

**THE IMPACTS OF CONCENTRATED AMBIENT PARTICULATES  
ON HEART RATE VARIABILITY IN RATS IN DETROIT, MICHIGAN  
AND STEUBENVILLE, OHIO**

**by**

**Ali S. Kamal**

A dissertation submitted in partial fulfillment  
of the requirements for the degree of  
Doctor of Philosophy  
(Environmental Health Sciences)  
in the University of Michigan  
2009

Doctoral Committee:

Professor Gerald J. Keeler, Chair  
Professor Bhramar Mukherjee  
Professor Marie Sylvia O'Neill  
Professor Jack Harkema, Michigan State University  
Professor James Wagner, Michigan State University

© Ali S. Kamal

---

All Rights Reserved  
2009



To all my teachers,  
academic and spiritual,  
thank you for believing in me.

## ACKNOWLEDGEMENTS

None of my graduate studies would have been possible without the continued support and guidance of my committee chair, Dr. Keeler. He brought me on in his Air Quality Laboratory early in 2001 and never stopped believing in me and I have constantly tried to repay my gratitude with my continuous commitment to the research projects in the lab. I thank him for keeping me aboard after my master's degree as a member of the lab because it gave me the opportunity to continue on and finish my doctoral degree. He never wanted me to just settle for working in his lab and saw potential in me beyond what I saw for myself. For that, I am forever grateful and hope to represent him and his reputation well where I may go.

I need to thank the other members of my committee for agreeing to see things through with me. Dr. Harkema, thank you for believing I could take on the great responsibilities of the mobile lab and for helping support my graduate degree. Dr. Wagner, thank you for your training and your continued guidance over the years and of course, for your sense of humor through it all. Dr. O'Neill, thank you for agreeing to support me and for your insights to prepare me to handle tough questions from other researchers in this field of heart rate variability. And finally, Dr. Mukherjee, you have been incredibly patient with me and I thank you for walking me through so much to understand the statistics behind my work. I wouldn't have much to say about the data without your help.

I have been fortunate to be part of so many other students' academic careers at the University of Michigan, and I must particularly thank the earlier generation of Fuyuen Yip, Mary Lynam, Molly Zwacki and Masako Morishita. You all believed in me and encouraged me on, especially Masako who helped put my future in motion for me. I have also become very close with Emily White, Lynne Gratz and Niama Hall who have all been great peers that made life in the lab and out in the field so enjoyable. And Emily, thank you for your friendship and your encouragement to make me better person along the way. But the Air Quality Lab would not be what it is without James Barres, who has

given me so much insight into myself, has trained me in so many ways to be a better person and a more capable scientist. Others who have helped me dearly through the years in the lab and out in the field includes Dr. Frank Marsik, Dr. Tim Dvonch, David Torrone, Matt Salvadori, Sue Crawford, Brenda Hadley and Ryan Lewandowski. Thank you all for guiding me through my degree and standing by me.

Most importantly, I thank my family who gave me the freedom to find out what I believe in and to pursue what I value in life. Thank you to all my friends here in Michigan and back in Illinois, and to all my personal mentors who never stopped believing in me that I could achieve the meaningful life I sought to live. You all made it possible that I am where I am today, and I only hope that I live a life that gives back to others and leave a positive impact on the world.

## TABLE OF CONTENTS

<b>DEDICATION.....</b>	<b>ii</b>
<b>ACKNOWLEDGEMENTS .....</b>	<b>iii</b>
<b>LIST OF TABLES .....</b>	<b>viii</b>
<b>LIST OF FIGURES .....</b>	<b>xii</b>
<b>LIST OF APPENDICES .....</b>	<b>xix</b>
<b>CHAPTER I INTRODUCTION .....</b>	<b>1</b>
I.1 Study Background .....	1
I.2 PM <sub>2.5</sub> Background.....	3
I.3 Heart Rate Variability.....	23
I.4 Research Objectives .....	31
I.8 Dissertation Structure .....	34
<b>CHAPTER II METHODOLOGY.....</b>	<b>36</b>
II.1 Site Selection.....	36
II.2 AirCARE1 Facility.....	41
II.3 Air Monitoring .....	44
II.4 Heart Rate Data Collection .....	52
II.5 Statistical Analysis .....	55
<b>CHAPTER III A SEASONAL COMPARISON OF THE IMPACTS OF PM<sub>2.5</sub> ON HRV IN RATS: DETROIT, MICHIGAN .....</b>	<b>62</b>
III.1 Detroit Summer Exposure.....	62
III.1.1 Synoptic Overview.....	62
III.1.2 Ambient Air Pollution Levels .....	70
III.1.3 CAPs PM <sub>2.5</sub> Characterization.....	76
III.1.4 High Temporal Resolution Air Pollution Findings.....	83
III.1.5 HRV Analysis .....	91

III.1.5.1 Eight-Hour Analysis .....	91
III.1.5.2 Thirty-Minute Analysis.....	99
III.1.6 Detroit Summer Summary .....	106
III.2 Detroit Winter Exposure .....	108
III.2.1 Meteorological Summary.....	108
III.2.2 Ambient Air Pollution Levels .....	111
III.2.3 CAPs PM <sub>2.5</sub> Characterization.....	118
III.2.4 HRV Summary.....	128
III.2.5 Detroit Winter Summary.....	134

**CHAPTER IV A SEASONAL COMPARISON OF THE IMPACTS OF PM<sub>2.5</sub> ON HRV IN RATS: STEUBENVILLE, OHIO ..... 146**

IV.1 Steubenville Summer Exposure.....	146
IV.1.1 Meteorological Summary .....	146
IV.1.2 Ambient Air Pollution Levels.....	150
IV.1.3 CAPs PM <sub>2.5</sub> Characterization .....	154
IV.1.4 Eight-Hour HRV Summary .....	160
IV.1.5 High-Resolution Air Pollution Measurements .....	168
IV.1.6 High-Resolution HRV Analysis .....	176
IV.1.7 Steubenville Summer Summary .....	184
IV.2 Steubenville Winter Study .....	185
IV.2.1 Meteorological Summary .....	185
IV.2.2 Air Pollution Measurements .....	191
IV.2.3 HRV Summary .....	204
IV.2.4 Steubenville Winter Discussion.....	212
IV.2.5 Steubenville Winter Conclusion .....	218
IV.3 Comparing Summer and Winter HRV Findings in Steubenville .....	219

**CHAPTER V ASSOCIATIONS OF HRV WITH SOURCE CONTRIBUTIONS IN SUMMERTIME EXPOSURES IN DETROIT, MIAND STEUBENVILLE, OH . 229**

V.1 Introduction .....	229
V.2 Source Factors in Detroit and Steubenville.....	234
V.3 Source Contributions Associated with HRV .....	241
V.4 Discussion and Conclusions.....	244

**CHAPTER VI CONCLUSIONS ..... 246**

VI.1 Revisiting the Study Objectives.....	246
---	-----

VI.2 Significant Method Developments .....	249
VI.3 Significant Discoveries .....	250
VI.4 Comparisons with Other HRV Studies.....	251
VI.5 Study Limitations and Future Advances in HRV Research .....	252
<b>APPENDICES.....</b>	<b>255</b>
<b>BIBLIOGRAPHY .....</b>	<b>284</b>



## LIST OF TABLES

### Table

I.1 USEPA estimated PM <sub>2.5</sub> emissions (2002) in the United States from classifiable point and mobile sources in tons/year .....	8
I.2 Historical progression of particulate matter regulations set by the USEPA .....	17
I.3 Definitions of HRV parameters and what each parameter modulates in the cardiovascular system .....	29
I.4 Summary of atmospheric measurements and heart rate variability parameters that were measured during the four exposure studies .....	33
II.1 Ambient and CAPs PM <sub>2.5</sub> concentrations are shown for each intensive, based upon 30-minute TEOM averages (µg/m <sup>3</sup> ) .....	36
II.2 Top point sources from all the surrounding counties of Detroit that emitted over 100 tons of PM <sub>2.5</sub> in 2002 .....	38
II.3 Table II.3 A list of the major PM <sub>2.5</sub> point sources in and around Steubenville, Ohio .....	41
III.1 Daily Concentrations of the major components of PM <sub>2.5</sub> CAPs collected during the 8-hour exposures (µg/m <sup>3</sup> ).....	79
III.2 Detroit summer average trace element concentrations of CAPs collected on Teflon filters in units of ng/m <sup>3</sup> (Except PM S and Fe which are in µg/m <sup>3</sup> ) .....	81

III.3 Averaged concentrations of PM and EC together with SEAS derived trace elements in the Detroit summer exposure study. ....	86
III.4 Detroit summer average statistics for unexposed (AIR) and exposed (CAPs) rats. ....	91
III.5 Eight-hour HRV mixed modeling results comparing AIR and CAPs Rats during the Detroit summer study.....	92
III.6 Least-squares means of ln(SDNN) for CAPs rats producing day-to-day comparative analysis during the Detroit summer exposure.....	93
III.7 Regression analysis of 8-hour average ln(SDNN) in CAPs Rats with integrated filter samples from the Detroit summer study .....	96
III.8 Thirty-minute mixed modeling results comparing AIR vs. CAPs Rats during the Detroit summer study.....	99
III.9 Average ambient PM <sub>2.5</sub> (µg/m <sup>3</sup> ) concentrations, during the two-week exposure period, according to wind direction .....	112
III.10 Comparison of the gaseous pollutants during the entire two-week exposure period for each seasonal intensive in Detroit .....	116
III.11 Daily Concentrations of the major components of PM <sub>2.5</sub> CAPs collected during the 8-hour exposures (µg/m <sup>3</sup> ) .....	119
III.12 Average CAPs concentrations of the PM <sub>2.5</sub> mass components in ng/m <sup>3</sup> (* µg/m <sup>3</sup> ) .....	121
III.13 Detroit winter average SEAS concentrations of PM <sub>2.5</sub> mass components (ng/m <sup>3</sup> ). *PM, EC and S are in µg/m <sup>3</sup> .....	127
III.14 Mixed modeling results from the Detroit winter study using 8-hour average for each HRV parameter.....	128
III.15 Detroit winter mixed modeling results for the 30-minute HRV dataset comparing AIR and CAPs Rats .....	132
III.16 Mixed modeling results comparing AIR and CAPs Rats ln(SDNN) in each season, based upon wind direction .....	138
III.17 Summary of the 30-minute HRV findings for each parameter for both summer and winter in Detroit.....	140

III.18 Summer and winter mean concentrations (ng/m <sup>3</sup> ) of SEAS trace elements for Detroit and the total range for each element in each season. (t-test, p<0.05)....	141
IV.1 Daily concentrations of the major components of PM <sub>2.5</sub> CAPs collected during the 8-hour exposures (µg/m <sup>3</sup> ) .....	156
IV.2 Daily trace element CAPs concentrations determined for Steubenville summer exposures.....	159
IV.3 Mixed modeling results comparing AIR and CAPs Rats from the Steubenville summertime intensive .....	160
IV.4 The ln(SDNN) parameter was investigated to determine if AIR and CAPs Rats differed within a specific day using the LS Means procedure.....	162
IV.5 HRV analysis within CAPs Rats parameter comparisons to determine if observed increases or decreases in ln(SDNN) were significantly lower (or higher) than on other observed days of exposure.....	162
IV.6 Eight-hour mixed modeling results from the Steubenville summer exposure after removing the first day of exposure (August 2) from the dataset .....	167
IV.7 Average SEAS concentrations of the PM <sub>2.5</sub> mass components during the Steubenville summer intensive, in ng/m <sup>3</sup> (* µg/m <sup>3</sup> ).....	172
IV.8 Thirty-minute mixed modeling results comparing AIR vs. CAPs Rats for the Steubenville summertime exposure .....	177
IV.9 Mixed modeling analysis broken down by NE and SW winds for the Steubenville summer intensive .....	178
IV.10 Daily concentrations of the major components of PM <sub>2.5</sub> CAPs collected during the 8-hour exposures (µg/m <sup>3</sup> ) .....	197
IV.11 Average CAPs mass and trace element concentrations in units of ng/m <sup>3</sup> .....	200
IV.12 Average SEAS fine fraction trace element concentrations in units of ng/m <sup>3</sup> .....	203
IV.13 Steubenville winter daily average statistics for unexposed (AIR) and exposed (CAPs) rats.....	204
IV.14 Steubenville winter study mixed modeling results for the 30-minute HRV parameters .....	205
IV.15 Least-squares means analysis showing that ln(SDNN) of CAPs Rats on February 17 was significantly lower than on all other days, except February 16.....	206

IV.16 Pearson's correlation table with two groups of constituents from the 8-hour Steubenville winter intensive that showed opposing effects on HRV .....	208
IV.17 The average of each component of PM <sub>2.5</sub> mass during the pollution episode (the first 4 hours of exposure on February 17) was compared to the average during all the other hours of exposure in ng/m <sup>3</sup> (* μg/m <sup>3</sup> ) .....	213
IV.18 Steubenville summer and winter mean concentrations (ng/m <sup>3</sup> ) of SEAS trace elements and the total range for each element in each season. (PM <sub>2.5</sub> mass in μg/m <sup>3</sup> ) The season in bold is to highlight that it has a higher concentration .....	222
V.1 The average mass and standard deviation for each pollutant during each intensive are shown with the associated percent reduction in ln(SDNN) .....	232

## LIST OF FIGURES

### Figure

I.1 Diagram conveying the relative size of coarse-mode ( $PM_{10}$ ) and fine-fraction ( $PM_{2.5}$ ) in contrast to the thickness of a human hair.....	4
I.2 Size distribution graph of particulate matter and the deposition of particles based on aerodynamic diameter .....	6
I.3 Eastern United States map depicting electric utility sources that emitted over 1000 tons/year of $PM_{2.5}$ in 2002 .....	9
I.4 CASTNET data for (a) $SO_4^{-2}$ and (b) $NO_3^{-1}$ (c) $NH_4^+$ in the Eastern United States from 2005-2007 .....	11
I.5 CASTNET ratios of $NH_4^+$ to $2[SO_4^{-2}] + [NO_3^{-1}]$ were used to determine the seasonal differences between the interaction of these constituents.....	13
I.6 Calculated ion ratios of $NH_4^+$ to $2[SO_4^{-2} + NO_3^-]$ from (a) Detroit and (b) Steubenville. ....	14
I.7 Average ion concentrations were plotted with the calculated $H^+$ ion.....	14
I.8 U.S. EPA map (2008) showing the non-attainment areas for $PM_{2.5}$ in the United States .....	19
I.9 The annual average $PM_{2.5}$ mass concentrations in the two counties observed in this study.....	20
I.10 Pathway of air pollution, from emission to adverse effects on the cardiopulmonary system .....	22

I.11 An example of a rat’s telemetry where the IBI is marked, measuring the distance between each detectable R peak in the ECG .....	26
I.12 Fast-Fourier transformation of a stressed and rested HR graph into frequency-domain parameters .....	28
II.1 AirData map of Wayne and Monroe Counties showing point source emissions (annual tons of PM <sub>2.5</sub> ) that contribute to the local air shed in Detroit .....	38
II.2 Map of Detroit denoting the major PM <sub>2.5</sub> within 10km of the sampling site in Detroit and their annual emissions in tons per year (2002).....	39
II.3 A map of Steubenville, Ohio with the largest PM <sub>2.5</sub> emission sources within 15km of the site, and tons of PM <sub>2.5</sub> emitted per year from the largest sources.....	40
II.4 Schematic layout of AirCARE1, the mobile air research laboratory.....	42
II.5 A diagram showing the Harvard PM <sub>2.5</sub> Concentrator and the Hinner exposure chamber inside AirCARE1 .....	43
II.6 A diagram of the major components to the function of the SEAS, the 30-minute trace element sampler .....	49
II.7 Regression analysis depicting a strong association between averaged 30-minute SEAS concentrations and 8-hour integrated filter data for S and Pb during the Detroit summer intensive (p<0.0001).....	50
II.8 Detroit summer AIR and CAPs Rats SDNN for each rat (bars) and the mean SDNN for each group (lines).....	56
II.9 Linear regression of the 8-hour Cu concentrations during the Detroit summer exposure with (a) the average SDNN for all CAPs and, and (b) the SDNN for each rat .....	59
III.1 Surface weather maps for two days during the Detroit summer intensive that observed the highest rainfall .....	63
III.2 Hourly temperature (°C) and relative humidity (%) with exposure hours highlighted in grey. Rainfall is denoted by purple horizontal bars .....	65
III.3 Wind rose for (a) the entire two-week study (July 16-28, 2005) and for (b) the 8 hours of exposure.....	66

III.4 HYSPLIT backward trajectory models for two days with different air mass histories .....	69
III.5 Thirty-minute ambient PM <sub>2.5</sub> concentrations from 7/17-28, 2005, during the Detroit summer study. Precipitation is shown to occur during the two-week study by the purple bars. The exposure hours are highlighted in grey .....	72
III.6 Twenty-four hour ambient PM <sub>2.5</sub> concentrations in Detroit based on 30-minute average mass and wind direction, for July 16-28, 2005 .....	73
III.7 Thirty-minute ambient gas concentrations measured at the Detroit site from July 16-28, 2005 with exposure hours highlighted by the grey bars .....	75
III.8 Wind roses for the exposure hours on (a) July 17 and (b) July 18, 2005 .....	77
III.9 Composition of PM <sub>2.5</sub> from analysis of CAPs filter samples collected during 8-hour exposures (µg/m <sup>3</sup> ) .....	79
III.10 Detroit summer 8-hour CAPs concentrations of PM <sub>2.5</sub> and constituents .....	82
III.11 Thirty-minute CAPs PM <sub>2.5</sub> and EC concentrations during Detroit summer exposure hours.....	84
III.12 Detroit summer Sb and S concentrations from 30-minute SEAS samples and 8-hour integrated filter samples.....	87
III.13 Pollutant concentration roses (ng/m <sup>3</sup> ) for (a) Sb, and (b) La (purple) and Ce (green) based on wind direction .....	89
III.14 Wind roses on July 28 broken down by (a) the first 2 hours of exposure and (b) the last 6 hours of exposure. PM <sub>2.5</sub> , Zn and Rb were plotted (c) over time.....	90
III.15 Box-and-whisker graph of daily ln(SDNN) for AIR and CAPs Rats .....	93
III.16 Detroit summer pollution concentrations of constituents associated with the changes in the average ln(SDNN) of CAPs Rats.....	95
III.17 Detroit summer confidence interval plots are for 8-hour average pollutant concentrations associated with HR, ln(SDNN) and ln(r-MSSD) .....	98
III.18 CI Plots using 30-minute pollution data associated with each health parameter, HR, ln(SDNN) and ln(r-MSSD).....	102
III.19 For the Detroit summer intensive, ln(SDNN) was associated with 30, 60, 90 and 120 minute moving average lags of pollutant concentrations .....	104

III.20 The lag effect on the percent reduction in ln(SDNN) for three pollutants most associated ln(SDNN) in real-time, PM, EC and Fe .....	105
III.21 Hourly temperature and relative humidity for the Detroit winter study with exposure hours shaded in grey .....	109
III.22 Wind rose illustrating air flow during the exposure hours in the Detroit winter study .....	110
III.23 Thirty-minute ambient PM <sub>2.5</sub> from February 10-23, 2006 in Detroit. Exposure hours are indicated with grey bands.....	113
III.24 Thirty-minute ambient PM <sub>2.5</sub> ambient concentrations (µg/m <sup>3</sup> ) for the Detroit winter study from February 10-23, 2006, by wind direction .....	114
III.25 Backward trajectories from the Detroit site showing the path of highest probability of air mass transport on February 11 and 16, 2006.....	115
III.26 Thirty-minute ambient gas concentrations measured at the Detroit site from February 11-23, 2006 with exposure hours highlighted by the grey bars .....	117
III.27 Composition of PM <sub>2.5</sub> from analysis of CAPs filter samples collected during 8-hour exposures for the Detroit winter study (µg/m <sup>3</sup> ) .....	120
III.28 Detroit winter 8-hour CAPs concentrations of PM <sub>2.5</sub> and constituents. Constituents in parentheses behaved similar to the pollutant being plotted. ....	122
III.29 Thirty-minute EC concentrations and CAPs PM <sub>2.5</sub> mass in the Detroit winter exposure study .....	124
III.30 Thirty-minute concentrations indicating the isolated early morning peaks in V and Sb on February 11, 2006.....	126
III.31 PM <sub>2.5</sub> and Zn associated with a spike on February 22, 2006 .....	126
III.32 CI Plots for 8-hour average concentrations of pollutants with each health parameter, HR, ln(SDNN) and ln(r-MSSD) from the Detroit winter intensive..	130
III.33 Detroit winter CI Plots using 30-minute concentrations of pollutants associated with each health parameter, (a) HR, (b) ln(SDNN) and (c) ln(r-MSSD) .....	133



III.34 Detroit summer CI Plot for ln(SDNN) after removing all data with mass greater than $600\mu\text{g}/\text{m}^3$ bringing summertime average mass down to wintertime concentrations. ....	136
III.35 Thirty-minute CI Plots comparing the percent change from the average (a) HR, (b) ln(SDNN) and (c) ln(r-MSSD) for each constituent of $\text{PM}_{2.5}$ during both Detroit exposure studies (Summer   Winter).....	142
IV.1 Hourly temperature and RH during the Steubenville summer study exposure .....	147
IV.2 Wind rose showing the prevailing surface flow for the August 2-14, 2006 summer exposure study in Steubenville .....	148
IV.3 Hysplit back trajectory models for August 2 during the exposure hours, observing an ambient $\text{PM}_{2.5}$ mass of $34.7\mu\text{g}/\text{m}^3$ (CAPs: $951\mu\text{g}/\text{m}^3$ ) .....	149
IV.4 Thirty-minute ambient $\text{PM}_{2.5}$ concentrations during the Steubenville summer study. ....	151
IV.5 Thirty-minute average ambient $\text{PM}_{2.5}$ ambient concentrations ( $\mu\text{g}/\text{m}^3$ ) according to wind direction, for 24-hours a day, during the Steubenville summer exposure .	152
IV.6 Thirty-minute average concentrations of gaseous pollutants measured in Steubenville during the summer exposure .....	153
IV.7 Daily CAPs concentrations obtained from the TEOM and from filter weights. Continuous TEOM concentrations are plotted in the background.....	155
IV.8 Composition of $\text{PM}_{2.5}$ from analysis of CAPs filter samples collected during 8-hour exposures for the Steubenville summer study ( $\mu\text{g}/\text{m}^3$ ).....	156
IV.9 Daily plots of CAPs concentrations during Steubenville summer exposures. $\text{PM}_{2.5}$ (a) and EC (b) were measured in $\mu\text{g}/\text{m}^3$ whereas trace element concentrations (c-f) are in $\text{ng}/\text{m}^3$ .....	158
IV.10 Steubenville summer CI Plots for the 8-hour integrated concentrations of pollutants associated with (a) HR and (b) ln(SDNN).....	165
IV.11 CI Plots for the 8-hour average pollutant concentrations in association with the frequency-domain parameters.....	166
IV.12 A CI Plot are for ln(SDNN) using 8-hour data from the Steubenville summer intensive but without the first day of exposure .....	168
IV.13 Thirty-minute EC concentrations during each exposure, as well as 8-hour integrated EC concentrations from the Steubenville summer intensive .....	170

IV.14 Thirty-minute continuous concentrations of S are plotted during the Steubenville summer exposure hours .....	171
IV.15 Thirty-minute pollution concentrations of La, S and EC based on wind direction during the Steubenville summer exposure hours .....	174
IV.16 Pollution ratios of air pollutants higher from the NE to SW (red) and ratios higher from the SW to NE (blue).....	176
IV.17 CI Plots for the Steubenville summer 30-minute measurements of HR, and according to NE and SW winds ( $p < 0.05$ ) .....	181
IV.18 Steubenville summer 30-minute CI Plots for $\ln(\text{SDNN})$ , and according to wind direction ( $p < 0.05$ ) .....	182
IV.19 Steubenville summer CI Plots for 30-minute $\ln(r\text{-MSSD})$ , by wind direction ( $p < 0.05$ ).....	183
IV.20 Hourly temperature and RH through each day's 8-hour exposure highlighted in blue.....	186
IV.21 The wind roses for (a) the entire 2-week period during the Steubenville winter intensive and (b) winds during February 17 .....	188
IV.22 Back trajectories for February 17 and February 19, two exposure days with low mixed depths (29m) .....	190
IV.23 Thirty-minute TEOM concentrations of ambient $\text{PM}_{2.5}$ ambient concentrations ( $\mu\text{g}/\text{m}^3$ ), exposure hours are highlighted by the grey bars .....	192
IV.24 Thirty-minute concentrations of gas measurements, exposure hours are highlighted by the grey bars .....	194
IV.25 Fine mass concentrations measured in Steubenville during the winter exposure from both the 8-hour exposure filter and the 30-minute TEOM data.....	196
IV.26 Daily concentrations of the major components of $\text{PM}_{2.5}$ CAPs collected during the 8-hour Steubenville winter exposures ( $\mu\text{g}/\text{m}^3$ ) .....	197
IV.27 Daily CAPs concentrations for (a) $\text{PM}_{2.5}$ and (b) S during Steubenville winter study .....	199
IV.28 Iron (Fe) and Sulfur (S) plots of 30-minute SEAS data during the Steubenville winter exposure hours .....	202

IV.29 Daily AIR and CAPs Rats averages for ln(SDNN) for the Steubenville winter exposure study .....	206
IV.30 CI Plots for the Steubenville Winter Exposure (8-hour data) (p<0.05).....	209
IV.31 Thirty-minute CI Plots from the Steubenville Winter exposure (p<0.05).....	211
IV.32 Average CAPs mass concentrations according to 4-hour averages during exposure hours.....	212
IV.33 CI Plots for the Steubenville winter intensive in the absence of the 4-hour data block on the morning of February 17 .....	217
IV.34 Pie graphs of the PM <sub>2.5</sub> CAPs composition from the Steubenville summer and winter intensives .....	221
IV.35 Thirty-minute CI Plots comparing the percent change from the average (a) HR, (b) ln(SDNN) and (c) ln(r-MSSD) for each constituent of PM <sub>2.5</sub> during both Steubenville exposure studies (Summer   Winter).....	225
V.1 Thirty-minute concentrations of Pb and P in Steubenville by wind direction.(ng/m <sup>3</sup> ) .....	235
V.2 Detroit and Steubenville summertime PM <sub>2.5</sub> source contributions to PM <sub>2.5</sub> mass during exposure hours.....	237
V.3 Thirty-minute PM <sub>2.5</sub> source contributions during exposure hours during the Detroit and Steubenville summer studies.....	239
V.4 Coal and Iron-Steel source contributions to Steubenville by wind direction based on 30-minute PMF results (µg/m <sup>3</sup> ) and SEAS results for S and Fe (ng/m <sup>3</sup> ) .....	240
V.5 Detroit confidence intervals of the effect estimate from each identified source for HR and HRV parameters. (msec).....	242
V.6 Steubenville confidence intervals of the effect estimate from each identified source for HR and HRV parameters. (msec).....	243

## LIST OF APPENDICES

### Appendix

- A.1 Backward wind trajectories (HYPSLIT) and surface wind roses for every 8- hour exposure period in Detroit during the summer and winter ..... 256
- A.2 Backward wind trajectories (HYPSLIT) and surface wind roses for every 8- hour exposure period in Steubenville during the summer and winter..... 271

# CHAPTER I

## INTRODUCTION

### I.1 Study Background

Associations between fine particulates in the ambient air, often referred to as PM<sub>2.5</sub> (particles with aerodynamic diameter < 2.5µm), and adverse human health effects are well documented in scientific literature.<sup>1,2,3</sup> However, neither the mechanisms nor the components of PM<sub>2.5</sub> related to cardiovascular effects are well described. While the toxicological effects of PM<sub>2.5</sub> mass in laboratory exposure studies have been reported, real-world atmospheric conditions that may affect the composition and chemistry of PM<sub>2.5</sub> have not been fully considered in an inhalation study.<sup>4</sup> In this thesis, a comprehensive characterization of ambient air pollution and an inhalation exposure study were integrated to investigate and potentially identify the most harmful components of PM<sub>2.5</sub> upon the cardiovascular system. The focus of this research is to investigate if PM<sub>2.5</sub> mass is the most effective measure to evaluate public health risk, or if a newer standard is needed that considers the composition of PM<sub>2.5</sub> mass.<sup>5</sup>

### Study Description

An “in-the-field” exposure assessment was conducted using a unique mobile air quality research laboratory. Spontaneously hypertensive (SH) rats were used to study the effects of inhaled concentrated ambient particulates (CAPs) on heart rate variability (HRV), a known indicator of autonomic tone of the cardiovascular system. The SH rats were exposed to CAPs in a whole-body exposure chamber for 13-day durations. For eight hours each day of the exposure study, cardiac parameters, including heart rate and electrocardiogram (ECG) waveforms were collected. Mixed modeling analysis was used

to determine if the HRV in CAPs-exposed rats was significantly different than the HRV in the control group, breathing HEPA-filtered air. Pollution concentrations were then modeled with HRV of CAPs-exposed rats to calculate the statistical strength of the associations (e.g. effect estimate), and determine which components of PM<sub>2.5</sub> were most strongly associated with changes in cardiovascular function in exposed rats.

### **Research Collaborators**

With 85% of electric energy generated by coal combustion in the United States, the Department of Energy (DOE) Office of Fossil Energy issued a request for proposals to examine the potential health risks associated with coal-fired power plant emissions.<sup>6</sup> Initially referred to as the “Tri-City CAPs Study,” this project was performed as a collaborative effort with the Electric Power Research Institute (EPRI), the University of Michigan Air Quality Laboratory (UMAQL), and Michigan State University. The main objective of the study was to characterize site and seasonal differences in the composition of PM<sub>2.5</sub>, and to associate pollutant concentrations with changes in cardiovascular function.

### **Sampling Locations**

The Tri-City CAPs Study was originally proposed to conduct summertime and wintertime exposures at three different locations (Detroit, MI, Steubenville, OH, and Goddard Park, PA) to determine how the composition of PM<sub>2.5</sub> may affect HRV. Air pollution in Detroit, MI, is an urban mixture of steel blast furnaces, coal-fired power plants, municipal waste and sewage sludge incineration, and significant tail-pipe emissions from motor vehicle traffic.<sup>6</sup> The exposure site was less than 2km from the Ambassador Bridge, the largest international crossing into Canada, potentially making diesel and motor vehicle traffic emissions a major contributor to the measured PM<sub>2.5</sub>. In Steubenville, OH, emissions from steel blast furnaces, coke ovens, coal-fired power plants, and chemical manufacturing dominate the PM<sub>2.5</sub> emissions inventory with less contribution from mobile sources. Two of the largest coal-fired power plants in the U.S. are located within 15km north and south of the site along the Ohio River Valley, the area in the United States with the highest concentrations of SO<sub>4</sub><sup>-2</sup>.<sup>8</sup> Also, the largest blast

furnace in the United States is 4km to the east in Weirton, WV.<sup>8</sup> The PA location was intended to be a background site with only regional source inputs, but was dropped from the study after DOE cut the funding for the project in the first year of study. Thus, this study will only compare results from Detroit and Steubenville.

## **Hypothesis**

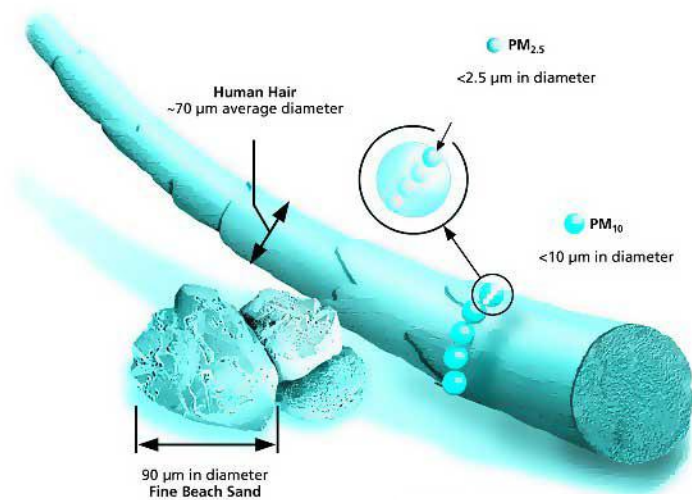
The objective of this thesis is to conduct a site and seasonal comparison of air pollution, and to identify the specific constituents of PM<sub>2.5</sub> that were associated with a cardiac response. If associations of specific constituents with HRV are found to be stronger than associations with PM<sub>2.5</sub> mass, then the results would suggest that pollutant-specific regulations may better mitigate adverse health effects.<sup>9</sup> Therefore, the hypothesis addressed here is that individual constituents of PM<sub>2.5</sub> are more strongly associated with changes in cardiovascular function than PM<sub>2.5</sub> mass in rats exposed to CAPs.

## **I.2 PM<sub>2.5</sub> Background**

### **PM Composition**

Particulate matter (PM) is a mixture of inorganic ions, organic matter, trace elements, water vapor, and naturally occurring wind-blown dust.<sup>10</sup> PM<sub>10</sub> refers to both coarse-mode particles (aerodynamic diameter 2.5-10microns) from natural sources, and fine-fraction particles (<2.5microns), primarily from anthropogenic combustion.<sup>10</sup> Fine-fraction particles are a greater risk to human health because particles of a smaller size can penetrate deep into the respiratory system, whereas coarse particles can be filtered out by the body's natural defenses before reaching the alveoli.<sup>10</sup> Figure I.1 from the USEPA provides a visual to capture the magnitude of these particles in relation to the thickness of a human hair.<sup>10</sup>

**Figure I.1 Diagram conveying the relative size of coarse-mode (PM<sub>10</sub>) and fine-fraction (PM<sub>2.5</sub>) particles in contrast to the thickness of a human hair.<sup>10</sup>**



Coarse-mode particles, referred to as PM<sub>10</sub>, are primarily composed of soil, sand, sea salts, pollen and other naturally occurring materials that are mechanically broken down to become wind-blown dust.<sup>10</sup> Depending on the location of the sampling site relative to industrialized areas, the majority of particulate matter the mass can be in the coarse-mode, whereas in downwind rural areas, there is less PM<sub>10</sub> and more fine-fraction mass.<sup>10</sup> Fine-fraction mass, referred to as PM<sub>2.5</sub>, is primarily generated by combustion of fossil fuels in electric utilities, motor vehicles and other industrialized processes that require an extreme amount of heat to process materials. PM<sub>2.5</sub> can be directly emitted as pulverized dust or hot fumes.<sup>10</sup> The gases emitted from industrialized processes, specifically SO<sub>2</sub> and NO<sub>2</sub>, are oxidized in the atmosphere by photochemical processes, and can then bind to trace elements or ion species (NH<sub>4</sub><sup>+</sup>) to form fine particles.<sup>11</sup> These gas-to-particle species of (NH<sub>4</sub>)<sub>2</sub>SO<sub>4</sub> and NH<sub>4</sub>NO<sub>3</sub> make up nearly 50% of the PM<sub>2.5</sub> mass in industrialized areas like Detroit and Steubenville.<sup>12,13</sup> These processes are enhanced in the summertime due to photochemical reactions resulting in strong seasonal variability of this component of PM<sub>2.5</sub>.<sup>11</sup>



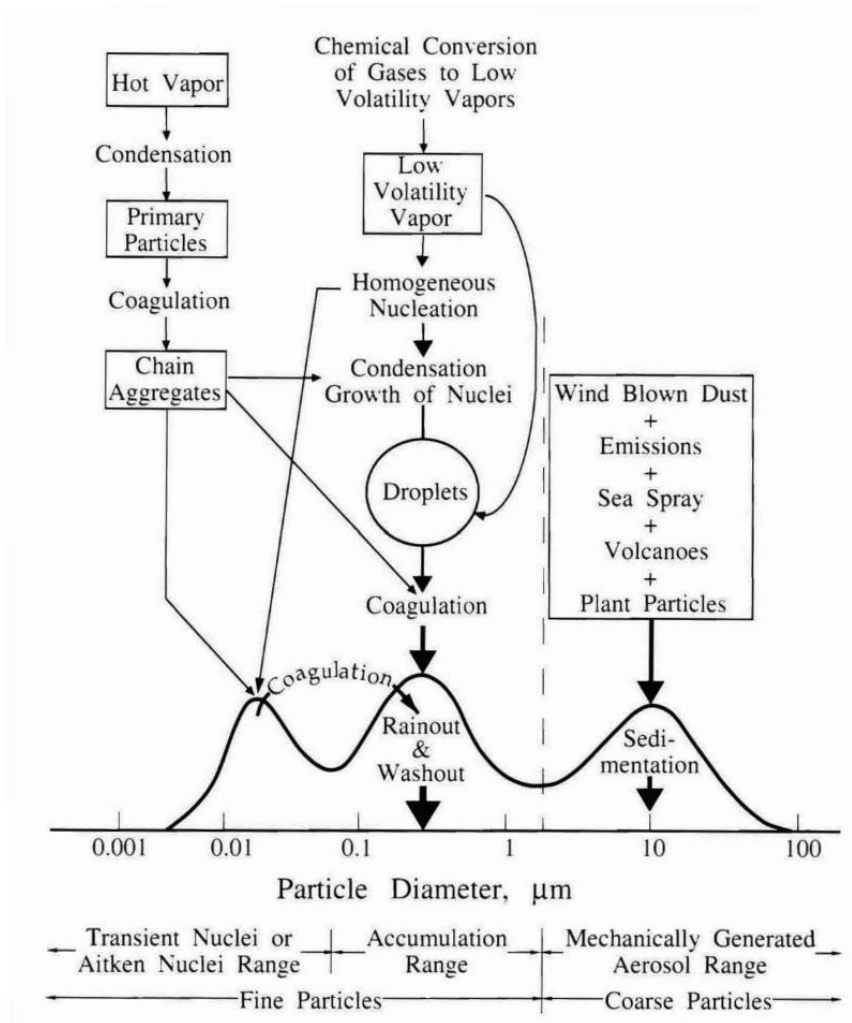
## Particle Size and Growth

Depending on atmospheric temperatures and relative humidity, primary emissions quickly coalesce into larger chains to form larger aerosols, but the particle size is still below 0.1 microns.<sup>14</sup> These ultrafine particles (e.g.  $PM_{0.1}$ ) are so small that they can interact on a cellular level and enter the bloodstream, causing toxicological effects directly upon target organs.<sup>15</sup> However, the lifetime of ultrafine particles is very short as they quickly coagulate into larger but still sub-micron particles. Therefore, if ultrafine particles are detected in an air shed, they most likely originated from a local source.<sup>14</sup>

The diameter of ultrafine particles is centered around 0.025 microns, but they quickly form aggregates with other particles and accumulate as fine-mode particles centered at 0.25 microns.<sup>14</sup> Figure I.2 shows the size-distribution of particles and the processes that they undergo from a primary ultrafine particle into an aggregate chain through coagulation into fine particles. Fine-fraction particles are transported long distances and contribute to the regional PM distant from the source.<sup>14</sup>

In the presence of water vapor, hygroscopic particles can grow into droplets and can be removed from the atmosphere through wet deposition, or settle over time on surfaces (e.g. dry deposition); both are mechanisms by which ambient air pollutants have been shown to pollute waterways and soil.<sup>10,14</sup> Coarse particles are typically not subject to the same chemical processes in terms of growth and coagulation, and are less subject to long-range transport.<sup>14</sup> The Harvard Six City Study found that  $PM_{2.5}$  is a better measure of relative health risk, and  $PM_{2.5}$  was adapted by the USEPA as the new regulatory standard in 2006.<sup>10</sup> This study attempts to go further by addressing the question of how the site and seasonal differences in the physiochemical characteristics of  $PM_{2.5}$  could modify the observable health effect (e.g. HRV).

**Figure I.2 Size distribution graph of particulate matter and the deposition of particles based on aerodynamic diameter.<sup>16</sup>**



### Seasonal Effects on PM<sub>2.5</sub>

Both temperature and relative humidity are major influences on particle growth and composition.<sup>14</sup> The Midwestern cities of Detroit and Steubenville both have considerable seasonal variability in ultra-violet (UV) light, strongly impacting the potential for photochemical reactions that can occur in the atmosphere with ambient air pollutants.<sup>14</sup> Increased UV light allows for more oxidation of species that can affect transition metals which become more toxic in the presence of oxygen.<sup>17</sup> Past studies have not shown that  $\text{SO}_4^{-2}$  and  $\text{NO}_3^-$  are well associated with human health effects.<sup>18,19</sup>

Thus, any seasonal impacts on the HRV may be related to PM<sub>2.5</sub> mass or the concentrations of trace elements, but are not likely to be associated with SO<sub>4</sub><sup>-2</sup> or NO<sub>3</sub><sup>-</sup>.

### **PM<sub>2.5</sub> Sources**

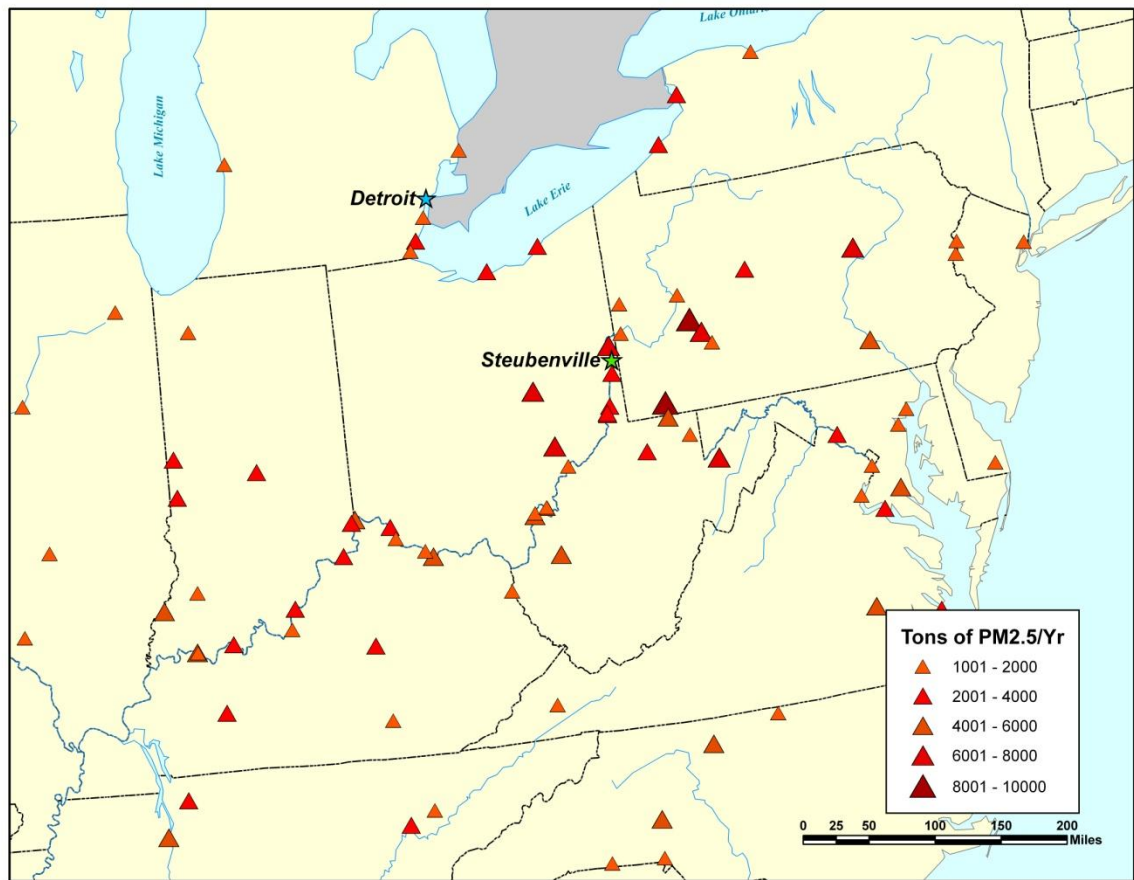
The PM<sub>2.5</sub> emissions from electric utilities reported by the United States Environmental Protection Agency (EPA) are estimated at 504,715 tons/year, primarily from coal combustion. Mobile source contributions from diesel trucks and automobiles, both on- and off-highway, are estimated over 501,338 tons/year.<sup>8</sup> Additional contributions from mobile sources are roadway dust and brake dust.<sup>20</sup> Other major point sources include oil refineries, waste incinerators, paper mills, metal processing facilities and chemical plants. Table I.1 summarizes the largest PM<sub>2.5</sub> emission sources in the United States in 2002.

In the entire United States, 160 coal-fired power plants each emit more than 1,000 tons of PM<sub>2.5</sub> annually.<sup>10</sup> Of those 160 facilities, 122 are found in the Eastern United States, most of which are shown in Figure II.3. The Ohio River Valley has a significant proportion of large power plants, mainly associated with the manufacturing core of the “rust belt” providing both coal and raw materials to produce steel. Despite the reduction in steel production in the United States over the last few decades, the number of coal-fired power plants emitting large amounts of PM<sub>2.5</sub> is still heavily concentrated along the river valley, stretching from southern Indiana and Ohio into western Pennsylvania.<sup>8</sup> There are also large electric utility plants in Georgia, Alabama, Tennessee and Florida, but the density of these facilities is much less, and the contributions from these emission sources may not impact the regional atmospheric chemistry (mainly SO<sub>4</sub><sup>-2</sup> concentrations) to the same extent as observed in the Midwest.<sup>21</sup>

**Table I.1 USEPA estimated PM<sub>2.5</sub> emissions (2002) in the United States from classifiable point and mobile sources in tons/year.<sup>10</sup>**

	<b>Point Source</b>	<b>Non-Point/ Mobile Source</b>
Electric Utilities Fuel Combustion	504,715	1,358
<i>Coal</i>	<i>-471,080</i>	<i>-1,048</i>
<i>Oil</i>	<i>-17,946</i>	<i>-300</i>
<i>Gas</i>	<i>-6,693</i>	<i>-8</i>
<i>Other</i>	<i>-2,182</i>	<i>0</i>
<i>Internal Combustion</i>	<i>-6,813</i>	<i>-2</i>
Industrial Fuel Combustion	90,486	81,551
Other Fuel Combustion	8,050	393,879
Manufacturing	29,683	24
Metals Processing	53,852	98
Petroleum & Related Industries	17,100	497
Other Industrial Processes	137,260	213,691
Solvent Utilization	5,061	1,683
Storage & Transport	22,442	432
Waste Disposal & Recycling	13,368	237,767
Highway Vehicles	0	156,145
Off-Highway	152	345,193
Miscellaneous	171	3,217,785
	<b>1,387,054</b>	<b>4,651,460</b>

Figure I.3 Eastern United States map depicting electric utility sources that emitted over 1000 tons/year of PM<sub>2.5</sub> in 2002.<sup>10</sup>



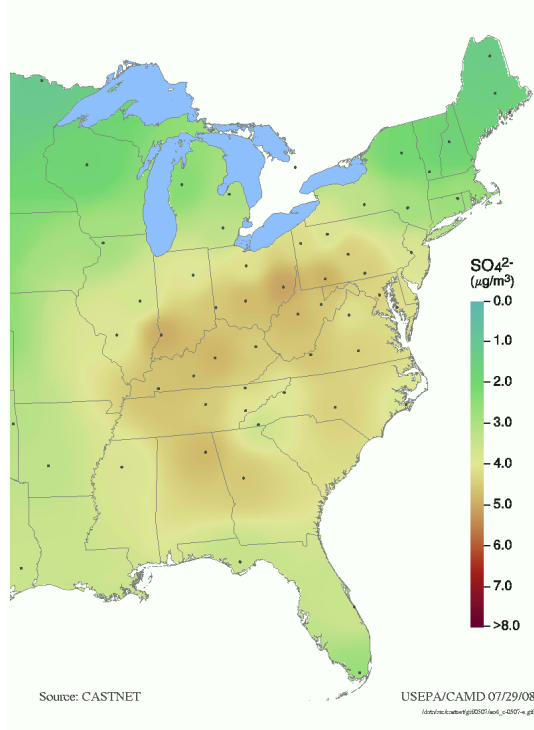
## The Atmospheric Chemistry of PM<sub>2.5</sub>

Historically, the major component of PM<sub>2.5</sub> found at locations in the Midwest was SO<sub>4</sub><sup>-2</sup>.<sup>12,13</sup> SO<sub>4</sub><sup>-2</sup> makes up 25% of the fine-fraction mass, but that typically decreases to 10% or less in the wintertime.<sup>14</sup> Acidic SO<sub>4</sub><sup>-2</sup> tends to bind with NH<sub>4</sub><sup>+</sup>, formed from gaseous NH<sub>3</sub> that results from the regional agricultural influences that surround Detroit and Steubenville.<sup>11</sup> The NH<sub>4</sub><sup>+</sup> binds to SO<sub>4</sub><sup>-2</sup> and acts to neutralize the acidic potential and eventually is deposited or transported as (NH<sub>4</sub>)<sub>2</sub>SO<sub>4</sub>.<sup>11</sup> In the wintertime, with less SO<sub>4</sub><sup>-2</sup> formation due to reduced UV light, more NO<sub>3</sub><sup>-</sup> can bind with NH<sub>4</sub><sup>+</sup> ion in the atmosphere.<sup>11</sup> Furthermore, NH<sub>4</sub><sup>+</sup> concentrations were increased in the absence of H<sup>+</sup> in the atmosphere, also caused by the reduction of UV in the winter months; thus more NH<sub>4</sub><sup>+</sup> binds to NO<sub>3</sub><sup>-</sup> forming NH<sub>4</sub>NO<sub>3</sub> rather than acidic species of HNO<sub>3</sub> or H<sub>2</sub>SO<sub>4</sub>.<sup>11</sup>

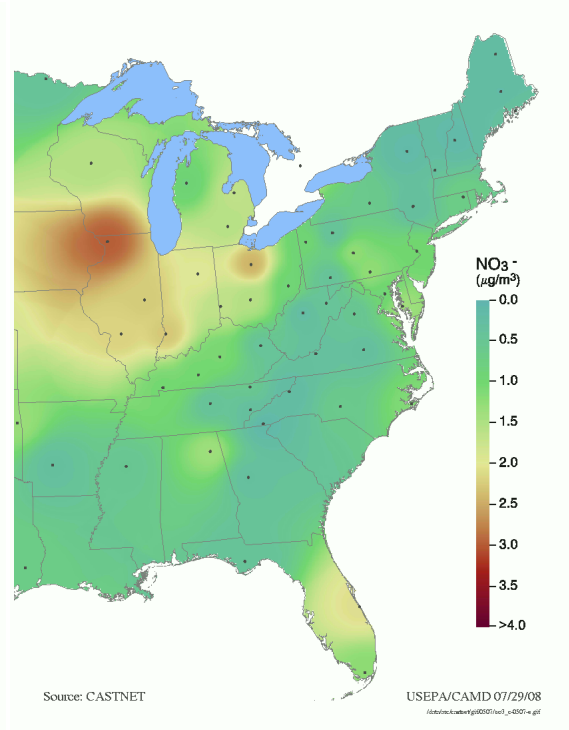
These chemical species have a great impact on the composition of PM in the Midwest. In Figure I.4, maps show the concentrations of SO<sub>4</sub><sup>-2</sup>, NO<sub>3</sub><sup>-</sup> and NH<sub>4</sub><sup>+</sup> in the Eastern United States compiled by the USEPA Clean Air Status and Trends Network (CASTNET). The concentrations of all these major species have dropped considerably over the last few decades. The average concentration of SO<sub>4</sub><sup>-2</sup> in the Ohio River Valley is half of what it was 20 years ago, from 8μg/m<sup>3</sup> to 4μg/m<sup>3</sup>; however, the river valley still has higher SO<sub>4</sub><sup>-2</sup> concentrations than the rest of the country.<sup>21</sup> Detroit does not have a high density of local power plants, but there is still a large contribution to PM<sub>2.5</sub> from secondary SO<sub>4</sub><sup>-2</sup>, largely attributed to the long-range transport of secondary SO<sub>4</sub><sup>-2</sup> from the Ohio River Valley where Steubenville is centrally located.<sup>7</sup> In Figure I.4.b, it is shown that the NO<sub>3</sub><sup>-</sup> concentration is low in the Ohio River Valley and is highest at the border of Iowa, Illinois and Wisconsin. Concentrations of NH<sub>4</sub><sup>+</sup> (Figure I.4.c) are higher throughout the Midwest (from agriculture and livestock) and where both SO<sub>4</sub><sup>-2</sup> and NO<sub>3</sub><sup>-</sup> are abundant and can bind with NH<sub>4</sub><sup>+</sup> to form particles. Together, the three CASTNET figures indicate a higher concentration of SO<sub>4</sub><sup>-2</sup> is surrounding the Ohio River Valley, and a higher concentration of NO<sub>3</sub><sup>-</sup> is seen where SO<sub>4</sub><sup>-2</sup> concentration is lowest in the Midwest.

Figure I.4 CASTNET data for (a)  $\text{SO}_4^{-2}$  and (b)  $\text{NO}_3^{-}$  (c)  $\text{NH}_4^{+}$  in the Eastern United States from 2005-2007.<sup>21</sup>

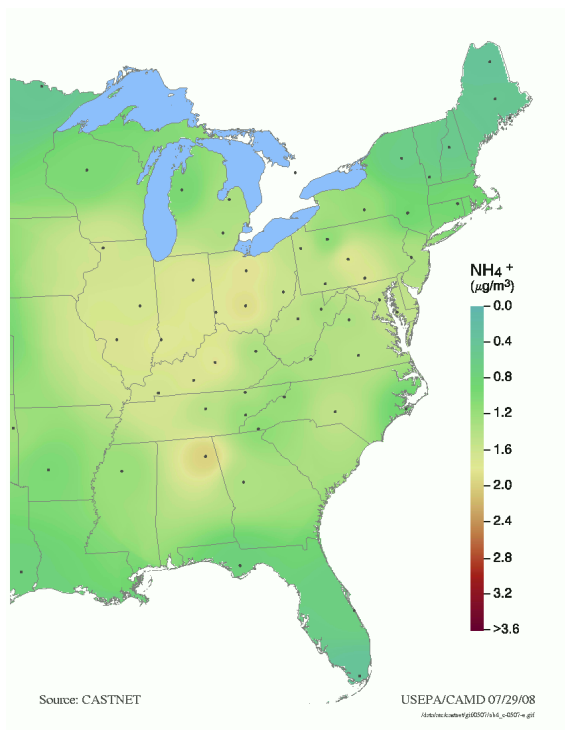
(a)  $\text{SO}_4^{-2}$



(b)  $\text{NO}_3^{-}$



(c)  $\text{NH}_4^{+}$



## H<sup>+</sup> Ion

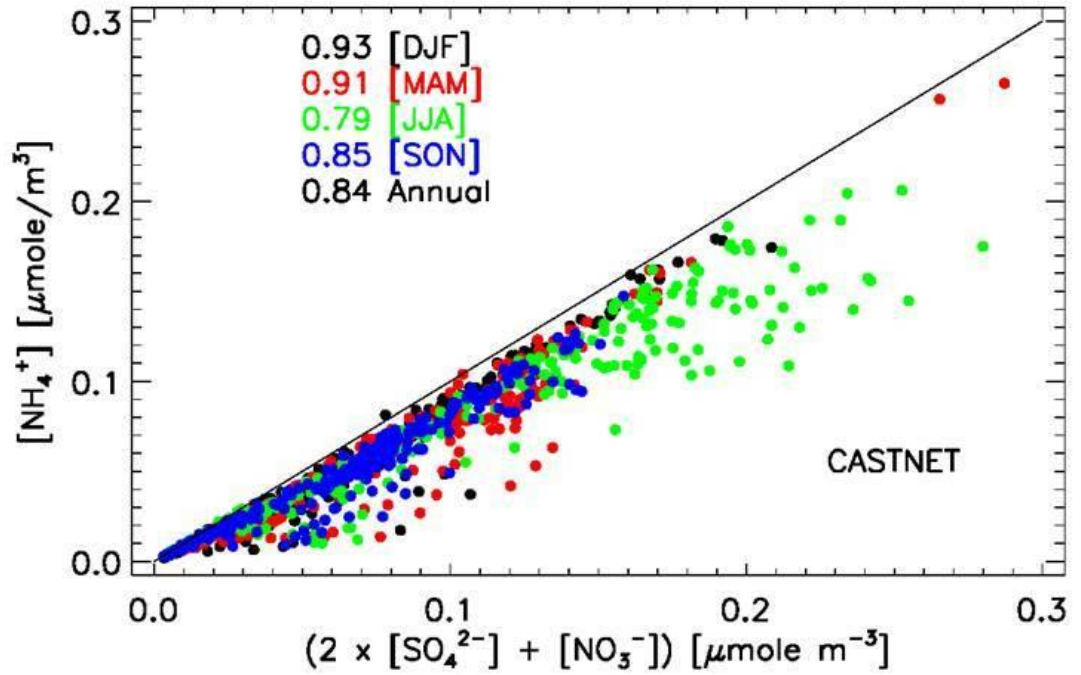
The seasonal abundance of SO<sub>4</sub><sup>-2</sup> concentrations in the summer in Detroit and Steubenville can lead to the saturation of NH<sub>4</sub><sup>+</sup> ions in the atmosphere.<sup>11</sup> In the absence of NH<sub>4</sub><sup>+</sup>, H<sup>+</sup> would be bound to the SO<sub>4</sub><sup>-2</sup> forming acid aerosols, H<sub>2</sub>SO<sub>4</sub>, the main contributor to acid rain.<sup>11</sup> However, multiple studies indicate that direct lung inflammation is not caused by the acidity of aerosols alone.<sup>18,22</sup> Instead, the acidic content could be another major factor in this study on health-related effects because the acidic content could alter transition metals forming more soluble, toxic species.<sup>7</sup> In this study, the H<sup>+</sup> concentrations were calculated for each day of exposure determine if there were significant differences in aerosol acidity from site-to-site and season-to-season that may lead to different chemical reactions in the atmosphere, but not a direct health effect on HRV.

Jacob *et al.* (2007) provided an analysis of the seasonal differences between the ratios of NH<sub>4</sub><sup>+</sup> concentrations of and the anion contributions of SO<sub>4</sub><sup>-2</sup> and NO<sub>3</sub><sup>-</sup> using the CASTNET network database of monitored sites across the United States (Figure I.5).<sup>23</sup> Quarterly regression analysis calculated that NH<sub>4</sub><sup>+</sup> to 2[SO<sub>4</sub><sup>-2</sup> + NO<sub>3</sub><sup>-</sup>] was lower in the summer months, leading to higher H<sup>+</sup>.

The same aerosol acidity analysis was conducted using the Detroit and Steubenville data, and the same μmole ratios were performed, and similar results were found (Figure I.6a and I.6.b). The H<sup>+</sup> ion was calculated using the formula: [H<sup>+</sup>] = 2[SO<sub>4</sub><sup>-2</sup>] + [NO<sub>3</sub><sup>-</sup>] - [NH<sub>4</sub><sup>+</sup>]. In Figure I.7, the average μmol of [NH<sub>4</sub><sup>+</sup>] and the 2[SO<sub>4</sub><sup>-2</sup>] + [NO<sub>3</sub><sup>-</sup>] was graphed with [H<sup>+</sup>]. The acidic aerosol in Detroit both seasonal intensives did not show a measurable amount of [H<sup>+</sup>], and was found negative due to the margin of error. The same result was seen in the Steubenville winter intensive where H<sup>+</sup> was below detection, however, during the summer in Steubenville, a measurable amount of H<sup>+</sup> was detected.

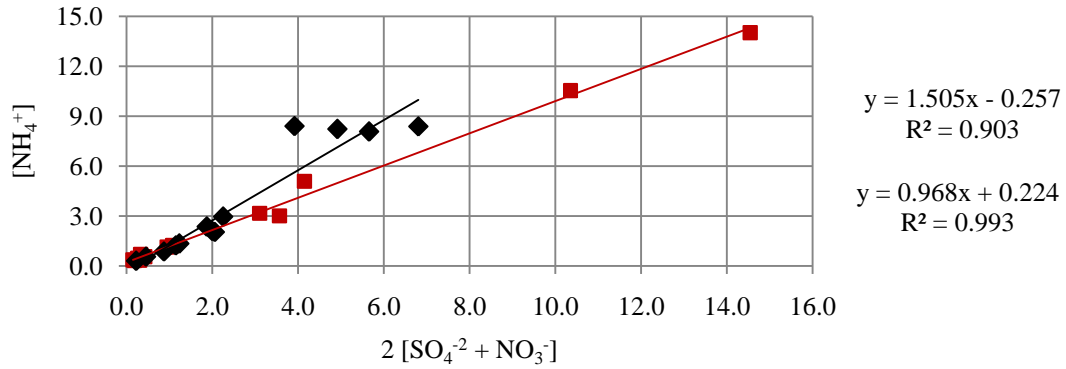


Figure I.5 CASTNET ratios of  $\text{NH}_4^+$  to  $2[\text{SO}_4^{2-}] + [\text{NO}_3^-]$  were used to determine the seasonal differences between the interaction of these constituents.<sup>23</sup>



**Figure I.6 Calculated ion ratios of  $\text{NH}_4^+$  to  $2[\text{SO}_4^{2-} + \text{NO}_3^-]$  from (a) Detroit and (b) Steubenville.**

**(a) Detroit Acidic Ratio (Red: Summer, Black: Winter)**



**(b) Steubenville Acidic Ratios (Red: Summer, Black, Winter)**

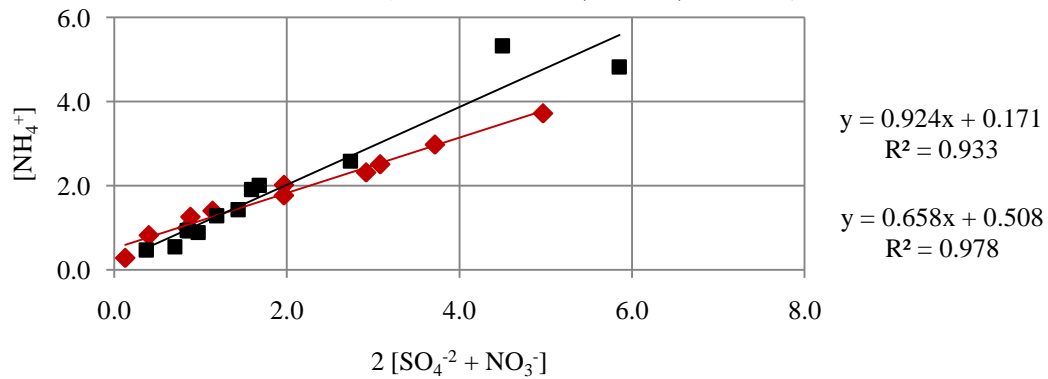
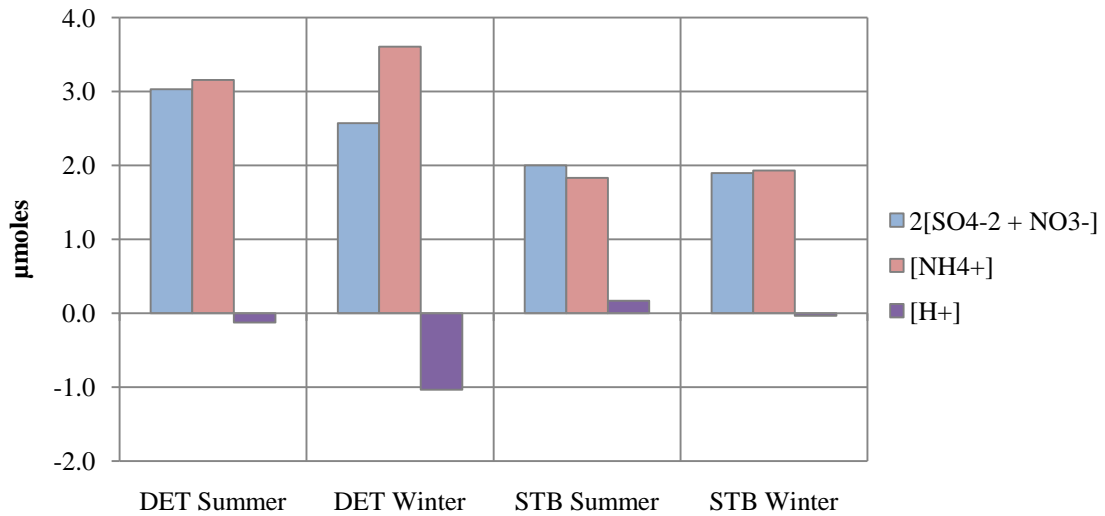


**Figure I.7 Average seasonal ion concentrations were plotted, along with the calculated concentration for the  $\text{H}^+$  ion.**



## **Carbon Species in Detroit and Steubenville**

The other major components of PM<sub>2.5</sub> in Detroit and Steubenville are elemental carbon (EC) and organic carbon (OC). EC, an indicator for diesel emissions, has shown to be relatively unchanged in Detroit between the summer and winter months because the reactions are few and governed by atmospheric conditions (e.g. wind speeds, mixed layer depth), not chemistry.<sup>7,24</sup> OC concentrations, however, are greatly affected by seasonal conditions. One explanation for the higher concentrations of OC found in Detroit and Steubenville in winter than in summer (30% compared to 5%, respectively) is that OC compounds vaporize at higher temperatures and are not effectively collected by air monitoring methods used in these studies.<sup>25</sup> In the winter, however, with lower ambient temperature, the vaporization temperatures of many OC compounds may not be reached and can therefore be collected on the filters and add to the fine-fraction mass.<sup>25</sup> Therefore, there is great value in conducting seasonal exposures at these two locations to determine the significant changes in PM<sub>2.5</sub> composition that is driven by temperature, humidity and photochemistry.

## **Historical Background on PM<sub>2.5</sub>**

The greatest air pollution disaster that occurred in the United States was in 1948 when the steel town of Donora, PA, experienced a temperature inversion, trapping emissions from the blast furnaces which resulted in the death of 20 individuals in a town of 14,000.<sup>5</sup> However, no greater episode in recent history was as severe as the London fog episode in 1952. Due to the large amount of coal-burning within the city, a five day temperature inversion resulted in a thick “Killer Fog” that was responsible for 4000 deaths.<sup>5</sup> Current air quality regulations, emissions controls and newer technology (e.g. higher smoke stacks, SO<sub>2</sub> scrubbers) prevent those extreme and catastrophic pollution episodes from occurring in the United States today.

These extreme examples show that there are acute effects of high air pollution; however, the greatest concern today is from prolonged exposures to lower-level urban and industrialized pollution. Despite current regulatory standards, heavy industrial productivity and increased automobile traffic in urban centers still experience an

increased occurrence of respiratory disease and an increased morbidity and mortality rate.<sup>1,26</sup> As a result, it became more important to understand the mechanisms by which air pollution is causing disease, and to identify the pollutants responsible for the adverse health effects. Epidemiological studies began to investigate long-term exposures to lower level concentrations, and it was found that concentrations are closely linked cardiopulmonary morbidity and mortality as well as respiratory diseases.<sup>27,28,29,30</sup> The study described in this thesis is important because it characterized the ambient air pollution in heavily industrialized areas to identify which components of PM<sub>2.5</sub> mass are most associated with the effects observed on HRV. Changes in HRV has been associated with air pollution concentrations in humans and experimental animal models.<sup>26,31,32</sup> These health data can help inform the development of future regulations to better reduce the health risks of low-level prolonged exposures.

### **Regulating PM<sub>2.5</sub>**

The health concerns associated with particulate matter exposure have changed through the years as scientific research and technological advances revealed that the composition of smaller particles is better associated with adverse health effects than larger particles. Early EPA regulations of PM controlled Total Suspended Particulates (TSP) were introduced in 1971 as one of the National Ambient Air Quality Standards (NAAQS) pollutants. NAAQS also included the monitoring and control of Pb, O<sub>3</sub>, NO<sub>x</sub>, SO<sub>2</sub> and CO. Once the EPA set the NAAQS, states were required to have Air Quality Control Regions (AQCR) maintain particular standards.

With TSP, the EPA was focused on reducing overall dust in urban areas, without yet understanding the health risks of continuous low-concentration exposures to particulate matter. Soon after its introduction, the control of TSP proved to be too difficult for states to regulate because TSP often included naturally occurring wind-blown dust (20-50 microns in aerodynamic diameter). At the same time, studies in the early 1980's found that the inhalable size-fraction particles, PM<sub>10</sub> (aerodynamic diameter < 10 microns), were penetrating deeper into the respiratory system and exacerbating respiratory disease.<sup>10</sup> Finally, in 1987, the EPA set the PM<sub>10</sub> standard to regulate particulates. As part of the 1987 mandate, the USEPA funded the Harvard Six City

Study to assess whether the PM<sub>10</sub> standard was, in fact, the best measure to control injurious ambient particulates. The study showed that adverse health effects were not well linked with PM<sub>10</sub> concentration, but rather with respirable-sized particles below 2.5 microns.<sup>33</sup> In 1997, PM<sub>2.5</sub> was finally added to the NAAQS, and was modified in 2006 to have a lower 24-hour standard (along with eradicating the PM<sub>10</sub> annual standard). Table 1.2 summarizes the progression of the PM standard.

**Table I.2 Historical progression of particulate matter regulations set by the USEPA.<sup>10</sup>**

Year	Pollutant	24-hour Standard	Annual Standard
1971	Total Suspended Particulates	<u>Primary:</u> 260µg/m <sup>3</sup> <u>Secondary:</u> 150µg/m <sup>3</sup>	75 µg/m <sup>3</sup>
↓			
1987	Particulate Matter < 10 microns	150	50
↓			
1997	Particulate Matter < 10 microns	150	50
	Particulate Matter <2.5 microns	65	15
↓			
2006	Particulate Matter < 10 microns	150	-
	Particulate Matter <2.5 microns	35	15

**Detroit and Steubenville Concentrations of PM<sub>2.5</sub>**

Detroit, MI, and Steubenville, OH, have been in non-attainment for the annual PM<sub>2.5</sub> NAAQS and both have been integral locations in addressing the health impacts of PM<sub>2.5</sub>. In Detroit, understanding the health implications of air pollution is critical due to the excessive number of deaths related to cardiovascular and respiratory diseases.<sup>34,35</sup> Steubenville, OH, was a critical site in the Harvard Six City Study as discussed in the earlier section and was shown to be an area in which adverse health effects were

associated with PM<sub>2.5</sub> concentrations.<sup>35</sup> In Figure I.8, the AirData map for 2008 shows the distribution of PM<sub>2.5</sub> non-attainment areas around the country.<sup>10</sup> Both Detroit and Steubenville are included and Figure I.9 shows the average PM<sub>2.5</sub> concentrations for the counties in which each city is located (Wayne County, MI, and Jefferson County, OH, respectively).<sup>10</sup> The gradual reduction in PM<sub>2.5</sub> concentrations is more likely attributed to the reduction in productivity in the steel and automotive industries rather than increased regulations.

**Figure I.8 U.S. EPA map (2008) showing the non-attainment areas for  $PM_{2.5}$  in the United States. Both Detroit and Steubenville are located in non-attainment areas.<sup>10</sup>**

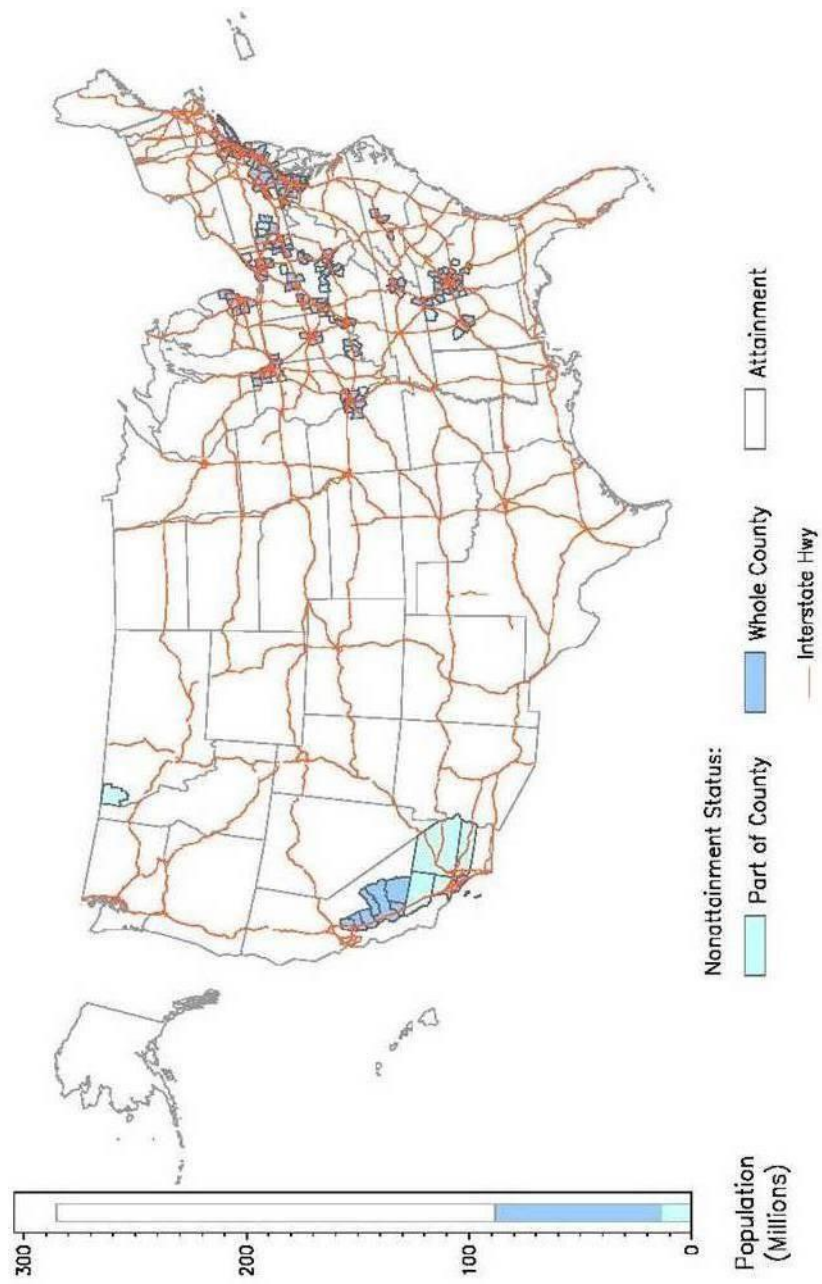
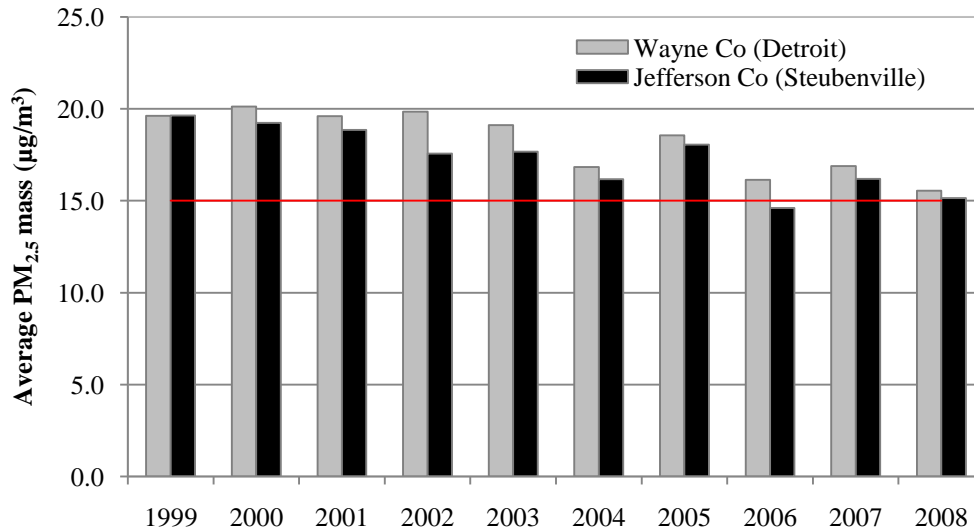


**Figure I.9 The annual average PM<sub>2.5</sub> mass concentrations in the two counties in which exposures were performed in this study. The red line indicates the U.S. EPA the annual NAAQS standard for PM<sub>2.5</sub> mass.<sup>10</sup>**



## Health Concerns of PM<sub>2.5</sub>

### Physical Defenses

Several studies suggest that regardless of the composition of PM, as particle size decreases, the toxicity of the PM increases.<sup>31,32</sup> Understanding the size distribution and behavior of particles in the atmosphere is therefore critical to characterize PM<sub>2.5</sub> in an exposure study. As small as PM<sub>10</sub> particles are, the respiratory system in humans has many defenses to protect against particles permeating into the lungs.<sup>32</sup> Nasal hairs and upper-airway mucus provide an initial filtration of coarse-sized particles to prevent them from even entering the tracheal or bronchial airways.<sup>32</sup> Particles that do reach these lower areas are controlled by a mucus layer that seizes these particles and prevents them from reaching the alveoli.<sup>32</sup> Macrophages then carry any attached particles up through the respiratory tract to be coughed out of the respiratory system.<sup>32</sup>

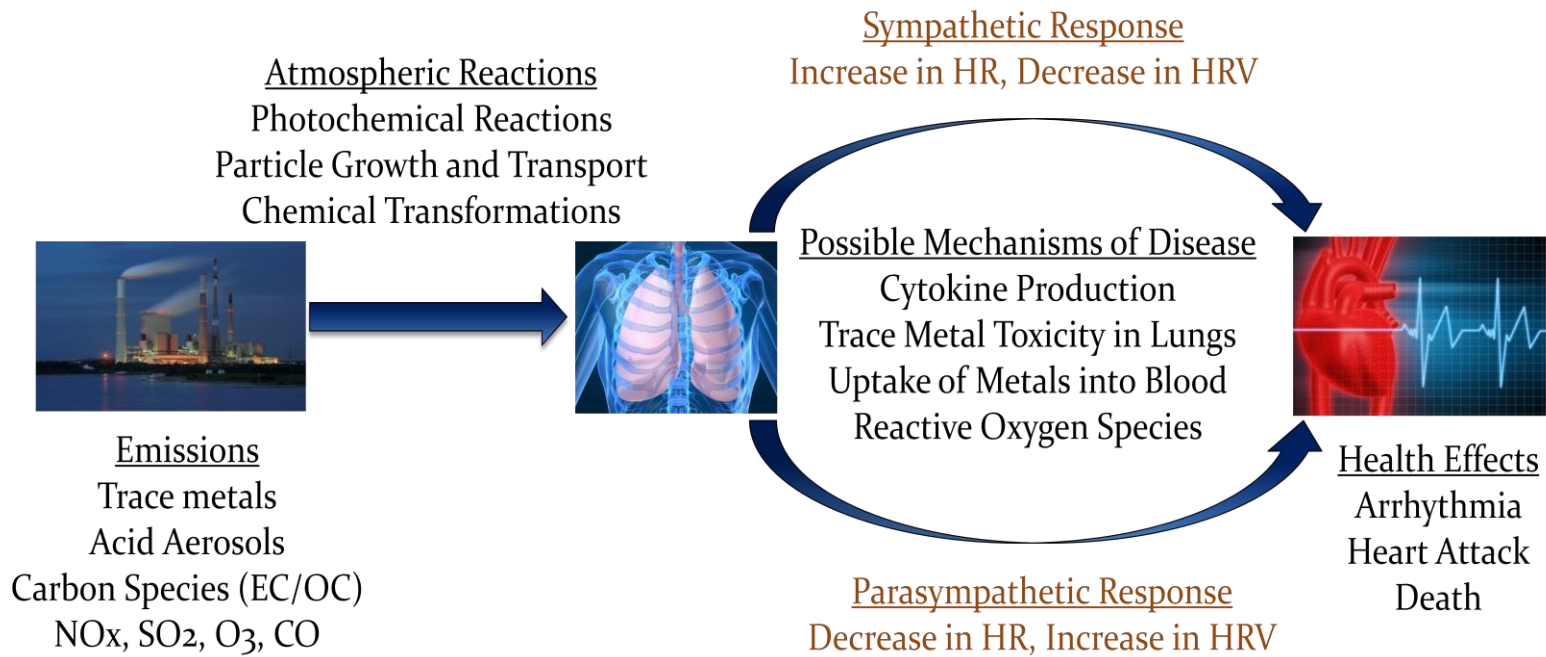


## **Fine-Fraction Health Effects**

PM<sub>2.5</sub> particles can penetrate deep into the respiratory system; the aerodynamic diameter of PM<sub>2.5</sub> is small enough that fewer collisions with the nasal passages and bronchial walls occur.<sup>10</sup> The smallest size-fraction within PM<sub>2.5</sub>, referred to as ultrafine particles (aerodynamic diameter <0.1 microns), can reach alveoli-blood exchanges in the lungs and have been identified to be taken up by the blood.<sup>10,15</sup> Ultrafine particles (PM<sub>0.1</sub>) are often the primary emissions from combustion, making the hazards of being in proximity to point sources and highways greater due to higher PM<sub>2.5</sub> concentrations as well as the mass consisting of smaller, and potentially more toxic particles.<sup>32,37</sup>

Multiple studies have confirmed that PM<sub>2.5</sub> has adverse health outcomes on the respiratory system, however, the mechanisms that effect the cardiopulmonary system are still unclear.<sup>38</sup> The most severe effects of PM<sub>2.5</sub> can be caused by hypoxia or respiratory distress; however, neither are associated with changes in autonomic tone.<sup>39</sup> Lung inflammation, indicated by an increase in cytokine production in the blood, may cause a direct effect on the conductivity of the autonomic nervous system.<sup>39,40</sup> Particles have also been identified to cross the blood-alveoli barrier, and trace elements have reached target organs, including cardiac tissue.<sup>15,41</sup> Brook *et al.* (2002) observed arterial wall constriction in the presence of PM<sub>2.5</sub> and O<sub>3</sub>. Together these studies indicate that exposure to air pollutants can drive changes in the cardiovascular system via the respiratory system.<sup>42</sup> Figure I.10 illustrates the possible mechanisms by which autonomic tone is affected by air pollution.

**Figure L.10 Pathway of air pollution, from emission to adverse effects on the cardiopulmonary system.**



## **The Need for Better Regulations on PM<sub>2.5</sub>**

When the new PM<sub>2.5</sub> standard was introduced in 1997, a large scientific debate began as to whether it was merely the size of the particles driving adverse health effects or whether the specific constituents of PM<sub>2.5</sub> were toxic.<sup>9</sup> Many studies have associated PM<sub>2.5</sub> mass concentration with adverse health outcomes (i.e. hospital admissions from pulmonary distress, morbidity and mortality rates).<sup>1,27,35</sup> Although PM<sub>2.5</sub> mass can penetrate deep into the lungs, the make-up can range from mostly inert (i.e. silica) to extremely toxic (e.g. heavy metals). It is therefore important to first understand which constituents are most harmful as well as the source of the particulates. However, the difficulty in monitoring PM<sub>2.5</sub> constituents as opposed to PM<sub>2.5</sub> concentrations has been difficult to conduct.

Studies have been conducted in urban areas and near roadways to investigate if mass contributions from specific sources are more strongly associated with adverse health effects than PM<sub>2.5</sub> mass.<sup>43,44</sup> Such studies might help determine if PM<sub>2.5</sub> mass is the best measure to protect public health, or if the control of specific source constituents is needed. But to discover this correlation, a comprehensive characterization of the particulates needs to be conducted first, then analysis can be conducted to determine which constituents or sources are most associated with adverse health outcomes. The study described in this thesis used HRV as a biomarker of cardiac function, and determined associations with specific constituents of PM<sub>2.5</sub> (e.g. trace elements, ion species, carbon species and source factors) to find the best measure associated with cardiovascular health.

## **I.3 Heart Rate Variability**

### **Background on HRV**

Normal cardiac function has a natural variability as a result of the collective balance of the sympathetic and parasympathetic autonomic nervous system.<sup>45</sup> Without any physiological controls, the pacemaker of the human heart would beat at 120bpm.<sup>45</sup> Most people have an average HR of 60-80bpm due to the activation of the parasympathetic autonomic response to keep the heart rate down for the body to conserve

energy and to provide rest.<sup>45</sup> In opposition, the sympathetic autonomic nervous response to the heart is responsible for speeding up HR in excess of 180bpm if necessary.<sup>45</sup> Whether it be standing up quickly or beginning an exercise, the sympathetic autonomic response reads the changes in demand and adjusts HR to maintain adequate blood flow and blood pressure throughout the cardiovascular system.<sup>45</sup> Together, these two systems work in conjunction to provide adequate rest and appropriate work upon the heart.

Under stress, the sympathetic autonomic system responds with an increase in HR and causes a decrease in the natural HR variability, or simply HRV. Therefore, a loss in HRV has typically been seen as an up-regulated autonomic response caused by the activation of the sympathetic nervous system.<sup>46</sup> However, the down-regulation of the parasympathetic nervous system can also cause a reduction in HRV.<sup>46</sup> Either way, a significant change in HRV indicates an autonomic response in the cardiovascular system, beyond changes in respiratory rate or the physiological impact on the respiratory system.<sup>46</sup>

For those cardiac patients who have already suffered from a heart attack, there is clear evidence that their autonomic responses are compromised and do not respond appropriately to changes in cardiac demands, resulting in very dangerous and even fatal situations.<sup>46</sup> Hospital studies have shown that cardiac patients experience a loss in their natural HRV before a heart attack.<sup>45</sup> The heart no longer receives the appropriate input to adjust to physical activity or stress as it would under normal circumstances. Nolan *et al.* (2006) confirmed the reciprocal relationship between the activation of the sympathetic autonomic response and the depression of the parasympathetic tone in cardiac patients that suffered from heart failure.<sup>47</sup>

### **HRV and Air Pollution**

There is a concern that PM<sub>2.5</sub> interferes with the autonomic tone and may be extremely dangerous for at-risk populations on high pollution days. If any pollutant or chemical were to disrupt the system's natural balance, a compromised situation would occur where the heart may not be able to adjust for the changes in demand.<sup>45</sup> Pope *et al.* (1999) found ambient PM concentrations aligned with increased heart rate (HR) and the root mean sum of successive differences (r-MSSD) and a reduction in the normal to

normal standard deviation (SDNN) in elderly subjects.<sup>31</sup> Meanwhile, spontaneously hypertensive (SH) rats exposed to ozone and particulate matter showed an observable reduction in HR and body temperature.<sup>49</sup> Corey *et al.* (2006) used mice to instill fine ambient particulates from Seattle, WA, into the nasal passages and experience an increase in HR followed by a reduction in HRV, thus concluding a change in autonomic tone.<sup>50</sup>

More recent human epidemiological studies have revealed that specific components of PM<sub>2.5</sub> are harmful to the cardiopulmonary system. Gold *et al.* (2006) studied non-smokers in Steubenville and observed reductions in SDNN, r-MSSD and the high frequency power spectral density (HF) with increased SO<sub>4</sub><sup>-2</sup> concentrations and PM<sub>2.5</sub> mass, with a one-day lag.<sup>51</sup> Furthermore, PM<sub>2.5</sub> constituents attributed to traffic were better associated to cardiovascular mortality than PM<sub>2.5</sub> mass.<sup>26</sup> Additionally, a reduction in r-MSSD occurred in congestive heart failure (CHF) and in healthy rats immediately following exposure to diesel exhaust.<sup>52</sup> Campen *et al.* (2003) and Chang *et al.* (2003) both conducted diesel exposures on SH rats and identified a significant increase in HR.<sup>53,54</sup>

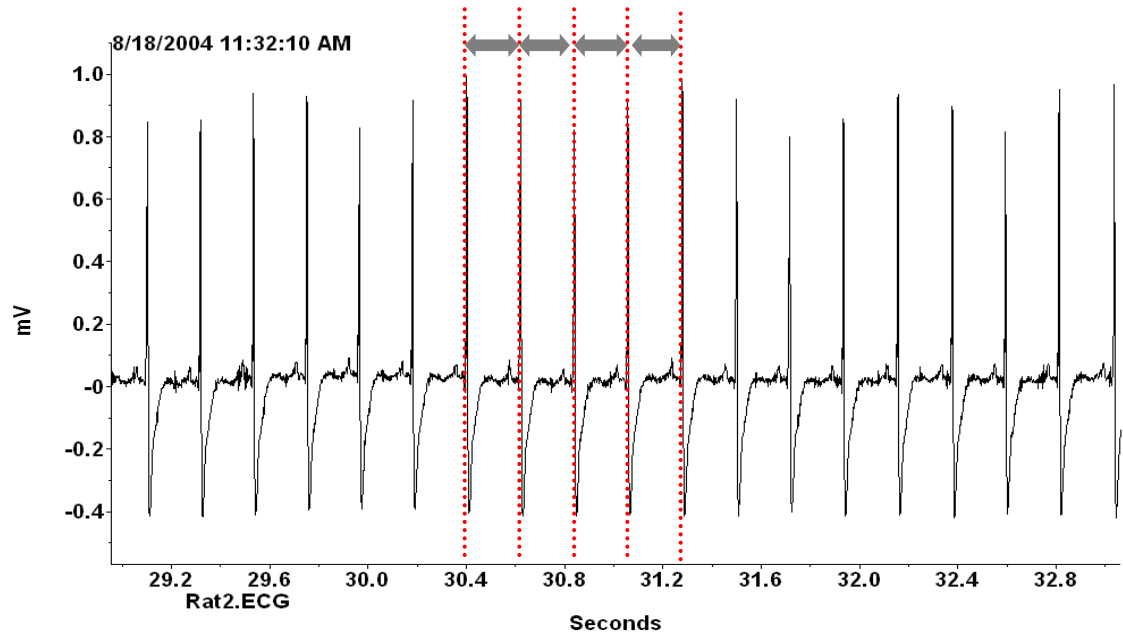
Many animal studies have been conducted in the laboratory, but the unique and critical aspect of the study presented in this thesis was the ability to take the rats into the field and monitor real-world interactions of pollutants. The benefit of this approach was described by Peretz *et al.* (2007) in human subjects exposed to diesel exhaust (200µg/m<sup>3</sup>) where increased HF and decreased low frequency to high frequency spectral density ratio (LF/HF) suggested an autonomic response.<sup>55</sup> Peretz concluded that diesel alone did not well associate with health impacts in this experimental study, and that an in-the-field exposure study with mixtures of ambient particulates would provide better, real-world cardiovascular effects.<sup>55</sup>

### **Measurements of HRV**

All HRV parameters were calculated using the inter-beat interval (IBI), or the distance from one R-peak to the next R-peak in an electrocardiogram (ECG) readout.<sup>46</sup> Each R-peak represents the point at which the heart is fully depolarized and blood is pumped out of the ventricles into the arteries.<sup>48</sup> In Figure I.11, a sample ECG readout from an SH rat is shown with the R peaks and IBI highlighted. Measuring the distance

between R-R peaks is the method by which the average heart rate (HR) was calculated. The IBI is continuously changing through the influence of sympathetic and parasympathetic inputs as previously discussed.<sup>45</sup>

**Figure I.11** An example of a rat's telemetry where the IBI is marked, measuring the distance between each detectable R peak in the ECG.



### Time-Domain HRV Parameters

To study the variability in HR over time, two factors were calculated, (1) the standard deviation of the IBI for each time segment (SDNN), and (2) the root mean square of successive differences of the IBI (r-MSSD).<sup>46</sup> HR, SDNN and r-MSSD are referred to as “time-domain” HRV parameters. Toxicological studies have found that a reduction in HRV occurs with drug interaction on the autonomic nervous system, and occupational studies of inhaled particles by boilermakers have also seen changes in HRV.<sup>46,56</sup> The European Task Force of Heart Rate Variability established that both SDNN and r-MSSD parameters reflect the modulation of autonomic tone and can be used as indicators of cardiac health.<sup>46</sup> HR is not a measure of autonomic tone, however, it is still be used in cardiovascular studies to see if biological responses to the cardiovascular

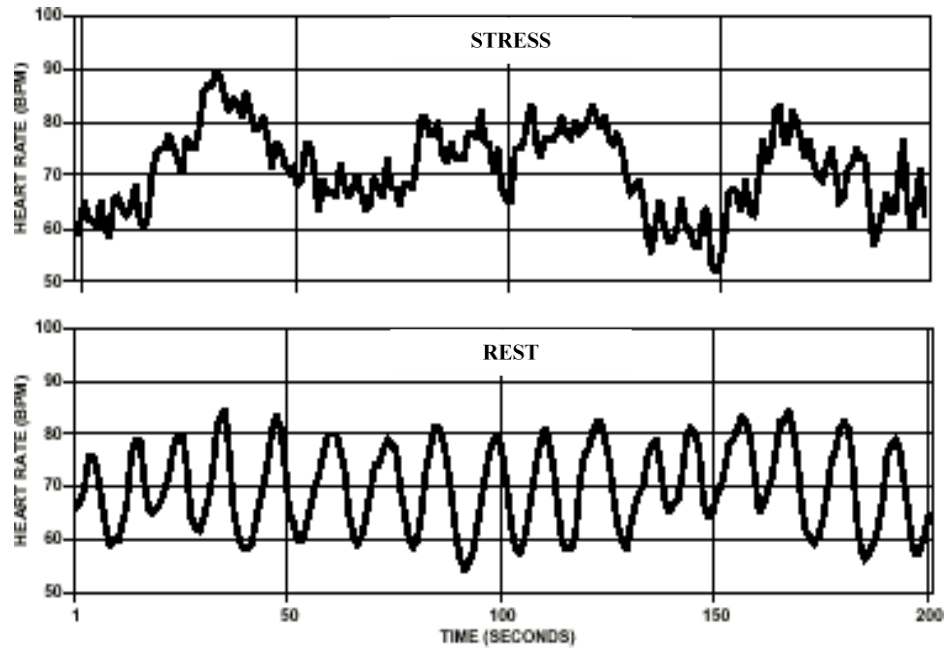
system can be associated with air pollution concentrations. This study will extensively look at HR, SDNN and r-MSSD parameters, both on an 8-hour time frame and on a 30-minute high-resolution time scale.

### **Frequency-Domain HRV Parameters**

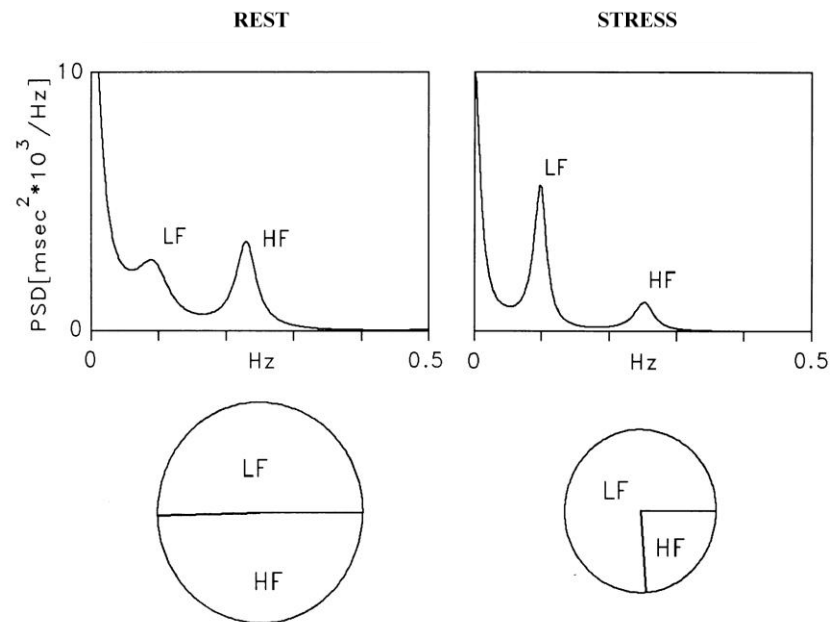
The combined input of the sympathetic and parasympathetic systems produces natural variability over time so that high frequency and low frequency wave oscillations in HR can be used as a measure of HRV. The measurement of these trends, referred to as “frequency-domain” (e.g. spectral analysis), and used as a measure of autonomic modulation of the sympathetic and parasympathetic autonomic nervous systems.<sup>46</sup> Continuous IBI data are converted into a spectral graph using Fast-Fourier transformation, categorized into high frequency (HF) waves (0.4-2.5 Hz) and low frequency (LF) waves (0.04-0.4 Hz) in a power spectral density graph like those shown in Figure I.12b.<sup>46</sup> Previous scientific studies have investigated the ranges for LF and HF, and have detected the influence of the parasympathetic and sympathetic nervous system responses on both parameters, as well as the ratio between them (LF/HF).<sup>45,46</sup> A reduction in LF, for example, represents increased heart activity and up-regulation in the sympathetic nervous system and/or a down-regulation in the parasympathetic.<sup>48</sup> An increase in the LF/HF ratio has been shown to strongly associate with a sympathetic response.<sup>46</sup> A visual description of these parameters is given in Figure I.12, and Table I.3 defines each HRV term and describes what physiological responses each parameter reflects.

Figure I.12 Fast-Fourier transformation of a stressed and rested HR graph into frequency-domain parameters.<sup>68,64</sup>

(a) Sample Average Heart Rates under “Stress” and at “Rest”



(b) Spectral analysis of a heart rat at “Rest” and under “Stress”





**Table I.3 Definitions of HRV parameters and what each parameter modulates in the cardiovascular system.**<sup>46,57</sup>

Time Domain	Definition	Modulation
HR	Average Heart Rate, Determined by the Difference between R-R Peaks	Combined Inputs from Sympathetic and Parasympathetic Neural Inputs, Closely Tied to Respiratory Rate
SDNN	Standard Deviation of all R-R Intervals	Parasympathetic Modulation of Overall HRV
r-MSSD	Root Mean Squares of Successive Differences	Parasympathetic Modulation of Short-Term Changes in HRV
Frequency Domain	Definition	Modulation
LF	Low Frequency Spectrum (0.04-0.4 Hz)	Both Sympathetic and Parasympathetic Inputs, with Sensitivity to Chemoreceptors, Thermoregulation, and the Rennin-Angiotensin System
HF	High Frequency Spectrum (0.4-2.5 Hz)	Occurring in Relation to the Respiratory Frequency, and Associated with Parasympathetic Activity with Pharmacological Blockage, Respiratory Sinus Arrhythmia
LF/HF	Ratio	Sympathovagal Balance of the Influences on the Cardiac Cycle

Frequency-domain findings are more accepted in the scientific community as a stronger measure of autonomic function because it measures the variability as a function of frequency rather than just calculating the arithmetic variability.<sup>64</sup> Frequency-domain parameters need to be calculated on short 5-minute intervals for humans.<sup>64</sup> This would be equivalent to about a 30-second reading for a rat. Due to the restriction on the software that collected the ECG of the rats, however, these parameters could not be calculated with this same resolution. Gehrman *et al.* (2000) used mice to draw a parallel with human heart rate data by multiplying the factors by 10, and SH rats have also been used in exposure studies to draw parallels with human cardiac function.<sup>68,69</sup> Therefore, the values for these parameters using the 8-hour dataset are only an estimate of the possible biological effects, but cannot be considered reliable if averaged over the 8 hours of exposure.

### **Statistical Methods**

To meet the study objectives, the two groups of rats must be distinguished from one another to determine a significant biological effect. The CAPs-exposed rats must exhibit significantly different HRV than the AIR Rats breathing HEPA-filtered air. To conduct this test, the independent variance in each rat's HRV data must be considered. Mixed modeling analysis between the two subject groups can properly compare the two groups to determine if AIR and CAPs are significantly different when considering each HRV parameter, both on the 8-hour and 30-minute time scale. This will be the main test to determine if a biological effect occurred.

Site-to-site and season-to-season differences in the composition PM<sub>2.5</sub> can be significant and may modify the effects upon HRV in CAPs-exposed rats. After a comprehensive characterization of CAPs is performed, PM<sub>2.5</sub> constituents will be modeled to the HRV in CAPs Rats to determine if significant associations exist. Again, mixed modeling will need to be conducted to account for the variance in each rat's HRV. This will be done on both the 8-hour and 30-minute time scales for each constituent. The unique feature of this study is that 30-minute trace elements were collected, and short-term changes in cardiac function can be viewed in relation to high-resolution air pollution concentrations.

#### **I.4 Research Objectives**

Objective 1: Develop a protocol to process and analyze HRV data to determine if and when significant differences in HRV exist between AIR and CAPs-exposed rats. Chapter II will discuss heart rate data collection methodology and the quality assurance procedures used to select viable data. Data analysis techniques, such as using mixed modeling to appropriately compare the exposure and control groups of SH rats, will be discussed in Chapter II and applied in Chapter III and IV for Detroit and Steubenville, respectively.

Objective 2: Characterize PM<sub>2.5</sub> constituents between distant sites and describe seasonal variability at each location based upon atmospheric chemistry and air mass transport. The atmospheric monitoring regimens used to describe ambient air pollution, as well as the method of PM<sub>2.5</sub> characterization for the exposure chamber is discussed in Chapter II. This particular research objective involved data from the entire 8-hour exposure period on each day, and high-resolution 30-minute air pollution data. Each exposure study will have a complete characterization of PM<sub>2.5</sub> given in Chapters III and IV.

Objective 3: Determine if a relationship exists between HRV in CAPs exposed rats and specific constituents found in concentrated PM<sub>2.5</sub>. Mixed modeling was used to compare changes in HRV to air pollution on the 8-hour time scale as well as the high-resolution 30-minute data. Chapters III and IV will discuss these findings for each study.

Objective 4: Determine if specific PM<sub>2.5</sub> source types are better associated with changes in HRV than PM<sub>2.5</sub> mass alone. Given the large number of trace metal samples for each study period using 30-minute trace element samples, it is possible to conduct source apportionment using a multivariate statistical model (Positive Matrix Factorization - PMF). The modeling results will produce a quantified percentage source contribution for every 30-minute period of the exposure study. In Chapter V, source contributions are investigated to see if associations existed between potential sources and changes in HRV of CAPs Rats.

To meet these objectives, a rigorous sampling protocol of both atmospheric monitoring and telemetry need to be performed over each exposure study. The sampling protocol for the air pollution measurements and the HRV collection is summarized in Table I.4. A complete description of the air monitoring instruments and HRV measurements are described in detail in Chapter II.

**Table I.4 Summary of atmospheric measurements and heart rate variability parameters that were measured during the four exposure studies.**

**Atmospheric Sampling**

	Pollutant	Methods	Measurement
Eight-Hour Integrated Sampling	PM <sub>2.5</sub> Mass	Teflon Filter, Gravimetric Mass	µg/m <sup>3</sup>
	Organic/Elemental Carbon	Quartz Filter, Sunset Labs EC/OC Analyzer	µg/m <sup>3</sup>
	Ions (NH <sub>4</sub> <sup>+</sup> , SO <sub>4</sub> <sup>-2</sup> , NO <sub>3</sub> <sup>-</sup> )	URG Annulated Denuders, Dionex Analyzer	µg/m <sup>3</sup>
	Trace Elements	Teflon Filter, ELEMENT2 ICP-MS	ng/m <sup>3</sup>
	Pollutant	Methods	Measurement
Thirty-Minute High-Resolution Sampling	PM <sub>2.5</sub> Mass	R&P TEOM (5-minute readings)	µg/m <sup>3</sup>
	Elemental Carbon	Anderson Aethalometer (5-minute readings)	ng/m <sup>3</sup>
	Trace Elements	SEAS, ELEMNT2 ICP-MS	ng/m <sup>3</sup>

**Heart Rate Sampling**

	Parameter	Description	Measurement
Eight-Hour Integrated Sampling	HR	Eight-Hour Mean Heart Rate for Each Rat	msec
	ln(SDNN)	Log of the Standard Deviation of Heart Rate over 8 Hours	msec
	ln(r-MSSD)	Log of the Root Mean Sum of Successive Differences	msec
	ln(LF)	Log of the Power Spectral Density (0.04-0.4Hz)	
	ln(HF)	Log of the Power Spectral Density (0.4-2.5Hz)	
	LF/HF	Ratio of Spectral Components	
	Parameter	Description	Measurement
Thirty-Minute High-Resolution Sampling	HR	Thirty-Minute Average of Heart Rate	msec
	ln(SDNN)	Log of the Standard Deviation, During Every 30-Minute Period	msec
	ln(r-MSSD)	Log of the Root Mean Sum of Successive Differences, During Each 30-Minute Period	msec

## **I.5 Dissertation Structure**

This thesis presents a complete air pollution analysis for each seasonal intensive as well as modeling the constituents of PM<sub>2.5</sub> for each HRV parameter. Chapter II introduces the methods used and provides examples to illustrate the value of the new protocols. The Semi-continuous Elemental Automated Sampler (SEAS), a 30-minute trace element sampler, is described in detail. HRV data will be discussed as well as the statistical techniques used to process the data and to test for significant effects in the CAPs-exposed rats. Together, the integration of an in-the-field animal exposure study using a fine particle concentrator inside a mobile research laboratory and semi-continuous trace element data allow an investigation of the effects of PM<sub>2.5</sub> on HRV that have not yet been reported.

The findings from the Detroit studies will be discussed in Chapter III. The summer intensive in Detroit provides an excellent example of PM<sub>2.5</sub>-driven health effects where health effects associated with the constituents could not be differentiated from fine-fraction mass. This is in contrast to the findings from the Detroit winter intensive where mass concentrations were much lower, and the effects of individual constituents were better associated with changes in HRV. A strong seasonal comparison of the constituents and the differences in HRV in the CAPs Rats is presented in this chapter.

Chapter IV details the two intensives conducted in Steubenville. During summer we observed the highest PM<sub>2.5</sub> concentrations, but specific constituents had stronger associations with HRV than the PM<sub>2.5</sub> mass concentration. Variability in the dominant wind direction over the exposure hours provides insights to the sources influencing the PM composition at the sampling site.

Chapter V incorporates the HRV findings from Detroit and Steubenville to investigate how the sources at each site are associated with changes in HRV. A summary of the constituent findings from each exposure study are presented, leading into a brief background on source-receptor modeling. The effect of each source factor at each site will be associated with HRV to determine if the contributions from sources more strongly associates with HRV than PM<sub>2.5</sub> mass or constituent concentrations.

In Chapter VI, the findings from all the previous chapters will be summarized and the hypothesis, that constituents of PM<sub>2.5</sub> provide a better effect estimate on HRV than

PM<sub>2.5</sub> mass, will be addressed. Each exposure study presented a unique set of conditions that was different enough to make an interesting point to help provide a model for future studies. The significance and implications of these findings, as well as the limitations and possible improvements of the study, will be discussed.

## CHAPTER II

### METHODOLOGY

#### II.1 Site Selection

##### **PM<sub>2.5</sub> Concentrations in Detroit, MI and Steubenville, OH**

Detroit and Steubenville have been historically been considered non-attainment areas based upon USEPA standards. Table II.1 shows the concentrations observed during the two-week seasonal studies. During both the summer and winter exposure studies, higher ambient concentrations were observed in Steubenville. However, the CAPs concentration for Detroit summer and winter were not statistically different than what was found for the Steubenville intensives. Differences in the concentration enrichment factor (CEF) may have been caused by meteorological factors, like temperature and humidity, or by the nature of the particles. For example, smaller particles may have acted like gases and may have been drawn out of the concentrator rather than accelerated into the exposure chamber.

**Table II.1 Ambient and CAPs PM<sub>2.5</sub> concentrations are shown for each intensive, based upon 30-minute TEOM averages ( $\mu\text{g}/\text{m}^3$ ).**

	Ambient	CAPs
<b>Detroit Summer</b>	<b>16.9±11.0</b> (2.8-57.7)	<b>795.0±582.8</b> (110.3-2778.2)
<b>Detroit Winter</b>	<b>9.8±5.1</b> (1.4-32.7)	<b>365.6±262.5</b> (22-1341.5)
<b>Steubenville Summer</b>	<b>23.8±12.4</b> (5.0-68.4)	<b>736.9±512.1</b> (81-2951.0)
<b>Steubenville Winter</b>	<b>13.1±10.3</b> (1.9-61.4)	<b>326.1±271.1</b> (49.2-1995.7)



## **Pollution Sources in Detroit, Michigan**

Detroit, Michigan, is a highly industrialized area with numerous PM<sub>2.5</sub> sources affecting the local air shed (Figure II.1). The sampling site was located next to Maybury Elementary School (42°18'57.58", -83°5'39.84"). Centered in *Mexicantown*, a Southwest neighborhood of Detroit, the site is in close proximity (<2km) to the heavy diesel truck and passenger vehicle traffic of the Ambassador Bridge leading into Windsor, Ontario. The largest international crossing connecting the United States to Canada, an estimated 10,000 commercial vehicles cross the bridge each day.<sup>58</sup> In Wayne County alone, highway vehicles contribute 1126 tons of PM<sub>2.5</sub> emissions annually.<sup>7</sup> Several industrial point sources also are in close proximity to the site: an oil refinery, steel blast furnaces, metal-plating plants, a municipal waste incinerator, a sewage sludge incinerator, a cement plant, and several coal-fired utility boilers (Figure II.2). The top PM<sub>2.5</sub> emission sources from the five counties that encompass Detroit are listed in Table II.1. Although the sewage sludge and municipal waste incinerators have relatively low PM<sub>2.5</sub> emissions compared to the other point sources in Detroit, (36 and 3.2 tons, respectively) their composition can be highly toxic; past studies have identified these two incinerators as source factors that significantly influence the composition of PM<sub>2.5</sub> at the Maybury sampling site.<sup>7</sup> Zug Island Industrial Park is located 4 km southwest of Maybury Elementary and operates a steel blast furnace and a coal-fired power plant. River Rouge Steel and Rouge Power are 5 km west of the site, and are two of the largest emitters of PM<sub>2.5</sub> in the vicinity.<sup>7</sup> Although Ontario, Canada, is directly across the Detroit River, none of their point sources exceed 53 tons of PM<sub>2.5</sub> per year, as reported by Environment Canada.<sup>59</sup> Additionally, air flow is rarely from the east, so these sources do not greatly impact Detroit. Due to the mixture of multiple point sources and a heavy diesel and motor vehicle input to the PM<sub>2.5</sub> in Detroit, the Maybury site is centrally located to capture many of the source contributions that influence PM<sub>2.5</sub> concentrations.

**Table II.2 Top point sources from Detroit’s surrounding counties that emitted over 100 tons of PM<sub>2.5</sub> in 2002.<sup>8</sup>**

Source Type	Plant Name	County	Tons PM <sub>2.5</sub> /Yr
Electric Services	Detroit Edison/Monroe Power	Monroe Co	2815
Blast Furnaces And Steel Mills	National Steel Corp	Wayne Co	1983
Blast Furnaces And Steel Mills	Rouge Steel Co	Wayne Co	1336
Electric Services	Detroit Edison Trenton Channel	Wayne Co	1128
Electric Services	J R Whiting Co	Monroe Co	1029
Cement, Hydraulic	Holcim Inc	Monroe Co	657
Electric Services	Detroit Edison River Rouge	Wayne Co	378
Petroleum Refining	Marathon Petroleum Company	Wayne Co	145
Flat Glass	Guardian Industries	Monroe Co	125

**Figure II.1 AirData map of Wayne and Monroe Counties showing point source emissions (annual tons of PM<sub>2.5</sub>) that contribute to the local air shed in Detroit.<sup>8</sup>**

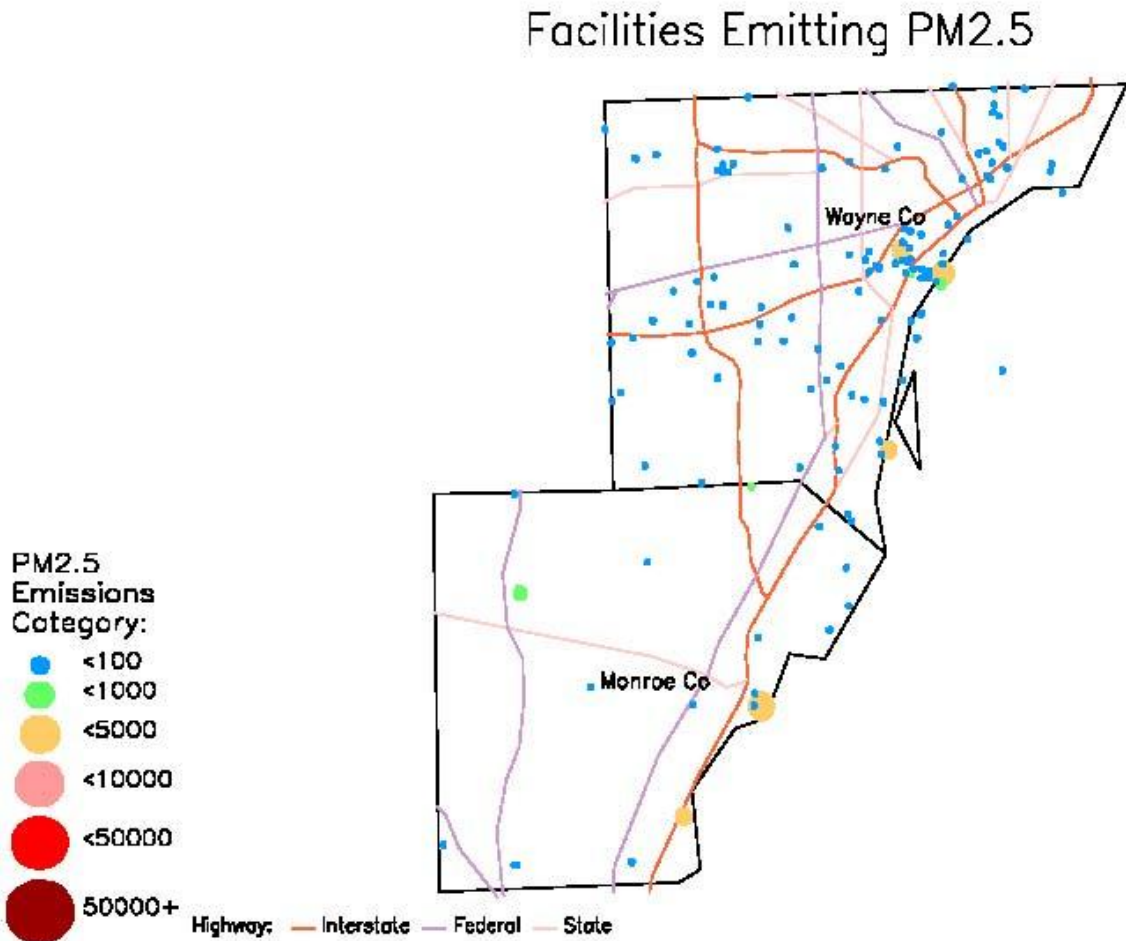
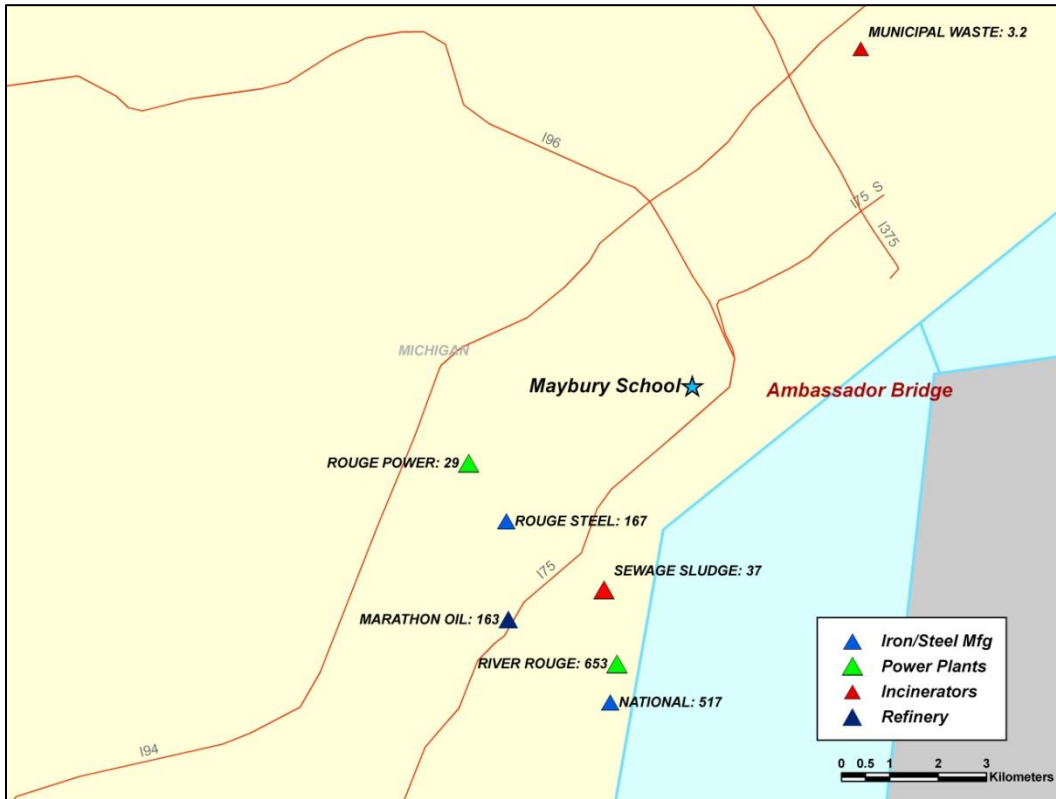


**Figure II.2 Map of Detroit denoting the major PM<sub>2.5</sub> within 10km of the sampling site in Detroit and their annual emissions in tons per year (2002).<sup>8</sup>**



### **Pollution Sources in Steubenville, Ohio**

Steubenville, Ohio, is located between two major coal-burning power plants and in close proximity to multiple steel and metal plants, provided this study with an industrialized area and is impacted very little by mobile source contributions (40°22'45.46"N, -80°37'11.65"W). The site was on the top of the 100m high valley wall that is along the Ohio River. Fifteen kilometers north of the site is Sammis Power, a 2456MW power plant that emits 6485 tons of PM<sub>2.5</sub> each year.<sup>8,60</sup> Thirteen kilometers south of the site is the Cardinal Power Plant, a 1200MW coal-fired power plant with multiple boilers producing 3581 tons of PM<sub>2.5</sub> annually.<sup>8,60</sup> These two power plants rank 12<sup>th</sup> and 33<sup>rd</sup> of all PM<sub>2.5</sub> emission sources in the United States.<sup>8</sup> Across the Ohio River in Weirton, WV, is Weirton Steel Corporation, emitting the most of any steel blast furnace in the country, with 3610 tons of PM<sub>2.5</sub> a year.<sup>8</sup> The entire Ohio River Valley has

several power plants and steel blast furnaces that make the region a primary emission source of  $\text{SO}_2$ , the cause of acid rain in New England through the formation of secondary  $\text{SO}_4^{-2}$ .

**Figure II.3 A map of Steubenville, Ohio with the largest  $\text{PM}_{2.5}$  emission sources within 15km of the site, and tons of  $\text{PM}_{2.5}$  emitted per year from the largest sources.<sup>8</sup>**

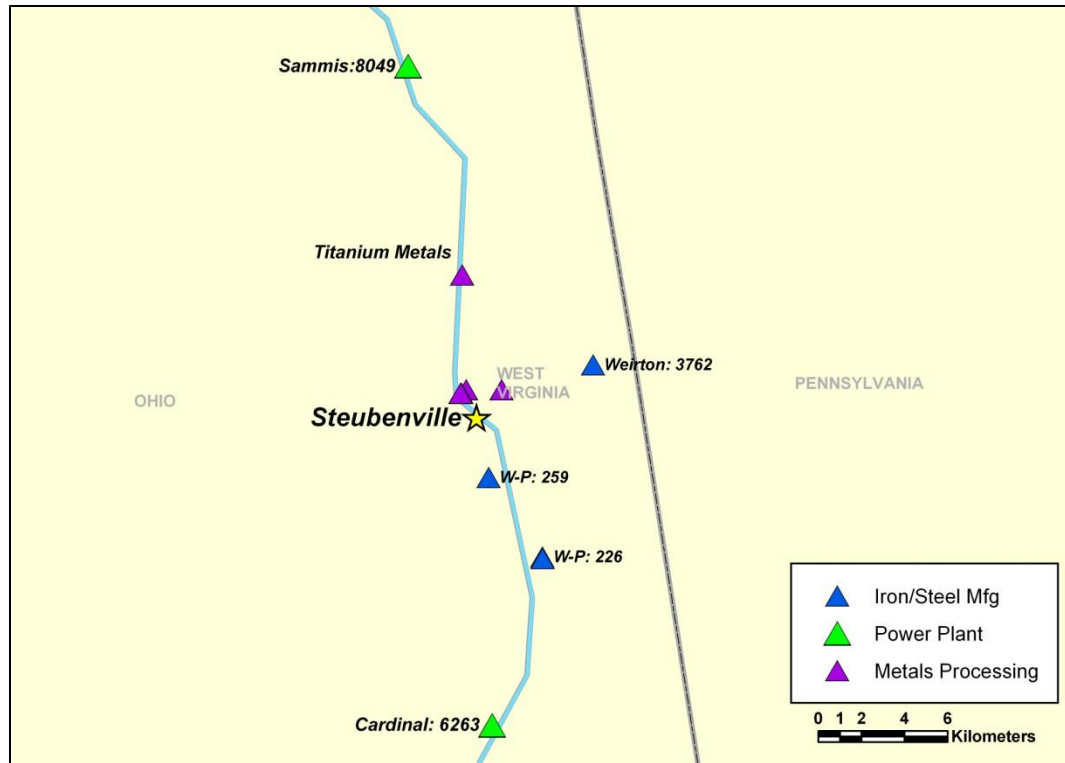


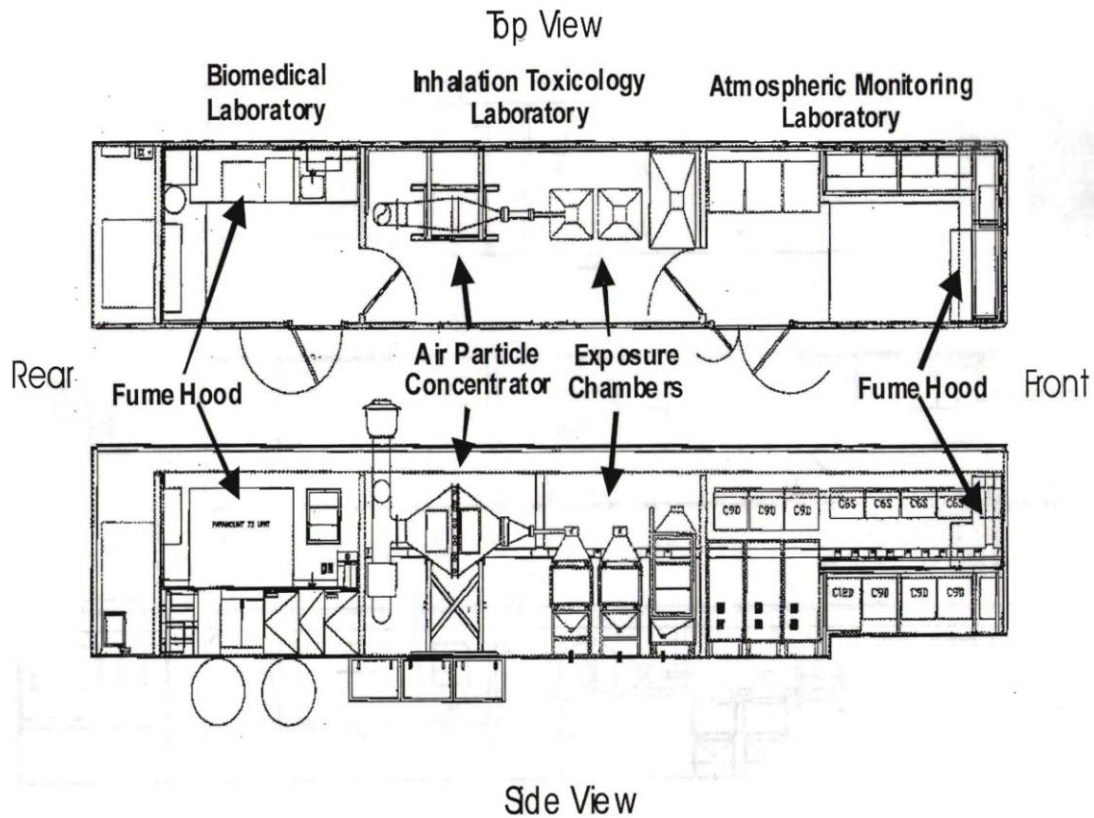
**Table II.3 A list of the major PM<sub>2.5</sub> point sources in and around Steubenville, Ohio.<sup>8</sup>**

<b>Source Type</b>	<b>Plant Name</b>	<b>County</b>	<b>State</b>	<b>Tons/Year</b>
Electric Services	Sammis Power	Jefferson Co	OH	6485
Blast Furnaces And Steel Mills	Weirton Steel	Hancock Co	WV	3610
Electric Services	Cardinal Power	Jefferson Co	OH	3581
Electric Services	Burger Power	Belmont Co	OH	2237
Blast Furnaces And Steel Mills	W-P Steel	Jefferson Co	OH	252
Blast Furnaces And Steel Mills	W-P Steel	Brooke Co	WV	224
Nonferrous Rolling	Titanium Metals	Jefferson Co	OH	33
Vitreous China	Homer Laughlin China	Hancock Co	WV	28
Metal Coating	Roll Coater	Brooke Co	WV	20

## **II.2 AirCARE1 Facility**

Each seasonal intensive was conducted with the AirCARE1, a mobile research facility shared between the University of Michigan Air Quality Laboratory and the Department of Animal Pathology at Michigan State University. The mobile laboratory is a custom-built 53' trailer able to be transported to a designated location. Inside, the facility has three temperature-controlled rooms: a biomedical lab, an inhalation toxicology lab and an atmospheric monitoring lab (Figure II.4). The biomedical lab has facilities necessary to conduct animal exposures and accommodates the rats when exposures are not in progress. Air monitoring instruments are housed inside the atmospheric monitoring lab with sampling ports on the roof of the trailer for ambient air pollution measurements. The exposure chambers and the particle concentrator are housed inside the inhalation toxicology lab with a port to sample off of the exposure chamber.

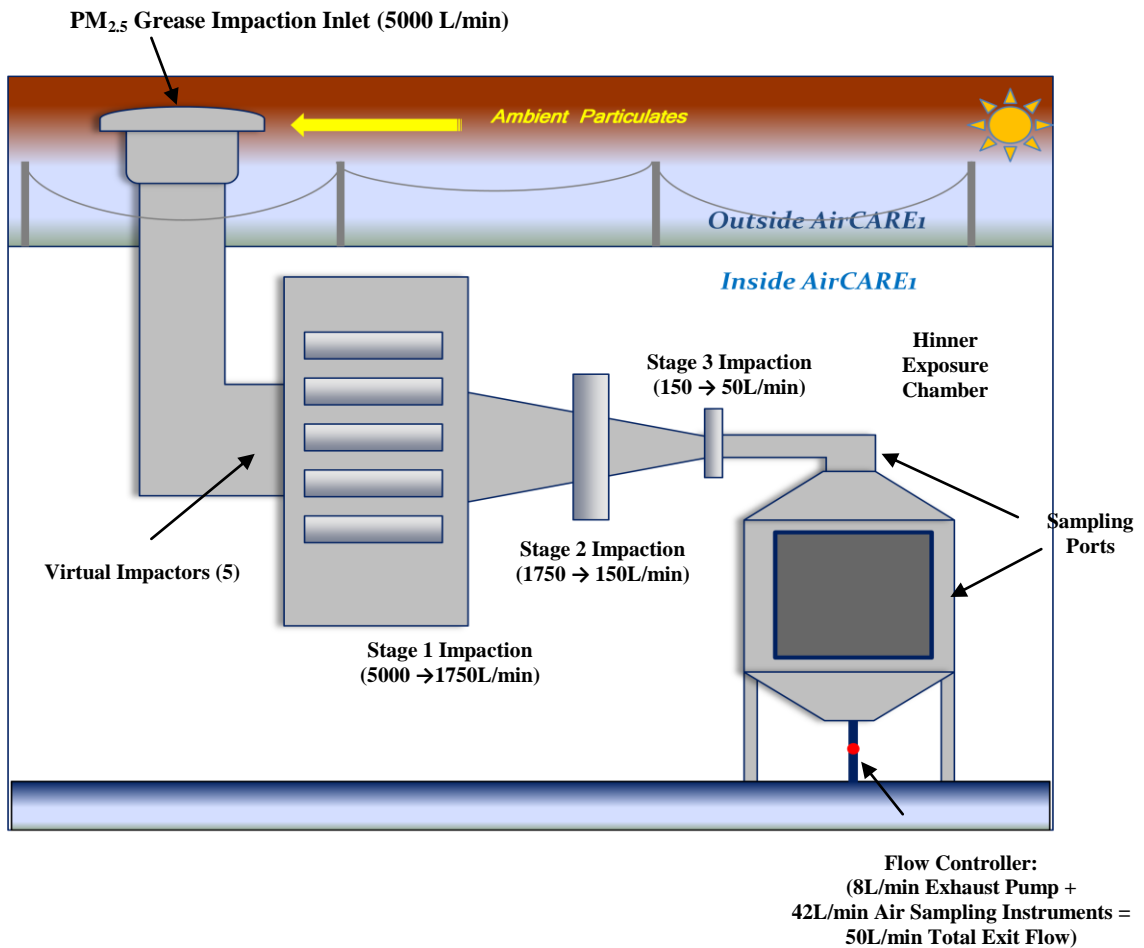
**Figure II.4 Schematic layout of AirCARE1, the mobile air research laboratory.**



### **Harvard Concentrator**

The inhalation toxicology lab is outfitted with an EPA/Harvard  $PM_{2.5}$  Concentrator and two air full-body animal exposure chambers. The Harvard  $PM_{2.5}$  Concentrator inside AirCARE1 was used to amplify the ambient concentration of  $PM_{2.5}$ . By drawing in 5000L/min of ambient air through a  $PM_{2.5}$  size-selective inlet and then through a series of virtual impactors, fine particulates are concentrated 20 to 30 fold, depending on particle size distribution and meteorological conditions.<sup>61</sup> The CAPs are drawn into the Hinner full-body exposure chamber (HC-I 00, Lab Products, Maywood, NJ) at 50L/min for inhalation by the CAPs Rats.

**Figure II.5 A diagram showing the Harvard PM<sub>2.5</sub> Concentrator and the Hinner exposure chamber inside AirCARE1.**



### Hinner Exposure Chambers

The Hinner chambers, shown in Figure II.5, are a sealed, of cast iron construction and are engineered such that CAPs entering from the top of the chamber will mix evenly throughout. Inside the chamber, a grid-like, custom-built cage separates all 16 rats from one another. Multiple air-tight sampling ports pull off of the CAPs chamber to conduct a thorough exposure assessment. Alongside the exposure chamber is an identical Hinner chamber pulling in HEPA-filtered air with matching flow rate which houses the control group, or AIR Rats. Air pressure and pressure were balanced in both exposure chambers by external pumps (Gast Manufacturing, Benton Harbor, MI). For the AIR chamber

50L/min of air was drawn out from the external pump, but in the CAPs chamber, the pump drew out only 8-10L/min to balance the total flow (50L/min) accounting for the flow drawn out from the sampling ports (40-42L/min).

### **II.3 Air Monitoring**

#### **Integrated 8-Hour Sampling**

Situated on the back of the exposure chamber, filter packs were tightly attached to threaded ports, sealing off the chamber from room air. During exposures, 3lpm of CAPs air was drawn through the filters via vacuum pump. Designed at UMAQL, a box housing 11 small vacuum pumps, Hoke valves and sample lines were used to control the flow needed to sample onto the filters. Flow was monitored prior to and after sampling using a Rotameter (Matheson, Montgomeryville, PA), which were calibrated using a Gillian flow calibrator before each study period. The sampling tubing was a combination of semi-rigid poly propylene or flexible rubber-like silicon. To calculate mass concentrations, a dry test meter (DTM, Schlumberger, Owenton, KY), inline to each filter pack, was used to calculate the exact volume of air during the sampling period. Acid denuders (URG, Chapel Hill, NC) were attached in-line with filters to collect-ion chromatography analysis (Dionex 600) to determine concentrations of  $\text{SO}_4^{-2}$ ,  $\text{NO}_3^{-1}$  and  $\text{NH}_4^+$ . A 10-stage multi-orifice impactor (MOI) sampler loaded with Teflon filters was used to collect size-segregated PM directly from the Harvard concentrator to determine mass and trace metal concentrations of particles of different aerodynamic diameter. These findings will be analyzed in future publications for associations between HRV and size-segregated PM mass. Quartz filters (Gelman Sciences) were used for sampling during the exposure period and analyzed for elemental and organic carbon analysis (Sunset Laboratories, Forest Grove, OR).

#### **Laboratory Filter Techniques**

To properly characterize pollution in the exposure chamber, filters were used to obtain sample during each 8-hour exposure. The Teflon membrane filters used in this study have an outer olefin ring (Gelman Sciences, Port Washington, NY) and have a



47mm sampling diameter with a 2 micron pore size. These filters were pre-and post-weighed in the University of Michigan Air Quality Laboratory (UMAQL) Class 100 Clean Room, maintaining fewer than 100 particles in one cubic meter of air through the use of several High-Efficiency Particulate Arrestors (HEPA) filters in a negatively-pressurized laboratory space. Room temperature (20-23°C) and humidity (30-40%) are controlled and maintained to minimize changes in conditions that would modify filter blanks by more than 15µg. Using a Mettler-Toledo (Toledo, OH) microbalance, UMAQL follows USEPA protocols for handling and weighing for gravimetric mass calculations (Code of Federal Regulations, 1997).<sup>10</sup> UMAQL implements a 20% replication check on every fifth filter weighed to correct for scale drift. A 10% check using calibrated weights (Troemner, Thorofare, NJ) as well as a “Lot Blank” check was implemented for every new batch of filters received from Gelman. Subsequent to sampling and mass determination, Teflon filters were acid digested and analyzed for trace metals. Quartz fiber filters (Gelman Sciences) were also used to collect sample in order to determine organic and elemental carbon concentrations. These filters were baked in a muffle furnace for 2 hours at 500° C to eradicate any potential carbonaceous species on the filter prior to sampling.

### **Preparation of Filter Supplies**

The University of Michigan Air Quality Laboratory has developed proven methods of ultra-clean techniques to prepare samples for nano-scale level atmospheric particulate sampling.<sup>62</sup> Cleaning supplies for air sampling was all conducted within UMAQL by employees trained on in-house laboratory standard operating procedures. For filter sample collection, Teflon filter packs (University Research Glass, Chapel Hill, NC) were used. These were disassembled, scrubbed with Alconox laboratory soap, and soaked for 3 days in 3.5% HNO<sub>3</sub>. After soaking, ultra-pure water (Milli-Q, Millipore, Billerica, MA) was used to rinse off acid residue and any trace metals extracted from the surfaces of the filter packs into the HNO<sub>3</sub>. The Petri dishes (Millipore) used to store filters were HNO<sub>3</sub> soaked for seven days in 3.5% HNO<sub>3</sub> and washed with Milli-Q water five times. For Teflon filters used for ions analysis, Petri dishes were rinsed with Milli-Q only to avoid potential contamination by NO<sub>3</sub><sup>-</sup> ion. Filters were kept in Petri dishes until

sampling began and were returned to their original Petri dish immediately following the 8-hour exposure. Petri dishes were sealed with Teflon tape and stored in triplicate plastic bags. Handling of filters in the field was performed in a HEPA work hood inside the atmospheric monitoring laboratory in AirCARE1, with particle-free gloves and acid-soaked and Milli-Q rinsed tweezers to pick up and transfer filters.

### **Continuous PM<sub>2.5</sub> Sampling**

Ambient and CAPs PM<sub>2.5</sub> mass concentrations were monitored by Rupprecht and Patashnick TEOMs (Tempered Element Oscillating Mass-Balance) (Thermo Scientific), which were logged at 5-minute intervals to track the concentration enrichment factor (CEF) of the Harvard Concentrator. The ambient TEOM inlet was on the roof of the mobile laboratory (approximately 20 feet from the ground) and had an in-line Nephalon drier to remove moisture from the sample. The CAPs TEOM does not have a drier and is more susceptible to relative humidity affecting the sensor that calculates mass. Furthermore, the TEOM was susceptible to the pressure changes when the concentrator was turned on and off. Therefore, a protocol to eliminate outlying data needed to be applied.

Initially, all CAPs data outside a range of 20-2995 $\mu\text{g}/\text{m}^3$  were eliminated from the dataset to select reasonable CAPs concentrations. After calculating the 30-minute averages for both the ambient and CAPs TEOM data, the CEF at each 30-minute period was calculated. A CEF range from 10 to 40 would eliminate data based on the performance of the concentrator. However, due to the effects on the CAPs TEOM caused by summertime humidity, especially in the Detroit summer study, this narrow cut-off would eliminate over 60% of the CAPs PM<sub>2.5</sub> mass. Therefore, a CEF range from 10 to 90 was methodically selected to maximize the number of samples while also maintaining a strong correlation between ambient and CAPs mass. As a result, the daily average PM<sub>2.5</sub> TEOM concentrations for the summer exposure studies were elevated over the filter concentrations. These data were still acceptable to use in statistical analysis because mass data was normalized. In associations of PM<sub>2.5</sub> mass with HRV, the variability of the data was more important than the scale.

### **Continuous Elemental Carbon**

The Anderson aethelometer provided continuous elemental carbon concentrations readings for the exposure chamber (Magee Scientific, Berkeley, CA). The aethelometer uses 7 light wavelengths to calculate the absorption of particles on a quartz filter, with the absorption from each wavelength a concentration estimate. For average EC concentrations, the average mass determined by all 7 wavelengths was taken. The concentration of EC was calculated by dividing the average mass collected on the quartz filter by the average flow. For every 5 minutes, an average concentration was recorded then a 30-minute average was calculated in SAS.

### **Continuous Gas Analyzers**

Continuous ambient gas analyzers were used to sample SO<sub>2</sub>, NO<sub>x</sub>, CO and O<sub>3</sub> (Thermo Scientific, Waltham, MA) with the inlets place on the roof. These instruments followed EPA QA/QC for calibration and data collection. SO<sub>2</sub> was measured using a pulsed fluorescence technique (Teco 43S) with a limit of detection (LOD) of 0.6ppm. The NO<sub>x</sub> instrument (Teco 42S) uses a chemoluminescence detector and calculates concentrations of NO, NO<sub>2</sub> and NO<sub>x</sub> with a LOD of 0.4ppb. The CO instrument (Teco 48S) implements an infrared detector with a LOD of 0.04ppm. O<sub>3</sub> (Teco 49) measurements are taken using UV photometric analyzer with a LOD of 1 ppb. These data were recorded on a Campbell Scientific (Logan, UT) data logger in 30-minute intervals.

### **Thirty-Minute Trace Element Sampling: Introduction of the SEAS**

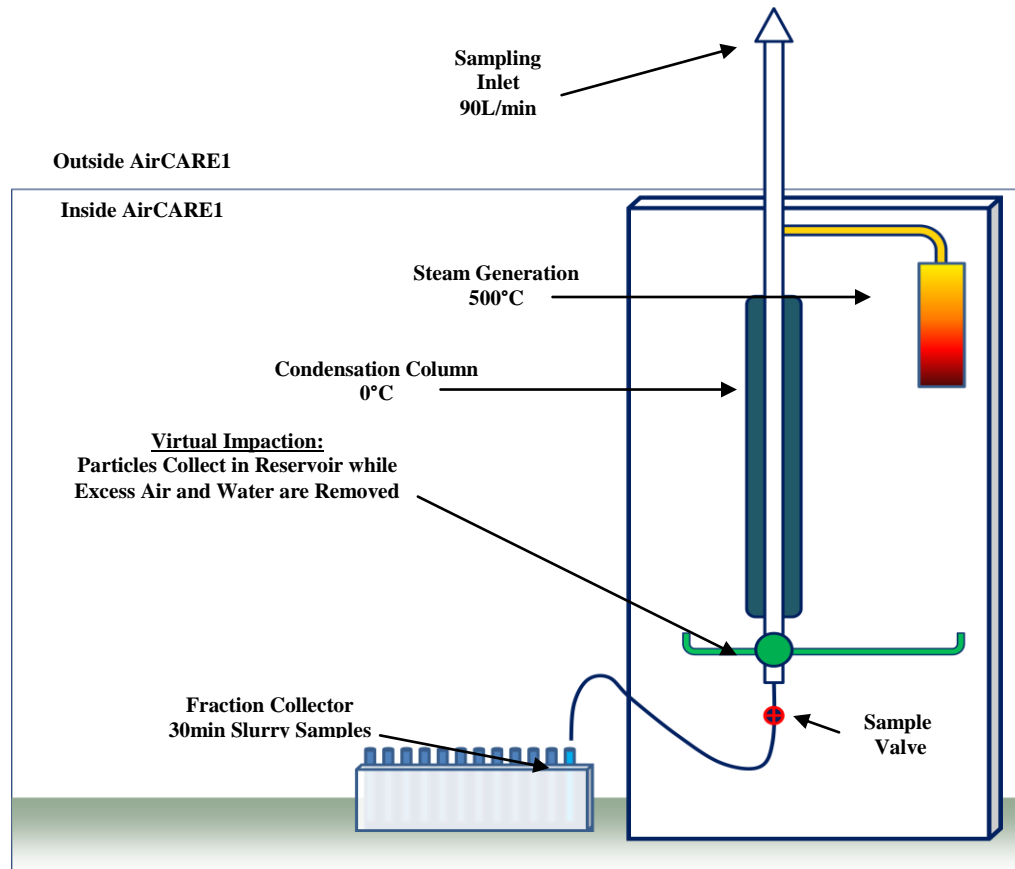
Past exposure studies were limited to identifying integrated trace element concentrations for the full exposure period (e.g. 8, 12 or 24 hours). A 30-minute trace element sample collected onto a filter sample was logistically not possible because not enough mass would be collected to exceed the detection limit of the analytical methods with flow rates as directed. However, a novel instrument was developed to concentrate ambient particles for generation of enough mass for trace metal analysis.

The Semi-continuous Element Automated Sampler (SEAS, Ondov Enterprises) was developed to obtain 30-minute trace metal samples. The SEAS pulls in ambient at

90L/min and introduces steam (from distilled water) at 500°C to form liquid aerosols. Air is then drawn through a glass cooling column at 0°C to condense the steam onto particles. Excess water that does not condense onto the particles is drawn out of the sample line at the virtual impactor, while the droplets with particulate nuclei are heavier and pass through the virtual impactor, and collect into a glass reservoir. Every 30 minutes, the sample valve is opened and the fraction collector automatically ejects a “slurry sample” into a test tube. Twice a day, the slurry samples were capped and removed from the fraction collector. They were then bagged and refrigerated. The samples were later acidified and analyzed for trace metals on the ICP-MS ELEMENT2.

The drawing in Figure II.8 provides a basic description of the components of SEAS. What is not shown are the sophisticated sensors and programming that maintain a gradient between the ambient temperature and humidity and the sample line. The steam generation rate must adjust automatically to provide the correct temperature and humidity so that sufficient condensation is supplied to incoming ambient particles to yield an adequate slurry sample concentrations and volume.

**Figure II.6 The major components of the SEAS, the 30-minute trace element sampler.**



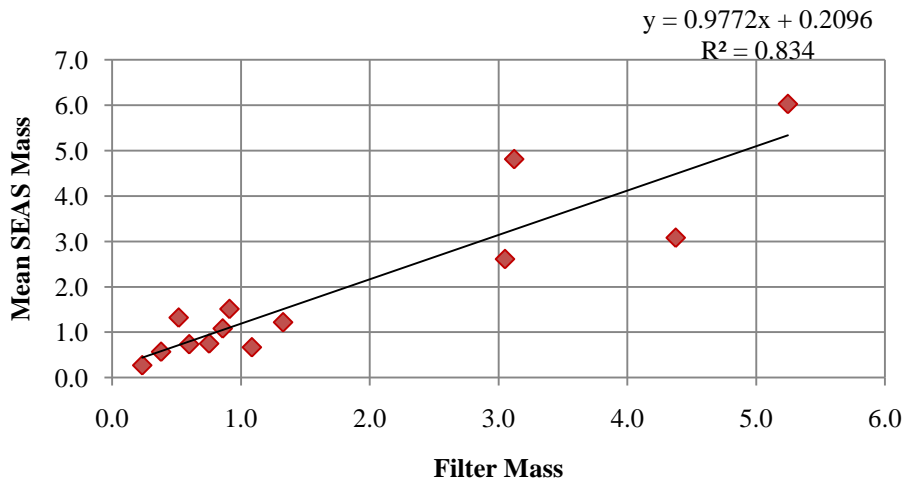
The development of the slurry sampler allowed for the collection of high-resolution trace metal data that (1) provided valuable information on source impact variability over the course of the day, and (2) provided high-resolution trace element concentrations that have the potential to be associated with 30-minute changes in HRV. The 30-minute dataset proved to be more valuable because the trace metal concentrations varied over the course of the day due to source emission, wind direction and atmospheric condition changes. As with HRV data, if these trace metal values were integrated over the 8-hour exposure, associations may be diluted and any inherent variability would be lost.

All elements from this high-resolution data were averaged and aligned with the integrated filter samples to test the accuracy the SEAS collected samples over the 8-hour ambient concentrations during the exposure. These results indicated that some 8-hour

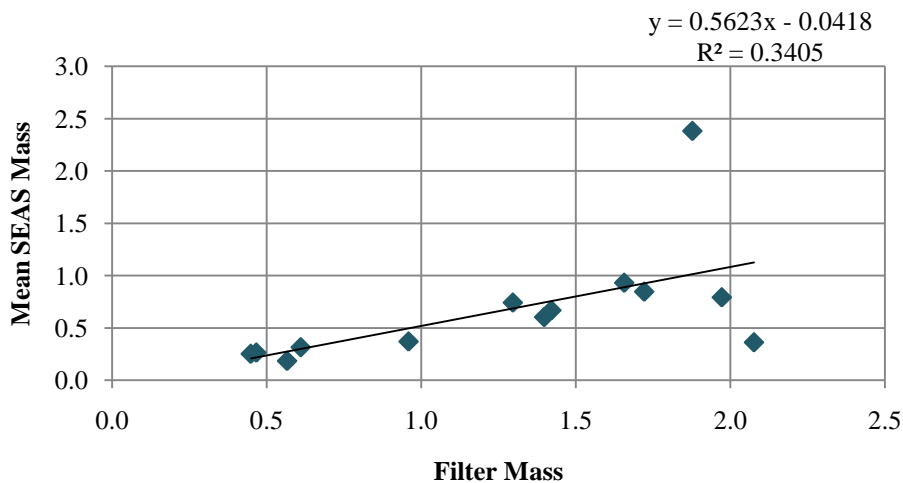
SEAS averages for individual trace element concentrations were better associated with the 8-hour integrated filter concentrations. These results indicated that some 8-hour SEAS averages for trace element concentrations were better associated to the 8-hour integrated filter concentrations than others. For example, Sulfur (S), an important pollutant often used as a tracer of sulfate concentrations (secondary pollutant), proved to be very well correlated between the two sampling methods (Figure II.7a).

**Figure II.7 Regression analysis depicting a strong association between averaged 30-minute SEAS concentrations and 8-hour integrated filter data for S and As during the Detroit summer intensive ( $p < 0.0001$ ).**

(a) S



(b) As



The greatest advantage of the SEAS was the ability to use high-resolution concentrations of trace elements to identify short-term peaks in concentrations that would normally be drowned out over an eight-hour integrated sample. Some elements, such as Arsenic (As), peaked in concentrations and these peaks could not be identified with the 8-hour integrated sample alone. The difference in collection methods and subsequently collection efficiencies of particular sizes of particle may call cause discrepancies. These explanations may describe the poor correlation of the SEAS and filter concentrations of As in Figure II.7b. Another advantage of the SEAS data is that a “pollution rose” for each trace element can be compiled to identify if a trace element is attributed to a specific wind direction. Pollution roses for PM<sub>2.5</sub> mass and several trace elements are shown in Chapter III and IV. However, the most important use of the 30-minute data is to provide a robust data set to link constituent concentrations with the high-resolution changes in HRV. Factor analysis for these intensives could not be conducted without the use of SEAS. PMF requires a large dataset to examine the variability and co-linearity of constituents in a dataset to detect potential source factors.

### **Trace Metal Analysis**

Utilization of the ICP-MS ELEMENT2 (Thermo Finnigan, San Jose, CA) allows for the determination of trace metal concentrations for filter and SEAS samples collected using a unique method established by the UMAQL. The ICP-MS was used to analyze a suite of trace metals: Rb, Sr, Mo, Cd, Sb, La, Ce, Sm, Pb, Mg, Al, P, S, Ti, V, Cr, Mn, Fe, Co, Ni, Cu, Zn, As, Se, Cs, Ba, U, Ca, and K. The sample is drawn through an auto-sampler and individually introduced to the argon plasma through an ultrasonic nebulizer.<sup>17</sup> The argon plasma (2000°C) atomized and ionized samples so that a magnetic field can separate each ion by its mass and energy content. Each ion is analyzed for mass content by an electrostatic analyzer.<sup>17</sup> Based upon the NIST standard curves before each run on the ICP-MS, the mass content can be quality assured if the replicates are within 15%.<sup>17</sup> The method detection limit of the instrument (MDL) is the lowest possible concentration that can be determined by the analyzer, calculated as the standard deviation of a 7 replicate analysis.<sup>17</sup> If the concentrations were measured below this limit, they were calculated as ½ the MDL.<sup>17</sup>

Teflon filters are first acid digested (200  $\mu$ L Ethanol + 10 ml of 10% v/v HNO<sub>3</sub>) in conical centrifuge tubes and are placed in a sonication bath for two days, then sit for two weeks to allow for full extraction of the metals into solution. Approximately 5 ml of solution is poured into scillation vials for the automated sampler of the ICP-MS to draw in sample. For the SEAS samples, 10% HNO<sub>3</sub> is added 24 hours prior to analysis. Four optimally mixed solutions of trace metal NIST standards were used to create a standard curve for every analysis run, and standard checks were kept within a 20% of the expected value for the duration of the run. A series of blanks were also run to check for drift. These quality assurance checks steps follow EPA protocol for trace metal analysis (Compendium Method IO-3.5, 1999).

### **Source Apportionment**

A multivariate, receptor-based model was used to assess the source factors that contributed to PM<sub>2.5</sub> mass in Detroit and Steubenville. In the past, source apportionment methods such as Principle Component Analysis (PCA), Positive Matrix Factorization (PMF) and UNMIX have been employed extensively on PM data sets to determine source profiles influencing a receptor site.<sup>7,63,64,65</sup> The chemical composition profiles are compared to elemental ratios and known tracers of specific sources. Each PM<sub>2.5</sub> mass data point is then transformed from an extensive vector of several trace elements to a reduced combination of source contributions.<sup>62</sup> The model terms and methods are described in detail by Henry (2002).<sup>63</sup> In Morishita *et al.* (2009) PMF was run on SEAS sample data collected for exposure hours of each seasonal intensive and 30-minute source contributions for the sampling sites were determined.<sup>65</sup>

## **II.4 Heart Rate Data Collection**

### **Subjects**

Spontaneously hypertensive (SH) rats (Charles River, Portage, MI) are genetically predisposed to hypertension were selected to increase the likelihood of observing a response in heart function during exposures. In previous studies, SH rats were more susceptible to changes in HRV when compared to other strains of rats, and therefore



believed to be more practical for this CAPs-exposed study.<sup>53,54</sup> As a result, the SH rats were used to identify changes in HRV that may be associated with air particulates. To minimize a multitude of long-term health effects hypertension rats could experience unrelated to the exposures, the rats were only 13 weeks old at the beginning of each exposure study. AIR and CAPs Rats were selected at random with no differences between them prior to exposure. To control for variability that may exist in female rats with their reproductive cycles, the rats were all male. During non-exposure, hours, the rats were kept in individual cages and had free access to distilled water (reverse osmosis system) and food (Tek Lad 1640, Harlan Sprague-Dawley, Indianapolis, IN). To control for biorhythms in the rats, indoor lights were set on a 12-hour cycle (light hours: 6am/6pm, local time). Temperature and humidity were maintained between 21–24°C and 40–55%, respectively.

### **Exposure Regimen**

Eight AIR Rats and eight CAPs Rats were outfitted with surgically implanted heart rate monitors. These monitors remotely transmit each rat's ECG to a receiver that collects the data onto a computer (DataQuest, Data Services International, St. Paul, MN). The battery-operated monitors are implanted at Charles River laboratory and use a radio transmitter. The receivers are housed in the Hinner exposure chambers. The chambers have an inner cage to keep the rats separated from each other. Each receiver picks up a signal from the nearest transmitter. Each rat and its receiver is situated as close as possible, while the 8 rats in the chamber with transmitters are separated as far as possible from each other to avoid mistaken signaling and crossed signals.

### **HRV Collection**

The SH rats have an average IBI of approximately 200 milliseconds, equivalent to a HR of 300 beats per minute. Due to the enormous amount of heart rate data that could be collected over a two-week period, a 30-second ECG was taken every 5 minutes. This protocol was adapted to allow for the adequate observation of HRV a 30-minute time period. Each study lasted for 13 days, and exposures ran from 7:00 am to 3:00 pm, local time.

## **HRV Parameters**

At the beginning of each sampling day, the DataQuest software was set to automatically start the heart rate sampling for the designated period. Each rat had a continuous file for a given day of sampling. For every sampling period, DataQuest recorded the interbeat interval (IBI) by measuring the timed distance (in milliseconds) between each R-R peak in the ECG reading. From the IBI, average Heart Rate, the standard deviation (SDNN) and the root mean square of successive differences (r-MSSD) of the IBI were calculated for every 30 minutes of exposure as well as averaged over the entire 8 hours of exposure. HR, SDNN and r-MSSD are referred to as the time-domain parameters and were calculated by observing the arithmetic changes in HRV.

Frequency-domain parameters were calculated by spectral analysis (Fast Fourier Transformation) on the 8-hour dataset using online software (WebStart). Spectral analysis was used to calculate Low Frequency (LF), High Frequency (HF) and a LF/HF Ratio.

## **Quality Control/Quality Assurance**

Processing these large data sets required a strategy to filter out erratic IBI readings caused by poor, crossed and missed signals that may have been caused by electronic noise, movement and arrhythmias. To remove any erroneous data, a scientifically and statistically sound method was implemented to maintain unbiased data. Outlying data beyond a reasonable physiological range of IBI (50-400 msec) were initially removed so as to not to distort the normal distribution of IBI when calculating the time-domain parameters. Subsequently, all IBI data points beyond two standard deviations (approximately 4% of the raw data set) were also eliminated.

Since data collection started and stopped throughout the exposure, breaks in the data often incurred a shift, resulting in a large, erroneous r-MSSD calculation when the dataset was merged together. This situation also occurred when an ECG signal was momentarily lost and restarted, greatly disturbing the r-MSSD calculation. Therefore, when consecutive IBI readings exceeded 30msec (r-MSSD >30msec), those r-MSSD points were removed to reduce misleading variability in the dataset. On some days, rat ECG signaling was so sporadic that only small patches of data remained. Analysis

showed that those data points often contained outlying data, and that the intermittent data did not give an adequate assessment of the true HRV. A transmitter may have had a poor signal on a given day or received cross signaling from other rats, thereby compromising the data. Therefore, if the number of samples for the 8-hour summary for each rat was below 1000 data points (and below 200 for each 30-minute time period), the data were removed from that given dataset.

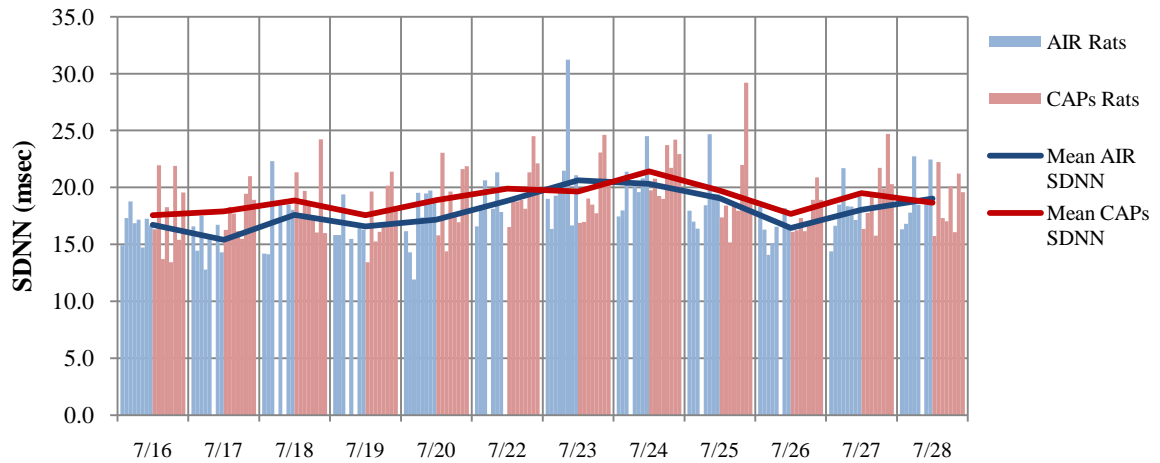
## **II.5 Statistical Analysis**

For each HRV parameter, descriptive summary statistics for AIR and CAPs Rats were calculated. These data were cleaned, processed and generated into a readable format for statistical analysis (SAS). SDNN, r-MSSD, LF and HF, distributions were not normally distributed, based on SAS Univariate analysis results. Mixed modeling analysis assumes that the effects are normally distributed. Therefore, the natural log was taken. Throughout the analysis,  $\ln(\text{SDNN})$ ,  $\ln(\text{r-MSSD})$ ,  $\ln(\text{LF})$  and  $\ln(\text{HF})$  were evaluated.

For HR,  $\ln(\text{SDNN})$  and  $\ln(\text{r-MSSD})$ , the parameters were calculated on both the 8-hour and 30-minute time scales for each rat and for the average of AIR and CAPs rat groups. The frequency-domain parameters could only be run on the 8-hour time scale and therefore will only be used as supporting data as proper spectral analysis was not run on short-term intervals.

It became apparent that averaging all the AIR Rats and all the CAPs Rats together masked the variability that existed within individual rats. Figure II.8 provides 8-hour SDNN data to illustrate the variability that exists within each of the rats in relation to the overall mean. Each column represents the daily mean SDNN for each rat. The average lines demonstrate how dramatically an average AIR and CAPs SDNN would weaken the pronounced variability within each subject. This effect was even more profound when analyzing 30-minute HRV data, as even more variability in HRV has the potential to be lost.

**Figure II.8 Detroit summer AIR and CAPs Rats SDNN for each rat (bars) and the mean SDNN for each group (lines).**



### **Mixed Modeling to Compare AIR and CAPs Rats**

Due to the presence of two components of variability in HRV: within-rats and between rats, and to incorporate the correlation between repeated HRV observations on the same rat, repeated measures ANOVA was used in a mixed model framework (PROC MIXED). The basic structure of a mixed model that tests for marginal differences in AIR and CAPs Rats as well as for changes in time profiles of HRV between AIR versus CAPs Rats is given below in Equation II.1. The same model was used for two datasets with different time-scale: to observe day-to-day HRV differences in the 8-hour dataset and high-resolution changes in HRV using the 30-minute dataset.

**Equation II.1 Description of the mixed model that was used to compare the difference in HRV measures of AIR and CAPS as averaged over time and to describe any changes in HRV profiles across time.<sup>65</sup>**

$$Y_{ij} = (\beta_0 + u_i) + \beta_1(\text{Group}_i) + \beta_2(\text{Time}_{ij}) + \beta_3(\text{Time}_{ij} * \text{Group}_i) + e_{ij}$$

*Y<sub>ij</sub> = Response or HRV measures (e.g. Heart Rate, ln(SDNN), ln(r-MSSD)) measured on the i<sup>th</sup> rat on the j<sup>th</sup> time point.*

*Group<sub>i</sub> = A binary variable indicating the Group that rat i belongs to, (e.g. AIR, CAPs)*

*Time<sub>ij</sub> = Time corresponding to the j<sup>th</sup> observation on the i<sup>th</sup> rat*

*β<sub>0</sub> = Overall intercept*

*u<sub>i</sub> = Random intercept corresponding to the i<sup>th</sup> rat*

*β<sub>1</sub> = overall effect of Group (e.g. CAPs versus AIR)*

*β<sub>2</sub> = overall effect of Time (e.g. Day1 versus Day2, averaged HRV across both groups)*

*β<sub>3</sub> = coefficient corresponding to Group and Time interaction*

*e<sub>ij</sub> = Measurement error corresponding to the j<sup>th</sup> observation on the i<sup>th</sup> rat. u<sub>i</sub> and e<sub>ij</sub> are assumed to be independently distributed random variables with mean zero and variance σ<sub>u</sub><sup>2</sup> and σ<sup>2</sup> respectively. Given this assumption, the resultant covariance matrix has a compound symmetry structure.*

### **Differences between 8-Hour and 30-Minute Datasets**

For the 30-minute data set, the model equation is the same, with one modification to account for every 30-minute time step during the exposure. Each 30-minute time variable can be “nested” within a day, allowing for the 16 time periods in a day to be grouped together to compare day-to-day differences using the high-resolution data. This function allows for each 30-minute period to be independent of all the others. High-resolution data alters the degrees of freedom by an order of magnitude with all additional data points being considered in the model. Consequently, these data indicate if higher resolution HRV data can find significant differences between AIR and CAPs Rats that would not be identified using 8-hour averages. The assumptions for the 8-hour mixed model (compound symmetry, repeated statement) were also made when using the high-resolution 30-minute dataset.

### **Identifying Specific Times AIR and CAPs Rats are Significantly Different**

Thus far, PROC MIXED has been described to compare overall differences between AIR and CAPs Rats, but it can also be used to perform tests to specifically

determine when a significant divergence in HRV occurred. The least-squares means test (LS Means) is a feature of mixed modeling that allows one to look at individual time points to determine if AIR and CAPs Rats are significantly different from each other. This test helped determine a specific day or 30-minute time point when the HRV of CAPs Rats revealed a notable departure from that of AIR Rats HRV even if the two-week trend did not show that the groups were significantly different from each other.

### **Isolating Significant Changes in HRV within CAPs Rats**

Another major feature of the LS Means procedure is the ability to conduct within-group comparisons to help identify when significant changes in HRV in relation to all other time points for CAPs-exposed rats. Although the focus of this study was to observe overall changes in CAPs Rats, the model must first distinguish the CAPs Rats from the control group (e.g. AIR Rats). However, AIR Rats have their own independent HRV occurring naturally. These normal changes in the HRV of AIR Rats can, in fact, mask significant changes in CAPs Rats. Therefore, this study did not rely on differences between AIR and CAPs Rats alone to determine if a health effect occurred. Instead, significant changes within the HRV of CAPs Rats will be investigated, independent of AIR Rats. The LS Means procedure was used to identify specific times (both 8-hour and 30-minute time points) when the HRV of CAPs Rats was significantly higher or lower than the other time points from the dataset.

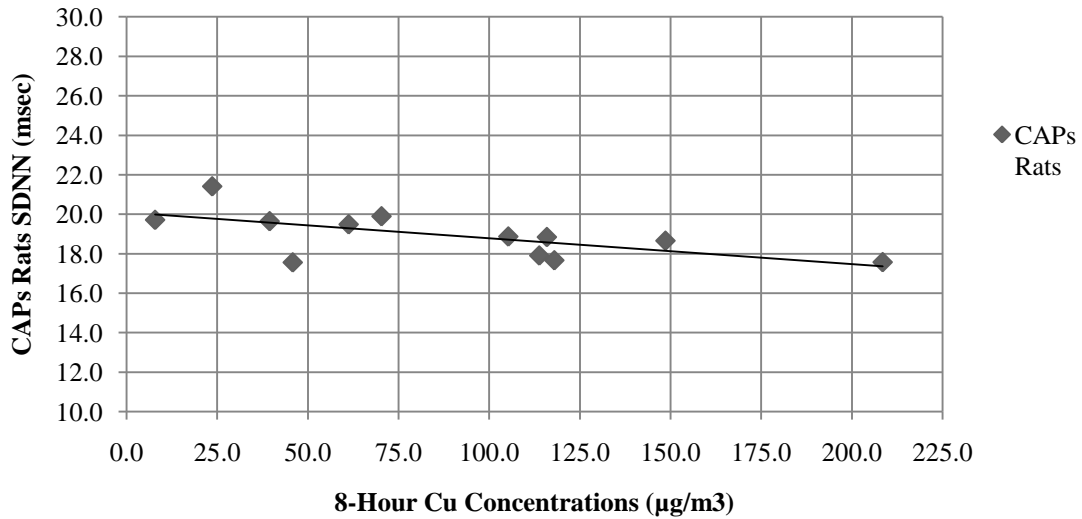
### **Mixed Modeling to Associate Pollution with CAPs Rats HRV**

The fundamental aim of this thesis was to determine if changes in the HRV of CAPs-exposed rats can be significantly associated with  $PM_{2.5}$  and its constituents. For both the 8-hour integrated dataset and 30-minute high-resolution dataset, a simple linear regression could be used to identify if a significant relationship exists, but this would require the average HRV for CAPs Rats to be calculated, losing the within-rat variability. In Figure II.7a, the daily average CAPs SDNN was regressed with 8-hour Cu concentrations. In Figure II.7b, the daily CAPs SDNN for each rat was regressed with Cu concentrations to show the variability in the slopes and intercept in each rat. Therefore, PROC MIXED was used to account for the variability in each rat when

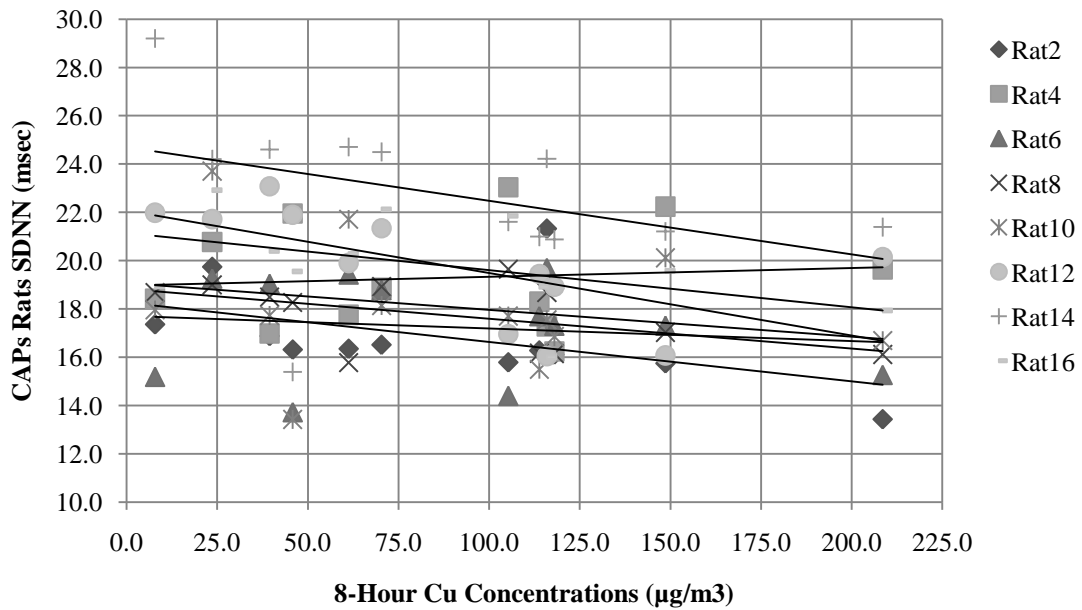
associating each HRV parameter in relation to individual pollutants. Compound symmetry is seen as the best model structure because the treatment (air pollution concentrations) was heterogeneous and can be assumed to be normally distributed.

**Figure II.9 Linear regression of the 8-hour Cu concentrations during the Detroit summer exposure against (a) average SDNN for all CAPs and, and (b) SDNN for each rat.**

(a)



(b)



## Processing Air Pollution Data

Pollutant concentrations were modeled with all the HRV parameters for CAPs Rats to determine the association and the significance of the relationship (e.g. Effect Estimate). Equation II.2 is a mixed model that will model each pollutant with each HRV parameter using both 8-hour and 30-minute data. This equation could be calculated using the raw mass values for each pollutant; however, since the scales for each constituent are on different orders of magnitude, it was more useful to normalize the data, allowing for a comparative analysis of the effect estimates of each pollutant. Therefore, the raw concentration for every component of PM<sub>2.5</sub> was normalized using its inter-quartile range:

$$\text{IQR} = 75^{\text{th}} \text{ \%ile} - 25^{\text{th}} \text{ \%ile}$$

The 75<sup>th</sup> and 25<sup>th</sup> percentiles were calculated in SAS using Univariate statistical analysis on each pollutant. IQR for each component was then internally scaled based on the pollutants inherent variability rather than its raw concentration. Now, the effect estimate of S (mean=3000ng/m<sup>3</sup>) can be reasonably compared against the effect estimate of La(mean=2ng/m<sup>3</sup>), to determine which pollutant was most associated with the observed changes in HRV.

### Equation II.2 Mixed modeling equation used to associate air pollution concentrations with the changes in HRV in CAPs-Exposed Rats.<sup>66</sup>

$$Y_{ij} = (\beta_0 + u_i) + \beta_1(\text{Pollutant}_j) + e_{ij}$$

*Y<sub>ij</sub>* = Response or HRV measures (Heart Rate, ln(SDNN), ln(r-MSSD))  
measured on the *i*th rat on the *j*th time point.

*Pollutant<sub>j</sub>* = A continuous variable indicating the concentration at the *j*th observation

*β<sub>0</sub>* = Overall intercept

*u<sub>i</sub>* = Random intercept corresponding to the *j*th time point

*β<sub>1</sub>* = overall effect of the Pollutant (e.g. Effect estimate)

*e<sub>ij</sub>* = Measurement error corresponding to the *j*th observation on the *i*-th rat. *u<sub>i</sub>* and *e<sub>ij</sub>* are assumed to be independently distributed random variables with mean zero and variance  $\sigma_u^2$  and  $\sigma_e^2$  respectively. Given this assumption, the resultant covariance matrix has a compound symmetry structure.



### **Additional Features of the Model**

Another component of PROC MIXED in these models was the maximum likelihood estimation (method=ML), used to calculate the upper and lower confidence interval for the effect estimate. The entire range of the confidence interval for the effect estimate must fall above (or below) the origin for determination of the statistical significance of the association ( $p < 0.05$ ). Any range that would cross the origin indicates that the effect estimate may be positive or negative, thus a significant directional association cannot be achieved. Furthermore, the narrower the range of the beta estimate, the stronger the statistical strength of the association between the component of  $PM_{2.5}$  and HRV.

### **Calculating Lag Periods**

Studies linking air pollution with HRV indicate that the effects may be delayed for a period of time.<sup>67,68</sup> Also, when examining the associations with HRV and air pollutants, it is possible that there is a cumulative effect on HRV from prolonged exposure. Although human epidemiological studies frequently observe a health response 24- or 48-hours after a pollution episode, the continuous sampling protocol over two-weeks does not allow for this observation in the current study. As a result, the high-resolution dataset was used to investigate the moving average lag (arithmetic mean) for each pollutant, and apply the lagged concentration to the model and determine the effect estimate for a 30, 60, 90 and 120 minute lag.

## **CHAPTER III**

### **A SEASONAL COMPARISON OF THE IMPACTS OF CONCENTRATED PM<sub>2.5</sub> ON HRV IN RATS: DETROIT, MICHIGAN**

#### **III.1 Detroit Summer Exposure**

##### **III.1.1 Synoptic Overview**

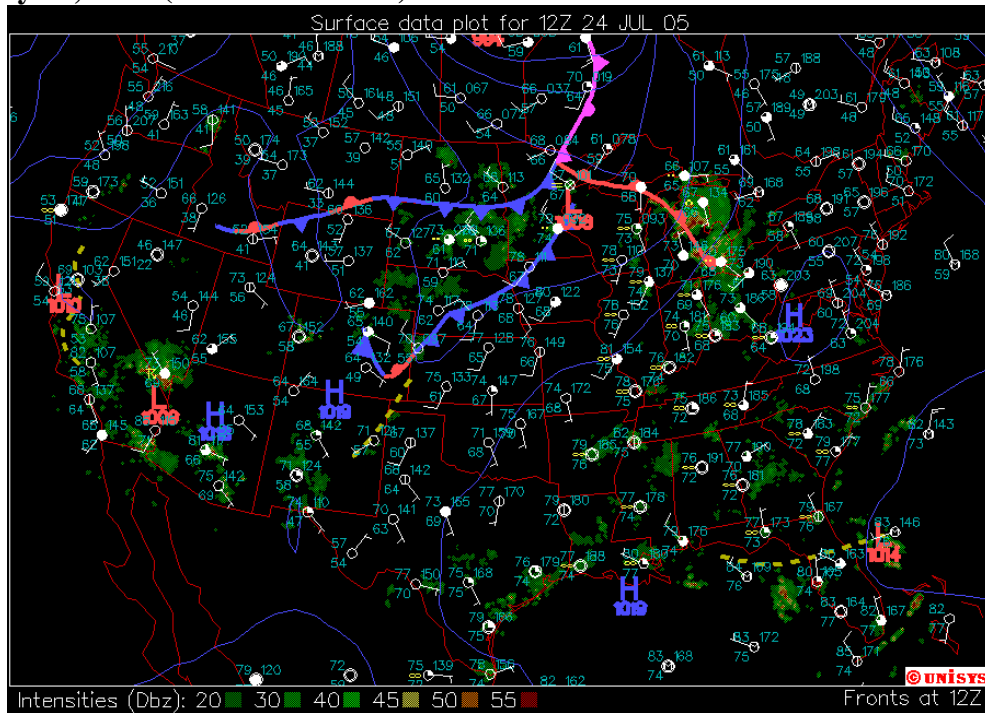
The weather during the summertime sampling period (July 16-28, 2005) was fairly typical for southeast Michigan. High-pressure systems moved through the Great Lakes region followed by areas of low pressure and associated fronts that brought rainfall. In the following sections, the most important meteorological observations will be discussed with respect to the wind directional changes, timing of precipitation with respect to the daytime exposure periods, and the importance of temperature and humidity.

##### **Frontal Systems and Precipitation**

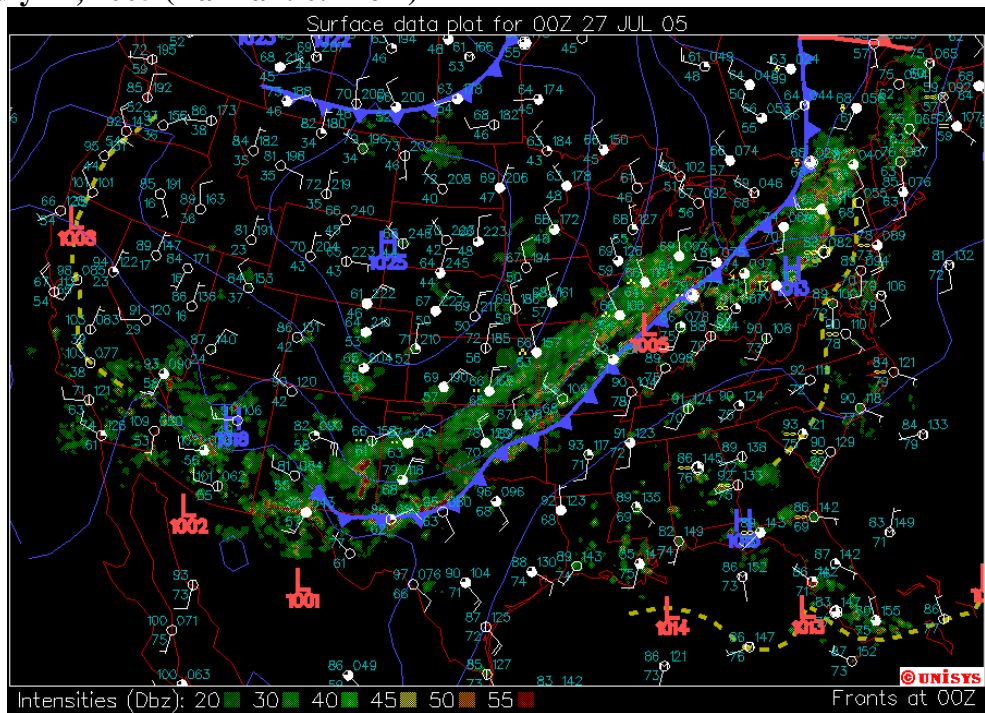
A total of 8.4 cm of rain fell during the two-week period, with half of the rain falling during exposure hours. On July 16 and 18, Detroit experienced isolated convective thunderstorms, 0.79 cm and 1.2 cm of rain was recorded on the two days, with the rain on the 18<sup>th</sup> falling after exposure hours. Two additional frontal passages had rainfall associated with them. The surface weather maps show the location of the warm fronts in Figure II.1. On July 24 and 27, rain fell across most of southeast Michigan, thus effecting regional air pollution contributions, with 1.01 cm and 0.77 cm of rainfall during the exposure hours on both days, respectively. Each of these events is shown in conjunction with the changes in temperature and RH in Figure III.2.

**Figure III.1 Surface weather maps for two days during the Detroit summer intensive that observed the highest rainfall.**

**(a) July 24, 2005 (Rainfall: 1.01cm)**



**(b) July 27, 2005 (Rainfall: 0.77 cm)**



## Temperature

The temperature and RH in Detroit over the two weeks of the study fell within the climatologic norms, averaging  $26.2 \pm 4.6^\circ\text{C}$  and  $60 \pm 18\%$ , respectively. Figure III.2 shows the strong diurnal changes in temperature and RH measured on-site over the two-week study period. Temperatures ranged from 14 to  $36^\circ\text{C}$  and RH ranged from 22-91%. Elevated temperatures, decreased humidity and increased photochemical activity were observed during daylight hours, which for late July in Detroit were approximately 6am to 9pm EDT.<sup>41</sup> Average daylight temperatures and RH were  $28.1 \pm 4.1^\circ\text{C}$  and  $53 \pm 18\%$ , whereas nighttime measurements were significantly different ( $p < 0.05$ ) for both temperature and RH,  $23.1 \pm 3.5^\circ\text{C}$  and  $71 \pm 11\%$ . Exposure hours are indicated in Figure III.2 as vertical gray bars. Within the exposure hours, RH was observed as high as 80-90% when exposures began at 7:00am EDT and decreased to 35-45% by the end of the 8-hour exposure. These changes in RH can have a significant impact on the airborne particle size distribution and concentrator performance.<sup>55</sup> Diurnal temperature increases were observed as well, having a significant impact on photochemical activity.<sup>56</sup> As seen in Figure III.2, precipitation events from frontal passages (i.e. July 26) and convective thunderstorms (July 16) were accompanied by decreased temperatures and increased RH.

**Figure III.2 Hourly temperature (°C) and RH (%) during the Detroit summer study with exposure hours highlighted in grey. Rainfall is denoted by purple horizontal bars.**

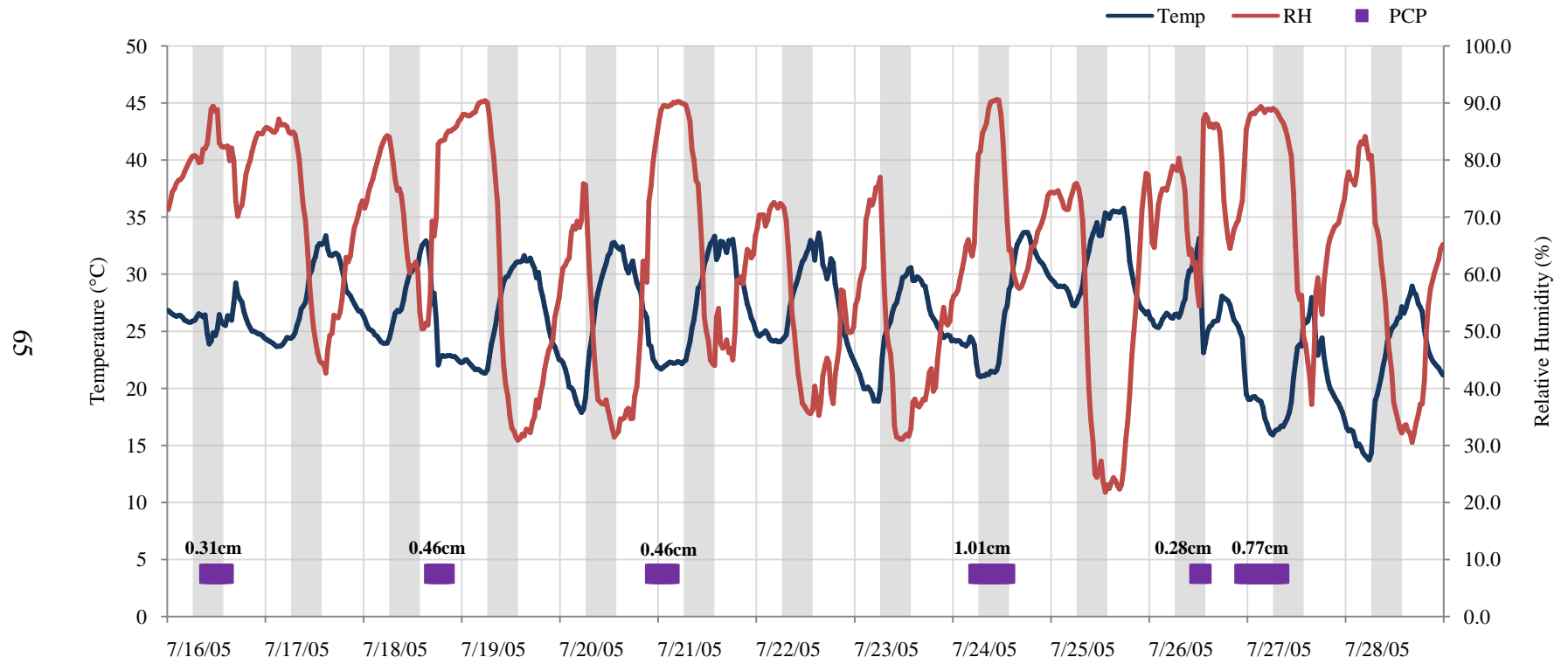
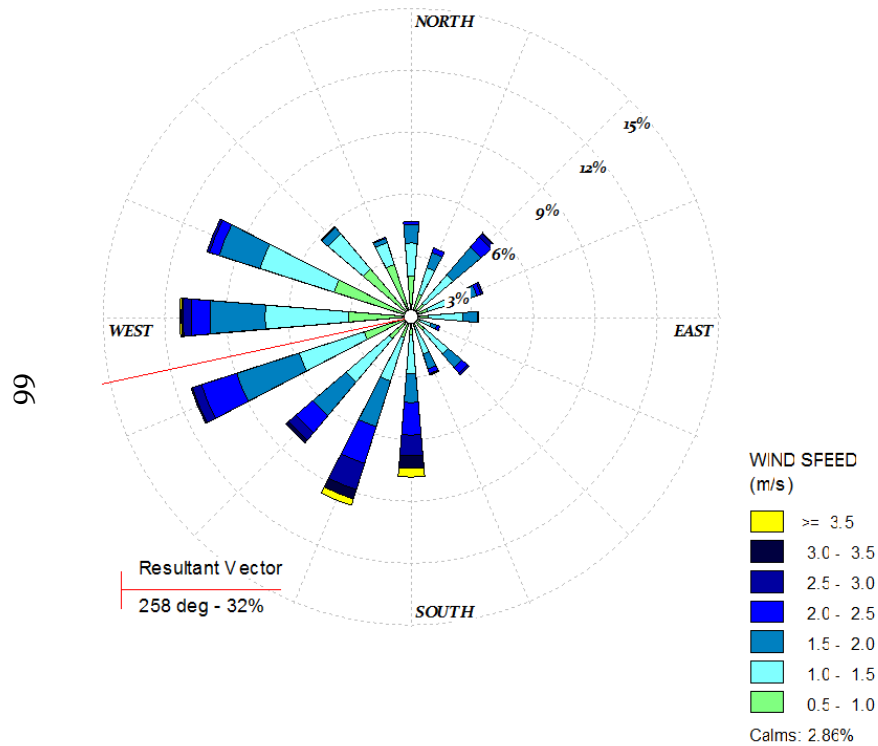
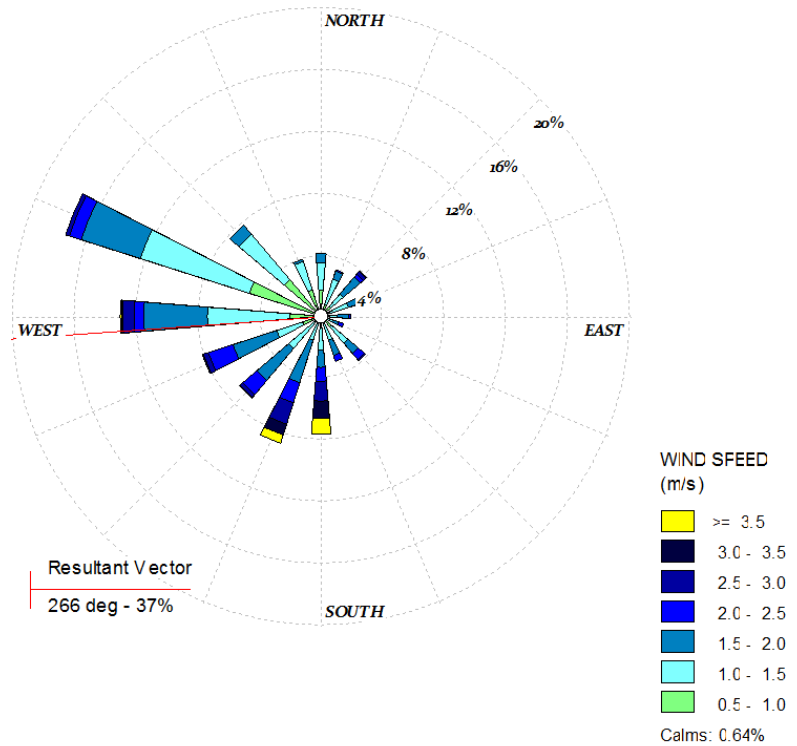


Figure III.3 Wind rose for (a) the entire two-week study (July 16-28, 2005) and for (b) the 8 hours of exposure.

(a) 24 Hours



(b) 8 Hours of Exposure



## **Wind Patterns**

Winds during the two-weeks were predominantly out of the west, southwest, and south as typically observed in Detroit during the summer months, with low wind speeds throughout most of the intensive period averaging 1.3 m/s. Increased southerly flow was observed on July 24 during a heavy precipitation event. Rapid wind speeds are typically associated with lower PM<sub>2.5</sub> mass concentrations.<sup>41</sup> Figure III.3 shows the wind rose for the entire exposure period as well as winds during the 8-hour exposure period only. These wind roses show that the 8 hours of exposure captured more flow from the west-northwest direction, slightly changing the resultant average vector from 258° to 266°. Individual daily wind roses are provided in Appendix A. On most days, the exposure hours experienced winds from a dominant direction. However, there were a few instances where significant changes in wind patterns occurred within the 8 hours of exposure. The most significant example is on July 28 when early morning winds were exclusively from the northwest until 9:00am EDT; then winds shifted to the southwest and south. This phenomenon is explored in depth in later sections, as Figure III.15 depicts two wind roses where changes in wind direction and speed brought about significant changes in PM<sub>2.5</sub> mass contributions.

## **Air Mass History**

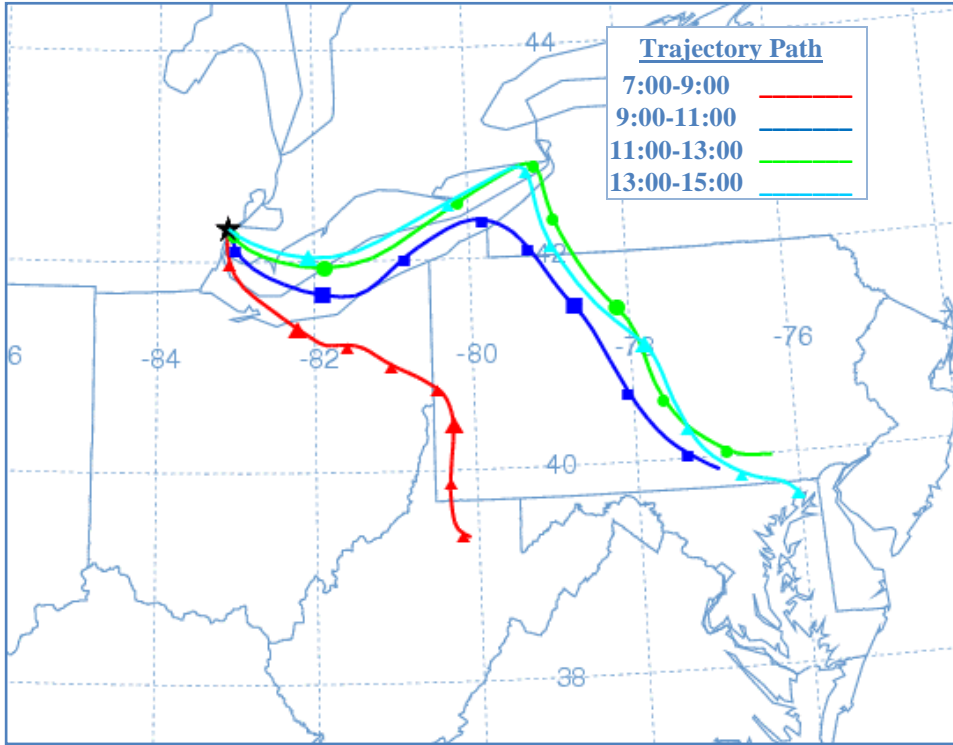
Air mass transport to Detroit and Steubenville was modeled using the Hybrid Single-Particle Lagrangian Integrated Trajectory (HYSPLIT) Model Version 4.8 (Draxler and Hess, 1997). Forty-eight hour back trajectories were calculated every two hours of the eight-hour exposure period on each day. HYSPLIT back trajectories were calculated using the Eta Data Assimilation System (EDAS) and were obtained from the National Oceanic and Atmospheric Administration's Air Resources Laboratory (NOAA-ARL). The starting height was set to one-half of the mixed-layer height, as determined from upper-air soundings, in order to best represent air mass transport within the boundary layer. Two back trajectories are shown in Figure III.4 indicating significantly different air mass histories that resulted in a high ambient PM<sub>2.5</sub> day (July 16) and a low ambient PM<sub>2.5</sub> day (July 23). On July 16, the model predicted that air masses reaching Detroit during the first two hours of exposure (shown in red) were slow moving and had a more

southerly path. The last 6 hours of the exposure were influenced by air mass transport from over Lake Erie to the east and then dropping down across central Pennsylvania. The mixed-layer trajectories matched well with the surface winds measured on-site. In fact, the wind roses for July 16 also identified the shift in wind, showing southeast flow in the morning and northeast flow in the later part of the day. Daily trajectories alongside wind roses are catalogued in Appendix A.

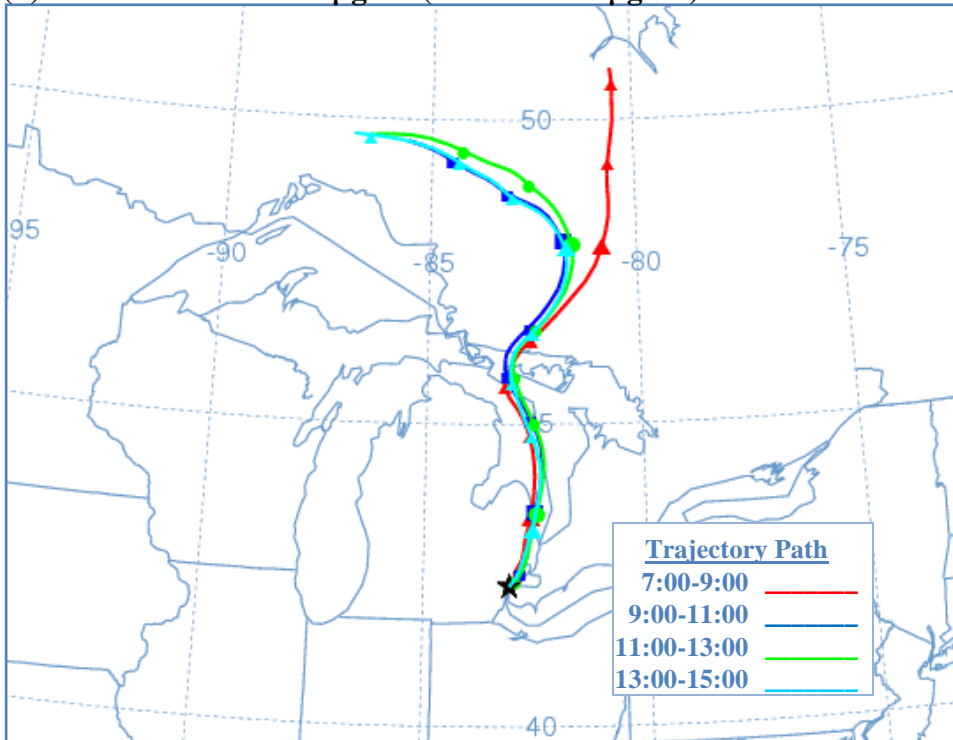


Figure III.4 HYSPLIT backward trajectories for two days with different air mass histories.

(a) 7/16/05: Ambient:  $30.4 \mu\text{g}/\text{m}^3$  (CAPs:  $1339 \mu\text{g}/\text{m}^3$ )



(b) 7/23/05 Ambient:  $6.2 \mu\text{g}/\text{m}^3$  (CAPs:  $115.5 \mu\text{g}/\text{m}^3$ )



### III.1.2 Ambient Air Pollution Levels

#### PM<sub>2.5</sub> Mass Concentration

During the two-week Detroit summer intensive, 24-hour TEOMs recorded an average PM<sub>2.5</sub> of 17.1±9.9 µg/m<sup>3</sup>. These ambient PM<sub>2.5</sub> concentrations were typical for Detroit; the average PM<sub>2.5</sub> concentration was found to be 16.8±8.4µg/m<sup>3</sup> in a similar study in July 2004. The 24-hour NAAQS standard for PM<sub>2.5</sub> mass (35 µg/m<sup>3</sup>) was not exceeded during the exposure; the 8-hour average on July 18 was 36.6 µg/m<sup>3</sup> but the 24-hour average remained below the standard at 28.0 µg/m<sup>3</sup>.

Ambient PM<sub>2.5</sub> concentrations during the 8-hour exposures in Detroit were also measured gravimetrically from Teflon filters and averaged 19.5±12.1µg/m<sup>3</sup>. In relation to other exposure studies, the summertime PM<sub>2.5</sub> mass in Detroit was lower than that found in Steubenville (23.8µg/m<sup>3</sup>), but was higher than the winter intensives at both Detroit and Steubenville (9.8 and 13.1µg/m<sup>3</sup>, respectively). The average PM<sub>2.5</sub> concentration from the TEOM instrument during the 8-hour exposures was less (16.9±11.0µg/m<sup>3</sup>), but as it was described in Chapter II, 30-minute concentrations can be lower due to the loss of semi-volatiles from the heated TEOM inlet.<sup>44</sup> In Detroit, the TEOM recorded short duration spikes in fine-fraction mass, e.g. 30-minute or hourly, that were not observed with the integrated filter sample. Figure III.5 illustrates this point as PM<sub>2.5</sub> recorded by the TEOM is plotted over the course of the 13-day summer exposure period. Most often, elevated PM<sub>2.5</sub> mass concentrations occurred in the early morning with declines over the 8-hour exposures, highlighted in grey. The data on July 19 provides the best example of a prominent rise in PM<sub>2.5</sub> in the early morning associated with a shallow morning boundary layer and limited mixing in the lowest portion of the atmosphere.<sup>41</sup> The highest 24-hour average ambient PM<sub>2.5</sub> concentrations were observed on July 16 and 18, at 26.8 and 28.0µg/m<sup>3</sup>, respectively. During exposure hours, concentrations of PM<sub>2.5</sub> were also higher, but dropped sharply at 3:00pm EDT. The afternoon and evening of July 24 showed the highest mass concentrations. During exposure hours on July 24, ambient PM<sub>2.5</sub> mass was normal at 14.6µg/m<sup>3</sup>, after the conclusion of the rain event by 2:00pm EDT, average mass increased significantly to 36.8µg/m<sup>3</sup> through midnight.

Fluctuations in  $PM_{2.5}$  mass can often be attributed to shifts in wind direction that change the source impacts at the sampling site. Thirty-minute  $PM_{2.5}$  concentrations as a function of wind direction are plotted in Figure III.6. The graph shows that concentrations were higher with southwesterly winds; only a few 30-minute concentrations had a mass  $>30\mu\text{g}/\text{m}^3$  with winds from the southeast. In addition, southwest winds resulted in the highest fine mass concentrations recorded at the site. Hence, ambient  $PM_{2.5}$  mass concentrations were heavily influenced by the prominent flow at the sampling location in Detroit.

**Figure III.5 Thirty-minute ambient PM<sub>2.5</sub> concentrations from 7/17-28, 2005, during the Detroit summer study. Precipitation is shown to occur during the two-week study by the purple bars. The exposure hours are highlighted in grey.**

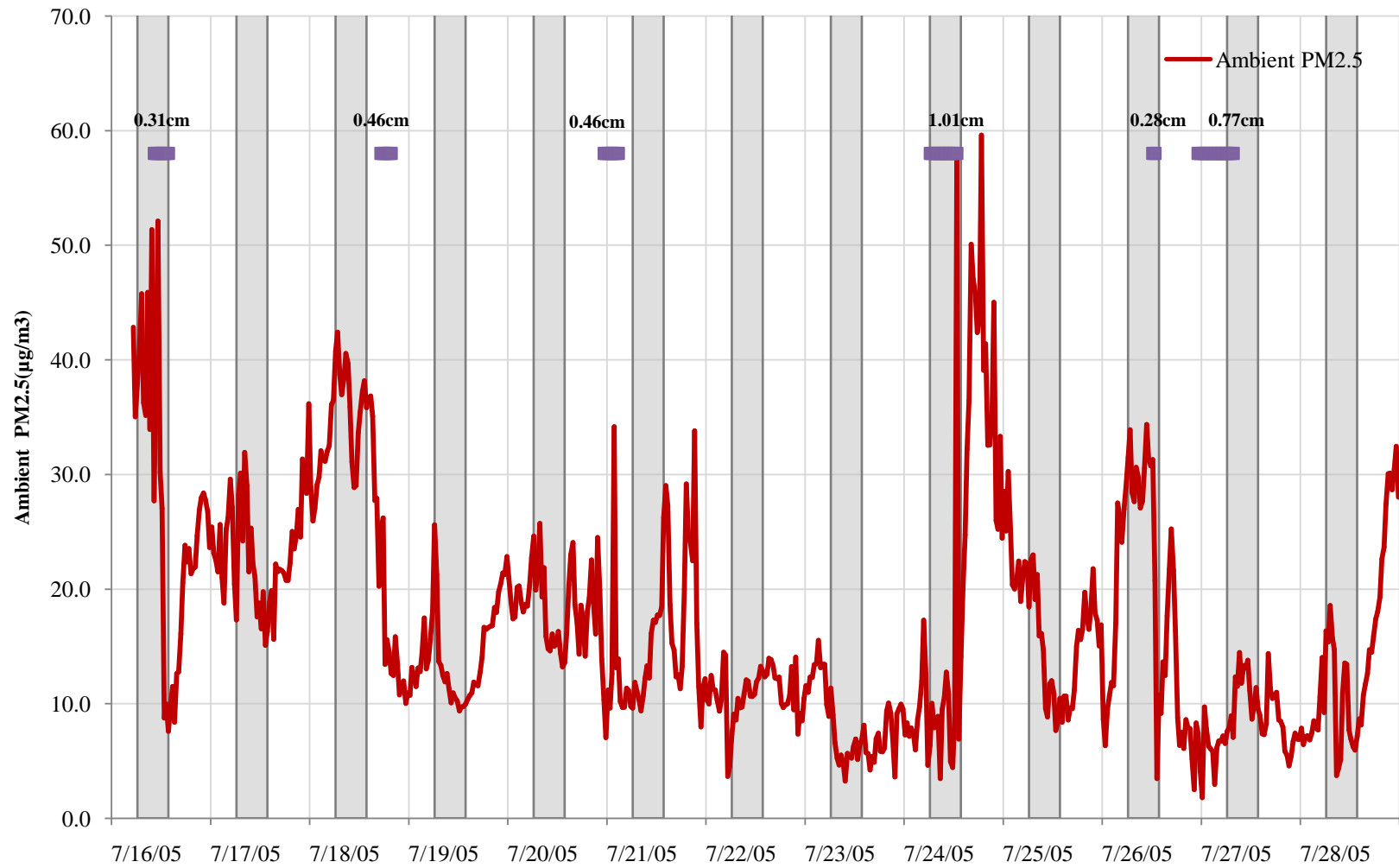
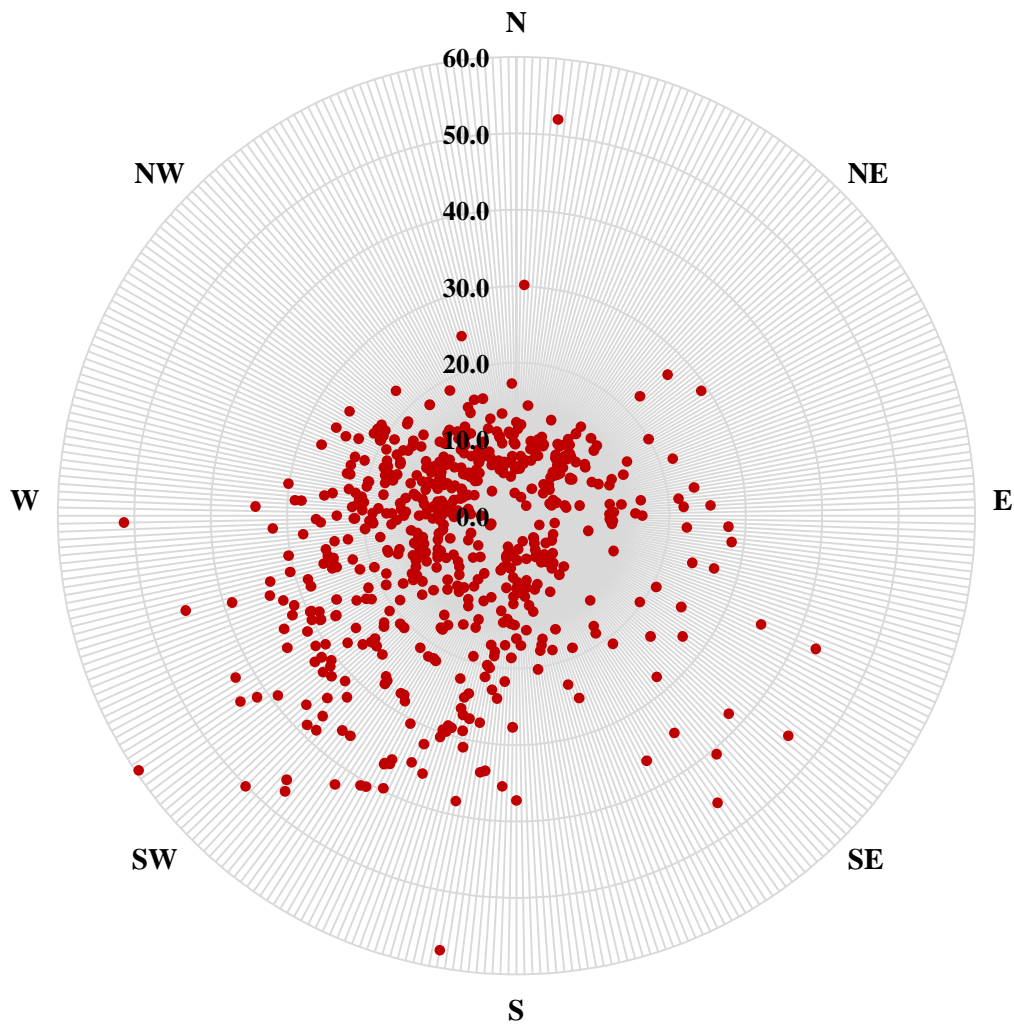


**Figure III.6 Twenty-four hour ambient PM<sub>2.5</sub> concentrations in Detroit based on 30-minute average mass and wind direction, for July 16-28, 2005.**

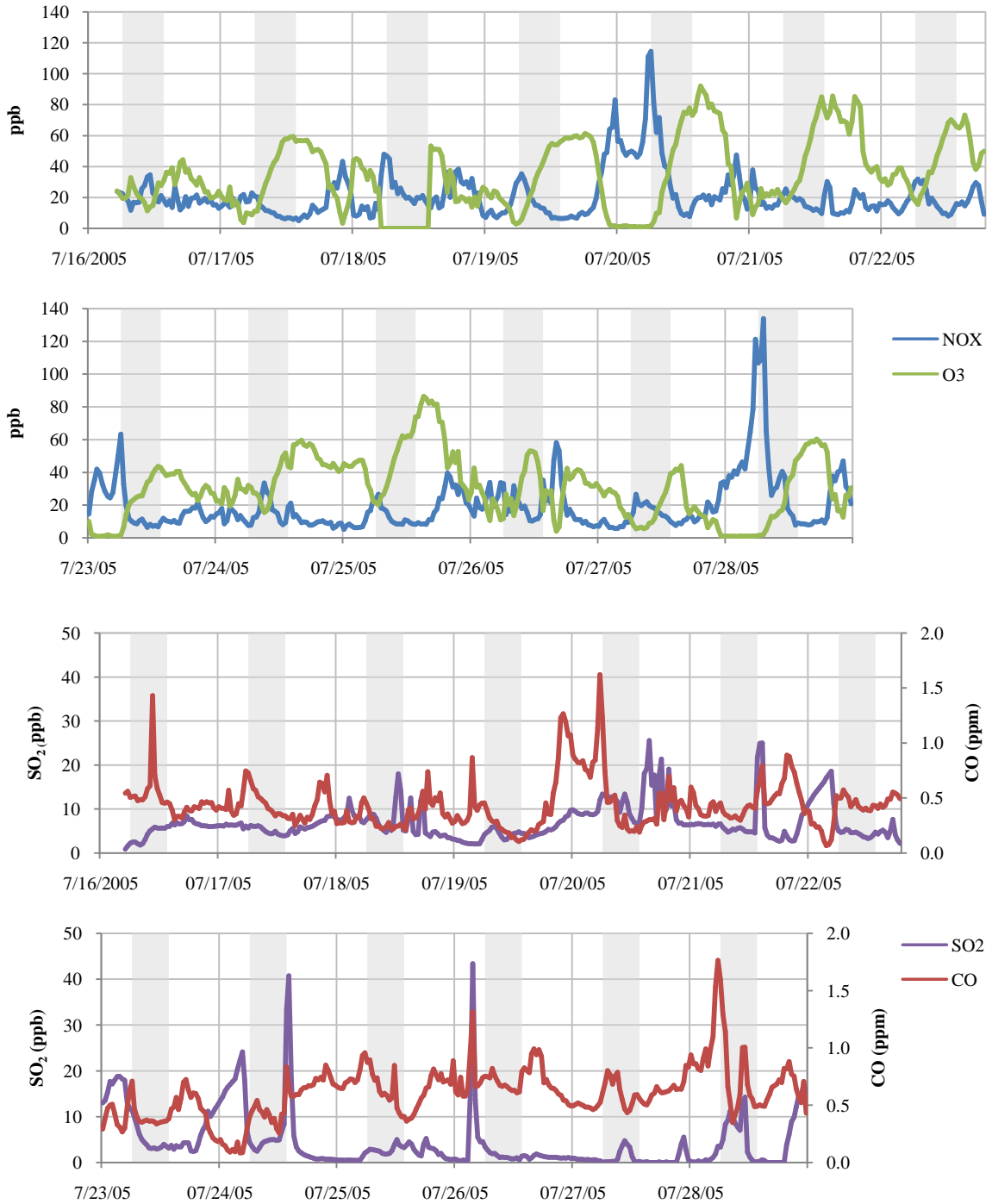


## Ambient Gas Concentrations

In addition to the fine mass and its components, the concentrations of ambient gaseous pollutants were monitored during the two-week period. Thirty-minute average ambient concentrations were calculated for NO<sub>x</sub>, SO<sub>2</sub>, O<sub>3</sub> and CO. The PM<sub>2.5</sub> concentrator works by accelerating particles through a series of virtual impactors, and the excess air is drawn out. Extensive tests on the concentrator system revealed that the more reactive gases deposited within the system inlet and slits, and the resulting gas phase concentrations in the exposure chambers were greatly reduced. The loss of gaseous pollutants in the Harvard concentrator varied as a function of the relative humidity, temperature, and the starting concentration of the gas phase pollutant. For this reason, these pollutants were not monitored in the exposure chamber itself, and the ambient gaseous pollutant concentrations are used to better understand the possible source influences on the levels and composition of the measured PM<sub>2.5</sub>.

Figure III.7 presents the concentration data recorded for the gaseous pollutants. There were two pronounced peaks in the CO and NO<sub>x</sub> concentration over the two-week summertime exposure in Detroit, but neither corresponded with elevated ambient PM<sub>2.5</sub> concentrations. During the early morning hours prior to the exposure periods on July 20 and 28, concentrations of CO reached ~1.5ppm and NO<sub>x</sub> concentrations reached ~120ppb; note the NAAQS NO<sub>x</sub> annual standard is 53ppb. The O<sub>3</sub> levels displayed typical diurnal changes in concentration with highest levels in the late afternoon and values going to zero overnight. Ozone was clearly titrated by NO<sub>x</sub> on occasion as it dropped when plumes of elevated NO<sub>x</sub> reached the site. Two peaks in SO<sub>2</sub> concentration were recorded with levels reaching ~50ppb. The peaks in SO<sub>2</sub> were also periods with elevated PM<sub>2.5</sub> concentrations. At the conclusion of the rain event on the 24<sup>th</sup>, a short-term peak in SO<sub>2</sub> concentrations occurred after the front passed and the wind direction shifted. NCDC data showed that conditions cleared after the frontal system passed through the area. Prior to the start of the exposure on July 26, SO<sub>2</sub> also peaked and subsequent PM<sub>2.5</sub> concentrations were elevated during this exposure period as well. On days like July 16 and July 18 when PM<sub>2.5</sub> was elevated during exposure hours, a corresponding peak in SO<sub>2</sub> was not recorded.

**Figure III.7 Thirty-minute ambient gas concentrations measured at the Detroit site from July 16-28, 2005 with exposure hours highlighted by the grey bars.**



### III.1.3 CAPs PM<sub>2.5</sub> Characterization

Characterization of the day-to-day changes in particulate matter in the exposure chamber, e.g. CAPs, was an important component of the health effects study. This section summarizes the trends in PM<sub>2.5</sub> composition, and discusses the CAPs concentrations relative to the concurrently measured ambient levels to document that CAPs PM<sub>2.5</sub> did mirror the ambient PM<sub>2.5</sub> behavior.

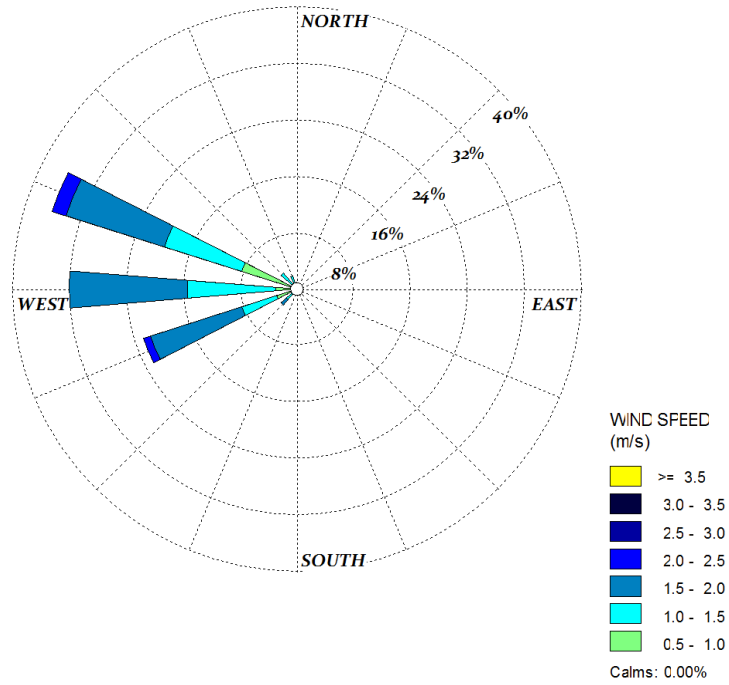
#### CAPs PM<sub>2.5</sub> Measurements

Eight-hour integrated CAPs fine mass concentrations in the Hinner exposure chamber during the Detroit summer intensive, measured using gravimetric analysis, averaged  $511.7 \pm 528.3 \mu\text{g}/\text{m}^3$ . The TEOM mass measurements were higher, at  $795.0 \pm 582.8 \mu\text{g}/\text{m}^3$ . Unlike the ambient TEOM, the CAPs TEOM does not have an in-line Nephelometer; therefore there is a greater likelihood that aerosol associated water and semi-volatiles affect the observed fine mass concentrations in the exposure chamber. Furthermore, a portion of the aerosol associated water vapor and other semi-volatiles may have degassed off the filters by the time of post-weighing back at the laboratory. TEOM data were initially filtered for CAPs mass, ranging from 20-2995  $\mu\text{g}/\text{m}^3$ . Higher short-duration peak concentrations may have been frequent enough to drive up the mean for each 30-minute average. The days with the highest ambient PM<sub>2.5</sub> concentrations, July 18, 16 and 26 ( $44.4$ ,  $42.2$  and  $28.0 \mu\text{g}/\text{m}^3$ , respectively), did not always result in the highest CAPs concentrations, and this may have been due to poor enrichment of the CAPs by the concentrator. The highest CAPs concentration was on July 18 ( $1638 \mu\text{g}/\text{m}^3$ ), followed by July 17 ( $1437 \mu\text{g}/\text{m}^3$ ) and July 26 ( $843 \mu\text{g}/\text{m}^3$ ). The ambient PM<sub>2.5</sub> concentration on July 17 during the exposure hours was  $22.3 \mu\text{g}/\text{m}^3$ . In Figure III.8, the wind roses for July 17 and July 18 are shown for the exposure hours; the prevailing winds recorded on these days were not from the same direction. Thus, other factors in addition to the winds influenced the CAPs mass. Specifically, the RH on both July 17 and July 18 were similarly high (69.4 and 70.3%, respectively) which may suggest that particle growth was important for concentrating the ambient PM<sub>2.5</sub> mass on these two days.

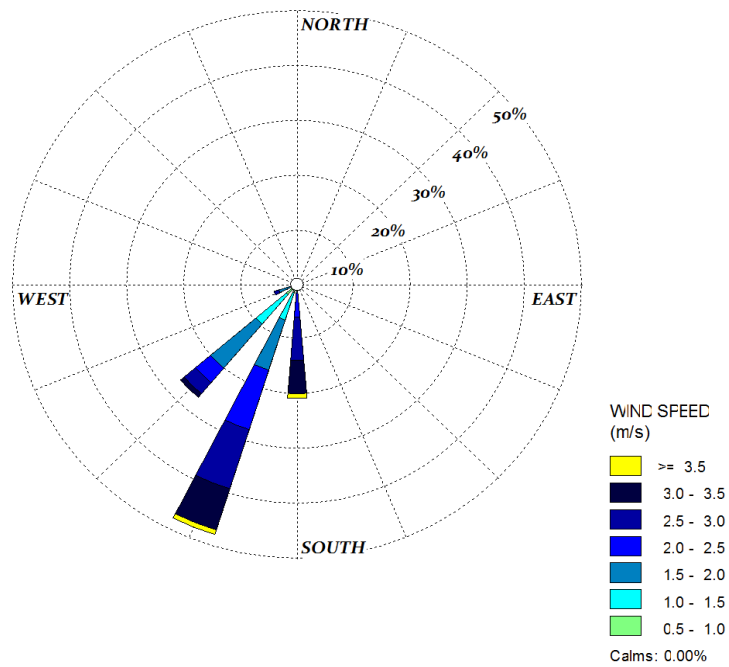


Figure III.8 Wind roses for the exposure hours on (a) July 17 and (b) July 18, 2005.

(a) 7/17/05 (CAPs mass: 1437 $\mu\text{g}/\text{m}^3$ )



(b) 7/18/05 (CAPs mass: 1638 $\mu\text{g}/\text{m}^3$ )



## CAPs PM<sub>2.5</sub> Composition

Substantial day-to-day differences in PM<sub>2.5</sub> composition were observed over the summer exposure period. Figure III.9 shows the daily contributions of SO<sub>4</sub><sup>-2</sup>, NO<sub>3</sub><sup>-</sup>, NH<sub>4</sub><sup>+</sup>, EC and OC. The total contribution of crustal material to the fine mass (~5% of PM<sub>2.5</sub>) was calculated using the following formula: 1.89(Al)+ 1.43(Fe) + 2.14(Si), where Si is estimated by K/0.15.<sup>65</sup> The “Other” category in the figure represents the unidentified mass: the difference of the gravimetric PM<sub>2.5</sub> mass and the sum of all the major constituents. This unidentified mass contributed to 23% of the mass, and largely consists of water vapor, typical for high humidity summertime conditions in Detroit.<sup>66,67</sup> Average SO<sub>4</sub><sup>-2</sup> concentrations were determined to be 124µg/m<sup>3</sup>, contributing nearly 25% of the fine-fraction mass. SO<sub>4</sub><sup>-2</sup> concentrations reflect regional contributions from coal combustion in Michigan.<sup>68</sup> NH<sub>4</sub><sup>+</sup> (11% of PM<sub>2.5</sub>) is highly correlated with SO<sub>4</sub><sup>-2</sup> (r<sup>2</sup>=0.98) due to the formation of (NH<sub>4</sub>)<sub>2</sub>SO<sub>4</sub> particles during summertime conditions in the Midwest with the availability of gaseous NH<sub>3</sub>. NO<sub>3</sub><sup>-</sup> accounts for only 5% of the mass in the summertime due to the high SO<sub>4</sub><sup>-2</sup> to bind with NH<sub>4</sub><sup>+</sup>. (NH<sub>4</sub>)<sub>2</sub>(SO<sub>4</sub>) is a major component of PM<sub>2.5</sub> in the Midwest and the largest mass contributor in Detroit, representing 35% of the fine-fraction mass. OC accounted for 31% of the fine mass on average. While OC concentrations varied substantially from day to day, it comprised a large percentage of the PM<sub>2.5</sub> on both high and low pollution days. EC, however, consistently represents a small percentage of PM<sub>2.5</sub>, averaging only 6% of PM<sub>2.5</sub>. EC is often identified as local contributions to urban areas like Detroit.<sup>69</sup> The three lowest PM<sub>2.5</sub> concentration days, July 23, 24 and 25, were associated with significantly different wind directions (northeast, south, and northwest, respectively) but had a similar PM<sub>2.5</sub> composition. Furthermore, the 24<sup>th</sup> had a substantial rain event (2.57cm) within the 8-hour exposure that may explain the lower pollution on the 24<sup>th</sup>, despite southerly flow which normally brought higher fine mass concentrations.

**Figure III.9 Composition of PM<sub>2.5</sub> from analysis of CAPs filter samples collected during 8-hour exposures for the Detroit summer study (µg/m<sup>3</sup>).**

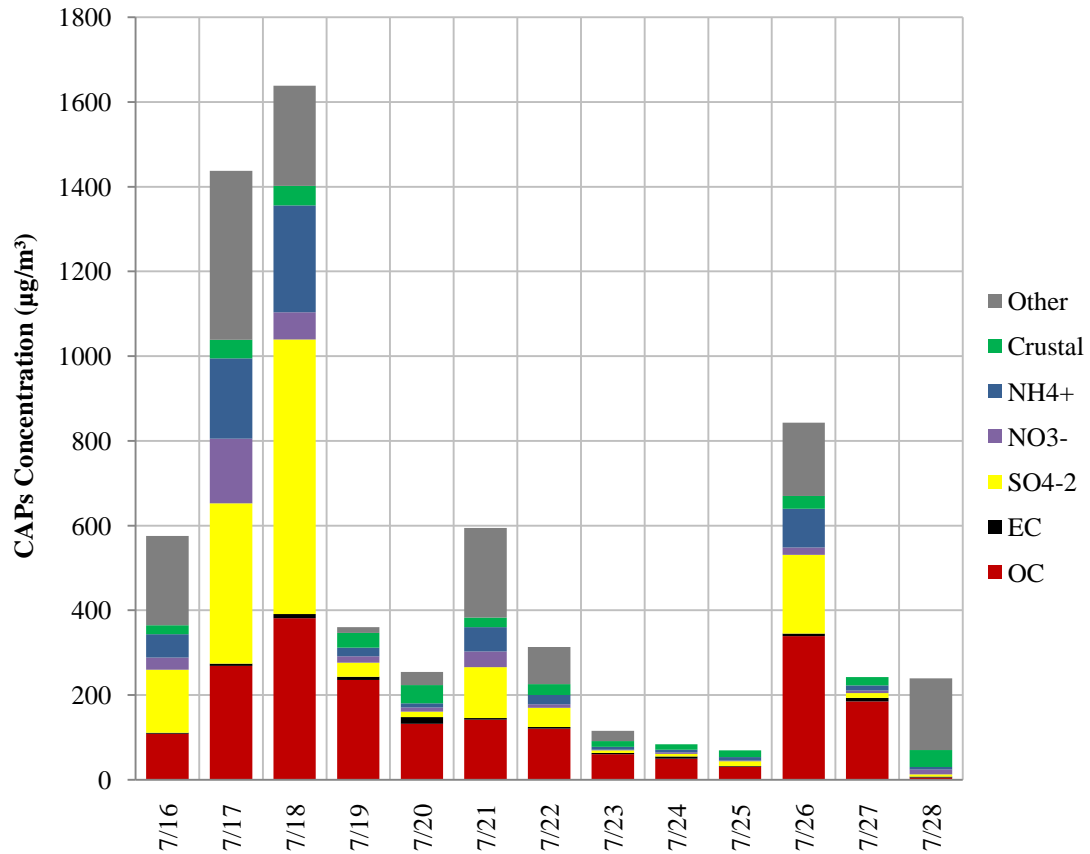


**Table III.1 Daily concentrations of the major components of CAPs collected during the 8-hour exposures during the Detroit summer study (µg/m<sup>3</sup>).**

	PM	OC	EC	SO <sub>4</sub> <sup>-2</sup>	NO <sub>3</sub> <sup>-</sup>	NH <sub>4</sub> <sup>+</sup>	Crustal
7/16	575.6	108.6	2.6	148.5	29.2	54.6	21.0
7/17	1437	269.3	4.9	378.8	152.1	189.7	43.6
7/18	1638	381.1	10.1	648.4	64.3	252.3	45.4
7/19	360.1	235.9	7.4	33.3	15.0	20.4	35.1
7/20	254.7	132.2	15.6	12.8	9.8	10.0	43.4
7/22	313.8	120.6	4.3	45.1	8.1	22.2	25.7
7/23	115.5	60.6	2.9	6.0	1.5	6.7	13.8
7/24	81.0	50.0	5.0	6.1	3.6	5.9	12.9
7/25	67.9	31.3	1.4	10.8	1.4	8.4	16.2
7/26	843.1	338.9	6.1	185.7	17.4	91.9	29.7
7/27	213.3	185.3	8.2	11.0	5.9	12.4	19.5
7/28	239.5	5.6	1.6	5.5	11.5	6.4	39.6
<b>Mean</b>	511.7	160.0	5.8	124.3	26.6	56.7	28.8
<b>Std Dev.</b>	505.9	117.8	3.9	191.2	41.3	78.4	12.3

## Trace Element Concentrations

Significant daily fluctuations in trace element concentrations were observed during the Detroit summer study. Even though these constituents make up a very small percentage of overall PM<sub>2.5</sub> mass, they are important to emphasize here because of (1) the potential toxicological effects that may be evident even in very small doses, and (2) the use of trace element concentrations in receptor models to estimate potential source contributions.<sup>70</sup> Table III.2 summarizes the average mass and standard deviation for each of the trace elements.

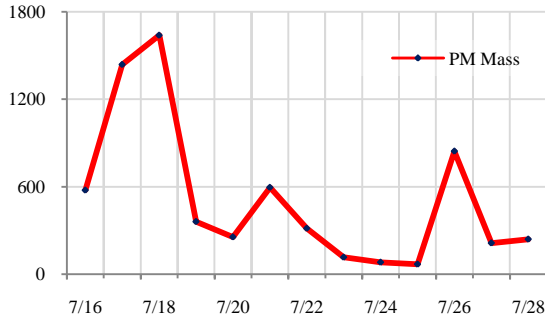
Figure III.10 shows the 8-hour ambient PM<sub>2.5</sub> together with NO<sub>3</sub><sup>-</sup> and EC and several trace elements that had daily concentrations patterns different from the PM<sub>2.5</sub> concentration. In Figure III.10a, PM<sub>2.5</sub> concentrations were correlated with NH<sub>4</sub><sup>+</sup>, SO<sub>4</sub><sup>-2</sup>, S, Se, OC, Co, Ti, Mo, La, Ce, Sm and Ni, with the only exception being V, which exhibited a spike in concentration on July 28. EC was plotted and correlated with the concentration to Al, Mg, Rb and Mn (Figure III.10.b). Fe also co-varied with EC, but like V, Fe also spiked on July 28. Concentrations of NO<sub>3</sub><sup>-</sup> were similar to K, As and Sr on each day (Figure III.10.c). P, Cu and Sb all shared a spike on July 19 with a secondary peak on July 27 and July 28 (Figure III.10.d). Pb, Co, Cd and Zn (Figure III.10.e-h) concentrations were all independent of the patterns found in the other constituents, including PM<sub>2.5</sub> mass. For example, Pb had a peak concentration of 921ng/m<sup>3</sup> on July 19 when PM<sub>2.5</sub> CAPs concentrations were below average (360µg/m<sup>3</sup>). These findings show that some trace elements displayed similar day-to-day variations while others did not co-vary with PM<sub>2.5</sub> mass.

**Table III.2 Detroit summer average trace element concentrations of CAPs collected on Teflon filters in units of ng/m<sup>3</sup> \*(Except PM, S, and Fe which are in µg/m<sup>3</sup>).**

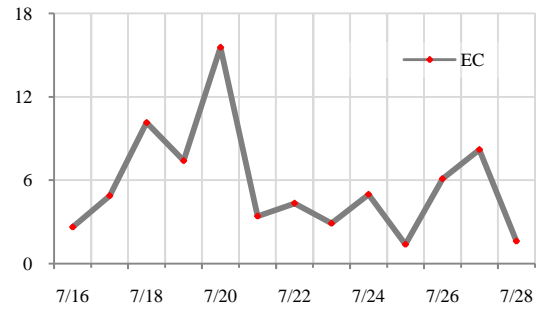
	PM*	Mg	Al	P	S*	K	Ti	V	Mn	Fe*	Co	Ni	Cu	Zn	As	Se	Rb	Sr	Mo	Cd	In	Sb	La	Ce	Sm	Pb
7/16	575.6	244.5	NA	307.7	58.2	1182	17.3	17.8	60.1	2.16	0.76	40.1	45.8	154.7	17.5	69.8	2.11	11.3	5.5	2.33	0.033	7.8	0.64	0.79	0.028	35.5
7/17	1437	475.2	245.6	179.4	132.0	2616	28.1	16.2	93.7	3.34	1.76	64.1	113.8	319.1	56.0	67.0	1.55	58.0	14.6	2.28	0.051	39.8	1.27	1.79	0.041	58.9
7/18	1638	1296	940.7	301.7	210.9	1722	88.5	21.3	205.3	7.04	6.45	211.0	115.9	768.8	40.9	164.7	3.60	34.3	62.5	4.10	0.131	20.9	24.38	16.49	0.186	354.5
7/19	360.1	894.4	371.3	603.6	15.9	1379	51.5	4.7	190.9	6.85	2.03	26.9	208.5	1629	17.2	20.5	1.93	19.1	11.2	4.98	0.248	116.9	1.23	1.94	0.105	921.1
7/20	254.7	1758.1	1245.3	426.4	6.0	1363	67.1	7.1	410.5	9.35	1.89	18.7	105.3	2419	11.5	13.1	3.88	38.2	16.1	3.96	0.090	74.0	21.96	14.20	0.184	788.7
7/22	313.8	799.7	875.4	109.5	18.9	1055	54.8	7.0	117.5	3.94	1.42	24.6	70.3	335.6	6.6	15.2	1.41	18.0	19.0	0.99	0.035	18.8	1.23	2.04	0.107	24.7
7/23	115.5	431.0	NA	146.2	3.8	650.8	20.8	4.2	39.2	1.67	0.60	12.4	39.4	47.9	5.5	7.4	0.72	8.8	5.0	1.04	0.067	5.2	0.40	0.71	0.030	35.6
7/24	81.0	189.3	448.6	4.1	3.0	571.0	8.3	2.9	53.3	1.94	1.59	43.2	23.6	35.3	3.8	4.0	1.06	9.3	4.3	0.39	0.005	2.9	1.27	0.96	0.031	10.8
7/25	67.9	119.1	308.0	142.8	5.5	1003	7.6	1.7	9.1	0.49	0.18	4.9	7.9	122.3	1.5	2.6	0.53	2.6	2.6	0.13	0.006	2.4	0.32	0.29	0.017	3.5
7/26	843.1	882.7	877.3	266.6	78.3	1335	37.0	13.3	190.1	3.21	1.51	26.6	118.0	965.8	16.9	60.4	3.63	17.6	4.3	2.45	0.060	9.1	6.35	4.54	0.128	53.5
7/27	213.3	278.6	278.4	571.1	5.1	980.4	26.9	1.9	84.4	2.58	1.59	48.6	61.2	272.1	4.7	4.4	2.11	7.2	16.6	1.38	0.015	10.7	0.32	0.79	0.022	17.0
7/28	239.5	1383	754.5	384.9	3.4	1356	70.7	62.8	528.8	8.53	3.56	98.1	148.6	16737	11.5	12.5	4.57	33.9	27.3	7.67	0.133	63.5	11.29	6.42	0.275	172.0
<b>Mean</b>	511.7	729.3	634.5	287.0	45.1	1268	39.9	13.4	165.2	4.26	1.95	51.6	88.2	1984	16.1	36.8	2.26	21.5	15.7	2.64	0.073	31.0	5.89	4.25	0.096	206.3
<b>Std Dev.</b>	505.9	509.8	329.6	176.7	63.1	510.8	25.2	16.2	150.8	2.80	1.58	53.8	55.2	4502	15.7	45.6	1.28	15.6	15.8	2.10	0.067	34.5	8.34	5.27	0.080	306.2

**Figure III.10 Detroit summer 8-hour CAPs concentrations of PM<sub>2.5</sub> and constituents. Constituents in parentheses behaved similar to the pollutant being plotted. PM<sub>2.5</sub>, NO<sub>3</sub><sup>-</sup> and EC are measured in µg/m<sup>3</sup> whereas trace elements are in ng/m<sup>3</sup>.**

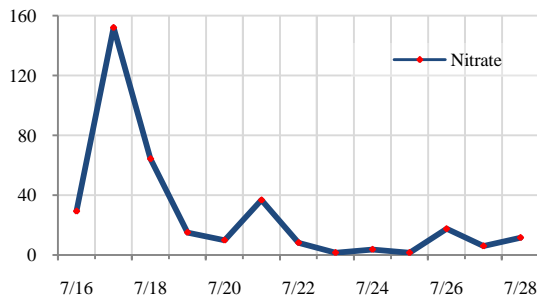
**(a) PM (NH<sub>4</sub><sup>+</sup>, SO<sub>4</sub><sup>-2</sup>, S, Se, OC, Co, Ti, Mo, La, Ce, Sm, Ni, V)**



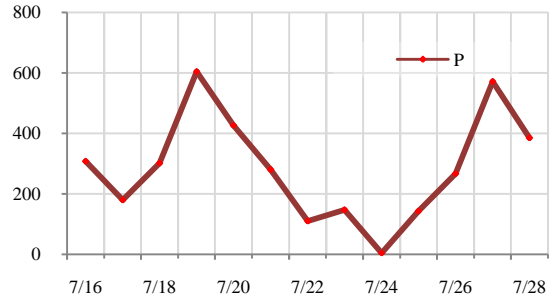
**(b) EC (Al, Mg, Rb, Mn)**



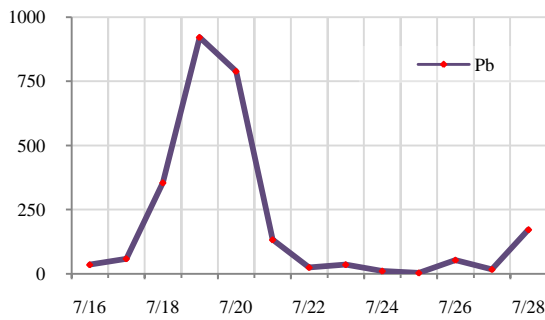
**(c) NO<sub>3</sub><sup>-</sup> (K, As, Sr)**



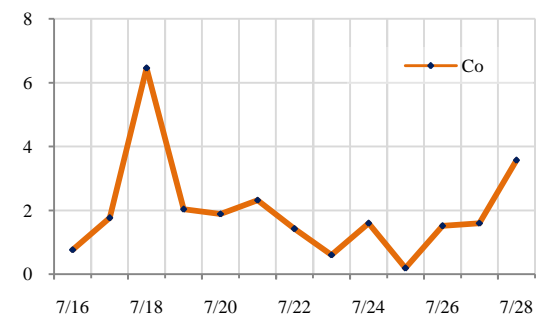
**(d) P (Cu, Sb)**



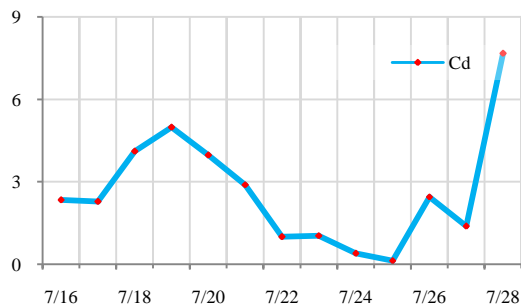
**(e) Pb**



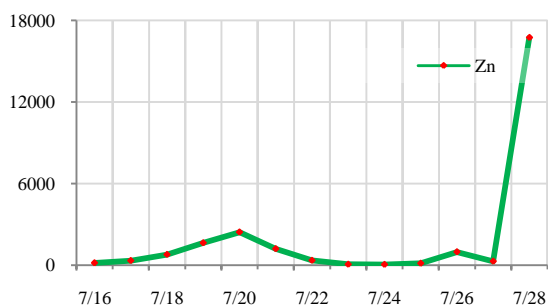
**(f) Co**



**(g) Cd**



**(h) Zn**



### **III.1.4 High Temporal-Resolution Air Pollution Findings**

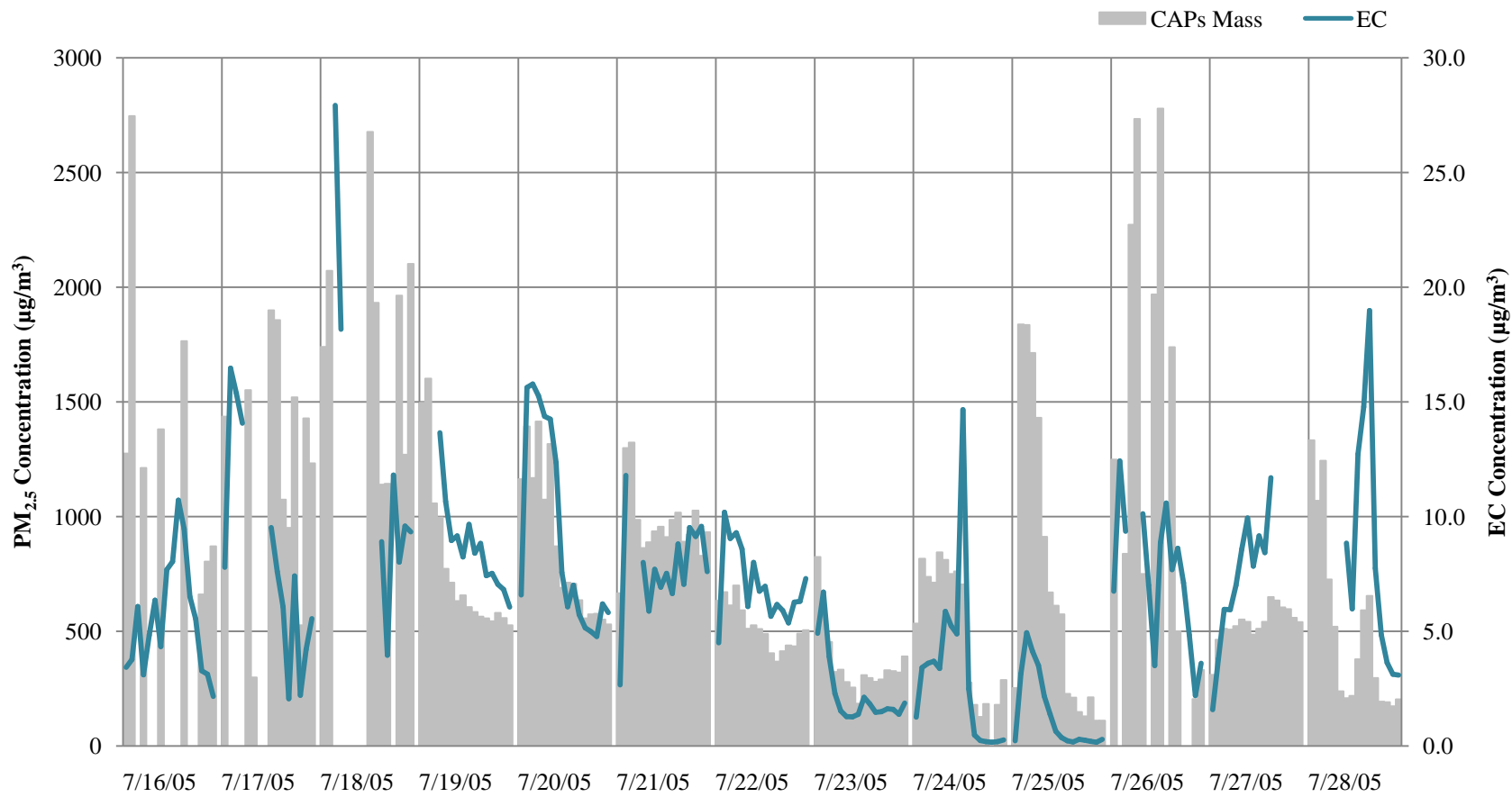
Monitoring air pollution on a high temporal-resolution, (e.g. high-resolution data or 30-minute data), is critical because winds can fluctuate rapidly over the course of the day, thus changing the pollutant concentration and source impacts at the sampling site. Furthermore, meteorology from a passing high-pressure system or a front can significantly affect atmospheric chemistry. Cloud cover can alter the amount of UV light, which will influence temperature, humidity and the mixing height. Air pollution concentrations collected over 30-minute periods better reflect the large variability that is typically observed in urban or source areas that would otherwise be lost within a single 8-hour integrated sample.

#### **Fine Mass and EC**

The large variability that occurred during the exposure hours in the CAPs mass was also seen in the fine mass constituents. In Figure III.11, EC is plotted with the CAPs mass and scaled to 1/10<sup>th</sup> of the mass concentration. On average, the fine-fraction mass in this study was composed of 6% EC, consistent with our previous findings in Detroit. Daily maximums in PM and EC were often observed in the early morning, likely due to the increase in traffic volume, indicated by elevated CO and NO<sub>x</sub> concentrations on July 20 and 28 (Figure III.3). A lower boundary layer would also reduce the available boundary layer mixing volume in the early morning, resulting in elevated concentrations. Observed on the morning of July 20 (mean mixing height: 208m), lowest mixing height was 98m, as determined by the HYSPLIT model.

Figure III.11 Thirty-minute averaged CAPs PM<sub>2.5</sub> and EC concentrations during Detroit summer exposure hours.

84





### **Ambient Trace Element Concentrations**

As seen with PM<sub>2.5</sub> and EC, trace element concentrations determined from SEAS 30-minute trace element samples also display significant sample-to-sample variability. Table III.3 summarized the SEAS data with daily averages of each trace element as well as the study mean, standard deviation, median, and the 5<sup>th</sup> and 95<sup>th</sup> percentiles. The Detroit summer study had several instances where a short-term peak in the concentration of a trace element was 20 times larger than the mean. In Figure III.12, 30-minute trace element concentrations of Sb and S were contrasted to integrated filter data to emphasize the significant variability that can occur within a day that would otherwise be masked over an 8-hour average. Sb and S had strong within-day variability that drove up the mean. On July 19, the elevated concentration (17.8ng/m<sup>3</sup>) was only for a short period of time, thus the potential impact on HRV would not be from a continuous exposure of Sb at 5.93ng/m<sup>3</sup>. Consequently, any associated effect on HRV from Sb would likely be different using the two time scales.

For S, the within-day concentrations were still noticeable, but did not have the same peaks in concentration as observed for Sb. Figure II.9 illustrates the strong correlation of SEAS findings with integrated data for S ( $r^2=0.921$ ). This observation was consistent with the plot in Figure III.12 where S is shown to have valleys and peaks in data, but overall average SEAS data appear similar to integrated concentrations. Integrated S mass followed PM<sub>2.5</sub> mass closely during the 8-hour data and was significantly associated with fine-fraction mass ( $p<0.0001$ ) as was 30-minute SEAS data with TEOM data ( $p<0.0001$ ). Therefore, S and some constituents of PM<sub>2.5</sub> can either act independent of PM<sub>2.5</sub> concentrations or be collinear and not diverge from the fine-fraction mass. As a result, the associations of trace elements and HRV need to be investigated on both the 8-hour and 30-minute time scales due to the independent variability that the constituents of PM<sub>2.5</sub> possess.

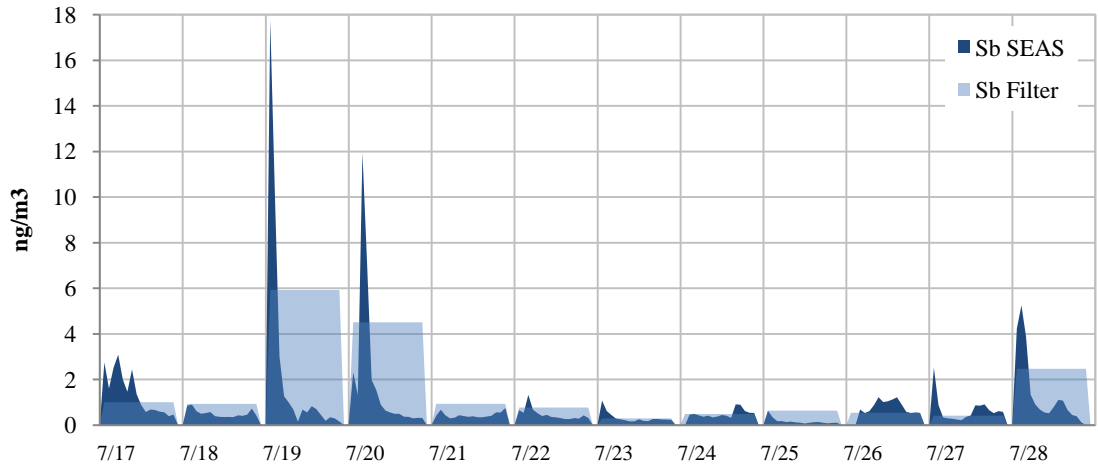
**Table III.3 Averaged concentrations of PM and EC together with SEAS derived trace elements in the Detroit summer exposure study. \* PM, EC and S are in  $\mu\text{g}/\text{m}^3$ , all other trace elements are in  $\text{ng}/\text{m}^3$ .**

	PM*	EC*	Mg	Al	P	S*	K	Ca	Ti	V	Cr	Mn	Fe	Co	Ni	Cu	Zn	As	Se	Rb	Sr	Mo	Cd	Sb	Ba	La	Ce	Pb
7/16	1339	1.52	115	34.8	72.3	3.08	258	629	1.21	4.24	1.47	5.63	50.6	0.45	3.19	17.9	85.9	0.36	0.67	0.29	2.03	0.82	0.66	0.88	9.72	0.09	0.16	2.1
7/17	1252	2.22	54.9	26.4	102	4.81	215	227	0.91	1.07	0.59	3.2	47.1	0.09	0.76	9.32	23.8	2.38	1.75	0.13	2.21	0.42	0.11	1.38	6.39	0.05	0.07	1.5
7/18	1782	3.37	76.2	38.7	28.7	6.02	155	517	1.84	0.75	1.01	6.19	99.8	0.08	0.99	18.5	29.6	0.85	1.66	0.19	1.81	0.88	0.21	0.52	5.7	0.35	0.24	7.6
7/19	777	2.31	33.2	11.4	8.67	0.74	46.4	235	0.49	0.1	0.18	3.97	35.5	0.04	0.29	4.05	51.8	0.6	0.52	0.08	0.9	0.46	0.26	2.39	4.2	0.02	0.03	12
7/20	871	2.49	100	27.6	11.5	1.51	65.8	685	1.42	0.23	0.33	13.6	94.9	0.06	0.31	3.61	65.4	0.79	0.74	0.24	3.41	0.7	0.26	1.94	8.61	0.49	0.3	23.9
7/21	964	2.15	48.9	10.4	13.6	1.22	37.2	218	0.43	0.14	0.21	3.45	45.4	0.03	0.15	2.23	23.7	0.37	0.43	0.07	4.89	0.36	0.15	0.44	5.23	0.03	0.03	6.5
7/22	519	1.99	50.9	18.8	28.1	0.75	631	242	0.7	0.25	0.17	3.14	47.3	0.04	0.11	2.64	17.3	0.25	0.27	0.09	0.94	1.19	0.24	0.47	5.07	0.03	0.04	4.3
7/23	362	0.64	20.6	10.1	6.32	0.57	23.1	92	0.34	0.25	0.14	1.43	29.6	0.08	0.23	3.31	13.8	0.32	0.19	0.04	0.31	1.43	0.13	0.32	3	0.01	0.02	1.4
7/24	527	0.86	20	8.8	6.37	1.08	45.4	78.4	0.28	0.75	0.25	2.22	19.7	0.06	0.29	3.4	16.4	0.67	0.76	0.1	0.58	0.11	0.22	0.5	3.72	0.05	0.04	6.5
7/25	687	0.39	10.4	2.4	0.85	0.67	16.3	37.9	0.04	0.09	0.05	0.52	2.6	0.01	0.03	0.75	1.9	0.18	0.3	0.02	0.14	0.03	0.02	0.17	1.02	0	0	0.2
7/26	1397	2.03	40.7	14.1	15.1	2.61	107	180	0.59	0.38	0.55	5.09	34.8	0.09	0.77	3.74	23.4	0.93	1.18	0.19	0.68	0.36	0.39	0.82	4.62	0.12	0.08	2.4
7/27	533	2.08	28.7	9.4	8.89	0.27	227	104	0.28	0.09	1.08	2.17	22.1	0.1	0.6	2.84	14.1	0.26	0.07	0.12	0.45	0.12	0.23	0.66	9.05	0.01	0.02	1.5
7/28	515	2.3	40.7	17.6	12.1	1.32	127	174	0.41	1.58	0.24	7.2	48.4	0.09	0.64	3.74	259	0.74	0.7	0.14	0.71	0.38	0.4	1.46	8.51	0.09	0.05	7.3
<b>Mean</b>	795	1.77	45.1	16.7	21.2	1.82	144	240	0.66	0.53	0.42	4.36	44.2	0.07	0.37	5.07	44.9	0.69	0.71	0.12	1.45	0.55	0.22	0.92	5.49	0.1	0.08	6.22
<b>Std Dev.</b>	583	1.19	49.5	18.6	25.6	2.11	235	273	0.74	0.66	0.54	4.98	50.3	0.08	0.78	6.28	61.8	0.8	0.82	0.14	2.11	0.74	0.26	1.18	6.27	0.15	0.1	7.59
<b>Median</b>	635	1.73	37.9	12.9	10	1.05	54.5	182	0.49	0.22	0.23	2.93	32.3	0.05	0.24	2.76	17.8	0.37	0.49	0.08	0.77	0.22	0.13	0.5	4.4	0.03	0.04	2.87
<b>5%ile</b>	185	0.07	9.6	0.5	0.4	0.24	11.1	34.9	0	0.04	0.02	0.47	0	0.01	0	0.31	1.6	0.09	0.04	0.02	0.13	0.01	0.02	0.13	0.89	0	0	0
<b>95%ile</b>	1931	4.04	113	42.4	93.5	5.7	363	848	1.99	2.54	1.29	13.4	150	0.14	1.56	17.9	125	2.03	2.34	0.3	3.9	1.61	0.64	2.75	12.0	0.33	0.24	25.0

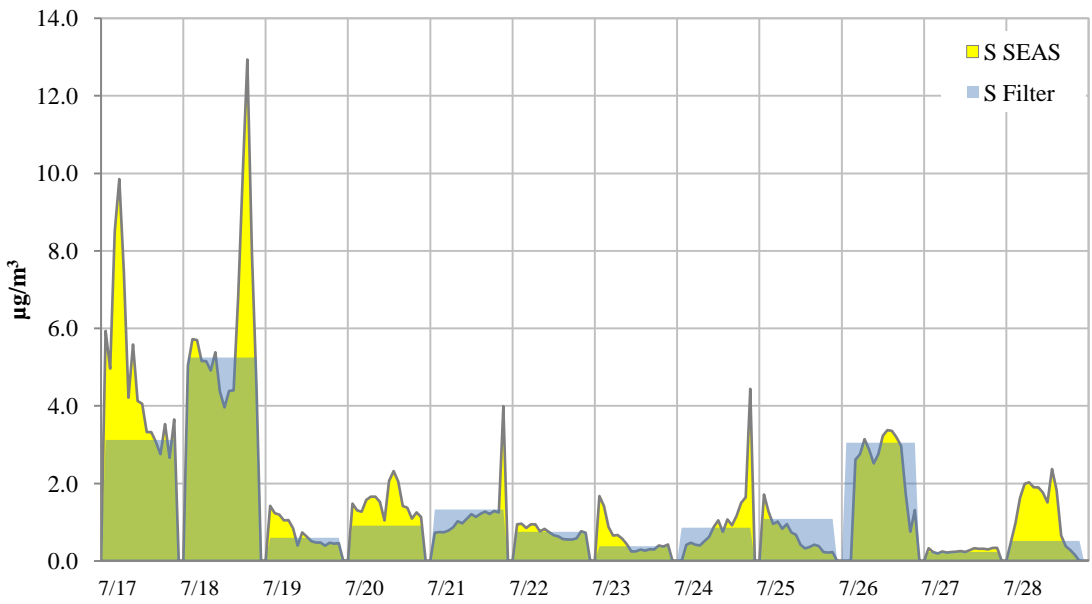
95

**Figure III.12 Detroit summer Sb and S concentrations from 30-minute SEAS samples and 8-hour integrated filter samples.**

**(a) Sb (Exposure Average: 0.922ng/m<sup>3</sup>)**



**(b) S (Exposure Average: 1.82µg/m<sup>3</sup>)**

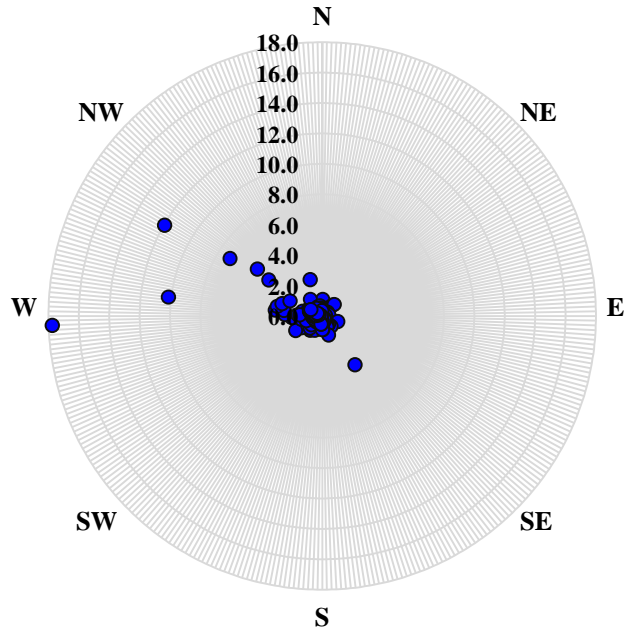


The concentrations of each trace element was plotted over time and made into a pollutant concentration rose, (e.g. “Pollution Rose”), to investigate if specific trace elements were higher with specific wind directions. The pollution roses in Figure III.13 show two examples how trace elements acted independently of  $PM_{2.5}$ , as observed in Figure III.10. Concentrations of Sb (III.13a) were higher with more westerly winds, whereas La and Ce concentrations (III.13b) were highest with winds from the southwest.

The SEAS derived data also gave the opportunity to observe significant changes in these trace elements over the course of a day due to synoptic scale changes in weather patterns. For example, Figure III.14a shows the wind rose for first 2 hours of exposure on July 28 and Figure III.14b shows the wind patterns for the remaining 6 hours of exposure. Concentrations of many constituents were greater than an order of magnitude for the first 2 hours of exposure. Very low wind speeds from the NW were observed and may have contributed to the higher observed mass. In Figure III.14c, Zn concentrations on July 28 were observed to reach nearly  $1000 \text{ ng/m}^3$  whereas the 8-hour integrated sample concentration was only  $416 \text{ ng/m}^3$ . Also,  $PM_{2.5}$  concentrations had an afternoon reemergence, where increased Rb peaked at  $0.530 \text{ ng/m}^3$  (Rb mean:  $0.173 \text{ ng/m}^3$ ). Rb, however, was unaffected by the elevated PM during the early morning. These data indicate how valuable it is to include high-resolution trace element in order to investigate the changes in mass that occur over the course of a day which would otherwise be masked in an integrated 8-hour sample. In future longitudinal studies, detecting short-term air pollution changes could be valuable in associating spikes in concentrations with acute and repeatable biological responses. However, the most important use of the 30-minute data in this study is to provide a robust data set to link constituent concentrations with the high-resolution changes in HRV. There is far more power behind high-resolution trace element concentrations, and if HRV findings can be observed on the shortened time scale, then the 30-minute data will be a better indicator of cardiac change.

**Figure III.13 Pollutant concentration roses (ng/m<sup>3</sup>) for (a) Sb, and (b) La (purple) and Ce (green) based on wind direction.**

**(a) Sb**



**(b) La (purple) and Ce (green)**

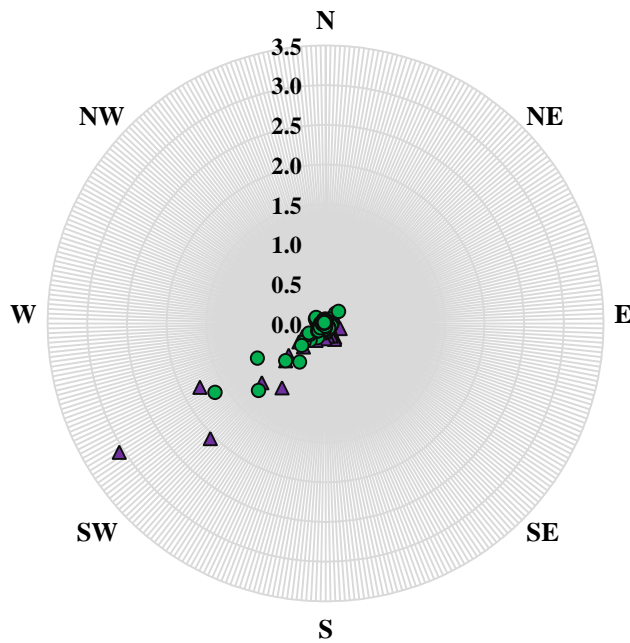
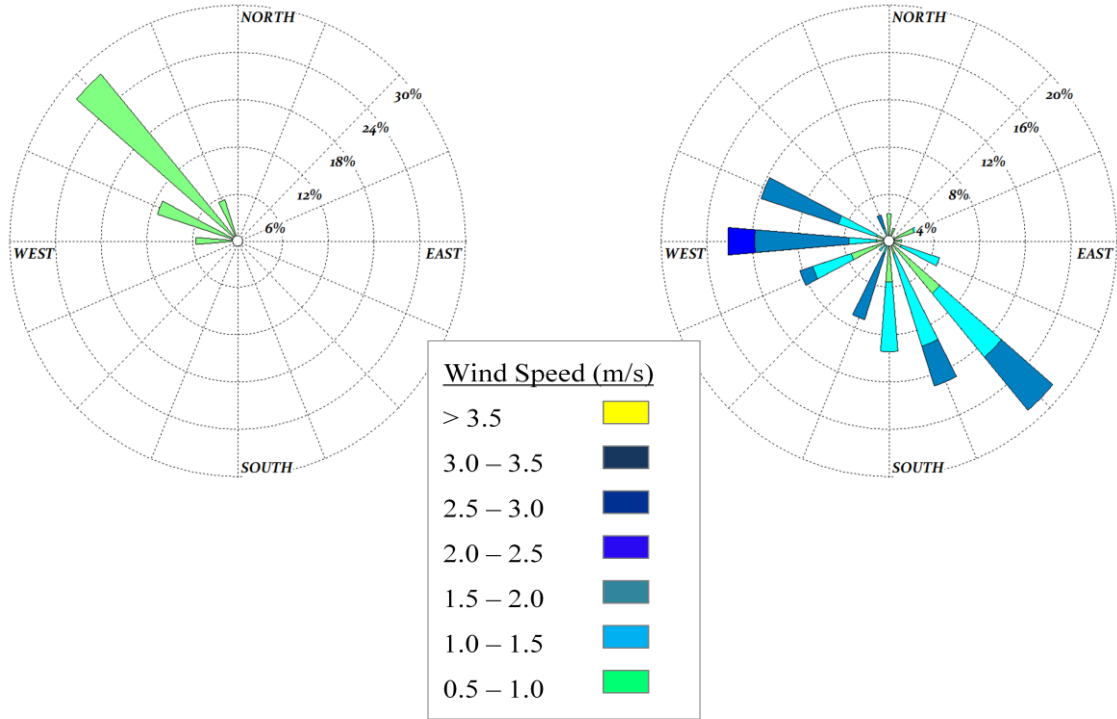


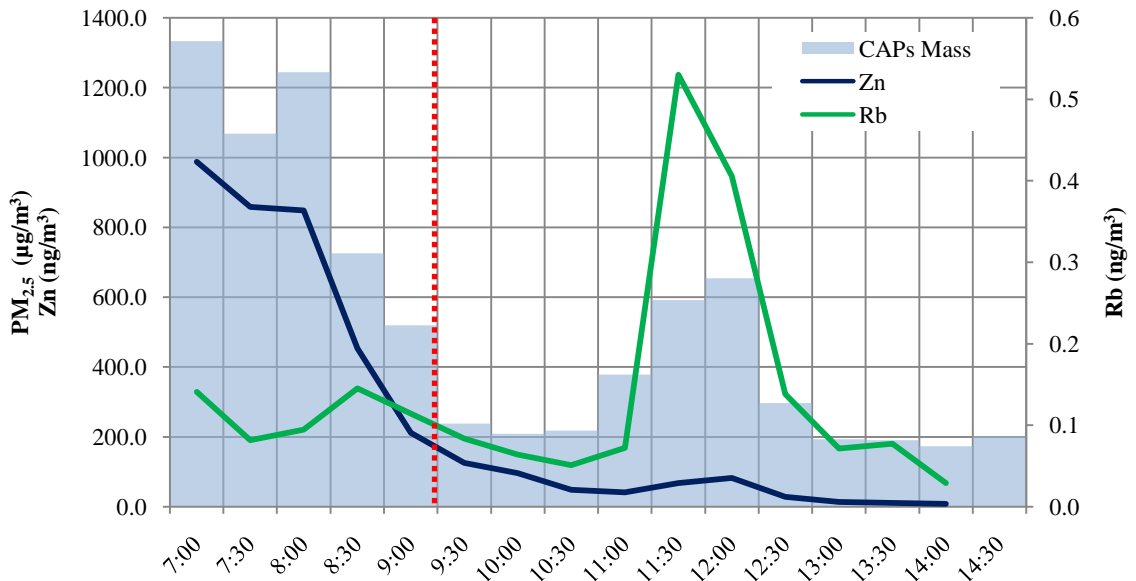
Figure III.14 Wind roses for Detroit on July 28 broken down by (a) the first 2 hours of exposure and (b) the last 6 hours of exposure. PM<sub>2.5</sub>, Zn and Rb were plotted (c) over time.

(a) 7:00-9:00

(b) 9:00-15:00



(c) AM/PM CAPs Concentrations of PM<sub>2.5</sub>, Zn and Rb



### III.1.5 HRV Analysis

#### III.1.5.1 Eight-Hour Analysis

The 8-hour statistical mean for HR and all HRV parameters were calculated for each rat to determine if CAPs-exposed rats could be statistically distinguished from the control subjects. Table III.4 summarized the means of AIR and CAPs Rats and it was found that there was a slight increase in the  $\ln(\text{SDNN})$  and  $\ln(\text{r-MSSD})$  parameters in CAPs Rats. This increase contradicts the anticipated outcome that HRV parameters decrease in the presence of elevated pollution concentrations. Statistical differences in the mean HRV for AIR Rats and the mean HRV of CAPs Rats were not identified for any parameter. In fact, mixed modeling analysis results did not indicate any 8-hour parameter that was significantly different between AIR and CAPs Rats. Table III.5 summarizes the mixed modeling results, showing all three terms in the model, Group, Date and Group\*Date. None of the p-values for the Group\*Date group are significant, thus, 8-hour data for Detroit summer was not adequate for differentiation between AIR and CAPs Rats.

**Table III.4 Detroit summer average statistics for unexposed (AIR) and exposed (CAPs) rats.**

	N	Heart Rate	$\ln(\text{SDNN})$	$\ln(\text{r-MSSD})$	$\ln(\text{LF})$	$\ln(\text{HF})$	LF/HF
AIR Rats	76	283.7	2.84	1.50	-2.39	-2.53	1.19
CAPs Rats	104	285.3	2.91	1.61	-2.42	-2.43	1.06

**Table III.5 Eight-hour HRV mixed modeling results comparing AIR and CAPs Rats during the Detroit summer study.**

<b>Parameter</b>	<b>Term</b>	<b>df N</b>	<b>df D</b>	<b>F Value</b>	<b>p Value</b>
<b>Heart Rate</b>	Group	1	12	0.18	0.6782
	Date	11	131	30.97	<.0001
	Group*Date	11	131	0.69	0.7465
<b>ln(SDNN)</b>	Group	1	12	2.24	0.1603
	Date	11	131	4.67	<.0001
	Group*Date	11	131	0.47	0.9212
<b>ln(r-MSSD)</b>	Group	1	12	1.65	0.2232
	Date	11	131	5.24	<.0001
	Group*Date	11	131	0.58	0.8412
<b>Low Frequency</b>	Group	1	12	0.35	0.5668
	Date	11	131	1.5	0.1371
	Group*Date	11	131	0.8	0.635
<b>High Frequency</b>	Group	1	12	0.82	0.3832
	Date	11	131	0.83	0.6143
	Group*Date	11	131	0.9	0.5464
<b>LF/HF Ratio</b>	Group	1	12	1.63	0.2253
	Date	11	131	1.97	0.0366
	Group*Date	11	131	0.9	0.5404

### **HRV Observed within CAPs Rats**

Even though mixed modeling results could not differentiate the CAPs-exposed rats from the control group, day-to-day variability within CAPs Rats did indicate significant changes in HRV. It is important to see if day-to-day changes in HRV in CAPs Rats are statistically different. In Figure III.15, the box-and-whisker graph shows ln(SDNN) plotted for AIR and CAPs Rats for each day of the exposure. There was profound day-to-day variability within the AIR Rats which may have created enough of a gradient to conceal the air pollution induced changes that may have occurred in the CAPs Rats. Consequently, it was worth investigating the HRV of just CAPs Rats to determine if day-to-day differences in HRV were significant. If so, then HRV in CAPs Rats can be reasonably linked with air pollution, despite the lack of significant difference from the control group.

The least-squares means method (LS Means) was applied on this dataset to determine if the ln(SDNN) of CAPs Rats was significantly different from one day to the next. In Table III.6 each day is cross referenced with all the other days and the



significance of the HRV differences was determined. The t-values are presented in order to reveal the directionality between the two days. If a significant difference existed between the days, the t-value was highlighted in red ( $p < 0.05$ ) or orange ( $p < 0.10$ ).

**Figure III.15 Box-and-whisker graph of daily ln(SDNN) for AIR and CAPs Rats.**

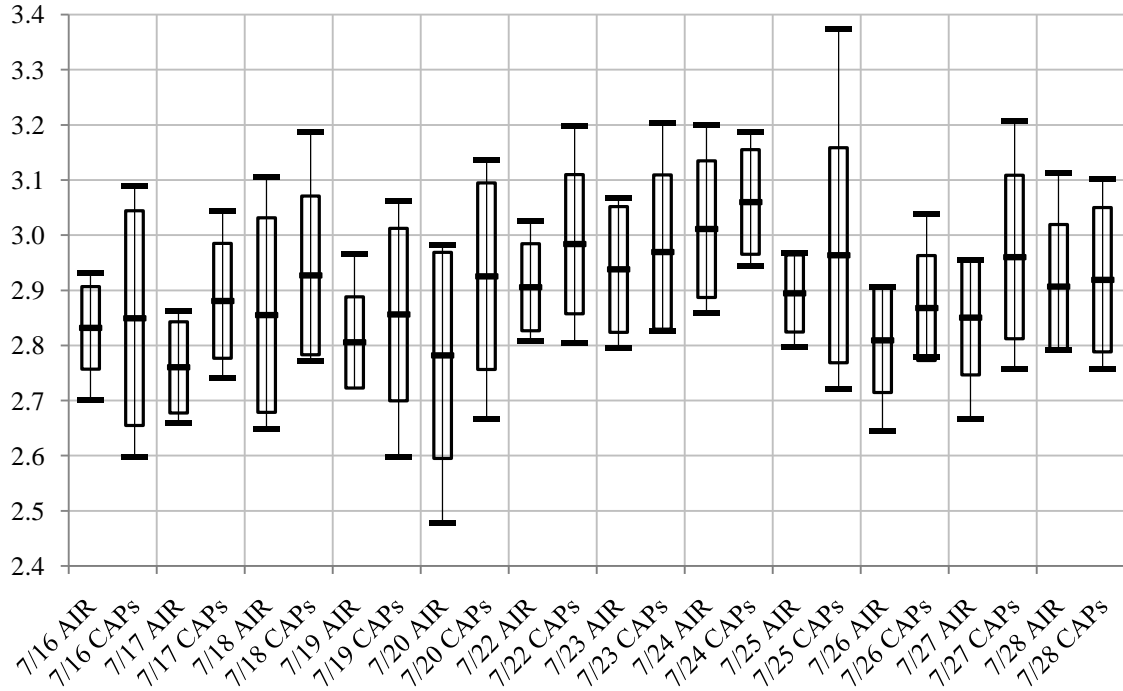


**Table III.6 Least-squares means of ln(SDNN) for CAPs rats producing day-to-day comparative analysis during the Detroit summer exposure. T-values were used to identify the strength and directionality of the relationship (Red:  $p < 0.05$ , Orange:  $p < 0.10$ ).**

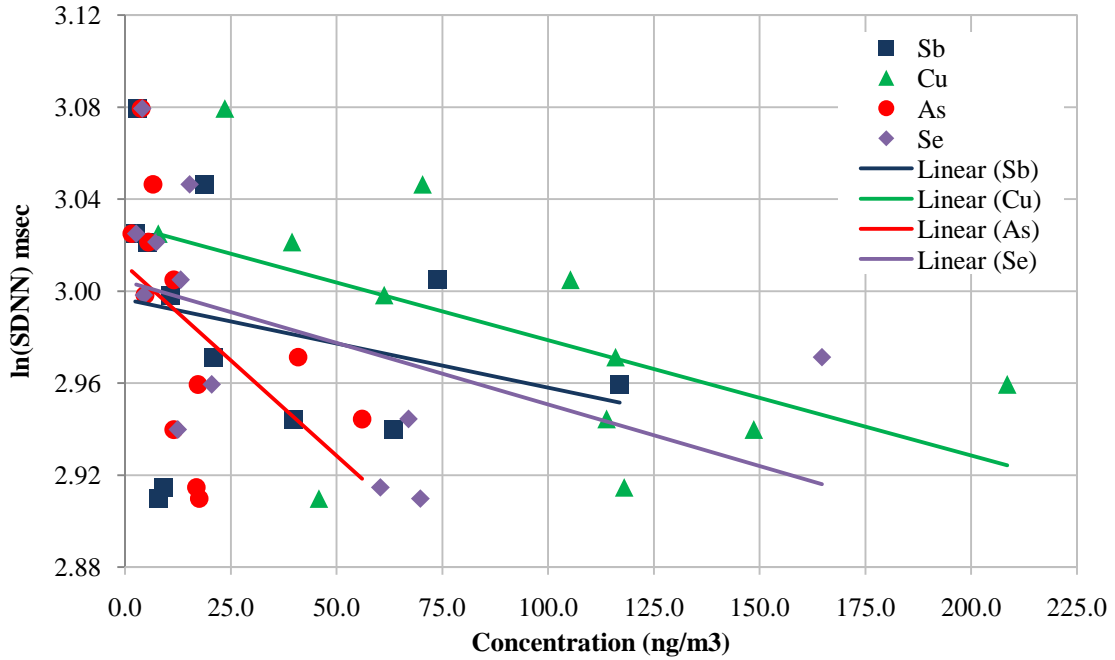
	7/17	7/18	7/19	7/20	7/22	7/23	7/24	7/25	7/26	7/27	7/28
7/16	0.55	1.37	0.12	1.34	<b>2.37</b>	<b>2.12</b>	<b>3.72</b>	<b>2.02</b>	0.33	<b>1.96</b>	1.23
7/17		0.82	-0.44	0.79	<b>1.82</b>	1.56	<b>3.17</b>	1.46	-0.23	1.4	0.67
7/18			-1.25	-0.03	1	0.74	<b>2.35</b>	0.65	-1.05	0.59	-0.14
7/19				1.23	<b>2.25</b>	<b>2</b>	<b>3.6</b>	<b>1.9</b>	0.21	<b>1.84</b>	1.11
7/20					1.03	0.77	<b>2.38</b>	0.68	-1.02	0.62	-0.11
7/22						-0.25	1.35	-0.35	<b>-2.04</b>	-0.41	-1.14
7/23							1.6	-0.1	<b>-1.79</b>	-0.16	-0.89
7/24								-1.7	<b>-3.39</b>	<b>-1.76</b>	<b>-2.49</b>
7/25									<b>-1.69</b>	-0.06	-0.79
7/26										1.63	0.9
7/27											-0.73

Within-group analysis of  $\ln(\text{SDNN})$  in CAPs Rats revealed several differences, with significantly higher  $\ln(\text{SDNN})$  on July 24 which was higher than other days of exposure. Seven of the 11 days showed significantly lower  $\ln(\text{SDNN})$  results than on July 24<sup>th</sup>. Strong southerly flow into Detroit on July 24 brought 2.57cm of rain, and subsequently lower  $\text{PM}_{2.5}$  mass during the exposure ( $11.5\mu\text{g}/\text{m}^3$ ). The significantly higher  $\ln(\text{SDNN})$  observed on this day indirectly supports the hypothesis that air pollution concentrations were associated with significant reductions in HRV. However, the most critical finding is that significant differences in CAPs Rats do exist from day-to-day. These differences can potentially be linked to CAPs concentrations. Therefore, all HRV parameters calculated for CAPs Rats were investigated for significant associations with  $\text{PM}_{2.5}$  and its constituents.

### **Eight-Hour Associations with Air Pollutants**

The LS Means findings determined that day-to-day differences in HR and HRV in CAPs Rats can occur even if overall statistical significance between AIR and CAPs Rats cannot be found. This function can test if significant changes in HRV in CAPs-exposed rats occurred, independent of the control group. Now, the HRV of CAPs Rats can be associated with air pollution concentrations to determine if a significant relationship may be statistically expressed. Descriptive analysis provided evidence that associations may exist. In Figure III.16, average  $\ln(\text{SDNN})$  for the CAPs Rats were plotted against CAPs constituent concentrations. The highest  $\ln(\text{SDNN})$  readings occurred on July 24, the same day with the lowest air pollution concentrations. These descriptive regression lines indicate that there was evidence that air pollution concentrations may influence HRV, even if  $\ln(\text{SDNN})$  was averaged over all 8 CAPs Rats. Furthermore, this observation may indicate that in the absence of air pollution,  $\ln(\text{SDNN})$  in CAPs Rats can be elevated. Specific constituents and total  $\text{PM}_{2.5}$  mass may be suppressing reductions in  $\ln(\text{SDNN})$ .

**Figure III.16 Detroit summer pollution concentrations of constituents associated with the changes in the average ln(SDNN) of CAPs Rats.**



In Table III.7, regression analysis showed the air pollutants associated with ln(SDNN) in CAPs Rats. Several constituents had a strong r-squared value than PM<sub>2.5</sub> mass, supporting the hypothesis that constituents, not PM<sub>2.5</sub> mass, may be better measures to changes in cardiovascular function. However, of all 33 pollutants investigated, only As and Cu were significantly associated with a reduction in ln(SDNN) (p<0.05). With mixed modeling analysis, these relationships were further investigated to better define the associations of each PM constituent with HRV.

**Table III.7 Regression analysis of 8-hour average ln(SDNN) in CAPs Rats with 8-hour filter samples from Detroit summer samples.**

Pollutant	r-Squared	Slope	Intercept	T Value	p Value
Cu	0.5180	-0.00058256	3.0395	-2.93	0.0189
As	0.4174	-0.00146	3.0066	-2.39	0.0436
Rb	0.3156	-0.01919	3.0260	-1.92	0.0910
V	0.2748	-0.00105	3.0021	-1.74	0.1198
Cd	0.2644	-0.01069	3.0101	-1.70	0.1284
P	0.2477	-0.0000013	2.9875	-1.62	0.1433
Co	0.2129	-0.00181	2.9919	-1.47	0.1795
NO <sub>3</sub> <sup>-1</sup>	0.1747	-0.00106	2.9965	-1.30	0.2293
PM	0.1713	-0.00004179	2.9984	-1.29	0.2344

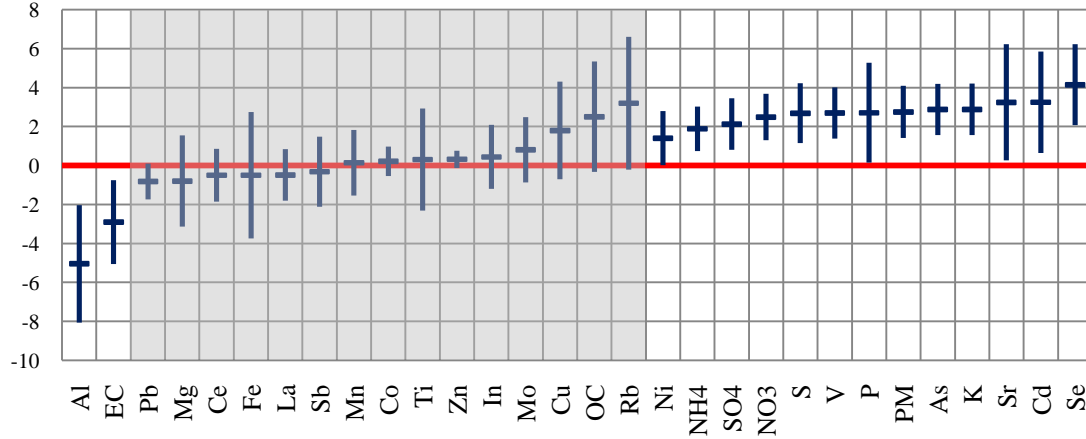
### Associating HRV with Air Pollutants

Mixed modeling was used to compare the differences in HRV across all 8 CAPs-exposed rats and normalized concentrations of the air constituents. The effect estimate of each constituent and the confidence interval (CI Plots) for each HRV parameter are given in Figure III.17 to determine which pollutants were most strongly associated with changes in cardiac function. By definition, the confidence interval must be either fully above (significant increase) or below (significant decrease) the origin to indicate that a constituent was statistically significant with changes in HRV ( $p < 0.05$ ). Specific trace elements were associated with significant increases in HR while significant decreases in ln(SDNN) and ln(r-MSSD) were also observed. For ln(SDNN), PM, As, Sb, In, K, Cd, OC, P, Rb and Cu were all found to be associated with a significant reduction. Many of the same constituents were also associated with ln(r-MSSD) but not PM, Sb, In or OC. HR did not associate with Cu, but all the other ln(SDNN) parameters were associated with a significant increase with the addition of Ni, NH<sub>4</sub><sup>+</sup>, SO<sub>4</sub><sup>-2</sup>, NO<sub>3</sub><sup>-</sup>, S, Sr and Se, as well as V that also associated with ln(r-MSSD). There were only four constituents that were significant in all 3 time-domain parameters: P, Cd, K and As. It was assumed that all four of these constituents would be highly correlated; however, K and As were significantly associated with one another ( $r^2 = 0.915$ ,  $p < 0.0001$ ) as were Cd and P ( $r^2 = 0.589$ ,  $p = 0.034$ ), but significance was not found across all four trace elements. For both ln(LF) and ln(HF), mixed modeling analysis did not reveal any trace metals or other

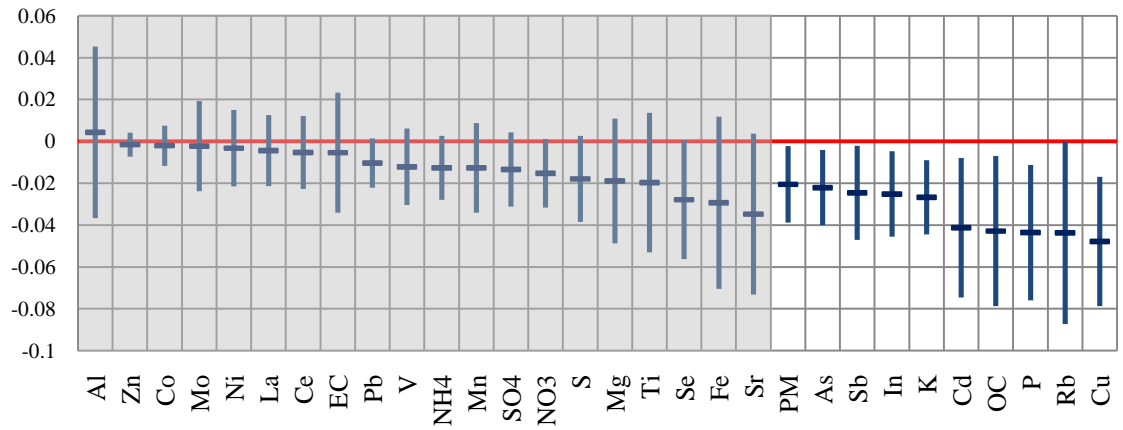
constituents associated with changes in their power. Al and Mg associated with an increase in the LF/HF ratio and only Al showed a decrease in HR, in opposition to the overall trend of HR. Therefore, frequency domain data for this model may be too vulnerable to allow for averages over an integrated time frame.

**Figure III.17 Detroit summer confidence interval plots for 8-hour average pollutant concentrations associated with HR, ln(SDNN) and ln(r-MSSD).**

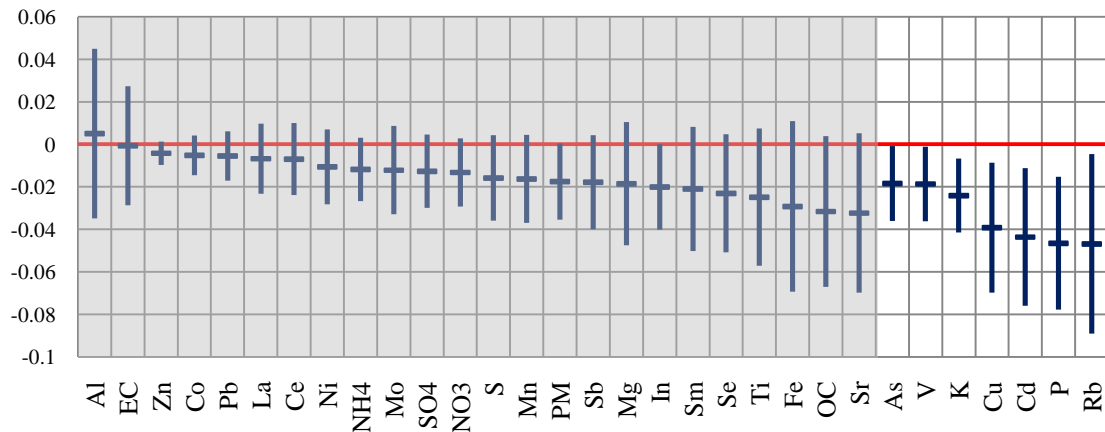
**(a) HR**



**(b) ln(SDNN)**



**(c) ln(r-MSSD)**



### III.1.5.2 Thirty-Minute Analysis

The 30-minute observations were capable of registering changes in HRV that occur within a day's exposure using mixed modeling analysis. Using the same ECG data, averaged over a shortened time scale, provided the mixed modeling with a considerably larger number of samples (16 fold) in which to identify significant changes in HRV in CAPs Rats in relation to AIR Rats. Table III.8 summarizes the three HRV parameters observed. Mixed modeling analysis of the 30-minute data revealed that  $\ln(\text{SDNN})$  was significantly different between AIR and CAPs ( $p=0.0029$ ). Heart rate showed a less than significant relationship,  $p=0.0576$ , but this helped provide supporting evidence that a biological effect in CAPs Rats occurred.

**Table III.8 Thirty-minute mixed modeling results comparing AIR vs. CAPs Rats during the Detroit summer study.**

Parameter	Term	df N	df D	F Value	p Value
Heart Rate	Group	1	12	0.21	0.6546
	Time(Date)	191	1872	11.19	<.0001
	Group*Time(Date)	191	1872	1.18	0.0576
$\ln(\text{SDNN})$	Group	1	12	1.7	0.2171
	Time(Date)	191	1872	2.87	<.0001
	Group*Time(Date)	191	1872	1.33	0.0029
$\ln(r\text{-MSSD})$	Group	1	12	1.57	0.2345
	Time(Date)	191	1872	2.54	<.0001
	Group*Time(Date)	191	1872	0.89	0.8458

### Daily HRV Comparisons

Mixed modeling analysis on 30-minute HRV data was conducted on individual days to help determine if the overall difference between AIR and CAPs Rats could be attributed to a certain day (or days) of exposure. The standard deviation in the heart rate in CAPs Rats  $\ln(\text{SDNN})$  exhibited significantly different behavior from the AIR Rats on July 16, 19 and 27. From observing the mean  $\ln(\text{SDNN})$  on each of these days, the  $\ln(\text{SDNN})$  in CAPs Rats was significantly lower in relation to AIR Rats only on July 16. SEAS data were unavailable for the majority of the exposure, but the last 90 minutes of

exposure did see elevated levels of V, Co, Ni and Cu (4.2, 0.45, 3.2 and 17.9 ng/m<sup>3</sup>, respectively). Integrated 8-hour filter samples were analyzed and concentrations of V (17.2ng/m<sup>3</sup>), S, and Se were notably higher than their means (5.8µg/m<sup>3</sup> and 69.8ng/m<sup>3</sup>, respectively). Winds on the 16<sup>th</sup> were from the southeast for the first 2 hours of exposure, and winds shifted to the northeast for the remaining six hours of exposure. For July 19, Table III.3 showed that the only trace element that exhibited a peak in concentration was Pb, with a mean of 12ng/m<sup>3</sup>. Concentrations of Pb were even higher on July 20 (23.9ng/m<sup>3</sup>), but no significant change in ln(SDNN) was observed. From the SEAS sample analysis, the elevated Pb concentration from the filter analysis may reflect the initial hours of exposure with Pb concentrations exceeding 40ng/m<sup>3</sup>. Higher than average concentrations of Sb and Zn were also observed on the morning of July 19 which may have contributed to the significant difference in ln(SDNN). Winds were consistently from the west throughout the exposure, thus early morning rise in concentration may have been a result of meteorological conditions rather than a change in source contribution. Similarly, on the morning of July 27 a peak in Cr and Ba was observed which may have caused a significant difference between AIR and CAPs Rats. The winds remained consistent throughout the day, and from the west, the same direction as seen on July 19.

### **Thirty-Minute Associations with Air Pollutants**

Thirty-minute CI Plots for the Detroit summer intensive increased the number of observations from 96 in the 8-hour dataset to 1134 observations. The CI Plots of 30-minute HRV and 30-minute pollutants are presented in Figure III.18. With SEAS data, PM<sub>2.5</sub> and 19 constituents were found to be associated with a reduction in ln(SDNN) whereas the 8-hour data set had associations with only 10. Only Sb, As and PM<sub>2.5</sub> were associated with both datasets; K, Cd, Cu, Rb and P were no longer found to be significant using the high-resolution data. Further investigation showed that the loss of significance in those five elements is likely due to the relatively low concentrations of these elements collected using the SEAS during the 30-minute collection. K, Cd, Cu, Rb and P had poor r<sup>2</sup> values between the filter data and the SEAS data (0.013, 0.134, 0.006, 0.390 and 0.021, respectively). The r<sup>2</sup> values for As and Sb concentrations were 0.736 and 0.899,



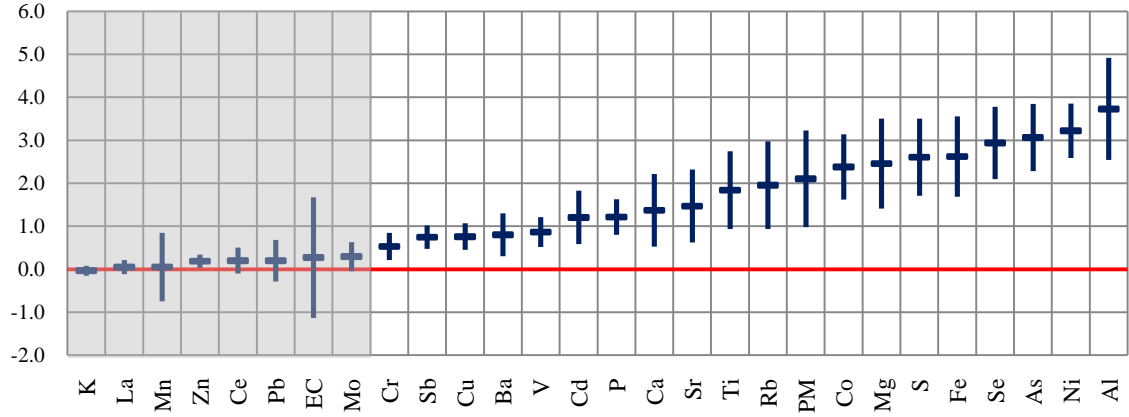
respectively, and could therefore be the reason these constituents were found significant in both datasets.

All three high-resolution CI Plots showed  $PM_{2.5}$  mass at the far right of the graph indicating that perhaps  $PM_{2.5}$  mass was driving HRV. Several constituents were also found in association with HRV, but their effect estimate was not as strong as was observed for  $PM_{2.5}$  mass. Although many constituents were found to be co-varying with  $PM_{2.5}$  mass concentrations, the only constituents associated with all three time-domain parameters were EC, As, Se and Fe. When looking at the constituents significantly associated with a reduction in  $\ln(SDNN)$ , most were significantly correlated with  $PM_{2.5}$ , but some were not (e.g. Sr, Ce, Pb, Co, Zn and Ba). In contrast, some constituents were significantly correlated with  $PM_{2.5}$  mass, but the CI Plots for  $\ln(SDNN)$  did not find a significant relationship (e.g. Rb, Cd, Al, P, S, Ni and Cu). Therefore, correlations (or co-linearity) with  $PM_{2.5}$  do not determine whether or not a constituent will also be significantly associated with HRV.

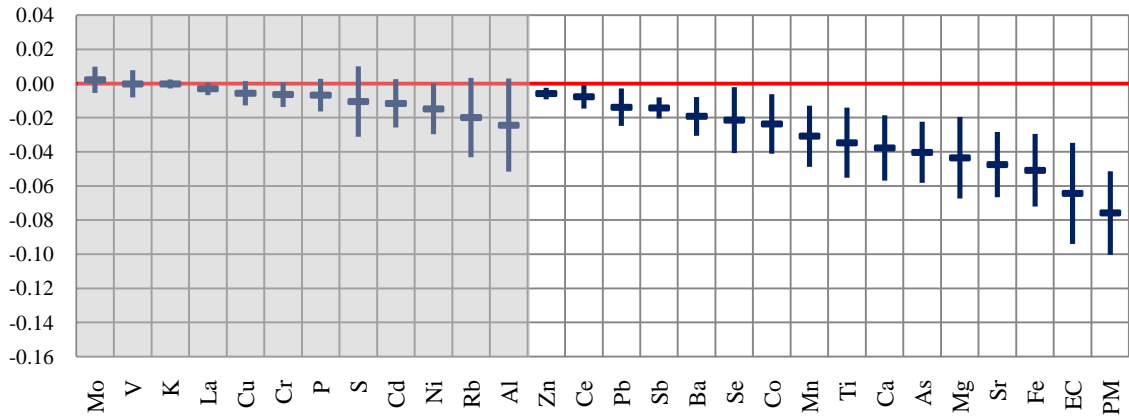
Since so many parameters were associated with HR and HRV, investigating the components not associated with HRV (K, Mo, La and V) may also be important. None of these constituents showed any association with  $\ln(SDNN)$  or  $\ln(r-MSSD)$  and may be assumed not to have any impact on HRV in Detroit, nor influence the increase in HR. K, Mo, La and V were all poorly associated with fine-fraction mass, even when removing outliers in the dataset that would have thrown off the regression with  $PM_{2.5}$  concentrations. The Pearson correlation coefficients between these 4 trace elements only found Mo and V were significantly associated with one another. This may indicate that a source contribution in Detroit that contributed Mo and V, as well as La and K, acted independently of  $PM_{2.5}$  and may have no significant impact on HRV.

**Figure III.18 Detroit summer CI Plots using 30-minute pollution data associated with each health parameter, HR, ln(SDNN) and ln(r-MSSD).**

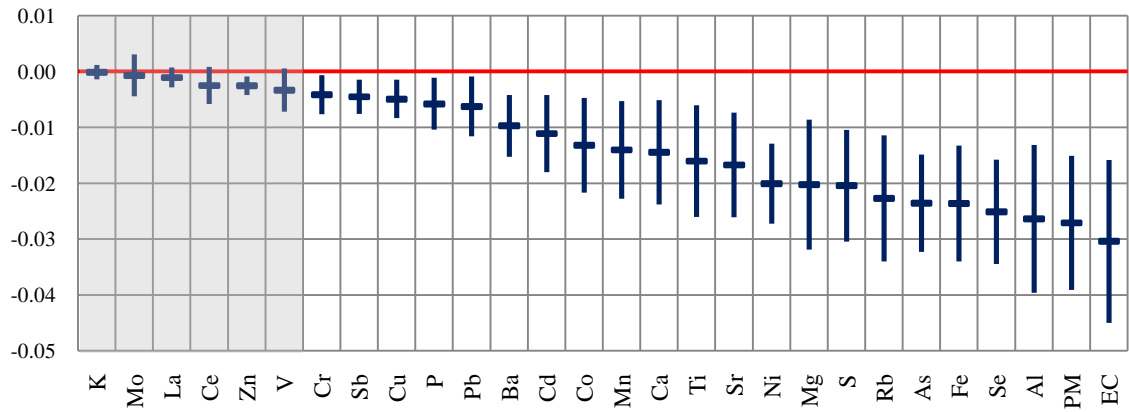
**(a) HR**



**(b) ln(SDNN)**



**(c) ln(r-MSSD)**

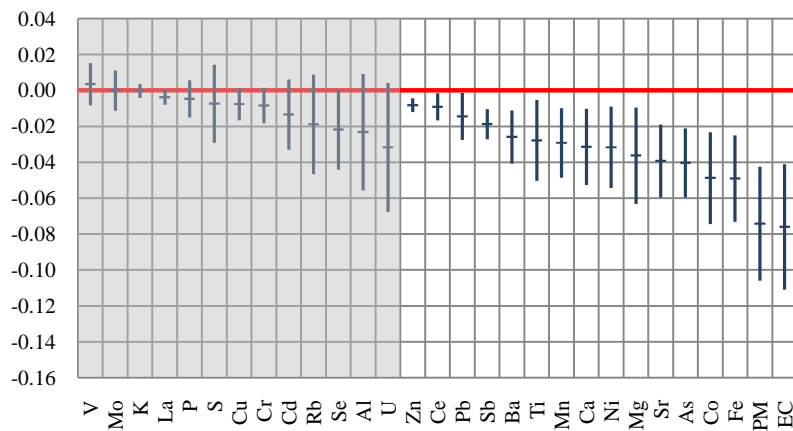


### **Testing for a Lag Effect in HRV**

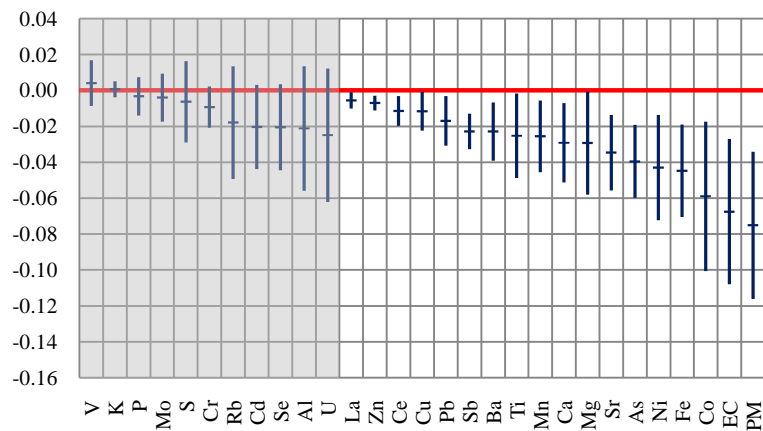
The 30-minute concentration data allowed for an analysis to determine if there is a delayed biological effect observed in the HRV due to the exposure to CAPs. A lag effect can be calculated by (1) shifting the data by increments of 30 minutes, or (2) calculating a moving average. The moving average would assume that HRV would be impacted by air pollution concentrations in real-time as well as the average air pollution concentrations from 30, 60, 90 and 120 prior. All four of these lag periods were explored. A shifted lag would assume that HRV was influenced by air pollution incrementally by 30, 60, 90 or 120, independent of real-time concentrations or concentrations at any prior point. Preliminary results from a shifted lag did not find as strong associations as those found using a cumulative lag. Thus the moving average was used to provide a better assumption on real-world exposures to ambient air pollution. In Figure III.19 the  $\ln(\text{SDNN})$  was used to provide an example how the CI Plots are shifted during a lag period.

**Figure III.19** For the Detroit summer intensive,  $\ln(\text{SDNN})$  was associated with 30, 60, 90 and 120 minute moving average lags of pollutant concentrations.

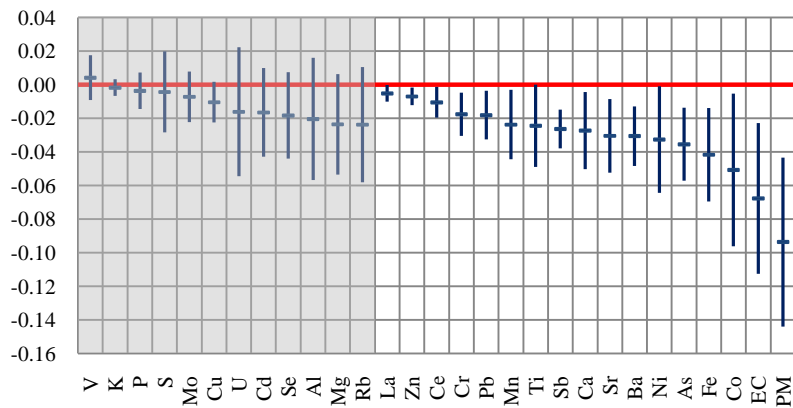
**(a.) 30-Minute Lag**



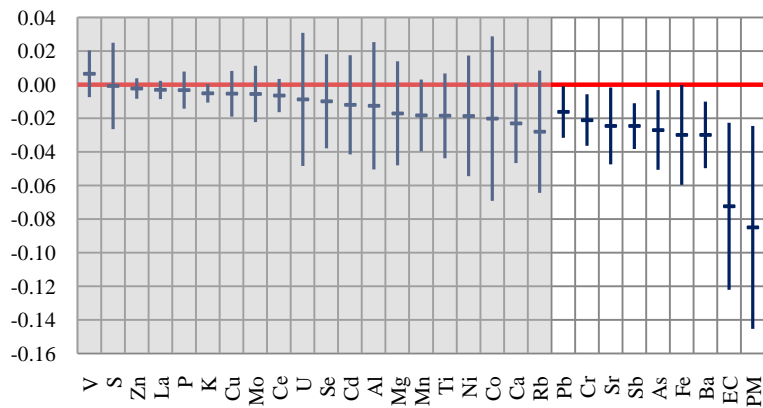
**(b.) 60-Minute Lag**



**(c.) 90-Minute Lag**

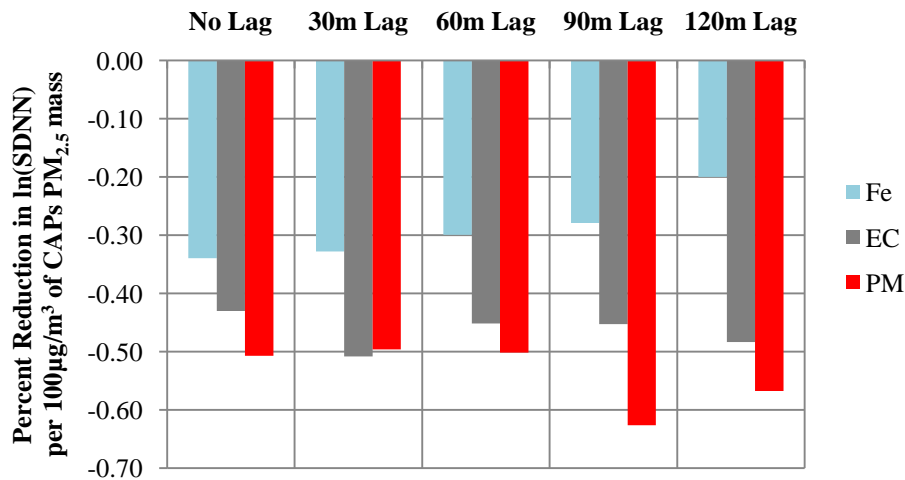


**(d.) 120-Minute Lag**



From the original CI Plot with real-time concentrations, 17 pollutants were associated with a reduction in  $\ln(\text{SDNN})$ , with Fe, EC and PM associated with the strongest reduction in  $\ln(\text{SDNN})$ . The effect estimates for these three pollutants were converted to a percent reduction and presented with their subsequent lag data in Figure III.20. As the lag period was applied, the associations with Fe were weakened. For most of the trace elements, the associations were not as strong as the concurrent concentrations associated with HRV. In some instances, constituents changed the order on the CI Plots, which in turn affected their statistical significance. After a 120-minute lag, only a few trace elements were still associated with a reduction in  $\ln(\text{SDNN})$ , and their percent reductions were not as large as they had been during real-time associations. EC, however, seemed unchanged during each lag period, but total PM mass was actually strengthened during the 90-minute lag. Concurrent data showed that a 0.50% reduction in  $\ln(\text{SDNN})$  was associated with every  $100\mu\text{g}/\text{m}^3$ , and the 90-minute lag period increased its influence to a 0.63% reduction in  $\ln(\text{SDNN})$ . With the mean concentration in Detroit over the summer at  $809\mu\text{g}/\text{m}^3$ , these concentrations would affect the total reduction in  $\ln(\text{SDNN})$  from 4% to nearly a 5% reduction. Thus, no significant influence of a lag in  $\text{PM}_{2.5}$  mass appears to exist; but with some trace elements, the lag analysis observed a change in the effect estimate, albeit that change was less than 1% different than the real-time association.

**Figure III.20 The lag effect on the percent reduction in  $\ln(\text{SDNN})$  for three pollutants most associated  $\ln(\text{SDNN})$  in real-time, PM, EC and Fe.**



### III.1.6 Detroit Summer Summary

Atmospheric concentrations and meteorology during the two weeks Detroit summer study were fairly typical for this location. The 8-hour daily exposure resulted in distinctly different  $PM_{2.5}$  composition and mass that enabled a meaningful day-to-day analysis of the importance of fine-fraction mass on CAPs-exposed rats. The only HRV parameter that found significant differences between AIR and CAPs Rats was  $\ln(\text{SDNN})$  using the 30-minute dataset.

The urban mix found in Detroit revealed that several constituents of  $PM_{2.5}$  were highly correlated with  $PM_{2.5}$  mass. Many of the same constituents that were associated with 30-minute  $\ln(\text{SDNN})$  were also found to reduce  $\ln(r\text{-MSSD})$  and were associated with an increase in HR. These findings are consistent with previous HRV studies indicating an up-regulation of the sympathetic nervous response or a down-regulation of the parasympathetic response.<sup>60,61</sup>

The strongest associations with all three time-domain parameters were  $PM_{2.5}$ , EC, Al, Fe, As, and Se. Subsequently, results from the Detroit summer study could not distinguish between the effects of individual constituents and fine-fraction mass in relation to HR and HRV. However, this first exposure study provided a strong example how fine-fraction mass may be driving the changes in HRV. One possible explanation is that  $PM_{2.5}$  mass was so high in Detroit that even if the effects of individual constituents were present, fine-fraction mass concentrations outweighed any other underlying effect. Another possibility is that the effect was a synergistic combination of  $PM_{2.5}$  and several constituents. However, the strong co-linearity of all the constituents was very high in the 30-minute dataset, and too few instances existed where constituents could have a different effect than fine-fraction mass.

The Detroit summer study took a comprehensive look at the differences in associations between the 8-hour and 30-minute datasets. Using 30-minute data provided a larger, more robust dataset, allowing for a greater likelihood of identifying significant differences between AIR and CAPs Rats and identifying associations between HRV and air pollution concentrations. Also, the high-resolution data was also allowed to capture more subtle, short-term peaks in air pollution concentrations that would be veiled under a single 8-hour average. Likewise, short-term declines or escalations in HRV would have

been lost using a single 8-hour average for each rat. Detroit summer findings supported this result with evidence that  $\ln(\text{SDNN})$  was significantly different in CAPs Rats using the 30-minute dataset, not the 8-hour dataset. Furthermore, the number of high-resolution constituents associated with HR and HRV was larger than it was identified in the 8-hour dataset. Although 30-minute data allowed for the investigation of lag effect in HRV, findings reported that the strongest associations with  $\text{PM}_{2.5}$  and constituents were more often strongest in real-time than with subsequent lags.

The Detroit summer intensive laid the groundwork to look at the remaining three exposures by comparing high-resolution HRV and air pollution against the 8-hour dataset. The HRV time-domain parameters behaved predictably, observing a significant increase in HR and reductions in HRV in association with  $\text{PM}_{2.5}$  and its constituents. The remaining three exposures did not have quite the same clear associations or the same statistical significance. Instead of repeating the same statistical tests done during the Detroit summer study, each of the remaining exposures will be investigated further to better understand the driving forces behind their distinctive findings.

## III.2 Detroit Winter Exposure

### III.2.1 Meteorological Summary

Differences in atmospheric conditions, from summer to winter exposures, at the Detroit sampling site were profound and allow for a strong comparison in the impacts of PM<sub>2.5</sub> between seasons at this site. The following section includes a discussion of the seasonal differences found in air pollution in Detroit and how these distinctions affected HRV in CAPs-exposed rats.

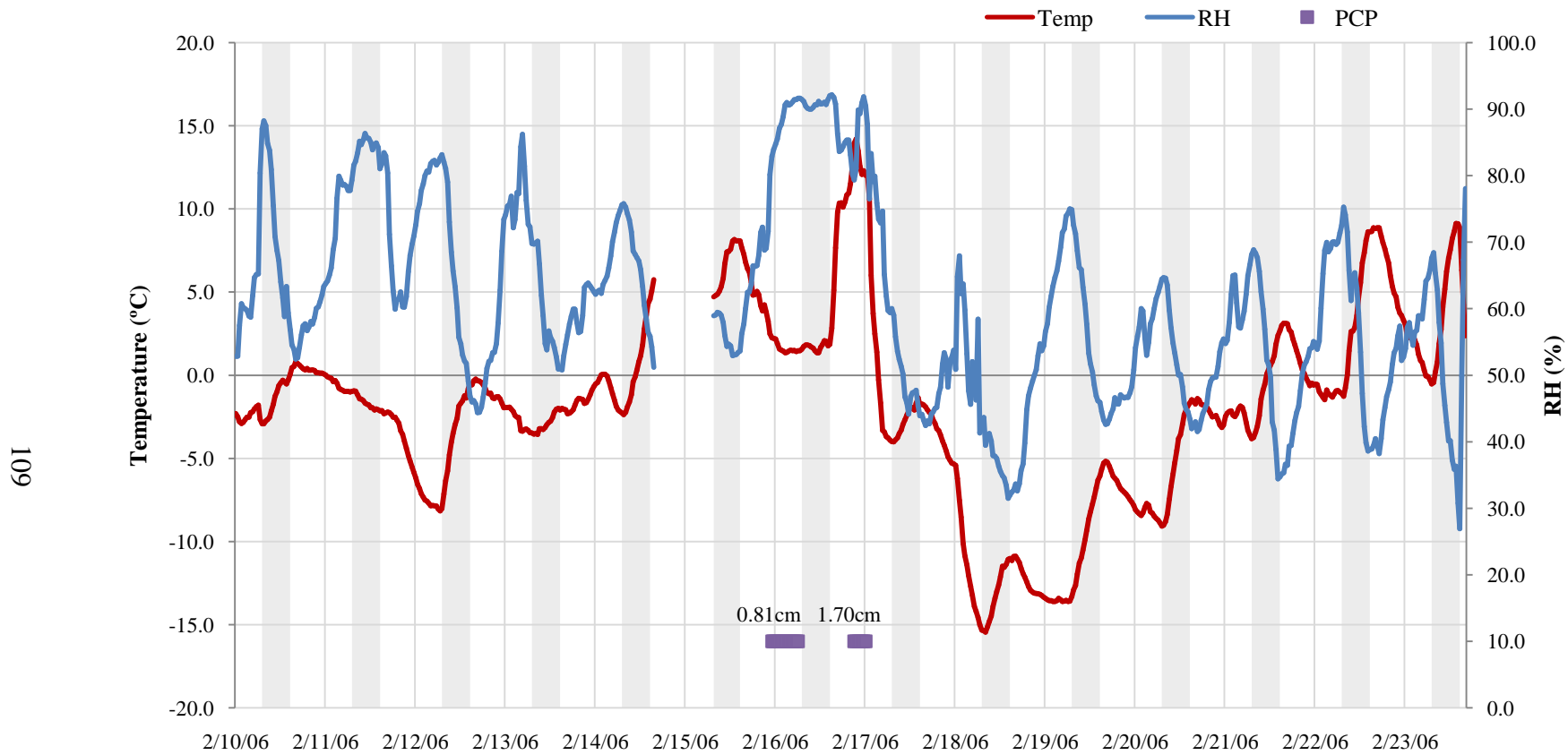
#### Climate and Precipitation

In the Midwestern region, wintertime reductions in solar radiation reaching the ground results in significantly lower atmospheric temperatures and significant changes in air pollution chemistry.<sup>41</sup> The loss of UV light hinders many of the photochemical reactions, especially the formation of secondary SO<sub>4</sub><sup>-2</sup> as described in Chapter I.<sup>66</sup> Average temperatures in the winter were  $-1.8 \pm 5.7^{\circ}\text{C}$  (Exposure Hours:  $-1.7 \pm 5.6^{\circ}\text{C}$ ) and relative humidity averaged  $69.1 \pm 17.5\%$  (Exposure Hours:  $61.0 \pm 16.2\%$ ). In Figure III.21, temperature and humidity expressed the same diurnal changes as was observed in the summertime exposures. Daylight hours (approximately 7:30am to 6:00pm, EST) had a slightly larger average temperature and humidity ( $-0.97 \pm 5.6^{\circ}$ ,  $58 \pm 17\%$ ) than the nighttime hours ( $-2.4 \pm 5.7^{\circ}$ ,  $64 \pm 13\%$ ). The differences in the means were not as large as the wide range in temperature and humidity suggests in Figure III.21. Both wintertime temperature and humidity were in the normal range for Detroit; and therefore the two-week period during exposure hours adequately represented the winter conditions.

Weather conditions during the two-week winter intensive were quite different than those that occurred during the summer. Two substantial snow events took place before the start of the exposure on February 16 (0.81cm) and before the exposure hours on February 17 (1.70cm). These two days were strongly influenced by a low-pressure system that remained static for an extended period of time directly over southeast Michigan. Other days during the two-week period observed trace amounts of snow flurries ( $<0.025\text{cm}$ ), but with no measureable accumulation.



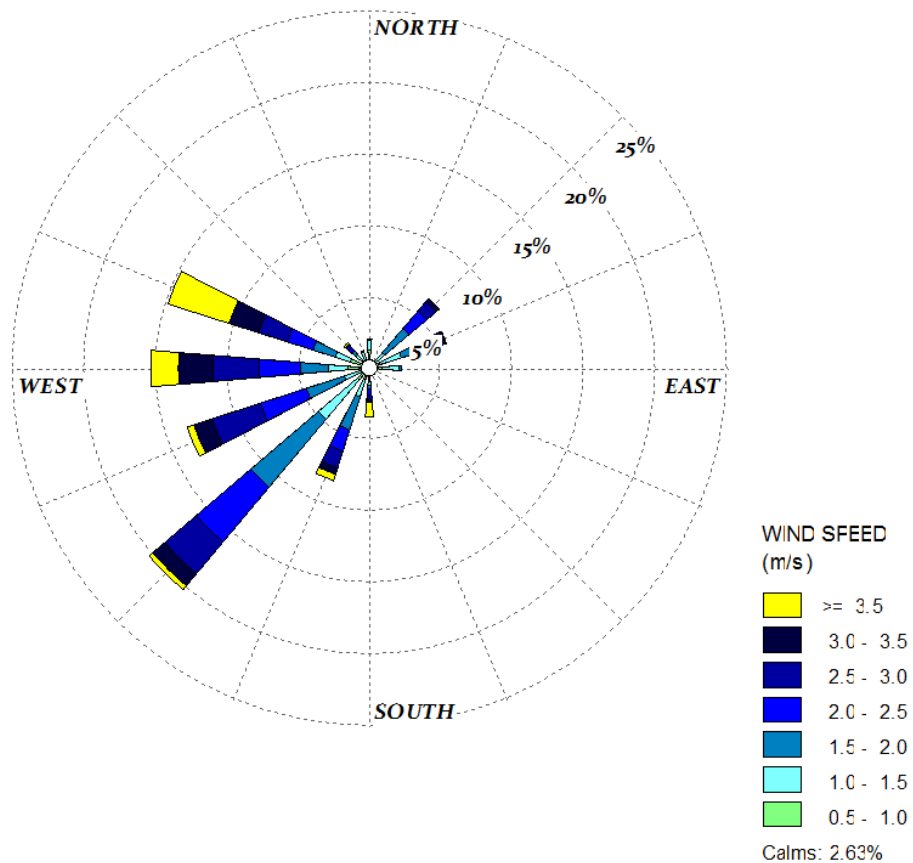
Figure III.21 Hourly temperature and RH for the Detroit winter study with exposure hours shaded in grey.



## Wind Patterns

The wind rose in Figure III.22 was plotted for the entire two-week winter exposure in Detroit. Winds from the west and southwest winds were still prevalent, but there was a much larger frequency from the northwest, which is typical during winter months. Somewhat surprisingly, winds coming from other directions were not common and the resultant wind vectors for the summer and winter were  $257^\circ$  and  $260^\circ$ , respectively. However, winds during the winter are typically stronger, consistent with this Detroit exposure period. Summertime wind speeds averaged 1.3m/s while the winter average speed averaged 2.0m/s.

**Figure III.22** Wind rose capturing air flow during the exposure hours in the Detroit winter study.



## III.2.2 Ambient Air Pollution Levels

### PM<sub>2.5</sub> Mass Concentration

The average ambient PM<sub>2.5</sub> concentration during the Detroit winter study was  $9.9 \pm 4.6 \mu\text{g}/\text{m}^3$ , (Exposure Hours:  $9.8 \pm 5.3 \mu\text{g}/\text{m}^3$ ), which was lower than the average fine mass observed during the summer exposure ( $16.9 \pm 11.0 \mu\text{g}/\text{m}^3$ ) in Detroit. The range in the 30-minute average PM<sub>2.5</sub> is shown in Figure III.23 and ranged from 1.3 to  $32.7 \mu\text{g}/\text{m}^3$ . This range was much narrower than the range observed during the summer study. Furthermore, the diurnal pattern observed during the summer intensive was not as defined during with winter study. Instead, a more jagged variability existed that did not strongly influence mean PM<sub>2.5</sub> concentrations during the daytime and nighttime hours ( $10.0$  and  $9.7 \mu\text{g}/\text{m}^3$ , respectively).

### PM<sub>2.5</sub> by Wind Direction

In the Detroit winter intensive, 30-minute mass concentrations had elevated concentrations from the south and southwest, similar to the pattern found in the summer intensive. In Table III.9, the average PM<sub>2.5</sub> concentration is given from each wind direction. The southeast has the highest mass, but was driven by only three 30-minute averages. In Figure III.24, the pollution rose for ambient PM<sub>2.5</sub> was plotted and identified a larger number of elevated measurements from the east. These easterly concentrations reflect air masses on two separate occasions: February 11 and 16. These two days showed surface wind exclusively from the east-northeast; however, the likely air mass transport was projected from the southwest. Figure III.25 shows the HYSPLIT models for both the 11<sup>th</sup> and the 16<sup>th</sup>. Therefore, the pollution rose may disproportionately show higher ambient pollution from the east-northeast when the contributions of high PM<sub>2.5</sub> on these two days were actually from the southwest.

**Table III.9 Average ambient PM<sub>2.5</sub> (µg/m<sup>3</sup>) concentrations during the two-week Detroit winter exposure period by wind direction.**

	<b>Frequency</b>	<b>PM<sub>2.5</sub> Mean</b>
N	16	7.3±3.9
NE	65	9.8±23.8
E	24	15.0±3.5
SE	3	20.2±3.9
S	42	17.3±5.2
SW	220	10.4±3.4
W	181	7.5±3.2
NW	59	7.4±4.4

**Figure III.23 Thirty-minute ambient PM<sub>2.5</sub> from February 10-23, 2006 in Detroit. Exposure hours are indicated with grey bands.**

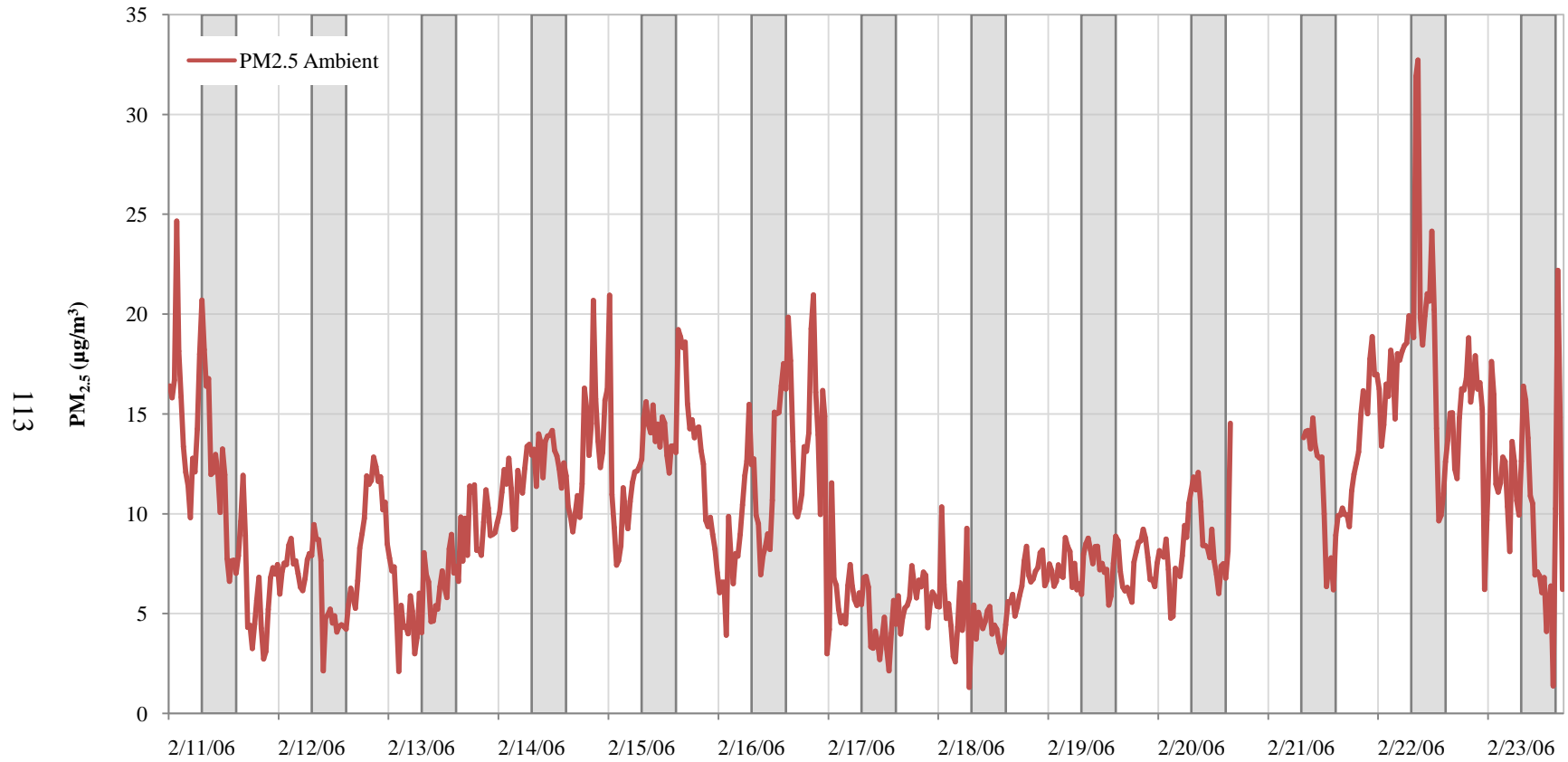


**Figure III.24 Thirty-minute ambient PM<sub>2.5</sub> ambient concentrations ( $\mu\text{g}/\text{m}^3$ ) for the Detroit winter study from February 10-23, 2006, by wind direction.**

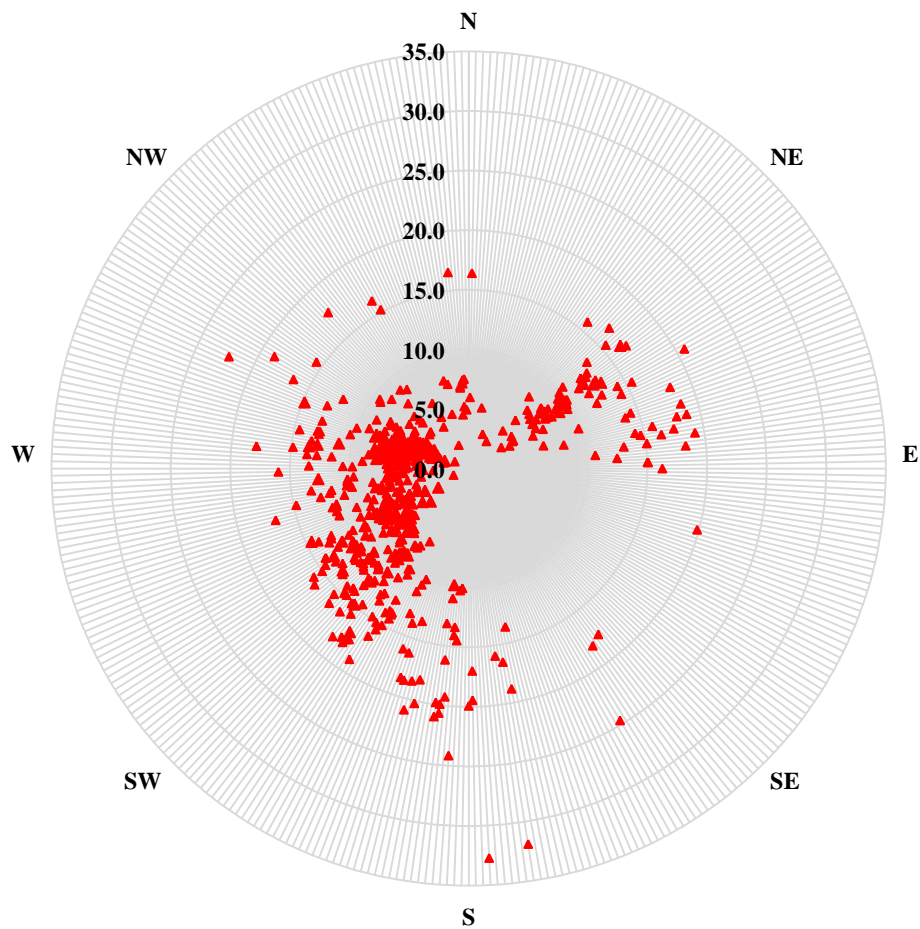
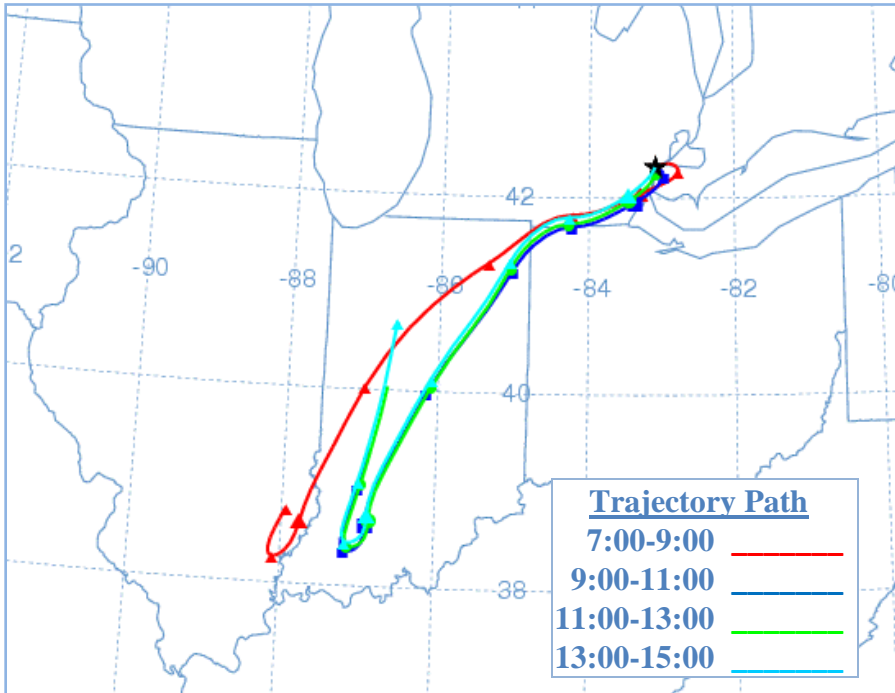
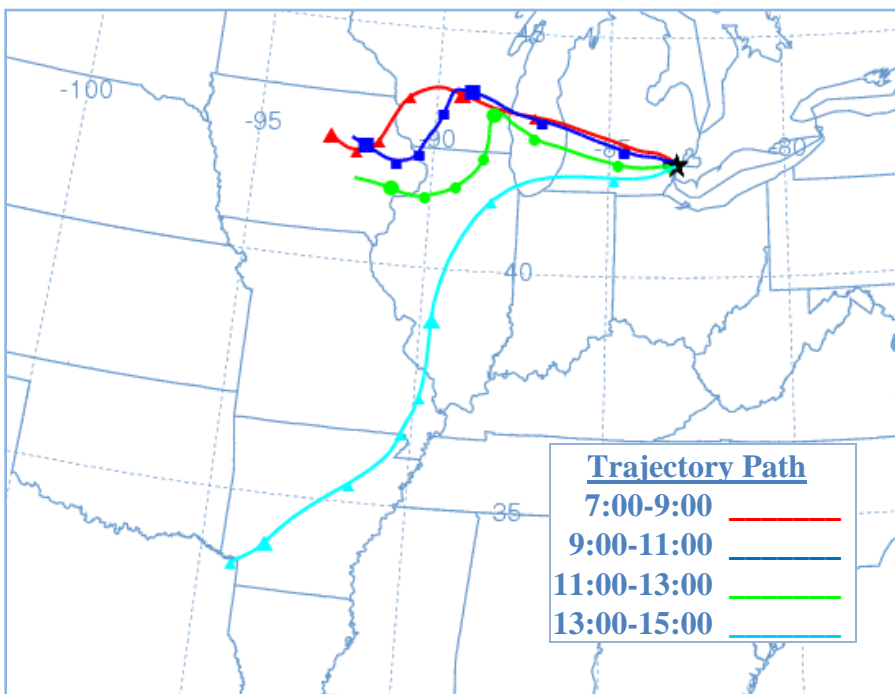


**Figure III.25 Backward trajectories from the Detroit site showing the path of highest probability of air mass transport on February 11 and 16, 2006.**

**(a) February 11, 2006**



**(b) February 16, 2006**



### Ambient Gas Concentrations

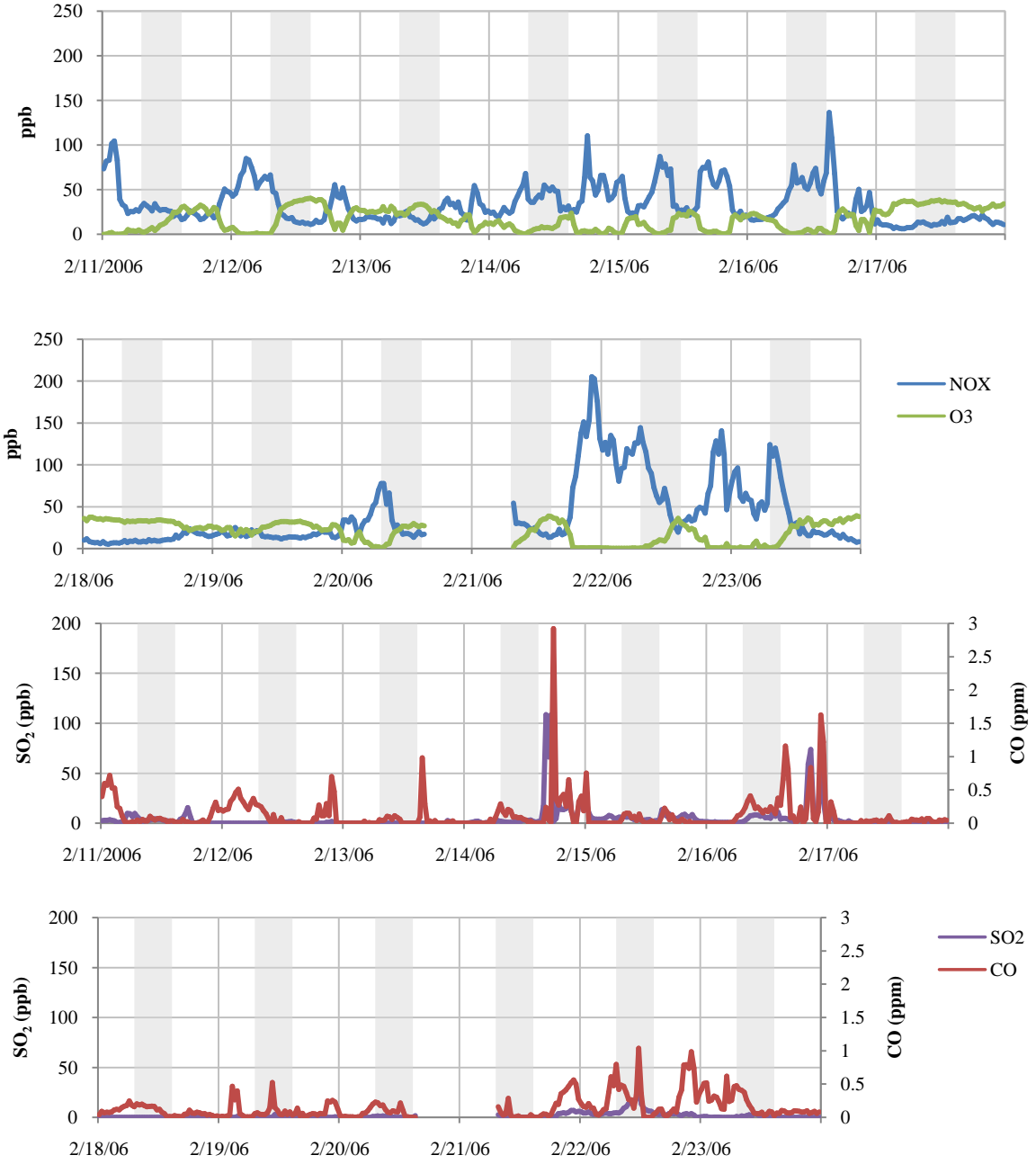
Ambient gaseous pollutants were plotted in Figure III.26 for the February 10-23, 2006 exposure period. Two periods during the winter intensive were observed with elevated concentrations of NO<sub>x</sub>, SO<sub>2</sub> or CO. On February 22, the overnight NO<sub>x</sub> concentrations were elevated for several hours and briefly exceeded 200ppb. The other gaseous pollutants did not appear to be correlated with NO<sub>x</sub>. However, PM<sub>2.5</sub> concentrations were greater than 20µg/m<sup>3</sup> in the early morning hours of the 22<sup>nd</sup> with southwest winds. NO<sub>x</sub> concentrations dropped before the exposure at 7:00am, at approximately the same time when the sun was rising and O<sub>3</sub> concentrations increased slightly. Short-term peaks in the concentrations of SO<sub>2</sub> and CO were observed on February 14, after exposure hours (108ppb and 2.9ppm, respectively). The elevated concentrations on February 14 were observed with a brief and moderate increase in ambient PM<sub>2.5</sub> (21µg/m<sup>3</sup>) while winds were from the south. Temperatures and RH were not significantly higher during the peaks on the 22<sup>nd</sup> or the 14<sup>th</sup>, nor did a synoptic event occur in the meteorology.

**Table III.10 A comparison of the gaseous pollutant concentrations from the two-week seasonal exposure studies in Detroit.**

	Detroit Summer	Detroit Winter
NO <sub>x</sub> (ppb)	20.5±16.3	36.6±32.2
CO (ppm)	0.52±0.25	0.17±0.26
O <sub>3</sub> (ppb)	33.5±21.2	18.4±12.7
SO <sub>2</sub> (ppb)	5.9±5.6	5.9±13.8



**Figure III.26 Thirty-minute ambient gas concentrations measured at the Detroit site from February 11-23, 2006 with exposure hours highlighted by the grey bars.**



### III.2.3 CAPs PM<sub>2.5</sub> Characterization

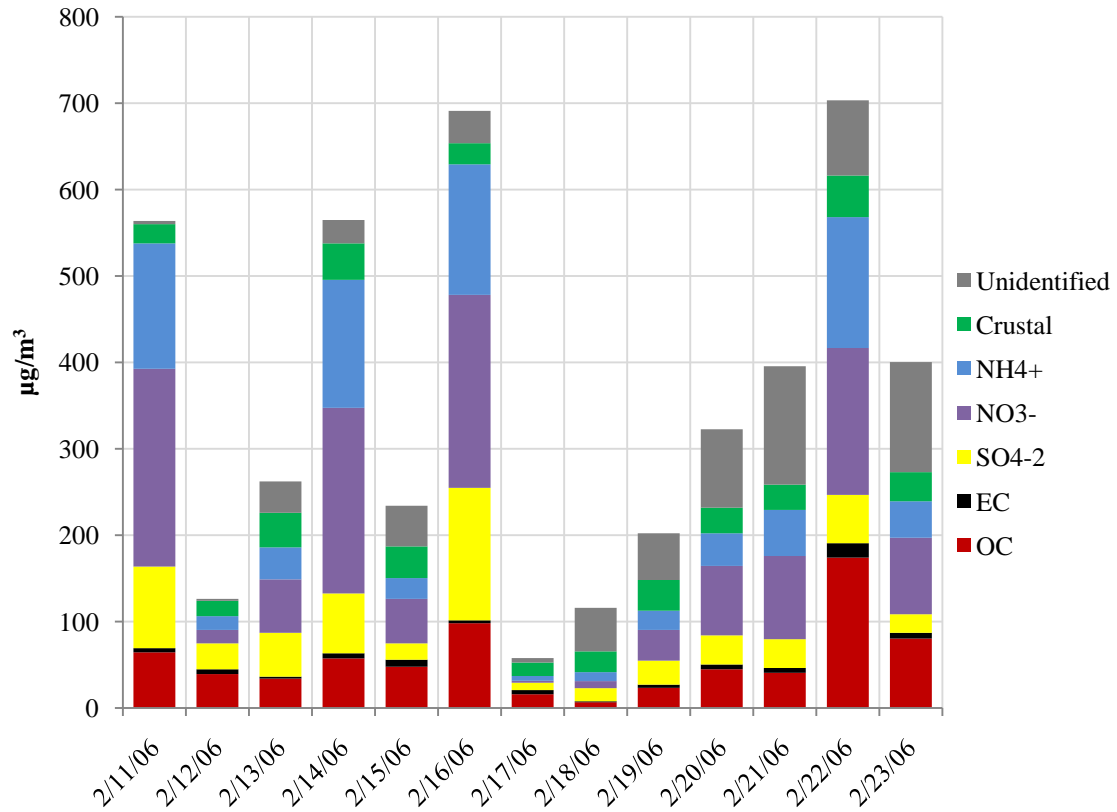
Thirty-minute PM<sub>2.5</sub> CAPs mass during the Detroit winter exposure ranged from 72 to 733  $\mu\text{g}/\text{m}^3$  and averaged  $366 \pm 262 \mu\text{g}/\text{m}^3$ . Although this mass concentration was considerably lower than the Detroit summer study (e.g.  $795 \mu\text{g}/\text{m}^3$ ), there may be enough daily variability in CAPs mass to associate with significant day-to-day changes in HRV. Also, there is not the large discrepancy between the TEOM and filter mass as was observed in the summer study. Gravimetric mass data for PM<sub>2.5</sub> CAPs during the Detroit winter study was nearly identical, averaging  $357 \pm 218 \mu\text{g}/\text{m}^3$ .

In Figure III.27, the graph shows the daily mass contributions of the major contributions to CAPs. The largest difference in the mass can be accounted for in terms of the  $\text{SO}_4^{-2}$  concentration peaking in the warmer months in the northeast U.S. and the increased formation of  $\text{NH}_4\text{NO}_3$  in the winter with the absence of the acidic  $\text{SO}_4^{-2}$ . The mean concentration of  $\text{SO}_4^{-2}$  accounted for only 13% of the CAPs mass in the winter, compared to 23% in the summer. On February 16, HYSPLIT determined that the air mass passed over Chicago, which may explain the larger than normal  $\text{SO}_4^{-2}$  contribution (22%) for the wintertime exposure. The EC concentrations did not show a seasonal difference in the contribution to CAPs; summer and winter EC mass contributions were both  $5.7 \mu\text{g}/\text{m}^3$ , attributing to 1.1 and 1.7% of the mass, respectively. Wintertime OC mass contributions were one-third of the mass in the summer composition (56 and  $159 \mu\text{g}/\text{m}^3$ , respectively), attributing to only 16% of the mass in the winter (summertime OC contribution: 31% of CAPs).

**Table II.11 Daily Concentrations of the major components of PM<sub>2.5</sub> CAPs collected during the 8-hour exposures (µg/m<sup>3</sup>).**

	<b>PM</b>	<b>OC</b>	<b>EC</b>	<b>SO<sub>4</sub><sup>-2</sup></b>	<b>NO<sub>3</sub><sup>-</sup></b>	<b>NH<sub>4</sub><sup>+</sup></b>	<b>Crustal</b>
2/11	563.5	64.5	4.9	94.2	228.9	145.3	22.2
2/12	126.4	39.4	5.6	29.8	15.6	15.8	18.1
2/13	262.2	34.1	2.3	50.7	61.9	36.8	40.0
2/14	564.9	57.4	5.7	69.3	215.1	148.0	42.1
2/15	234.0	47.9	8.0	18.8	51.6	24.2	36.4
2/16	691.2	98.1	3.3	153.3	223.6	150.9	24.6
2/17	57.9	15.9	4.7	8.7	2.3	5.5	15.6
2/18	116.1	6.8	1.0	15.1	8.3	10.2	24.1
2/19	202.3	23.4	3.7	27.5	35.6	22.3	35.8
2/20	322.8	44.7	5.8	33.5	80.5	37.8	29.6
2/21	395.4	40.8	5.4	33.4	96.3	53.2	29.2
2/22	703.4	173.9	16.7	56.2	170.0	151.3	48.2
2/23	400.4	80.4	6.7	21.6	88.2	42.5	33.7
Mean	357.0	55.9	5.7	47.1	98.3	64.9	30.7
Std Dev.	218.1	43.4	3.8	39.9	83.5	59.7	9.7

**Figure III.27 Composition of PM<sub>2.5</sub> from analysis of CAPs filter samples collected during 8-hour exposures for the Detroit winter study (µg/m<sup>3</sup>).**



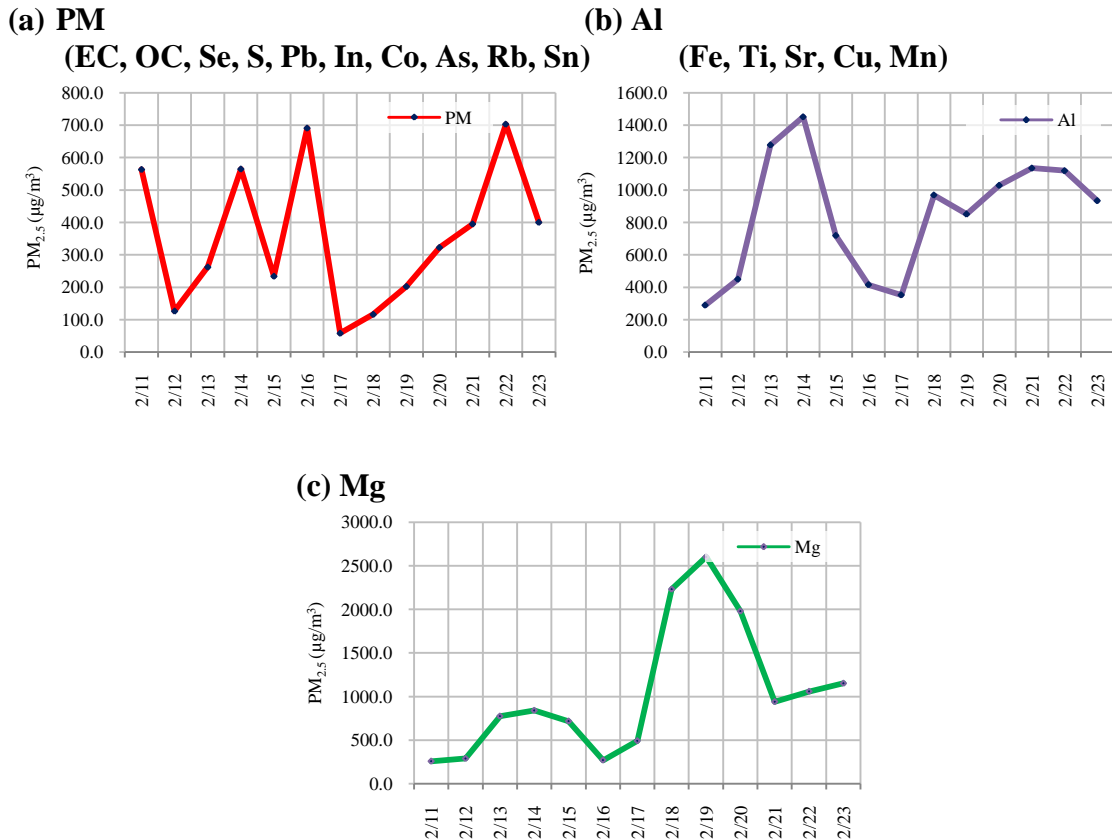
### Trace Element Concentrations

Not all trace element concentrations obtained from the integrated filter samples on the exposure chamber were well correlated with the total CAPs fine mass. This was not unexpected as these compositional differences in PM<sub>2.5</sub> were hypothesized to influence the day-to-day differences in HRV better than fine mass. Table III.12 summarizes the daily concentrations and Figure III.28a shows plots of these findings for PM<sub>2.5</sub>, and prominent peaks are present on February 11, 14, 16 and 22. Constituent concentrations of EC, OC, Se, S, Pb, In, Co, As, Rb and Sn appeared co-linear to PM<sub>2.5</sub>. S, La, Ce, Sm, V Mo and Ni had their highest peak on the 16<sup>th</sup>, but otherwise co-varied with PM<sub>2.5</sub>. Similarly, Sb and Cr had the highest mass on the 11<sup>th</sup>, Cd had an independent peak on February 21, Zn had a peak February 13 and K had a peak on February 19; otherwise, all these trace elements were co-linear to PM<sub>2.5</sub>. Al, shown in Figure III.28b, had its highest mass on the February 14 and 13, respectively; Fe, Ti, Sr, Cu, Mn co-varied with Al. Mg behaved independent of all other trace elements as shown in Figure III.28c.

**Table III.12 Average CAPs concentrations of the fine mass components in ng/m<sup>3</sup> \*Units for PM, S, K and Fe are µg/m<sup>3</sup>.**

	PM*	Mg	Al	P	S*	K*	Ti	V	Cr	Mn	Fe*	Co	Ni	Cu	Zn	As	Se	Rb	Sr	Mo	Cd	Sn	Sb	La	Ce	Pb
2/11	563.5	258.2	289.1	197.1	36.1	1.3	13.6	11.3	149.2	68.3	1.6	0.88	13.7	46.5	443.1	16.4	44.4	2.43	5.4	4.4	1.74	8.8	37.9	1.3	0.7	42.3
2/12	126.4	289.4	449.5	208.4	12.6	0.9	17.5	3.2	34.4	28.8	2.1	0.78	22.9	45.8	322.6	12.3	9.9	1.34	8.7	2.8	1.37	3.0	14.0	0.6	0.6	18.9
2/13	262.2	774.9	1278	376.3	20.9	1.6	23.4	4.7	35.4	197.5	5.0	0.79	21.6	62.7	2098	9.6	6.4	3.73	14.8	5.3	1.66	5.4	6.1	7.8	4.8	43.6
2/14	564.9	840.9	1451	276.9	28.6	1.9	48.7	8.0	34.4	203.3	4.8	0.86	5.1	93.6	1518	12.9	28.9	4.17	20.4	6.7	3.52	13.4	8.9	38.1	22.3	68.1
2/15	234.0	717.8	719.1	NA	7.1	1.4	36.2	6.8	26.6	127.0	4.7	0.85	17.6	60.4	751.5	8.6	19.6	3.13	24.7	6.4	2.43	10.1	11.4	5.5	3.6	62.2
2/16	691.2	270.8	415.7	277.6	49.4	1.3	24.8	240.6	18.3	138.2	2.5	1.03	54.5	68.4	837.9	12.3	32.8	2.52	10.8	396.2	5.04	15.6	14.8	4.4	1.9	71.6
2/17	57.9	492.5	352.4	87.0	3.5	0.7	11.7	2.0	14.3	35.6	0.9	0.39	3.5	25.9	106.4	7.8	2.0	0.95	9.7	2.3	1.09	2.6	11.0	0.3	0.6	31.8
2/18	116.1	2232	968.7	136.3	6.3	1.3	10.3	2.3	4.5	20.6	0.9	0.21	0.7	12.2	135.1	4.3	1.3	1.47	17.0	0.9	0.80	2.1	2.8	0.2	0.5	16.9
2/19	202.3	2603	851.3	149.5	10.8	1.9	26.0	4.7	58.1	184.1	3.7	0.50	8.3	19.9	1105	8.8	5.5	3.33	25.7	1.9	2.46	4.9	3.7	17.3	9.4	48.2
2/20	322.8	1980	1028	189.5	13.1	1.6	41.8	6.4		164.8	3.4	0.74	5.3	50.4	863.3	10.0	8.0	3.35	37.5	6.2	2.41	6.7	7.4	20.0	9.9	72.0
2/21	395.4	940.9	1135	169.3	13.1	1.3	34.8	6.4	31.9	118.3	2.6	0.84	12.7	64.0	669.9	11.8	15.3	3.13	25.0	14.8	11.68	8.8	13.6	9.7	5.3	89.9
2/22	703.4	1059	1119	435.0	22.6	2.6	45.2	11.6	30.1	213.6	5.0	1.23	13.3	79.1	1497	24.0	86.0	9.14	34.0	9.5	6.52	18.3	20.4	2.4	1.9	111.2
2/23	400.4	1152	933.9	33.2	9.7	1.2	45.5	5.2	75.7	194.6	6.7	1.01	24.0	78.5	511.8	9.2	9.8	2.48	35.3	8.0	1.89	8.7	9.8	8.7	4.8	98.3
Mean	357.0	1047	845.5	211.3	18.0	1.5	29.2	24.1	42.7	130.3	3.4	0.78	15.6	54.4	835.4	11.4	20.8	3.17	20.7	35.8	3.28	8.3	12.5	9.0	5.1	59.6
Std Dev.	218.1	766.4	374.2	114.8	13.3	0.5	13.7	65.1	38.5	70.9	1.8	0.27	13.9	24.2	588.1	4.8	23.5	2.03	10.7	108.4	3.00	5.0	9.0	10.8	6.1	29.4

**Figure III.28 Detroit winter 8-hour CAPs concentrations of PM<sub>2.5</sub> and constituents. Constituents in parentheses behaved similar to the pollutant being plotted. PM<sub>2.5</sub> is measured in µg/m<sup>3</sup> whereas Al and Mg are in ng/m<sup>3</sup>.**



### High-Resolution CAPs Concentrations

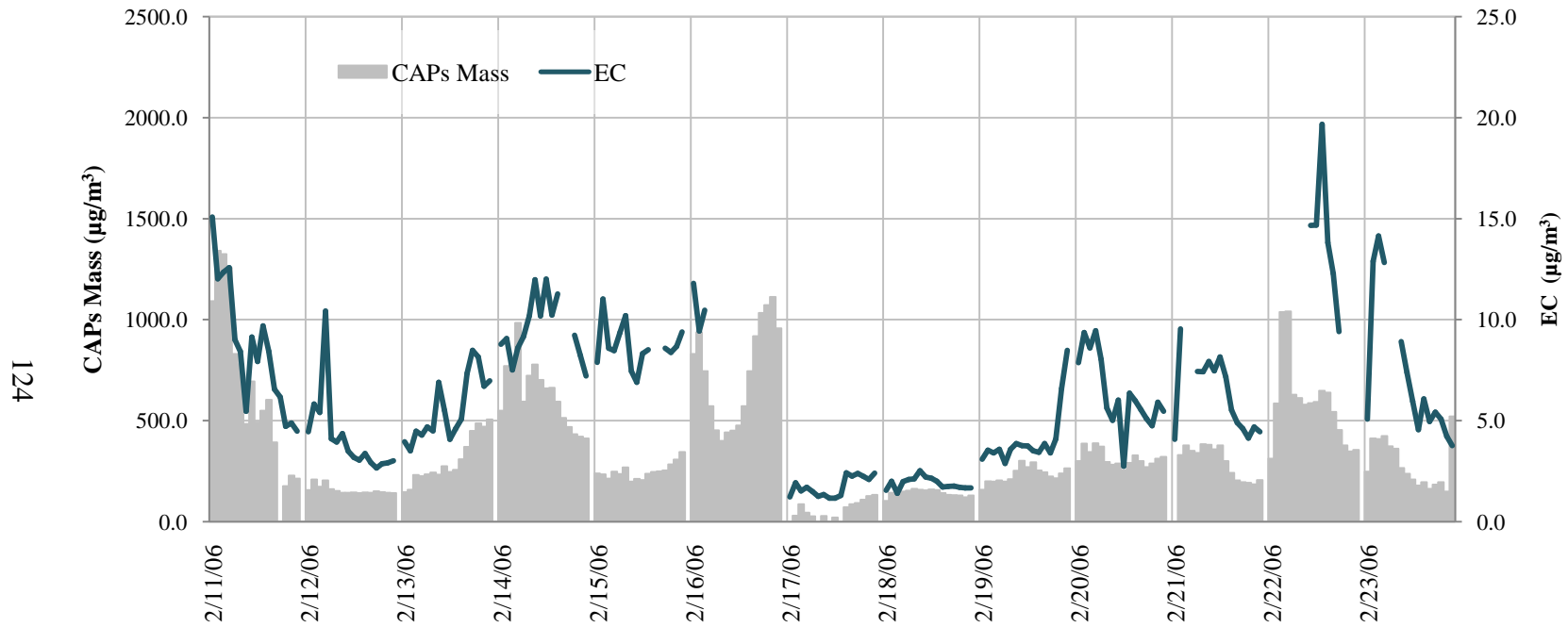
Fewer extreme changes in meteorology occurred during the winter exposure hours than during the summer intensive. Therefore, there were fewer instances where the SEAS trace element analysis diverged from the 8-hour integrated concentration. Stable conditions were seen when the daily wind roses and back trajectories from the winter exposures were taken into consideration. These figures (Appendix A.1) do not show any major shifts in the directionality of local surface winds within a day, nor do the trajectories show a shift in the air masses that were observed in Detroit. The only day when winds were variable during the exposure hours was on February 16 when mid-day winds shifted from the northeast to east. In the last 2-hours of exposure (1:00pm to

3:00pm EST), the trajectory shows that the air mass passed directly over Chicago (Figure III.25a).

### **CAPs Concentrations of PM and EC**

Thirty-minute  $PM_{2.5}$  and EC CAPs concentrations behaved differently in the wintertime study, with far fewer diurnal changes and maintaining strong co-linearity, as seen in Figure III.29. The high-resolution concentrations of EC were calculated to be just moderately lower in the wintertime exposures than in the summer, without much discrepancy from the 8-hour integrated concentration. Winds from the east-northeast, primarily on February 11 and 16, showed an increase in the EC concentrations, following closely to  $PM_{2.5}$  mass concentrations, which may have reflected diesel exhaust emissions from the Ambassador Bridge. However, the largest high-resolution peak in EC was on February 22 with strong southerly flow throughout the day, and high CAPs mass concentrations were observed as well. Therefore, the elevated EC on the 22<sup>nd</sup> may be caused by the co-linearity with  $PM_{2.5}$  rather than a tracer of a specific source impacting the sampling site.

Figure III.29 Thirty-minute EC concentrations and CAPs PM<sub>2.5</sub> mass in the Detroit winter exposure study.





## Ambient Concentrations of Trace Elements

Wintertime climatic conditions in Detroit were often stable throughout the exposure hours resulting in very few instances of peaks in trace element concentrations above the 8-hour mean. Nevertheless, significant changes in concentrations of constituents through the course of the two days were observed. In Figure III.30, 30-minute SEAS data for February 11 showed distinct peaks in some of the constituent concentrations. V peaked at  $3.11 \text{ ng/m}^3$  (Exposure Mean:  $0.633 \pm 1.66 \text{ ng/m}^3$ ), and Sb at  $3.05 \text{ ng/m}^3$  (Exposure Mean:  $0.519 \pm 0.784 \text{ ng/m}^3$ ). These significant peaks were reflected in higher 8-hour filter concentrations as well; both trace elements had the highest filter concentration on the 11<sup>th</sup>. However, from the 8-hour filter sample, we would have only been able to assume that V and Sb were consistent over the duration of the exposure, and could not identify that concentrations of V and Sb actually impacted the chamber concentrations only during the first few hours of exposure.

The other day for which significant changes were observed within the exposure hours was February 22, when CAPs concentrations exceeded  $1000 \mu\text{g/m}^3$  in the early morning (Figure III.31). On that day, Zn was the only constituent for which there was a substantially elevated concentration ( $100 \text{ ng/m}^3$ ) over the mean ( $23.3 \mu\text{g/m}^3$ ). The concentration of Zn, determined from the 8-hour filter, was not particularly high on the 22<sup>nd</sup>. This substantial difference in Zn between 8-hour and 30-minute data may show that Zn can be associated with HRV using high-resolution data.

**Figure III.30 Thirty-minute concentrations indicating the isolated early morning peaks in V and Sb on February 11, 2006.**

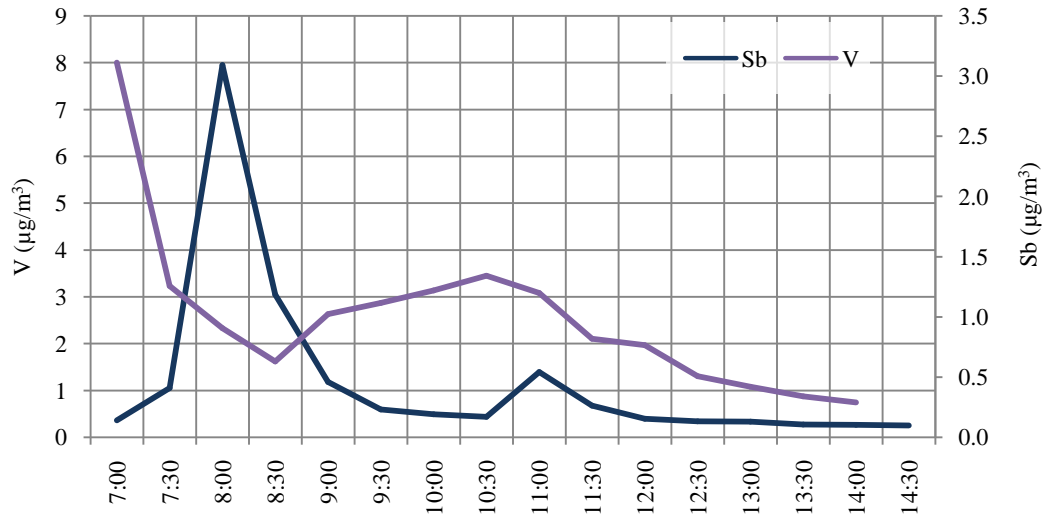


**Figure III.31 Thirty-minute concentrations of PM<sub>2.5</sub> and Zn with a spike in concentration on the morning of February 22, 2006.**

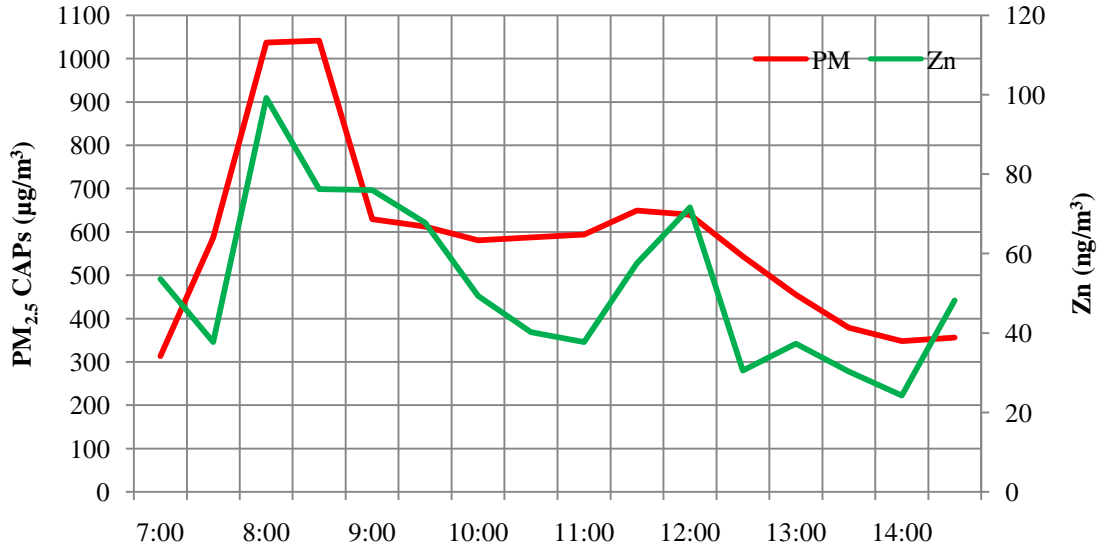


**Table III.13 Detroit winter average SEAS concentrations of PM<sub>2.5</sub> mass components (ng/m<sup>3</sup>). \*PM, EC and S are in µg/m<sup>3</sup>.**

	PM*	EC*	Mg	Al	P	S*	K	Ca	Ti	V	Cr	Mn	Fe	Co	Cu	Zn	As	Se	Rb	Sr	Mo	Cd	Sb	Ba	La	Ce	Pb
2/11	697	8.6	35.6	39.3	6.7	1.9	41.7	101	0.44	0.95	0.13	2.4	32.9	0.070	4.4	21.8	0.49	1.32	0.12	0.37	0.24	0.114	1.19	3.59	0.043	0.031	3.38
2/12	157	4.1	31.9	22.0	4.0	0.8	38.4	111	0.56	0.15	0.06	1.3	39.8	0.048	3.6	13.5	0.23	0.67	0.09	0.56	0.09	0.079	0.45	4.98	0.021	0.022	1.77
2/13	303	5.6	47.9	36.0	3.4	0.9	25.4	188	0.69	0.18	0.38	4.0	55.2	0.026	4.4	29.2	0.22	0.59	0.14	0.91	0.17	0.067	0.49	3.80	0.209	0.130	1.67
2/14	630	9.5	83.0	41.5	2.1	1.5	50.5	403	1.61	0.30	0.35	6.1	93.2	0.036	4.1	36.6	0.30	0.96	0.17	1.92	0.24	0.152	0.35	5.73	1.273	0.709	2.88
2/15	249	8.7	87.7	45.6	8.8	1.2	68.7	430	1.65	0.33	0.31	7.4	100.7	0.154	3.7	36.7	0.51	1.09	0.23	2.48	0.45	0.159	0.63	14.22	0.171	0.139	2.19
2/16	733	10.8	27.6	23.3	31.1	2.6	31.4	108	0.38	6.07	0.42	2.0	52.8	0.034	3.5	24.2	0.22	0.95	0.06	0.36	6.48	0.145	0.46	4.74	0.084	0.052	2.96
2/17	72	1.8	45.7	39.8	3.2	0.2	22.1	179	0.56	0.11	0.10	1.7	30.9	0.026	1.9	5.6	0.15	0.43	0.03	0.76	0.29	0.060	0.27	2.87	0.013	0.025	0.76
2/18	142	1.9	91.8	28.1	4.0	0.4	55.6	233	0.84	0.10	0.30	2.4	63.6	0.023	1.4	4.7	0.07	0.37	0.02	1.06	0.12	0.044	0.08	2.45	0.013	0.023	0.86
2/19	234	4.1	102.8	34.8	2.8	0.7	39.1	311	1.11	0.16	0.26	5.8	61.2	0.026	1.6	16.5	0.13	0.48	0.11	1.53	0.09	0.077	0.12	2.72	0.434	0.243	1.30
2/20	315	6.4	160.6	52.2	12.0	1.0	51.0	738	2.10	0.30	0.36	8.7	116.2	0.058	2.0	19.8	0.35	0.47	0.15	4.23	0.31	0.090	0.26	6.12	0.691	0.358	2.23
2/21	295	6.3	174.2	47.2	53.2	1.3	60.1	895	2.31	0.33	0.34	10.6	107.3	0.048	4.4	21.5	0.50	0.89	0.20	5.47	0.64	0.197	0.72	5.76	0.279	0.192	3.42
2/22	584	13.9	152.7	55.7	20.7	3.1	199.6	701	2.62	0.61	0.71	11.5	200.6	0.080	13.2	52.4	0.80	3.03	0.55	3.99	0.81	0.370	1.14	11.34	0.140	0.146	7.65
2/23	284	7.2	185.5	57.1	22.0	1.5	162.8	1066	3.56	0.42	0.70	14.9	206.1	0.087	19.2	23.8	0.69	0.58	0.28	5.31	0.58	0.215	0.56	10.26	0.374	0.279	8.04
Mean	366	6.2	97.7	40.9	14.6	1.3	67.0	435	1.46	0.63	0.34	6.2	90.9	0.052	5.3	23.3	0.36	0.91	0.17	2.31	0.66	0.136	0.52	5.82	0.302	0.188	3.06
Std Dev	262	3.6	88.1	31.2	20.1	0.9	110.4	491	1.62	1.66	0.36	7.1	87.7	0.060	13.7	17.3	0.29	0.93	0.18	2.87	3.50	0.112	0.78	3.92	0.639	0.338	2.80
Median	273	5.5	82.6	33.0	6.3	1.1	39.4	274	0.99	0.25	0.27	4.3	61.9	0.039	2.8	19.8	0.28	0.64	0.12	1.28	0.24	0.102	0.32	4.35	0.090	0.092	2.23
5%	109	1.5	25.5	12.3	1.9	0.2	10.7	76	0.30	0.09	0.03	1.0	17.9	0.013	0.5	4.0	0.04	0.25	0.01	0.30	0.07	0.028	0.08	2.13	0.010	0.017	0.61
95%	958	12.7	257.3	100.3	48.2	3.1	184.6	1067	3.59	2.03	0.89	15.1	267.2	0.111	13.5	57.6	0.98	2.23	0.65	5.76	1.07	0.408	1.40	14.11	1.238	0.807	8.64

### III.2.4 HRV Summary

The Detroit summer findings determined that 30-minute HRV analysis provided better statistical results than 8-hour analysis. The same comparison between the two data sets was conducted again to see if the high-resolution data provided better results during the winter exposure study as well. Table III.14 summarizes the mean HRV parameters for AIR and CAPs Rats and it also presents the p-values for each term in the mixed modeling analysis. Eight-hour mixed modeling analysis revealed HR in CAPs Rats to be significantly different from AIR Rats ( $p < 0.0001$ ). No other parameters were found to be significantly different using the 8-hour data.

Using the least-squares means procedure (LS Means), HR in CAPs Rats was found to be significantly lower than in AIR rats on February 22 ( $p = 0.0087$ ). February 22 had the highest  $PM_{2.5}$  mass and therefore some evidence was present to indicate that the effect on the HRV of the CAPs Rats may be a result of air pollution concentrations. A significant difference in CAPs Rats ( $p = 0.0917$ ) was seen on the 11<sup>th</sup>, which is difficult to qualify as a health effect because it was the first day of exposure, but also a day with higher than average mass. No days with in which HRV of AIR and CAPs Rats were significantly different were identified through LS Means.

**Table III.14 Mixed modeling results from the Detroit winter study using 8-hour average for each HRV parameter. P values are in bold if significant ( $p < 0.05$ ).**

	AIR Rats (N=53)	CAPs Rats (N=102)	Mixed Modeling Results		
			Group	Date	Group*Date
Heart Rate	298.1	298	0.9017	<b>&lt;.0001</b>	<b>0.0194</b>
ln(SDNN)	2.74	2.71	0.5089	<b>&lt;.0001</b>	0.5488
ln(r-MSSD)	1.52	1.49	0.6835	0.0015	0.6125
ln(LF)	-2.76	-2.92	0.5251	0.3300	0.3009
ln(HF)	-2.24	-2.33	0.6352	0.2134	0.6336
LF/HF	0.6	0.58	0.9832	0.3275	0.1033

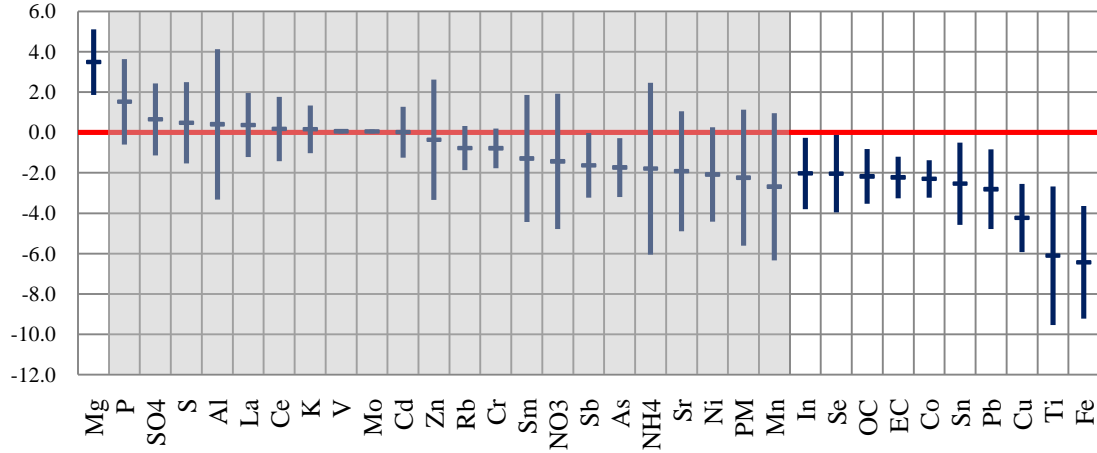
### **Eight-Hour Associations with Air Pollutants**

Even though significant differences could not be identified between AIR and CAPs Rats, significant associations with HRV and air pollutants were identified across all three time-domain parameters. Figure III.32 presents the CI Plots for HR,  $\ln(\text{SDNN})$  and  $\ln(\text{r-MSSD})$  and the associations of the 8-hour pollution concentrations collected on each day of exposure. In Figure III.32a, Mg associated with an increase in HR, but Fe had the greatest effect estimate in association with a reduction in HR. Ti, Cu, Pb, Sn, Co, EC, OC, Se and In were also significantly associated with a reduction HR. PM mass was not associated with HR and was not well correlated with Fe concentrations ( $r^2=0.3345$ ). The constituents that were significantly associated with HR were significantly correlated with Fe. These HR findings imply that  $\text{PM}_{2.5}$  mass was not driving HR in the winter intensive; instead, Fe and other co-varying pollutants were strongly associated with a decrease in HR.

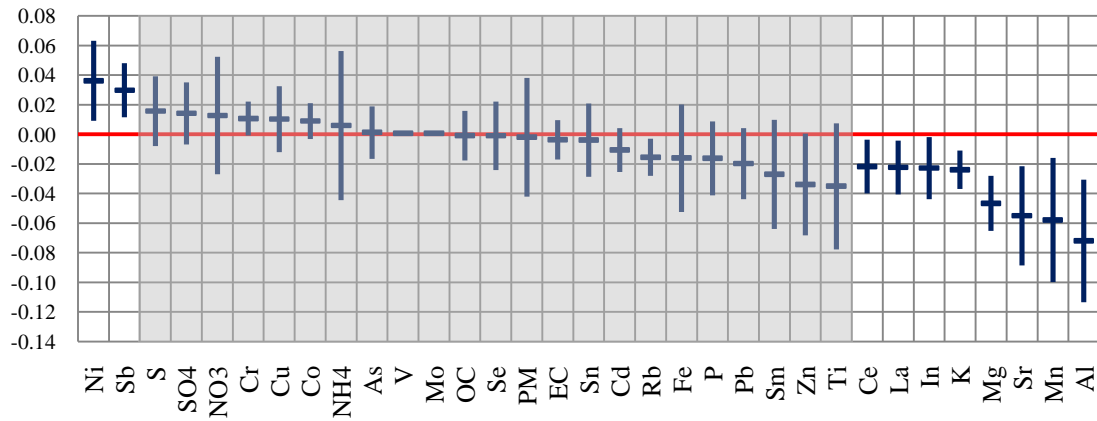
No significant differences between AIR and CAPs Rats existed based on the 8-hour HRV parameters; however, relationships were still explored to identify any constituents that may have been significantly associated between the  $\ln(\text{SDNN})$  and  $\ln(\text{r-MSSD})$  within CAPs Rats. The multi-directionality found in HR was also identified in HRV. Ce, La, In, K, Mg, Sr, Mn and Al were all associated with a decrease in  $\ln(\text{SDNN})$ , but Sb and Ni were associated with an increase. The  $\ln(\text{r-MSSD})$  parameter showed only Mg associated with a significant reduction, and Mg was also the only constituent associated with a significant increase in HR. However, the CI Plot for  $\ln(\text{r-MSSD})$  revealed an interesting trend. While Mg and P were closely associated with a reduction in  $\ln(\text{r-MSSD})$ , Fe, Ti and Cu were all associated with an increase, although not significant. This pattern was the inverse of the observations from HR where a reduction in HR was associated with Fe, Ti and Cu, and an increase in HR was associated with Mg and P, although P was not associated significantly with HR. Pollution roses showed that they were all primarily from the west and did not have contrasting wind direction. It is therefore possible that the effects of Fe, Ti and Cu diametrically opposed the effects of Mg and P. Nevertheless, this in-the-field study does not provide enough statistical strength to confirm these findings, but provides an interesting groundwork for future HRV studies.

**Figure III.32 CI Plots for 8-hour average concentrations of pollutants with each health parameter, HR, ln(SDNN) and ln(r-MSSD) from the Detroit winter intensive.**

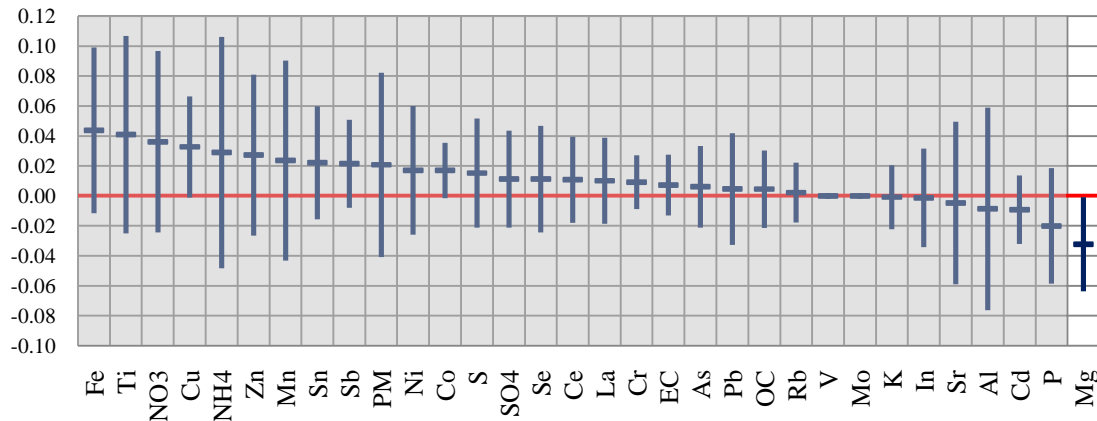
**(a) HR**



**(b) ln(SDNN)**



**(c) ln(r-MSSD)**



### **Spectral Analysis and Air Pollutants**

Spectral analysis was not discussed for the Detroit summer intensive because there were no associations with  $\ln(\text{LF})$  or  $\ln(\text{HF})$ ; however, during the winter intensive, increases in  $\ln(\text{LF})$  and  $\ln(\text{HF})$  were significantly associated with Sr and Ti. With the same constituents associated with both time-domain and frequency-domain parameters, there may be an effect on the cardiovascular function identified. Trace element concentrations for Sr and Ti were highest from the west, and were significantly correlated with each other, in both the 8-hour and 30-minute datasets, ( $r^2=0.79$  and  $0.71$ , respectively). Therefore, significant changes in the frequency-domain parameters may be legitimately associated with specific constituent concentrations from the west, even on an 8-hour scale. In future studies, with supporting high-resolution spectral analysis, these findings could possibly be confirmed.

### **High-Resolution HRV Findings**

Thirty-minute HRV data confirmed a significant difference in HR (also found in 8-hour analysis) and  $\ln(r\text{-MSSD})$  between AIR and CAPs Rats. As discussed in the summer findings, the 30-minute data can provide a much better comparison between the outcomes of CAPs Rats against a control group because the continuous changes in HRV were not diluted over a daily average. The winter study was no exception. In Table III.15, the mixed modeling results for 30-minute data are presented. HR was still significantly different between the AIR and CAPs Rats, supporting the 8-hour findings with an even stronger p-value. In addition,  $\ln(r\text{-MSSD})$  was also found to be significantly different ( $p=0.0278$ ) between the groups.

**Table III.15 Detroit winter mixed modeling results for the 30-minute HRV dataset comparing AIR and CAPs Rats.**

Parameter	Term	df N	df D	F Value	p Value
<b>Heart Rate</b>	Group	1	11	0.11	0.7416
	Time(Date)	204	1802	7.14	<0.0001
	Group*Time(Date)	204	1802	1.68	<0.0001
<b>ln(SDNN)</b>	Group	1	11	.05	0.8294
	Time(Date)	204	1802	2.60	<0.0001
	Group*Time(Date)	204	1802	1.07	0.2478
<b>ln(RMSSD)</b>	Group	1	11	.33	0.5748
	Time(Date)	204	1802	2.72	<0.0001
	Group*Time(Date)	204	1802	1.21	0.0278

With high-resolution data, the significant difference between AIR and CAPs Rats can be determined within a given day. For this analysis, both ln(SDNN) and ln(r-MSSD) were found to be significantly different in the CAPs Rats on February 22, a day with high PM<sub>2.5</sub> and with the largest spike in many constituents. HR was lower as well (p<0.10), and mean data showed that HR was reduced while ln(SDNN) and ln(r-MSSD) were increased. Therefore, the biological effect of SH rats in the winter appears to be a reverse response to that observed in the summer.

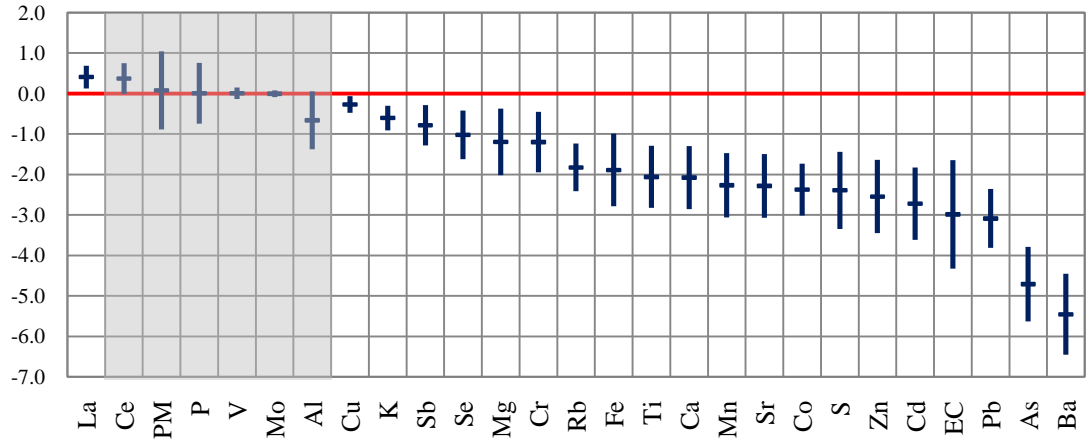
### **Thirty-Minute Associations with Air Pollutants**

The 30-minute CI Plots for the Detroit winter intensive indicated the same increase in the number of constituents associated with HR and HRV as was observed during the summer intensive. However, the patterns are not as straightforward with regards to the associations of the constituents with the changes in HRV. In Figure III.33, the CI Plots revealed that some pollutants increased the effect estimate of a parameter while other constituents worked to decrease the effect estimate. This multi-directionality is a clear divergence from the Detroit summer findings. Furthermore, the 30-minute dataset did not reveal any associations with PM<sub>2.5</sub> mass, another divergence from the Detroit summer study findings.

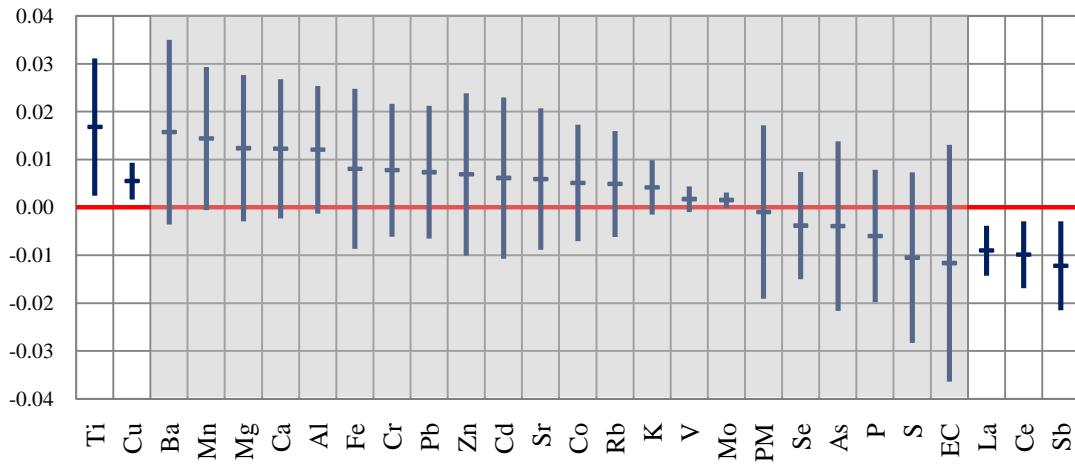


**Figure III.33 Detroit winter CI Plots using 30-minute concentrations of pollutants associated with each health parameter; (a) HR, (b) ln(SDNN) and (c) ln(r-MSSD).**

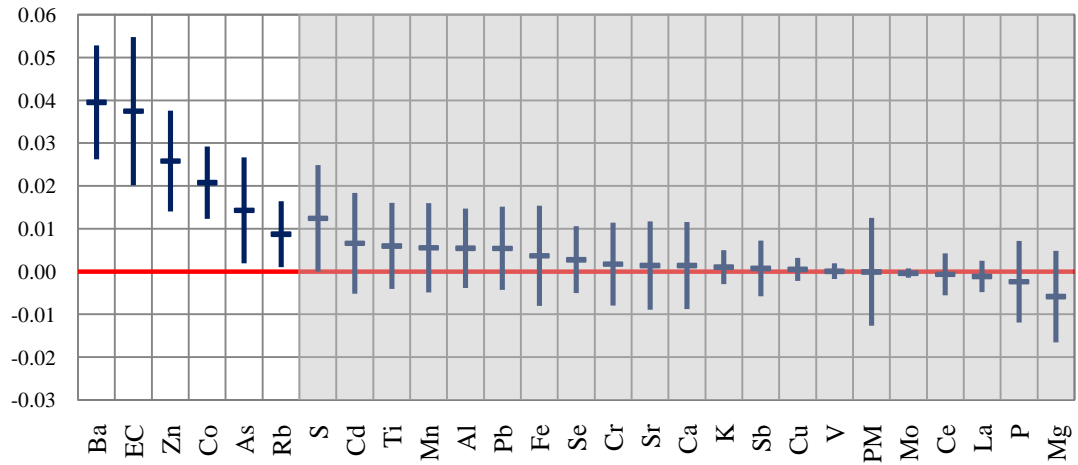
**(a) HR**



**(b) ln(SDNN)**



**(c) ln(r-MSSD)**



Thirty-minute mixed modeling analysis results revealed similar multi-directional patterns when associating HRV with air pollutants. Several constituents associated with a reduction in HR; Ba and As were most strongly associated with the reduction in HR, while La was significantly associated with an increase in HR. For ln(SDNN), Ti and Cu were significantly associated with an increase, while La, Ce and Sb were associated with a decrease. For ln(r-MSSD), Mg was the only 8-hour constituent associated with a reduction in this parameter, and in Figure III.37c, Mg had the lowest effect estimate, but it was not significant. Thirty-minute findings revealed Ba, EC, Zn, Co, As and Rb as associated with an increase in ln(r-MSSD). What is clear from all three CI Plots is that PM<sub>2.5</sub> mass was not associated with HRV during the wintertime exposure. It is possible that fine-fraction mass was not large enough to observe the same strong significant associations like those found in the summertime CI Plots. The role of PM<sub>2.5</sub> and the patterns in HRV will be explored more in the following section.

### **III.2.5 Detroit Winter Summary**

#### **HRV Findings**

In the winter study, heart rate (HR) was significantly different in CAPs Rats in relation to AIR Rats when using the 8-hour dataset. In addition, HR and ln(r-MSSD) were also significantly different within the high-resolution data. However, when trying to associate air pollutants with these significant changes in HR and HRV, it became apparent that the findings were unlike the summertime associations. Individual constituents of PM<sub>2.5</sub> associated with both an increase and decrease in HRV. The seasonal differences in how air pollutants associated with HRV needed to be discussed further.

#### **Understanding the Role of PM<sub>2.5</sub> Mass**

One of the most interesting differences observed in the Detroit winter exposure was that PM<sub>2.5</sub> mass was not associated with HRV in either 8-hour or 30-minute datasets. PM<sub>2.5</sub> may not have associated with HRV because the Detroit winter study observed much lower fine mass concentrations than were observed in the summer, when PM<sub>2.5</sub>

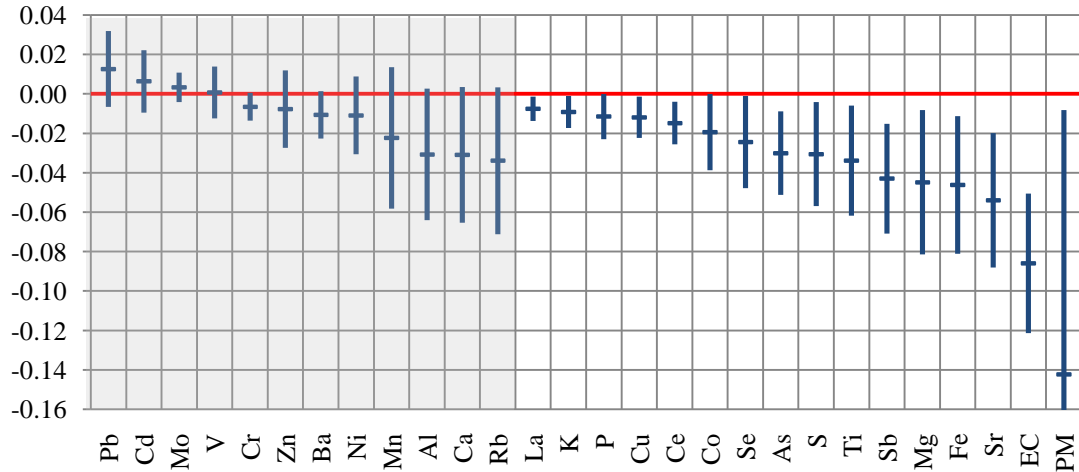
mass associated with HRV. The wintertime reduction in CAPs mass may not have reached an unknown threshold of CAPs mass that was achieved in the summer. If a threshold was in fact the reason, then it could be assumed that if the winter had reached this threshold, the same associations that were identified in the summer study would also be observed. The inverse of this speculation, that higher PM<sub>2.5</sub> mass in the summer achieved a threshold to affect HRV, can be indirectly tested. Looking back at Detroit summer data, the study mean was 795µg/m<sup>3</sup>, nearly twice as high as the average CAPs mass observed during the winter intensive. If high mass concentrations could be eliminated from the summer dataset to reduce the summer mean to 365µg/m<sup>3</sup>, then the summer and winter mean mass would be equivalent. Therefore, if a threshold in the summer was the reason for the associations, it would no longer be reached as the high mass concentrations were removed from the dataset.

This test was conducted by eliminating the highest mass concentrations from the summer dataset. By trial and error, a cut-off of high mass was applied to the summer data to reduce the mean CAPs mass down to winter concentrations. Eventually, it was determined that removing PM<sub>2.5</sub> concentrations above 600µg/m<sup>3</sup> from the 30-minute dataset reduced the summer CAPs to average CAPs mass of 365µg/m<sup>3</sup>. This cut-off reduced the total number of data points by 48%. Associations with HRV were reanalyzed by repeating mixed modeling analysis to see if the associations with constituents would remain the same with the reduced summer data set.

When summertime associations for ln(SDNN) were re-calculated in terms of reduced mass, the overall trend was not affected by the loss in high concentration values. Figure III.34 shows the new CI Plot for ln(SDNN), which can be compared to the findings in Figure III.19a. PM<sub>2.5</sub>, EC, Fe, Sr and Mg were still the most associated with the reduction in ln(SDNN). In fact, PM and EC had even larger effect estimates than all summertime data. There were some changes in the constituents that were found significantly associated with HRV: La, K, P and Cu were now significant with a reduction in ln(SDNN) and Pb, Ba, Ca and Mn were no longer found significant. Overall, the associations were nearly identical, thus indicating that the higher concentrations in the summer intensive did not drive the changes in ln(SDNN). The same effect was true for HR and ln(r-MSSD). Therefore, the compositional differences

in air pollution between the summer and winter in Detroit may be driving the patterns found in HR and HRV, not merely high PM<sub>2.5</sub> concentrations.

**Figure III.34 Detroit summer CI Plot for ln(SDNN) after removing all data with mass greater than 600µg/m<sup>3</sup>, bringing summertime average mass down to wintertime concentrations.**



### Differences due to Winds

Seasonal differences in the HRV findings could have also been caused by the differences in the dominant wind directions in the summer and winter exposure studies in Detroit. Therefore, mixed modeling analyses were conducted to determine if AIR and CAPs Rats were significantly different based on wind direction. In Table III.16, CAPs PM<sub>2.5</sub> mass, the average ln(SDNN) for AIR and CAPs Rats, and the mixed modeling analysis significance (p<0.05) is shown for each wind direction. Also included in the table is the frequency of recordings (Freq) found for each wind direction.

These mixed modeling analyses indicated that in the summer, the SW-W-NW wind directions were associated with significant changes in the ln(SDNN) of CAPs Rats in comparison to the AIR Rats. Northerly flow in the winter showed significant differences in ln(SDNN). The frequency of samples from the north may not have been large enough for identification of significant differences between AIR and CAPs over the course of the winter exposure study. These findings indicate that the seasonal differences in air flow may impact HRV findings; however, more evidence was needed to demonstrate that SW-W-NW winds are in fact having a significant impact on HRV.

Although AIR and CAPs Rats were significantly different from the SW-W-NW wind directions, the  $\ln(\text{SDNN})$  of CAPs Rats from the SW-W-NW directions needed to be significantly different than the rest of the wind directions. A mixed model similar to the one in Equation II.2 was used, replacing *Pollutant* with *Wind Category*. All 30-minute data was placed into 1 of 2 categories: SW-W-NW Winds and All Other Wind Directions. This test found that  $\ln(\text{SDNN})$  was not significantly different in CAPs Rats when winds were from the NW-W-SW direction, but HR and  $\ln(\text{r-MSSD})$  were significantly different. These results indicate that the significant differences between AIR and CAPs Rats in the summertime were not driven by  $\ln(\text{SDNN})$  being lower from the NW-W-SW directions. In the winter, when HR and  $\ln(\text{r-MSSD})$  were significantly different between AIR and CAPs Rats, HR was identified as being significantly different from the NW-W-SW direction, as well as from the N. These statistical tests showed that AIR and CAPs differences could be associated with wind direction, and within-group changes in HR and HRV were identified. These analyses were conducted to demonstrate that HR and HRV were in fact significantly influenced by dominant wind flows, and the first indication in this study that source types, with impacts varying due to shifting wind directions, may modify HR and HRV.

**Table III.16 Mixed modeling results comparing AIR and CAPs Rats ln(SDNN) in each season, based upon wind direction.**

**Detroit Summer**

Direction	Freq	CAPs PM <sub>2.5</sub> (µg/m <sup>3</sup> )	ln(SDNN) AIR Rats	ln(SDNN) CAPsRats	p Value
N	136	710	2.44	2.48	0.0566
NE	82	801	2.44	2.42	0.2493
E	154	495	2.59	2.56	0.7038
SE	163	747	2.38	2.44	0.8400
S	281	806	2.53	2.55	0.5679
SW	287	1281	<b>2.34</b>	<b>2.48</b>	<b>0.0500</b>
W	466	733	<b>2.42</b>	<b>2.50</b>	<b>0.0426</b>
NW	381	710	<b>2.41</b>	<b>2.47</b>	<b>0.0109</b>

**Detroit Winter**

Direction	Freq	CAPs PM <sub>2.5</sub> (µg/m <sup>3</sup> )	ln(SDNN) AIR Rats	ln(SDNN) CAPs Rats	p Value
N	68	149	<b>2.38</b>	<b>2.35</b>	<b>0.0258</b>
NE	189	634	2.40	2.42	0.9832
E	95	908	2.59	2.53	0.2692
SE	0	-	-	-	-
S	127	647	2.41	2.39	0.0515
SW	856	374	2.48	2.42	0.2841
W	556	211	2.49	2.46	0.3186
NW	257	151	2.39	2.43	0.1860

**Differences in Constituent Associations**

In the previous section, PM<sub>2.5</sub> mass was not determined as the factor that influenced HRV. However, the mass of constituents could be contributing to the HRV differences between summer and winter in Detroit. Therefore, seasonal differences in constituent concentrations were explored to determine if a greater concentration of constituents associated more strongly with HRV.

When looking at the overall constituents associated with the changes in HR and HRV between summer and winter, the differences between the seasons become quite pronounced. The greatest seasonal difference observed was that the CI Plots in winter revealed a reduction in HR and an increase in ln(r-MSSD), in direct contrast to the

summertime findings. From Table III.17, the Detroit summer study showed As, Ba, Ca, Co, Fe, Mg, PM, Sb, Se, Sr and Ti associated with all three time-domain parameters. Of those, only PM, As, Co and Sb had higher concentrations during the summer. Therefore, if the remaining pollutants, Ba, Ca, Fe, Mg, Se, Sr and Ti, did influence HRV, they all should show some response to HRV in the winter months as well. Some were associated with HR, like Ba, Sr, Ti and Se, but in the opposite direction than in the summer. This was true for Ti and  $\ln(\text{SDNN})$  as well as Ba and As with  $\ln(\text{r-MSSD})$ .

In Table III.18, the seasonal concentration of each pollutant is shown. It was then possible to determine if a larger concentration of a constituent was observed in conjunction with a stronger association with HR and HRV. This is illustrated in the CI Plots in Figure III.35, where the effect estimate for summer and winter are positioned side by side. These figures show the calculated percent change in HR,  $\ln(\text{SDNN})$  and  $\ln(\text{r-MSSD})$  for each pollutant.

From Figure III.35, it is clear that mass was not the factor determining a significant association with a pollutant. These unexpected findings may indicate three possible mechanisms occurring between air pollutants and HRV: (1) there were some false associations that appear from the model during the winter months without overall mass strong enough to cause substantial health response, (2) the associations in the winter are truly the correct pattern for those constituents, but constituents were strongly correlated to total  $\text{PM}_{2.5}$  mass during the summer such that they could not be dissociated, and (3) summertime  $\text{PM}_{2.5}$  mass was driving the HRV and drowned out the more subtle effects of the constituents that could be observed during the winter study when mass was less. All of these theories are speculative at best. But what has been established is that there were significant seasonal differences in air pollution in Detroit, and it is likely that the composition of the air pollution caused the differences in the health effects, not simply that total mass differences.

**Table III.17 Thirty-minute directional HRV outcomes for each season in Detroit.**

	Detroit Summer		Detroit Winter	
Heart Rate	↑	Al, Ni, As, Se, Fe, S, Mg, Co, PM, Rb, Ti, Sr, Ca, P, Cd, V, Ba, Cu, Sb, Cr	↑	La
	↓	-	↓	Ba, As, Pb, EC, Cd, Zn, S, Sr, Mn, Ca, Ti, Fe, Rb, Cr, Mg, Se, Sb, Cu, Al
ln(SDNN)	↑	-	↑	Ti, Cu
	↓	PM, EC, Fe, Sr, Mg, As, Ca, Ti, Mn, Co, Se, Ba, Sb, Pb, Ce, Zn	↓	Sb, Ce, La
ln(r-MSSD)	↑	-	↑	Ba, EC, Zn, As, Rb
	↓	EC, PM, Al, Se, Fe, As, Rb, S, Mg, Ni, Sr, Ti, Ca, Mn, Co, Cd, Ba, Pb, P, Cu, Sb, Cr	↓	-

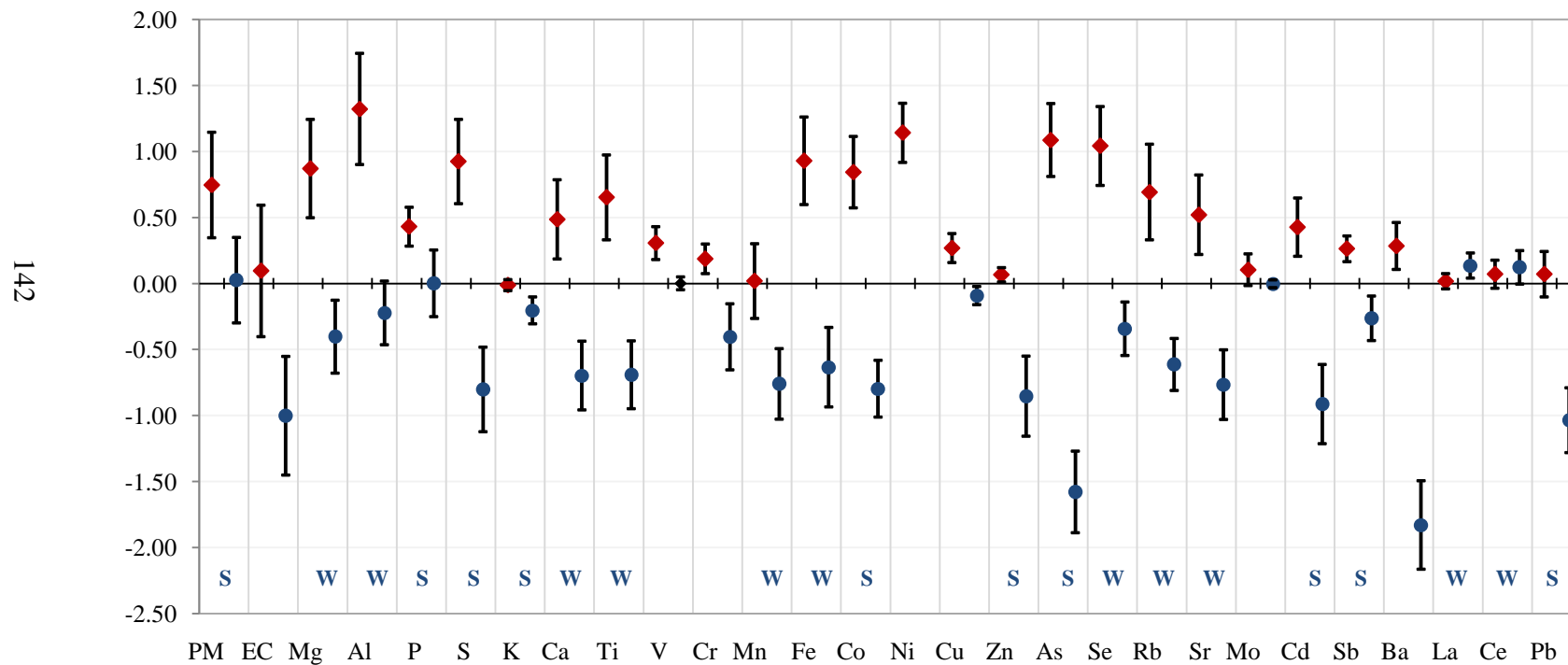


**Table III.18 Summer and winter mean concentrations (ng/m<sup>3</sup>) of SEAS trace elements for Detroit and the total range for each element. Significantly larger average concentrations are shown in bold (t-test, p<0.05).**

	Summer		Winter	
	Mean ± SD	Range	Mean ± SD	Range
PM	<b>809.9±560.4</b>	<b>(110.3-2778)</b>	365.6±262.5	(22-1341.5)
EC	6.42±4.35	(0.16-27.9)	6.20±3.60	(1.17-19.7)
Mg	45.1±49.5	(5.63-166.9)	<b>97.7±110.2</b>	<b>(17.8-863.8)</b>
Al	16.7±18.6	(0.051-85.0)	<b>40.9±45.3</b>	<b>(3.66-259.2)</b>
P	<b>21.2±25.6</b>	<b>(0.264-175.0)</b>	14.6±17.7	(0.155-126.5)
S	<b>1817±2107</b>	<b>(156.6-12934)</b>	1273±1401	(76.3-4174)
K	<b>144.1±234.6</b>	<b>(3.83-8490)</b>	67.0±82.9	(0.167-1030)
Ca	240.4±273.3	(17.3-1257)	<b>435.1±505.2</b>	<b>(46.4-4772)</b>
Ti	0.656±0.742	(0.002-3.61)	<b>1.46±1.69</b>	<b>(0.018-17.5)</b>
V	0.525±0.658	(0.014-8.43)	0.633±0.870	(0.020-17.3)
Cr	0.417±0.540	(0.006-10.8)	0.343±0.394	(0.001-3.36)
Mn	4.36±4.98	(0.242-27.9)	<b>6.21±7.22</b>	<b>(0.525-76.4)</b>
Fe	44.2±50.3	(1.05-214.3)	<b>90.9±103.4</b>	<b>(1.22-708.9)</b>
Co	<b>0.0705±0.0814</b>	<b>(0.004-0.821)</b>	0.052±0.061	(0.003-0.734)
Cu	5.07±6.28	(0.170-57.2)	5.34±7.29	(0.091-168.5)
Zn	<b>44.9±61.8</b>	<b>(0.268-987.8)</b>	23.3±25.7	(0.748-99.2)
As	<b>0.688±0.802</b>	<b>(0.003-5.27)</b>	0.361±0.402	(0.002-1.33)
Se	0.708±0.815	(0.015-4.12)	<b>0.907±1.04</b>	<b>(0.074-7.06)</b>
Rb	0.120±0.135	(0.010-0.625)	<b>0.168±0.194</b>	<b>(0.003-1.03)</b>
Sr	1.45±2.11	(0.080-63.6)	<b>2.31±2.72</b>	<b>(0.223-23.1)</b>
Mo	0.545±0.735	(0.005-15.6)	0.659±1.16	(0.028-46.8)
Cd	<b>0.222±0.261</b>	<b>(0.004-2.65)</b>	0.136±0.152	(0.008-0.575)
Sb	<b>0.922±1.18</b>	<b>(0.07-17.8)</b>	0.519±0.631	(0.013-7.95)
Ba	5.49±6.27	(0.495-64.2)	5.82±6.38	(0.425-21.1)
La	0.103±0.148	(0.000-3.10)	<b>0.302±0.393</b>	<b>(0.002-5.08)</b>
Ce	0.0775±0.103	(0.000-1.64)	<b>0.189±0.237</b>	<b>(0.004-2.76)</b>
Pb	<b>6.22±7.59</b>	<b>(0.087-61.2)</b>	3.06±3.47	(0.078-18.0)

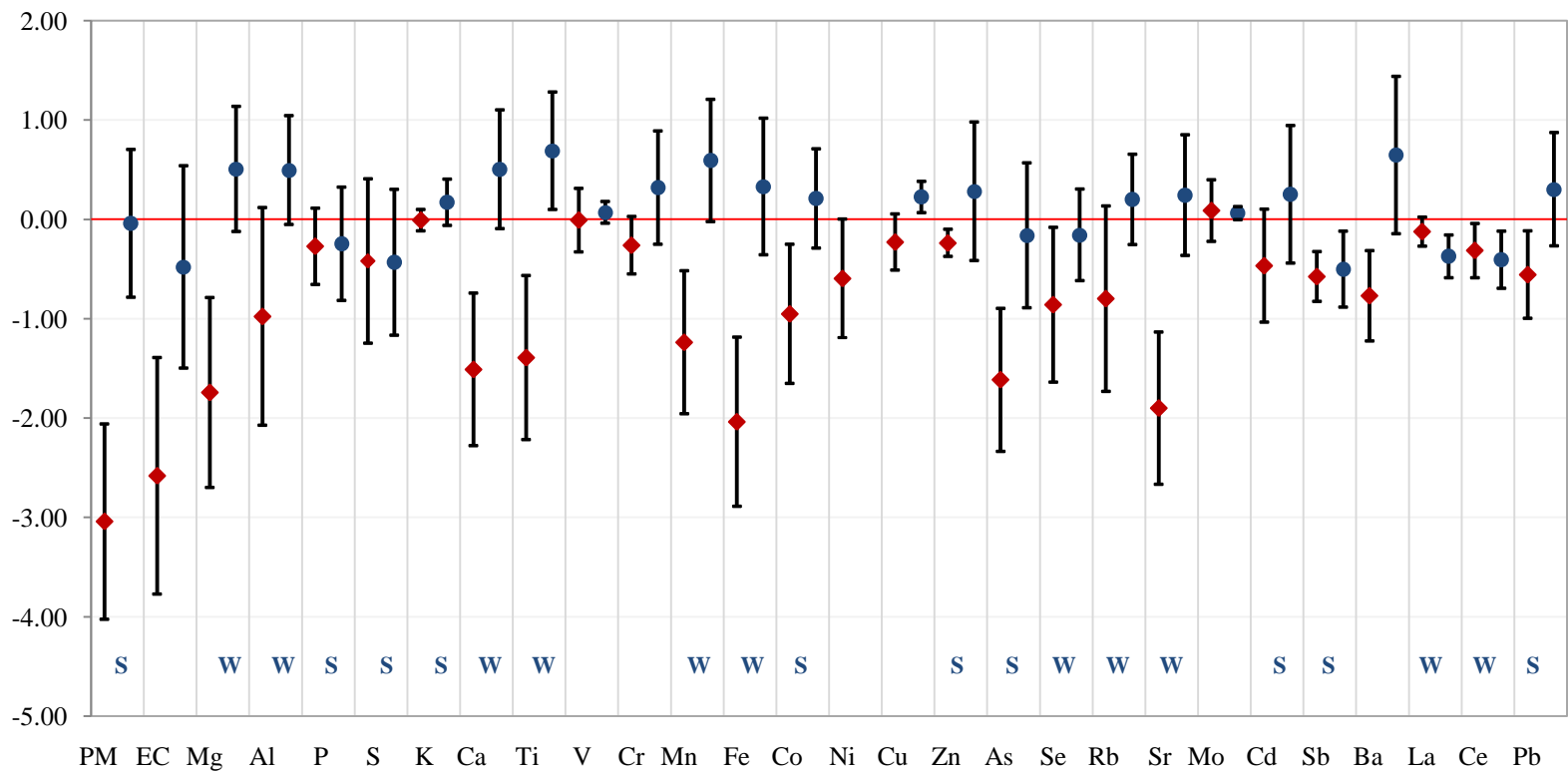
**III.35 Thirty-minute CI Plots comparing the percent change from the average (a) HR, (b)  $\ln(\text{SDNN})$  and (c)  $\ln(r\text{-MSSD})$  for each constituent of  $\text{PM}_{2.5}$  during both Detroit exposure studies (Summer | Winter). An S or W indicates the season for which the mass for that pollutant was significantly higher.**

**(a) Detroit HR**

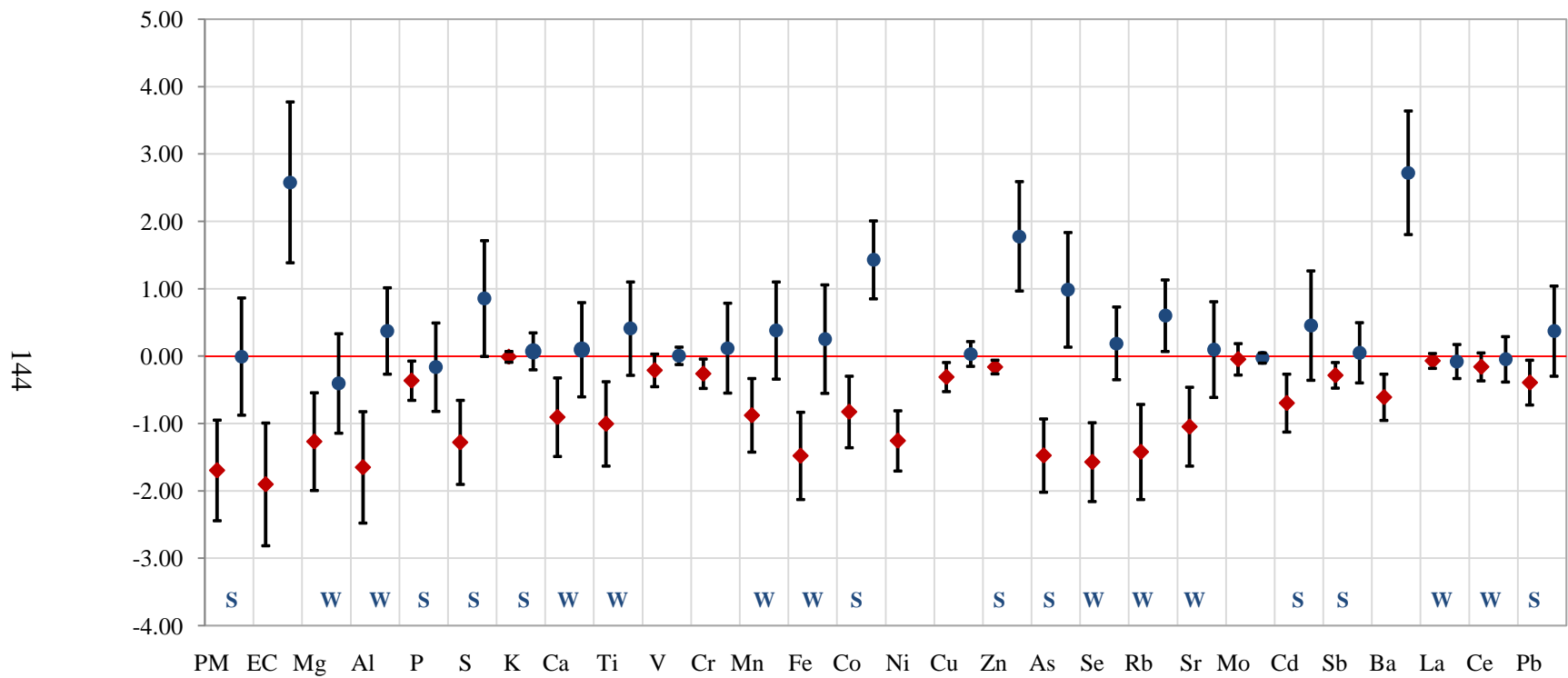


(b) Detroit ln(SDNN)

143



(c) Detroit ln(r-MSSD)



### **Possible Autonomic Effects**

Detroit summer findings indicate that  $PM_{2.5}$  was strongly associated with changes in HR and HRV, and several  $PM_{2.5}$  constituents followed this trend. With an increase in HR and a reduction in HRV, there is a possibility that summertime air pollution has a sympathetic autonomic response in the SH rats. Future studies with 30-minute spectral analysis may help support this hypothesis. Although the winter findings were not as succinct as the summer findings, it is possible that air pollution composition is different enough such that different effects upon HR and HRV were observed.

### **Conclusions**

Comparisons between the summer and winter intensives in Detroit showed that HRV in CAPs Rats was affected differently, but the reasons why are not well defined. Summertime  $PM_{2.5}$  mass, and several constituents had associations with an increase in HR and reductions in  $\ln(SDNN)$  and  $\ln(r-MSSD)$ , evident of a sympathetic autonomic response in cardiovascular function. Winter findings were multi-directional, but it appeared that trace elements (and not  $PM_{2.5}$  mass) associated with a reduction in HR and an increase in  $\ln(r-MSSD)$  in CAPs Rats. Often, when concentrations were higher in one season, the effects were not associated with HRV, whereas the season with lower mass did result in significant associations with HRV. There are only a few trace element examples (e.g. PM, La, Ce and Sb) where higher mass in one season could be attributed to changes in HRV. A statistical test was conducted to determine if high mass concentrations during the summer drove the observed effects that were not found during the winter. Even without high concentrations, there was the same distinct association between constituent concentrations and  $\ln(SDNN)$ . Therefore, this chapter finds that the seasonal differences in HRV associations were due to seasonal differences in atmospheric conditions and subsequent  $PM_{2.5}$  composition and not simply due to higher total summer  $PM_{2.5}$  mass.

## CHAPTER IV

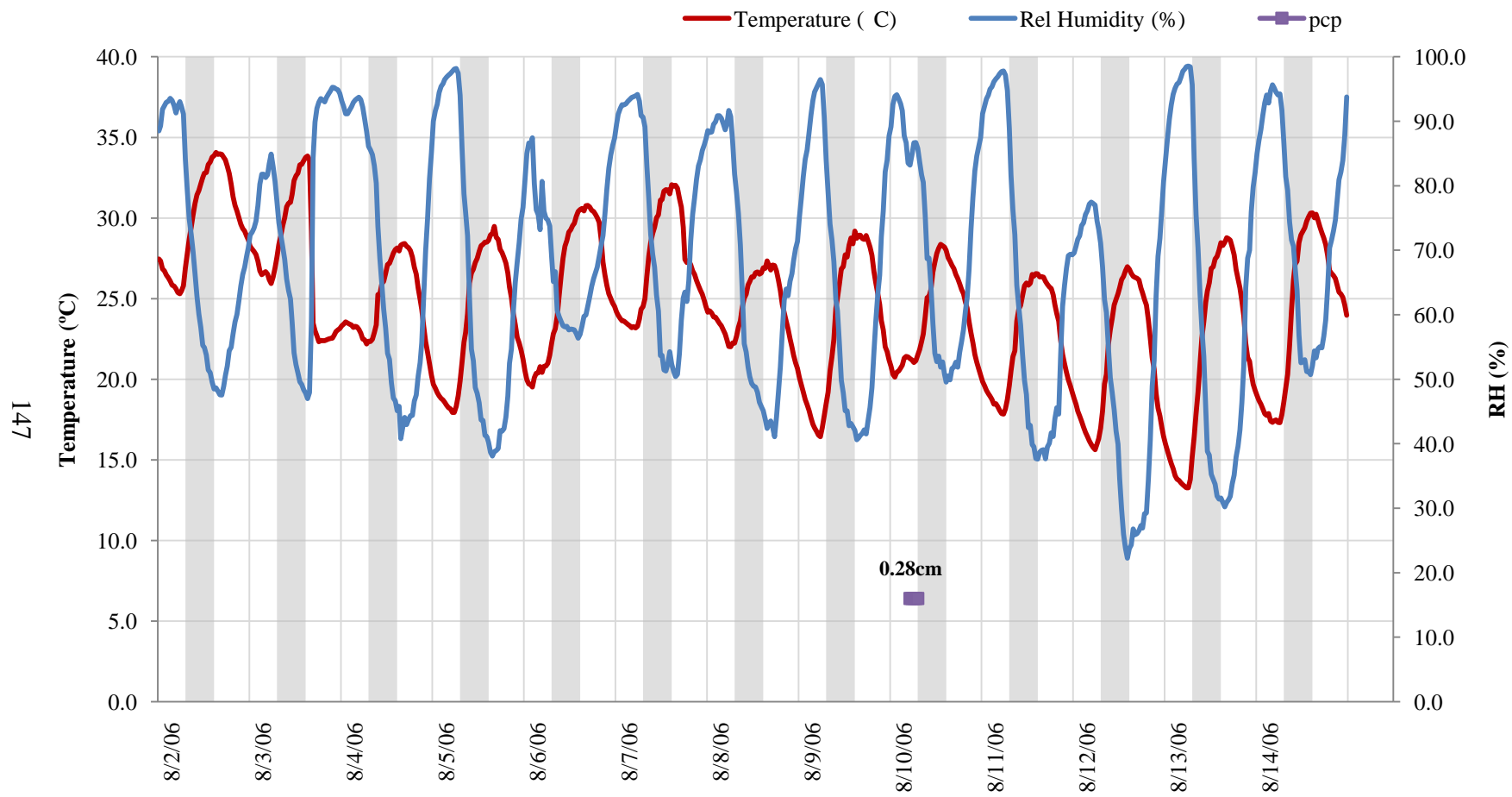
### A SEASONAL COMPARISON OF THE IMPACTS OF CONCENTRATED PM<sub>2.5</sub> ON HRV IN RATS: STEUBENILLE, OHIO

#### IV.1 Steubenville Summer Exposure

##### IV.1.1 Meteorological Summary

During the two-week period of air monitoring in Steubenville, Ohio, daily weather conditions were calm and little precipitation or few synoptic events occurred. As shown in Figure IV.1, the diurnal patterns were pronounced, but daily maximums and minimums were not substantially different from one another. The two-week average temperature was  $24.6 \pm 4.5^\circ\text{C}$  (Exposure Mean:  $26.5 \pm 3.8^\circ\text{C}$ ) and a RH of  $68.0 \pm 19.9\%$  (Exposure Mean:  $58.8 \pm 15.1\%$ ). Daylight hours in early August in Steubenville were approximately 6:20am to 8:30pm, EDT. The daytime/nighttime differences in temperature ( $26.4$  and  $21.9^\circ\text{C}$ , respectively) and RH (59 and 82%, respectively) were statistically significant ( $p < 0.0001$ ). As typically seen during the summer in the Midwest, the significant change in RH occurred shortly after sunrise. The only day that did not show the same strong RH changeover the course of day was August 6, which had overcast conditions throughout the day that may have limited mixing of the atmosphere due to less surface heating. Most days recorded several hours of clear conditions that would help promote photochemical reactions throughout the exposure period and enhance the formation of secondary  $\text{SO}_4^{-2}$  and  $\text{O}_3$  production.

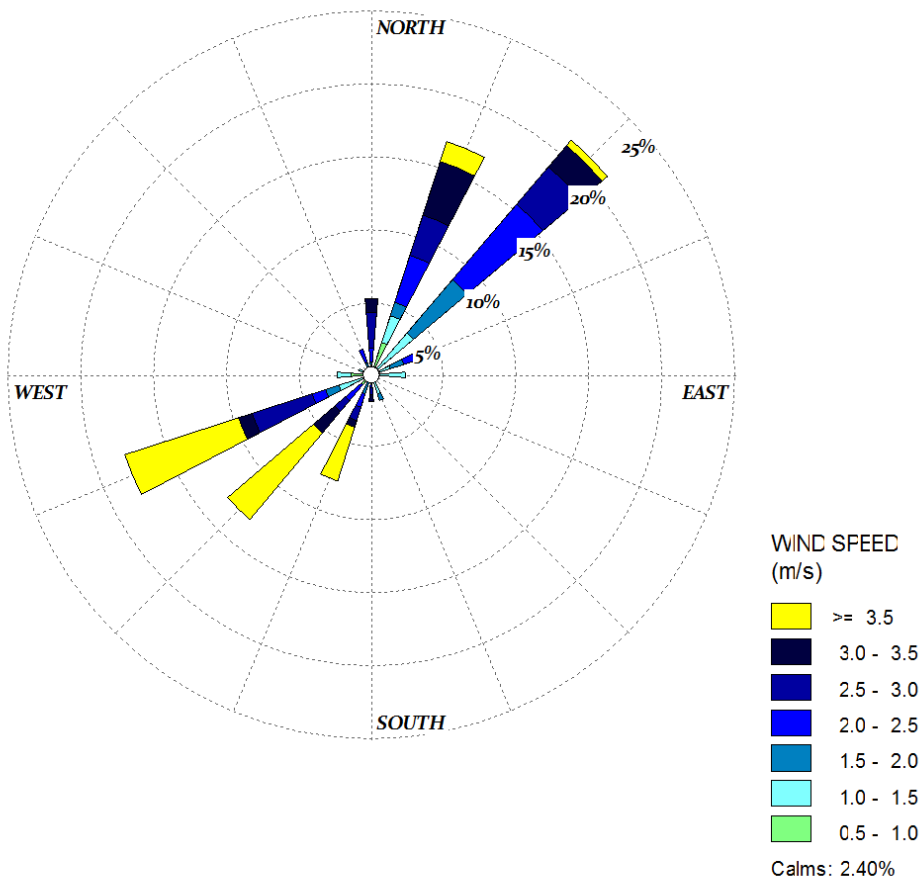
**Figure IV.1 Hourly temperature and RH during the Steubenville summer exposure study.**



## Wind Patterns

Wind patterns in Steubenville were often influenced by the ~100 meter cliffs on either side of the Ohio River Valley which channeled the winds. The Steubenville site was situated on top of the bluff, with predominant winds coming to the site from the northeast (NE) or from the southwest (SW). The wind rose for the two weeks of exposure captures this flow pattern (Figure IV.2). As discussed in Chapter II, two of the largest point source emissions for PM<sub>2.5</sub> in the vicinity of Steubenville are the Sammis and Cardinal coal-fired power plants. The wind rose suggests that NE winds can capture emissions from Sammis while SW winds will capture Cardinal emissions.

**Figure IV.2 Wind rose showing the prevailing surface flow for the August 2-14, 2006 summer exposure study in Steubenville.**

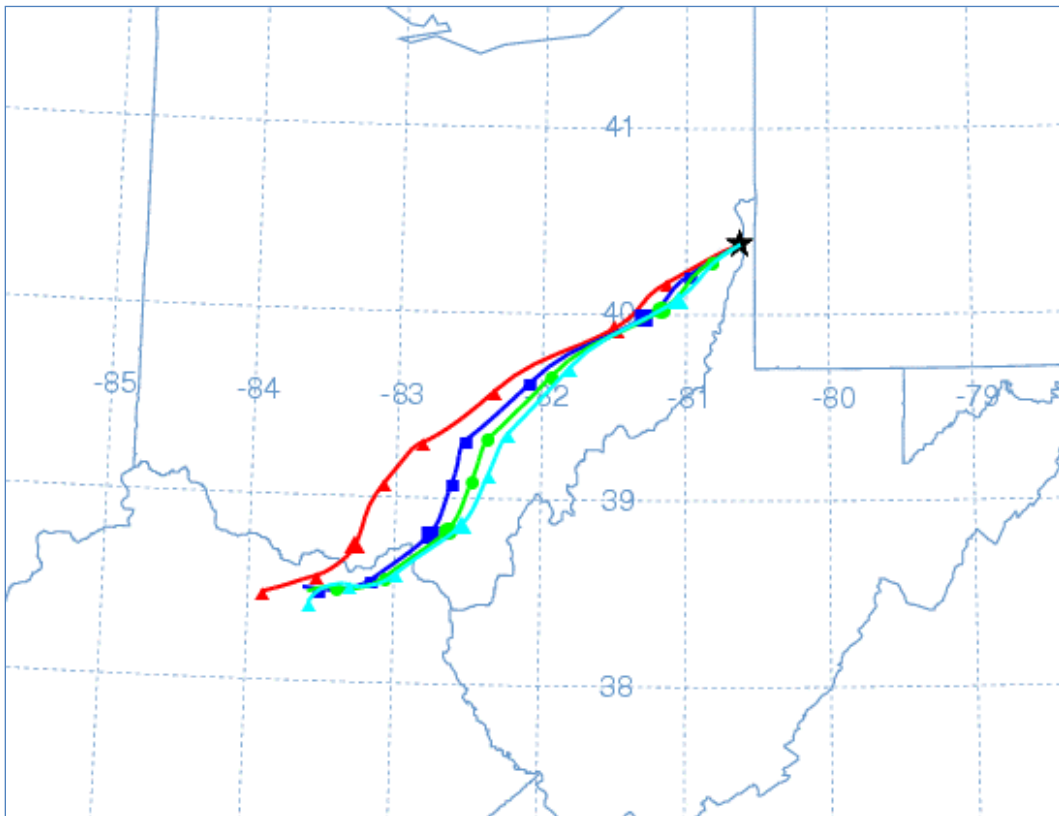




### Back Trajectories

Air mass transport to the site was modeled using the Hybrid Single-Particle Lagrangian Integrated Trajectory (HYSPPLIT) Model Version 4.8 (Draxler and Hess, 1997). Backward trajectories were calculated for each two-hour block of exposure starting at one-half the mixed depth for each day of the study. The trajectories illustrated that most air masses that reached Steubenville during the summer study were out of the SW and NE, showing similar trends observed in the surface winds. Appendix A shows the trajectories alongside the surface winds for each day of exposure. The on-site surface winds often matched the trajectory generated wind data indicating little wind shear through the mixed layer of the atmosphere. In Figure IV.3 the air mass path moving backward in time from the Steubenville site on August 2 was from the SW. Relatively slow, southwesterly air mass transport in the summer months often results in elevated concentrations of  $PM_{2.5}$  in broad areas around the Ohio River Valley.

**Figure IV.3 Hysplit back trajectories for August 2 during the exposure hours associated with ambient  $PM_{2.5}$  mass of  $34.7\mu\text{g}/\text{m}^3$  (CAPs:  $951\mu\text{g}/\text{m}^3$ ).**



## **Precipitation**

High-pressure dominated the weather for the two-week exposure period and kept conditions in Steubenville stable with very little precipitation. August 10 was the only day with rain (0.28cm), and the precipitation ended just prior to the exposure period that morning. The rain was associated with a warm front that passed through the region overnight. Trace amounts of precipitation were also recorded on the August 7 from isolated convective storms during the evening after exposure hours.

In summary, the meteorological conditions during the summer in the Ohio River Valley were often dominated by slow-moving high-pressure systems that led to large areas of poor air quality that encompassed the Steubenville site. Due to the large areas of stagnation that were observed in the eastern Ohio area changes in PM<sub>2.5</sub> were typically more gradual. Site-to-site comparisons between Detroit and Steubenville in a later chapter will discuss in more detail the pollution concentrations and HRV during the exposures.

### **IV.1.2 Ambient Air Pollution Levels**

#### **PM<sub>2.5</sub> Mass Concentration**

The average PM<sub>2.5</sub> concentration in Steubenville over the exposure period, as determined from the 30-minute TEOM data, was  $25.0 \pm 14.0 \mu\text{g}/\text{m}^3$  with fine mass ranging from 0.4 to  $82.2 \mu\text{g}/\text{m}^3$ . The average PM<sub>2.5</sub> for the 8-hours of exposure was nearly identical to the 24-hour average fine mass concentration ( $24.1 \pm 14.1 \mu\text{g}/\text{m}^3$ ). In Figure IV.4, the 30-minute PM<sub>2.5</sub> concentrations were plotted, with the exposure hours highlighted by grey bars. The diurnal changes in the PM<sub>2.5</sub> concentrations were not significant; daytime and nighttime ambient concentrations were 25.1 and  $24.9 \mu\text{g}/\text{m}^3$ , respectively ( $p=0.8618$ ). This is quite different from what was observed in the two Detroit intensives. Instead, synoptic-scale meteorology strongly influenced the PM<sub>2.5</sub> levels in Steubenville with the migration of strong high-pressure and weak low-pressure systems moving across the Midwest region. Figure IV.5 indicates that highest concentrations of PM<sub>2.5</sub> were observed with SW winds. The mean PM<sub>2.5</sub> from the NE was lower at  $15.8 \pm 8.3 \mu\text{g}/\text{m}^3$ . From the SW direction, the mean concentration was  $32.5 \pm 13.6 \mu\text{g}/\text{m}^3$ , over twice the concentration observed from the NE.

**Figure IV.4 Thirty-minute ambient PM<sub>2.5</sub> concentrations during the Steubenville summer study with exposure hours marked with grey bars.**

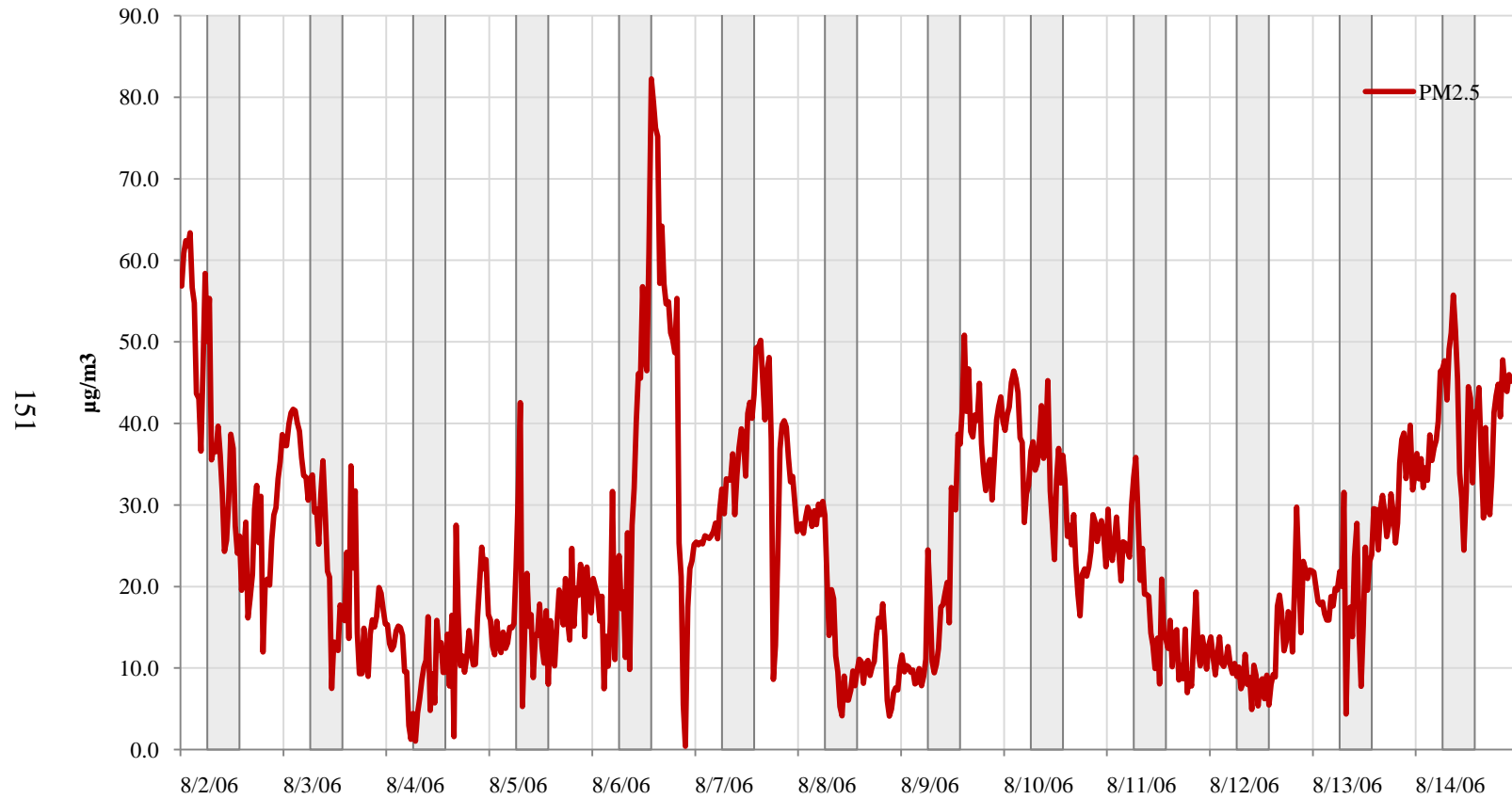
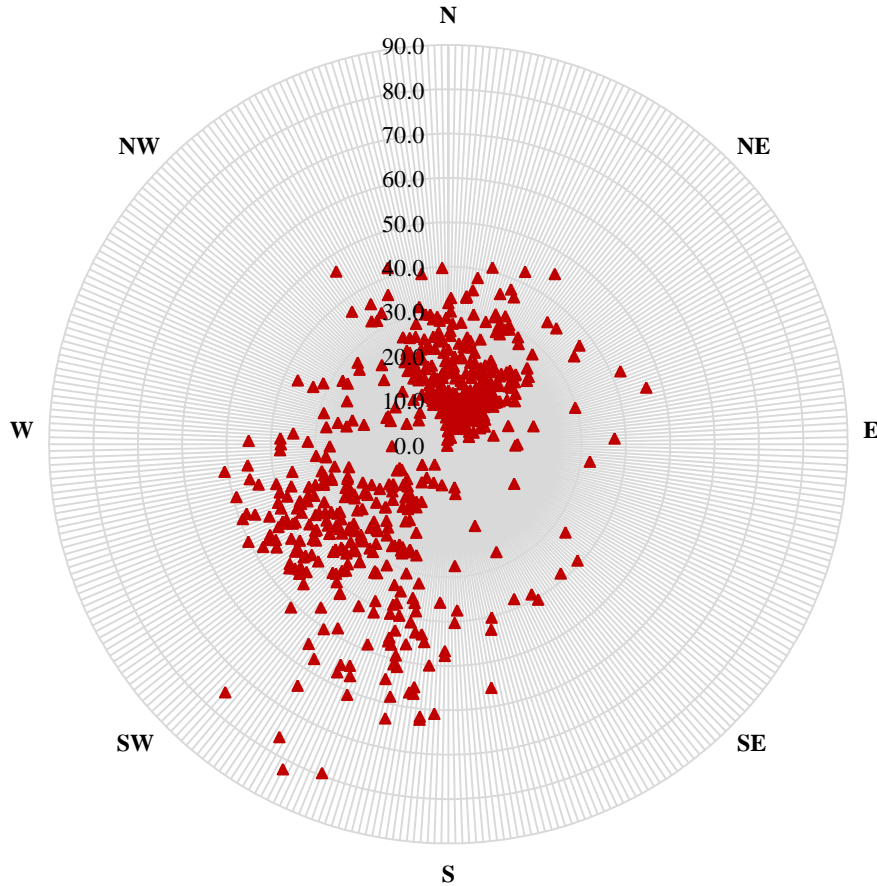


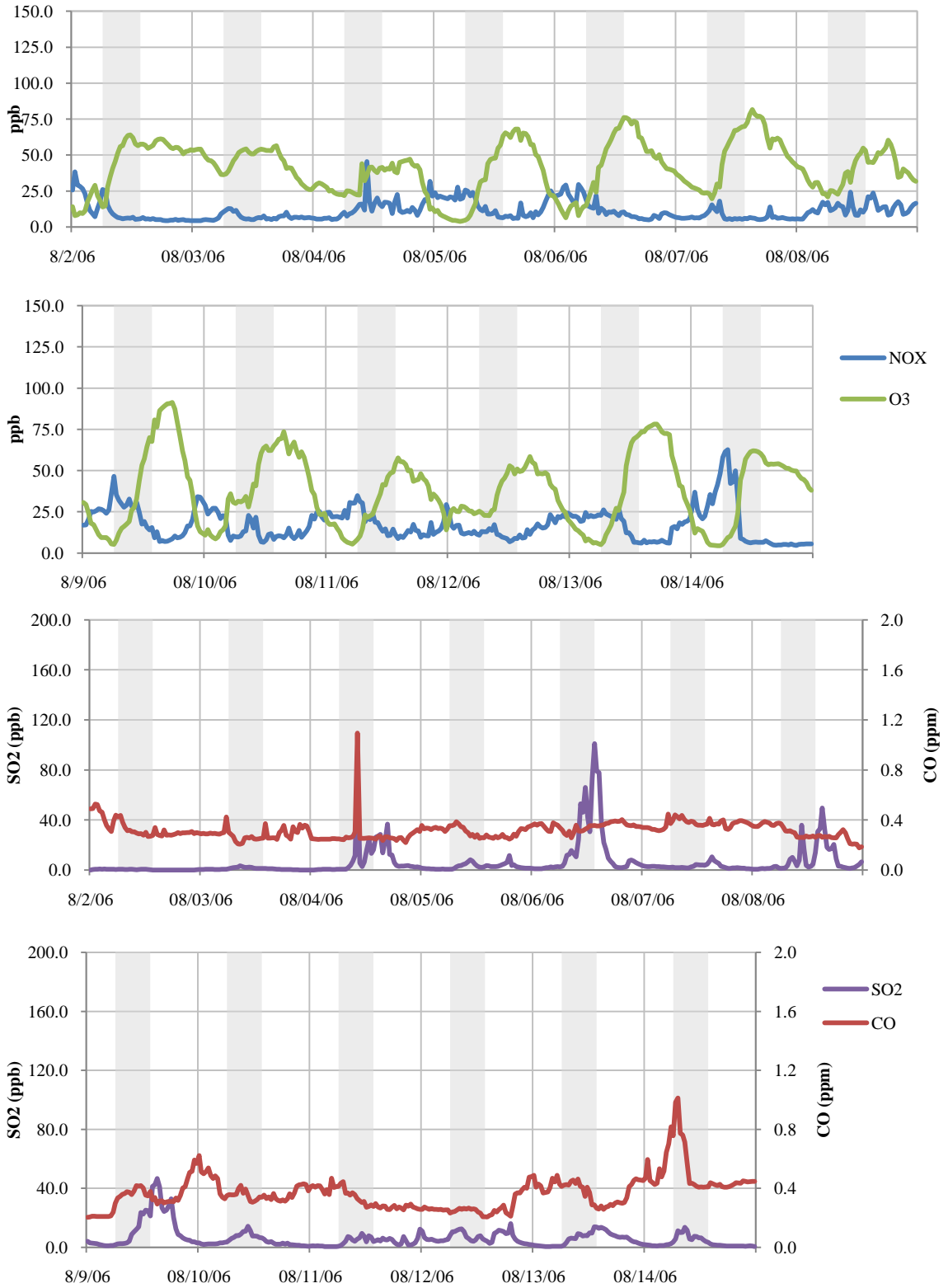
**Figure IV.5 Thirty-minute average ambient PM<sub>2.5</sub> ambient concentrations ( $\mu\text{g}/\text{m}^3$ ) according to wind direction, for 24-hours a day, during the Steubenville summer exposure.**



### **Ambient Gas Concentrations**

Thirty-minute concentrations of NO<sub>x</sub>, SO<sub>2</sub>, CO and O<sub>3</sub> were plotted in Figure IV.6. O<sub>3</sub> concentrations revealed a typical diurnal trend reaching 0ppb at night to ~75ppb during the late afternoon. There were a few significant peaks in NO<sub>x</sub>, SO<sub>2</sub> and CO during the two-week study, particularly on August 4 when all three gases had an early morning elevation in concentration, but did not correspond with PM<sub>2.5</sub> mass. On August 6 and 9, a gradual increase in PM<sub>2.5</sub> and gaseous SO<sub>2</sub> were observed. Furthermore, NO<sub>x</sub> had a significant peak in the early morning of August 14 corresponding with ambient PM<sub>2.5</sub> concentrations that reached 55 $\mu\text{g}/\text{m}^3$ . Winds during this day were fairly constant throughout.

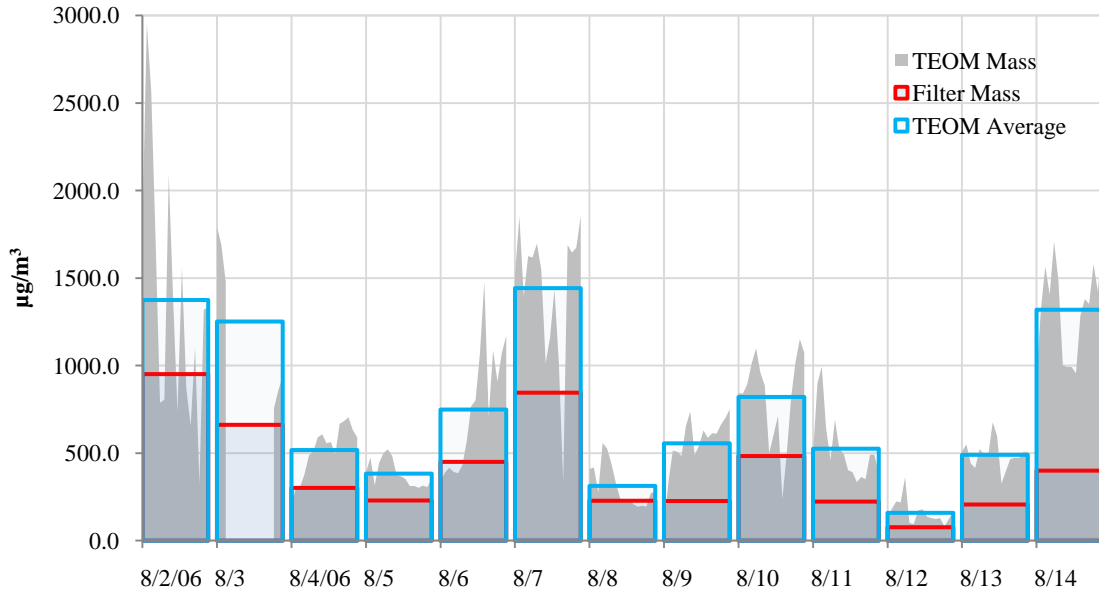
**Figure IV.6 Thirty-minute average concentrations of gaseous pollutants measured in Steubenville during the summer exposure.**



### IV.1.3 CAPs PM<sub>2.5</sub> Characterization

PM<sub>2.5</sub> mass concentrations in the exposure chamber during the Steubenville summer intensive averaged  $406.4 \pm 266.3 \mu\text{g}/\text{m}^3$  from daily, integrated filter weights. The chamber TEOM had a considerably higher average mass ( $719.4 \pm 423.1 \mu\text{g}/\text{m}^3$ ). The 8-hour average fine mass measured with the TEOM correlated highly with the fine mass from the filter ( $r^2=0.811$ ). In Figure IV.7, the continuous TEOM data is shown with the TEOM exposure average and the gravimetric mass concentration obtained from the filters. Differences in the fine mass concentration between the TEOM and the filters were not believed to be a malfunction with the TEOM. Instead, the heavy OC component to PM<sub>2.5</sub> mass in Steubenville may explain the discrepancy. OC in the summer may partially be in the semi-volatile form and affect the TEOM, and even though the semi-volatile OC was probably collected on the filter, but may have de-gassed prior to calculating the post-weight in the laboratory weeks after sampling.<sup>66</sup> Furthermore, ambient concentrations of PM<sub>2.5</sub> correlate better with the TEOM mass concentrations than with the filters, thus supporting that the concentrations recorded using 30-minute data were valid. In this respect, the TEOM was likely recording a more accurate representation of the PM mass during the exposure.

**Figure IV.7 Daily CAPs concentrations obtained from the TEOM and from filter weights. Continuous TEOM concentrations are plotted in the background.**



### PM<sub>2.5</sub> Composition

The major components of PM<sub>2.5</sub> were analyzed on each day from the filter extracts showing that (NH<sub>4</sub>)<sub>2</sub>SO<sub>4</sub> and OC made up over 50% of the mass composition in Steubenville. In fact, the percentages of the major components of PM<sub>2.5</sub> were nearly identical to the summertime composition found in Detroit. Organic matter (OC) may have a strong contribution in Steubenville due to (1) volatile organic compounds from metal processing and coke ovens along the river valley, and (2) more wind-blown agricultural dust from the surrounding farmland that parallels the Ohio River. NH<sub>4</sub><sup>+</sup> remains high and likely bound to sulfate ions, whereas nitrates were in small quantities either because of the prominence of SO<sub>4</sub><sup>-2</sup> binding to NH<sub>4</sub><sup>+</sup> to form particles or because a significantly lower NO<sub>3</sub><sup>-</sup> contribution occurs in Steubenville with the absence of heavy vehicle traffic as seen in metropolitan areas like Detroit. The unidentified mass (mean: 110.9µg/m<sup>3</sup>) was a relatively large percentage of daily mass, and the majority of unidentified mass was water vapor associated with the hygroscopic aerosols.

**Figure IV.8 Composition of PM<sub>2.5</sub> from analysis of CAPs filter samples collected during 8-hour exposures for the Steubenville summer study (µg/m<sup>3</sup>).**

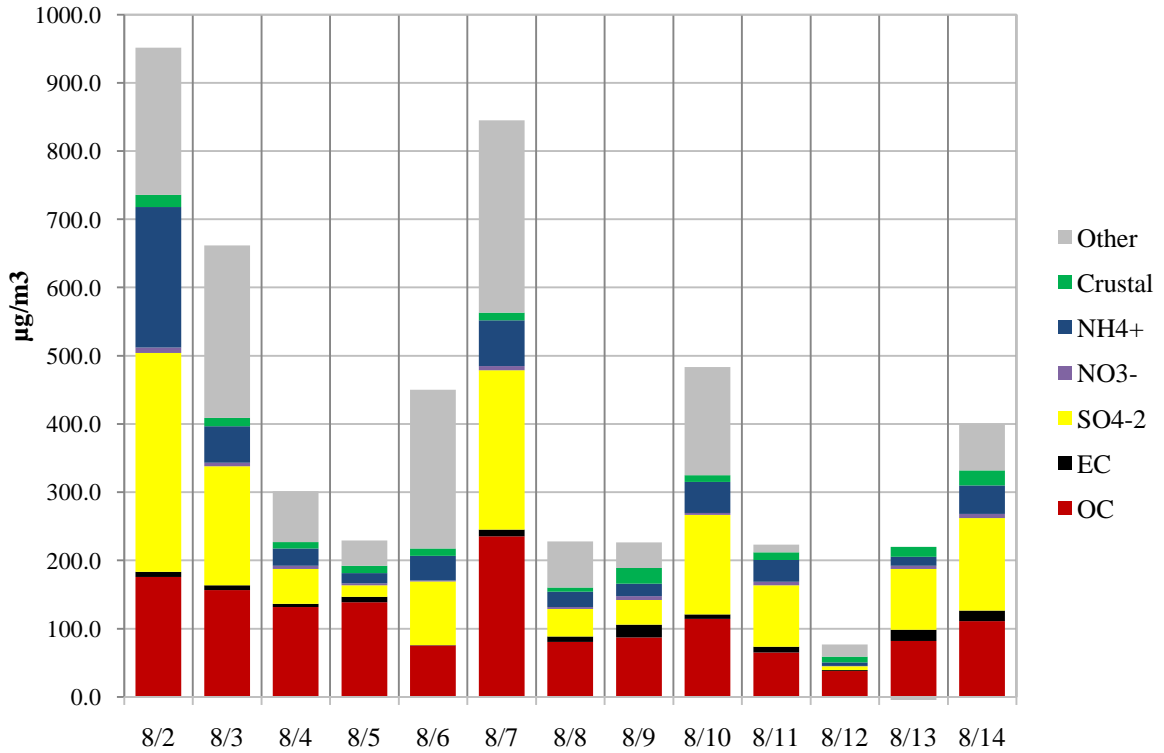


**Table IV.1 Daily concentrations of the major components of PM<sub>2.5</sub>CAPs collected during the 8-hour exposures (µg/m<sup>3</sup>).**

Date	PM	OC	EC	SO <sub>4</sub> <sup>-2</sup>	NO <sub>3</sub> <sup>-</sup>	NH <sub>4</sub> <sup>+</sup>	Crustal
8/2	951.3	176.0	7.4	320.9	7.6	206.1	19.8
8/3	661.6	156.7	6.8	174.7	4.8	53.6	13.9
8/4	301.4	131.5	4.8	51.0	4.7	25.3	11.4
8/5	229.4	138.5	8.1	16.9	3.0	14.8	12.1
8/6	450.1	75.3	0.5	93.5	1.1	36.3	10.8
8/7	845.2	235.3	9.7	233.6	6.3	67.0	12.5
8/8	228.0	80.5	8.0	40.3	2.6	22.7	8.0
8/9	226.6	87.1	18.8	36.3	5.7	17.9	30.8
8/10	483.3	114.5	6.6	145.5	3.1	45.2	11.3
8/11	223.2	65.2	8.2	90.4	5.1	31.8	18.7
8/12	76.7	37.9	1.3	5.7	0.5	5.1	10.1
8/13	206.6	82.0	16.1	89.4	4.8	12.9	18.7
8/14	400.0	110.9	15.8	135.6	5.9	41.7	26.3
<b>Mean</b>	406.4	114.7	8.6	110.3	4.2	44.6	15.7
<b>Std Dev.</b>	266.3	53.1	5.4	91.4	2.1	51.6	6.8



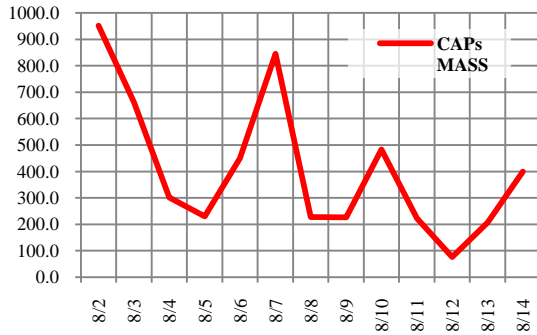
### Trace Element Concentrations

Substantial day-to-day differences in trace elements concentrations were observed and specific trace elements appeared to vary independently from PM<sub>2.5</sub>. The highest PM<sub>2.5</sub> concentration was observed on August 2, with secondary peaks on August 7 and 3 (951.3, 845.2 and 661.6 µg/m<sup>3</sup>, respectively). All three of these days had winds coming from the SW into Steubenville; as Figure IV.9 indicates, had generally the same component concentrations. Winds were from the NE August 12 when the lowest day of PM<sub>2.5</sub> CAPs was recorded (76.7 µg/m<sup>3</sup>). With calm winds, clear conditions and no precipitation, it appears that the only factor of a large high-pressure system could have created conditions for considerable lofting of air pollutants away from the surface causing low concentrations of PM<sub>2.5</sub> and its constituents.

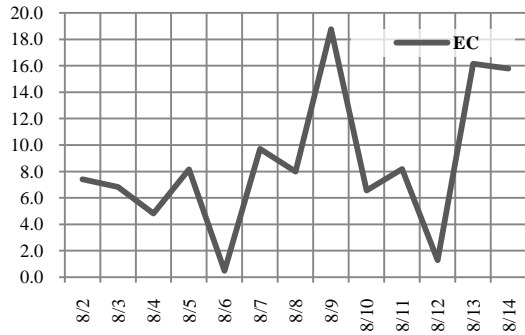
The following constituents generally followed the same day-to-day pattern in concentration as PM<sub>2.5</sub> with only minor variability: NO<sub>3</sub><sup>-</sup>, SO<sub>4</sub><sup>-2</sup>, NH<sub>4</sub><sup>+</sup>, OC, S, Al, P and Se. Elemental carbon (EC), however, peaked on August 9 and had two secondary peaks on August 13 and 14, as did many other trace elements, like Fe, K, Mn, Mg, Ca, Zn, Mo, Rb, Cr, Ba, Pb and In. La, Ce and Sm all had maximums on August 2 and did not observe significant day-to-day differences in concentration.

**Figure IV.9 Daily plots of CAPs concentrations during Steubenville summer exposures. PM (a) and EC (b) in units of  $\mu\text{g}/\text{m}^3$  and trace element concentrations (c-f) in units of  $\text{ng}/\text{m}^3$ .**

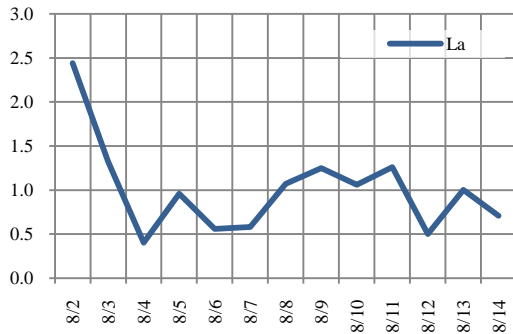
**(a) PM,  $\text{NO}_3^-$ ,  $\text{SO}_4^{2-}$ ,  $\text{NH}_4^+$ , OC, S, Al, P, Se**



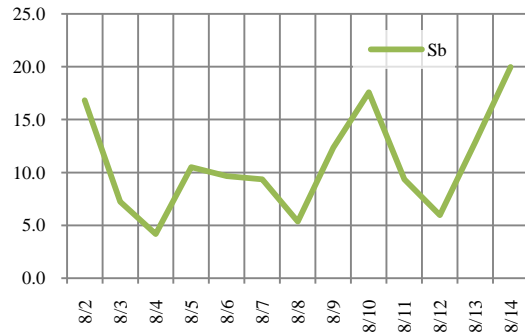
**(b) EC, Fe, K, Mn, Mg, Ca, Zn, Mo, Rb, Cr, Ba, Pb, In**



**(c) La, Ce, Sm**



**(d) Sb**



**(e) Co**



**(f) Cu**

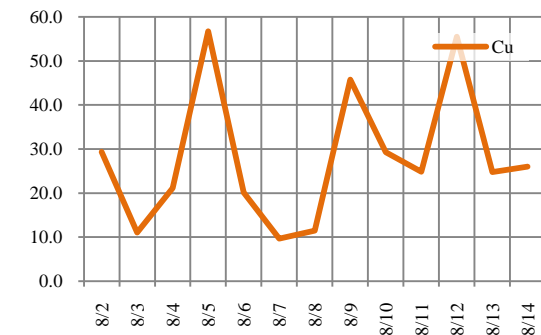


**Table IV.2 Daily trace element CAPs concentrations determined for Steubenville summer exposures. Units are ng/m<sup>3</sup> except PM, S, Ca and Fe in µg/m<sup>3</sup> (\*).**

	PM*	Mg	Al	P	S*	K	Ca*	Ti	V	Cr	Mn	Fe*	Co	Cu	Zn	As	Se	Rb	Sr	Mo	Cd	In	Sb	Ba	La	Ce	Sn	Pb
8/2	951	544	1391	430	78.9	778	1.46	33.8	22.6	11.3	71.3	2.84	1.03	29.3	200	16.1	88.6	2.71	12.5	2.8	20.7	0.05	16.8	44.7	2.44	3.22	13.5	123
8/3	662	550	957	212	42.5	565	1.22	27.7	18.9	9.3	45.1	1.65	1.82	11.0	94.2	9.3	63.4	2.15	11.1	2.1	7.4	0.02	7.2	34.6	1.32	2.12	9.7	57.6
8/4	301	210	234	207	13.1	533	1.35	61.1	8.5	0.0	55.6	1.01	0.24	21.2	97.3	9.9	46.9	1.08	5.6	0.9	5.7	0.03	4.2	32.7	0.40	0.83	5.8	58.5
8/5	229	243	442	181	6.0	601	0.70	148.6	25.6	34.4	83.0	1.17	0.50	56.7	1031	10.1	17.4	1.59	6.0	5.7	34.7	0.23	10.5	43.8	0.96	1.21	8.4	250
8/6	450	247	225	158	24.5	618	0.14	122.0	28.7	8.4	79.0	0.97	0.70	20.1	152	9.8	180	1.35	9.1	14.6	7.6	0.04	9.7	36.0	0.56	0.84	7.5	83.7
8/7	845	283	418	76.0	57.9	589	0.99	22.0	7.0	10.1	135	1.35	0.52	9.6	53.4	13.6	70.9	1.20	7.5	2.4	4.9	0.02	9.3	28.8	0.58	1.16	7.3	55.6
8/8	228	268	216	128	10.3	265	1.24	87.5	13.9	38.5	148	1.46	1.54	11.4	365	7.9	21.1	1.21	5.3	6.4	3.4	0.10	5.4	24.3	1.07	1.34	4.9	74.2
8/9	227	764	1033	246	12.8	1046	5.49	275.2	38.4	56.2	225	4.38	1.27	45.8	1635	11.8	38.0	2.53	14.0	39.1	15.1	0.20	12.4	74.6	1.25	2.43	10.4	208
8/10	483	259	246	113	42.2	529	0.84	20.9	6.1	28.7	67.1	1.47	0.38	29.3	587	16.2	45.1	1.11	6.6	5.5	8.0	0.03	17.6	38.1	1.06	1.64	7.8	79.6
8/11	223	674	762	113	11.9	418	5.50	83.3	11.2	19.8	155	2.48	0.62	24.9	474	8.9	13.8	1.45	13.2	9.1	11.4	0.09	9.3	53.4	1.26	2.35	7.1	101
8/12	77	321	215	194	2.6	469	1.17	18.4	1.6	13.2	45.9	0.92	0.50	55.5	635	2.8	8.4	1.04	4.8	11.9	7.9	0.01	6.0	36.6	0.50	0.89	4.3	65.2
8/13	207	495	462	127	7.6	827	2.98	148.6	29.2	32.1	84.7	1.32	0.79	24.8	1770	19.6	22.4	1.49	12.7	38.7	35.2	0.34	12.9	44.7	1.00	1.60	22.9	311
8/14	400	718	521	320	41.3	1015	2.91	31.3	15.0	14.3	307	4.73	0.79	26.0	4821	13.4	42.0	4.32	9.3	4.7	16.4	0.06	20.0	39.8	0.71	1.40	10.5	208
Mean	406	429	548	193	27.0	635	2.00	83.1	17.4	21.3	116	1.98	0.82	28.1	917	11.5	50.6	1.79	9.0	11.1	13.7	0.09	10.9	40.9	1.01	1.62	9.2	129
SD	266	202	378	96.5	23.5	226	1.74	75.0	10.9	15.7	77.8	1.28	0.47	15.6	1303	4.3	45.6	0.94	3.3	13.0	10.6	0.10	4.9	12.6	0.53	0.72	4.8	85.7

#### IV.1.4 Eight-Hour HRV Summary

The integrated Steubenville dataset allowed for an analysis of the frequency-domain and provided dramatic results for HR and HRV; however, the driving factors need to be further examined in order to better understand the mechanisms behind these changes. Table IV.3 summarizes the average HRV parameters for AIR and CAPs Rats. At first glance there appeared to be no significant differences, but as described in previous sections, averaging these parameters masks the day-to-day variability within each individual rat. Mixed modeling results for the Steubenville summer exposure found that  $\ln(\text{SDNN})$ ,  $\ln(\text{LF})$  and  $\ln(\text{HF})$  were significantly different between AIR and CAPs Rats.

The unique finding from the 8-hour dataset was the significant response in frequency-domain parameters,  $\ln(\text{LF})$  and  $\ln(\text{HF})$ . Although these changes were significant, the spectral analysis performed on HR used the 8-hour data, which included breaks in the data from one sampling point to the next. As discussed in Chapter II, spectral analysis should be conducted on short segments of continuous data. Nevertheless, the significance in these findings was worth further investigation to determine if patterns existed with the changes in  $\ln(\text{LF})$  and  $\ln(\text{HF})$ . If a specific data point (e.g. date) could be identified as significantly different in  $\ln(\text{SDNN})$  along with  $\ln(\text{LF})$  and  $\ln(\text{HF})$ , then there was a possibility that the observed changes in frequency-domain were valid. Likewise, if the same constituents associated with  $\ln(\text{SDNN})$  are also associated with  $\ln(\text{LF})$  and  $\ln(\text{HF})$ , then this may be strong indication that frequency-domain parameters in SH Rats were affected by CAPs exposure in Steubenville

**Table IV.3 Mixed modeling results comparing AIR and CAPs Rats from the Steubenville summertime intensive.**

	AIR Rats	CAPs Rats	Mixed Modeling Results		
	N=81	N=88	Group	Date	Group*Date
Heart Rate	218.9	218.8	0.7382	<.0001	0.8843
$\ln(\text{SDNN})$	2.886	2.902	0.7258	<.0001	<b>0.0127</b>
$\ln(r\text{-MSSD})$	1.640	1.685	0.6414	0.2286	0.9087
$\ln(\text{Low Frequency})$	-3.082	-2.934	0.2000	0.6612	<b>0.0076</b>
$\ln(\text{High Frequency})$	-2.624	-2.593	0.7081	0.044	<b>0.0173</b>
LF/HF Ratio	0.654	0.722	0.2895	0.0747	0.7698

## Days with Significant Changes in HRV

With significant differences observed across three HRV parameters, it was valuable to learn if significant changes in HRV occurred on a specific day (or days). The LS Means function sought to determine the specific dates that AIR and CAPs rats significantly differed from each other. For  $\ln(\text{SDNN})$  the first two days of exposure, August 2 and 3, showed that there was a significant *increase* in CAPs Rats over AIR Rats (Table IV.4). These findings were supported with the intra-group comparison of  $\ln(\text{SDNN})$  showing that  $\ln(\text{SDNN})$  of CAPs Rats on the first day of exposure varied considerably than all other days (Table IV.5). August 3 did not observe the same level of significance in CAPs Rats  $\ln(\text{SDNN})$  against CAPs Rats  $\ln(\text{SDNN})$  on all the other exposure days. When looking at  $\ln(\text{LF})$ , the first day of exposure showed a moderate decrease in the CAPs Rats in relation to AIR Rats ( $p=0.064$ ), whereas August 9 showed a significant increase in  $\ln(\text{LF})$  for CAPs Rats ( $p=0.027$ ). For  $\ln(\text{HF})$  in CAPs Rats, the 2<sup>nd</sup> and 9<sup>th</sup> showed moderate differences from the AIR Rats, ( $p=0.097$  and  $0.059$ , respectively). Inter-group statistical analysis found that neither  $\ln(\text{LF})$  nor  $\ln(\text{HF})$  in CAPs Rats were significantly different from one day to the next. Therefore, the only frequency-domain finding to align with time-domain findings was when a significant decrease in  $\ln(\text{LF})$  corresponded with a significant increase in  $\ln(\text{SDNN})$  on August 2, the day with the highest CAPs concentrations.

**Table IV.4 The ln(SDNN) parameter was investigated to determine if AIR and CAPs Rats differed within a specific day using the LS Means procedure.**

	Date	Estimate	SE	df	t Value	p Value	Direction
AIR - CAPs	<b>2-Aug-06</b>	<b>-0.1842</b>	<b>0.05646</b>	<b>131</b>	<b>-3.26</b>	<b>0.0014</b>	<b>Increase</b>
AIR - CAPs	<b>3-Aug-06</b>	<b>-0.1342</b>	<b>0.05646</b>	<b>131</b>	<b>-2.38</b>	<b>0.0189</b>	<b>Increase</b>
AIR - CAPs	4-Aug-06	0.02269	0.05646	131	0.4	0.6884	
AIR - CAPs	5-Aug-06	-0.01917	0.05829	131	-0.33	0.7428	
AIR - CAPs	6-Aug-06	0.001062	0.05829	131	0.02	0.9855	
AIR - CAPs	7-Aug-06	-0.00717	0.05829	131	-0.12	0.9023	
AIR - CAPs	8-Aug-06	-0.0061	0.05829	131	-0.1	0.9168	
AIR - CAPs	9-Aug-06	-0.02421	0.05829	131	-0.42	0.6786	
AIR - CAPs	10-Aug-06	0.02869	0.05829	131	0.49	0.6235	
AIR - CAPs	11-Aug-06	0.0607	0.05829	131	1.04	0.2997	
AIR - CAPs	12-Aug-06	0.051	0.05989	131	0.85	0.396	
AIR - CAPs	13-Aug-06	0.03268	0.06204	131	0.53	0.5993	
AIR - CAPs	14-Aug-06	0.01113	0.05829	131	0.19	0.8488	

**Table IV.5 HRV analysis within CAPs Rats parameter comparisons to determine if observed increases or decreases in ln(SDNN) were significantly lower (or higher) than on other observed days of exposure.**

	8/2	8/3	8/4	8/5	8/6	8/7	8/8	8/9	8/10	8/11	8/12	8/13
8/3	4.27											
8/4	2.00	-2.27										
8/5	3.75	-0.42	1.80									
8/6	5.22	1.05	3.26	1.44								
8/7	3.49	-0.68	1.54	-0.26	-1.70							
8/8	2.05	-2.12	0.09	-1.68	-3.12	-1.42						
8/9	2.25	-1.92	0.30	-1.48	-2.92	-1.22	0.21					
8/10	2.67	-1.50	0.72	-1.06	-2.50	-0.8	0.62	0.41				
8/11	3.05	-1.12	1.09	-0.7	-2.14	-0.44	0.99	0.78	0.37			
8/12	3.62	-0.46	1.71	-0.05	-1.46	0.20	1.60	1.40	0.99	0.63		
8/13	4.71	0.73	2.84	1.11	-0.26	1.36	2.72	2.52	2.13	1.78	1.15	
8/14	3.36	-0.81	1.40	-0.39	-1.83	-0.13	1.29	1.09	0.67	0.31	-0.33	-1.49

On August 2 significant changes in CAPs-exposed rats were observed along with the highest air pollution concentrations. However, August 2 was also the first day of exposure and the significant differences in HRV in CAPs Rats may have a result of the

stress of their new surroundings and atmosphere. The fact that  $\ln(\text{SDNN})$  was significantly different in CAPs Rats than the AIR Rats was important because the AIR Rats underwent the same handling and change in environment. Furthermore, neither of the Detroit intensives nor the Steubenville winter intensive observed quite the same effect in HRV on the first day of the Steubenville summer exposure. Therefore, the biological effects seen in  $\ln(\text{SDNN})$  and  $\ln(\text{LF})$  were likely due to air pollution concentrations and not influenced by confounding factors.

The significance of this first day of exposure was also evident when a test was done to remove the first day of exposure from the mixed model. When mixed modeling was conducted on the 12 remaining days of exposure, the strong significant differences between AIR and CAPs Rats are reduced. Table IV.6 shows that only  $\ln(\text{HF})$  remains as the parameter by which AIR and CAPs Rats differ, which coherent with the earlier findings that  $\ln(\text{HF})$  was only moderately different in CAPs Rats from the AIR Rats. Without August 2,  $\ln(\text{SDNN})$  and  $\ln(\text{LF})$  are no longer distinguishable from the control group. In the next section, the significant associations of  $\ln(\text{SDNN})$  with pollution concentrations will also be lost. Furthermore, the influence of August 2 was greater than that of August 7. Even though August 7 was the second highest day of pollution, removal of this day does not change the overall significance of the parameters. As a result, the air pollution on August 2 was the most significant influence on HRV and determined the health outcomes observed in the 8-hour dataset.

### **Associations between Daily HRV and Air Pollution**

This section discusses the significant changes in HRV in conjunction with 8-hour integrated pollution data. Although all HRV parameters were investigated, the focus will be on  $\ln(\text{SDNN})$ ,  $\ln(\text{LF})$  and  $\ln(\text{HF})$ . In Figure IV.10, the CI Plots for the time-domain parameters (HR and  $\ln(\text{SDNN})$ ) are shown, and ordered by strength of the effect estimate of each pollutant. No significant associations with  $\ln(\text{r-MSSD})$  were identified. Figure IV.11 shows the CI Plots for  $\ln(\text{LF})$ ,  $\ln(\text{HF})$  and the LF/HF ratio.

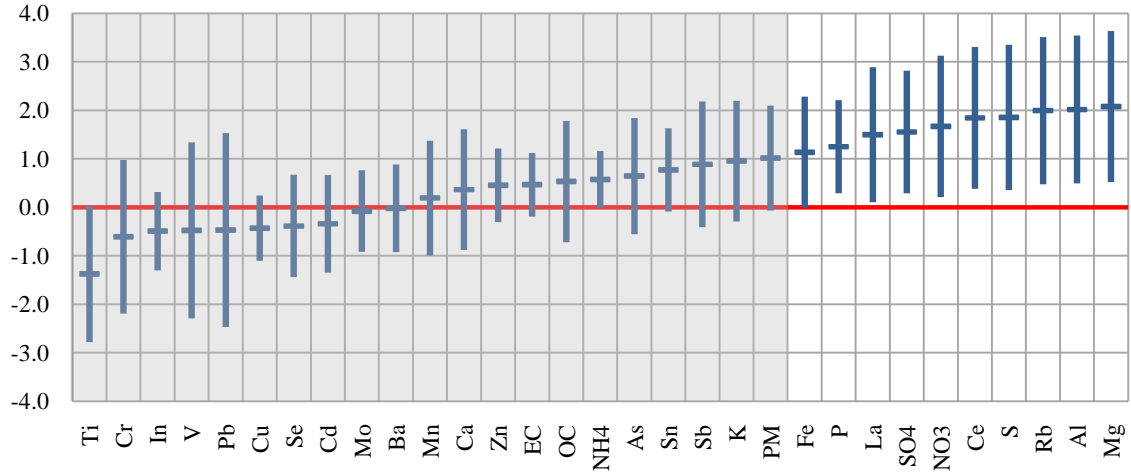
For HR and  $\ln(\text{SDNN})$ , both parameters observed an increase in association with pollutants. Shared among the parameters were Al, La, Ce, S,  $\text{NO}_3^-$ ,  $\text{SO}_4^{2-}$ , S and P. HR also saw significant associations with Fe, Rb and Mg while  $\ln(\text{SDNN})$  was associated

with  $\text{NH}_4^+$ , PM and OC. Reductions were observed for both  $\ln(\text{LF})$  and  $\ln(\text{HF})$ . Constituents associated with  $\ln(\text{HF})$  and  $\ln(\text{LF})$  were  $\text{NH}_4^+$ , PM,  $\text{SO}_4^{-2}$  and S. Additional constituents that associated with  $\ln(\text{LF})$  included Al, La, Ce and P. These four constituents were the only constituents significantly associated with a reduction in the LF/HF ratio; none of these four constituents were associated with  $\ln(\text{HF})$  alone. The concentrations of Al, La, Ce, P, S and  $\text{SO}_4^{-2}$  crossed with both time-domain and frequency-domain HRV parameters. This correlation may indicate that the reliable observations in the time-domain may, in fact, also be affecting the frequency-domain parameters, even if the values were not calculated on the appropriate time scale. Future studies conducted with spectral analysis and semi-continuous ion sampling will help explain this effect more clearly.



**Figure IV.10 Steubenville summer CI Plots for the 8-hour integrated concentrations of pollutants associated with (a) HR and (b) ln(SDNN).**

**(a) HR**



**(b) ln(SDNN)**

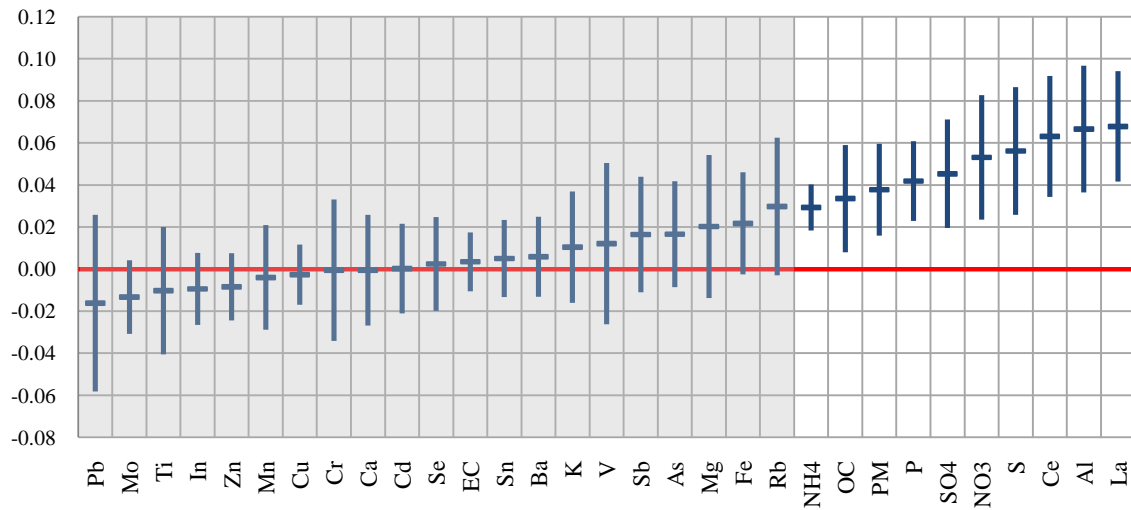
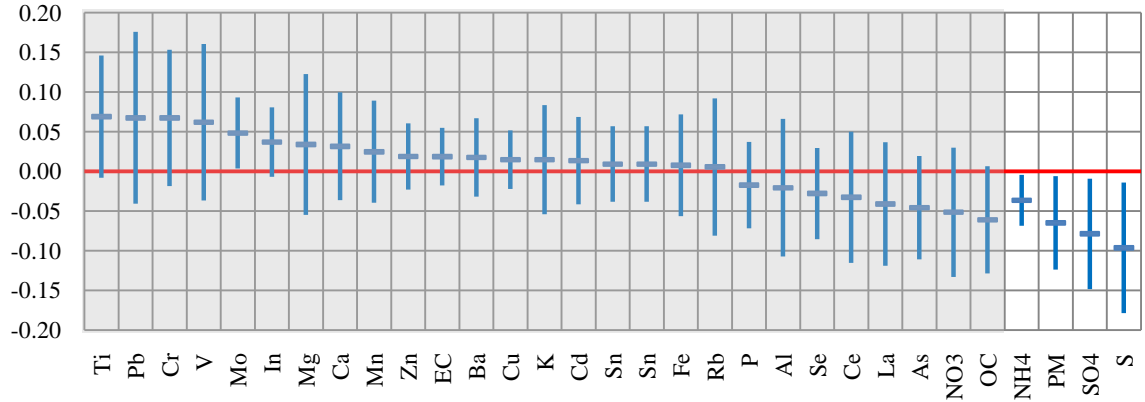
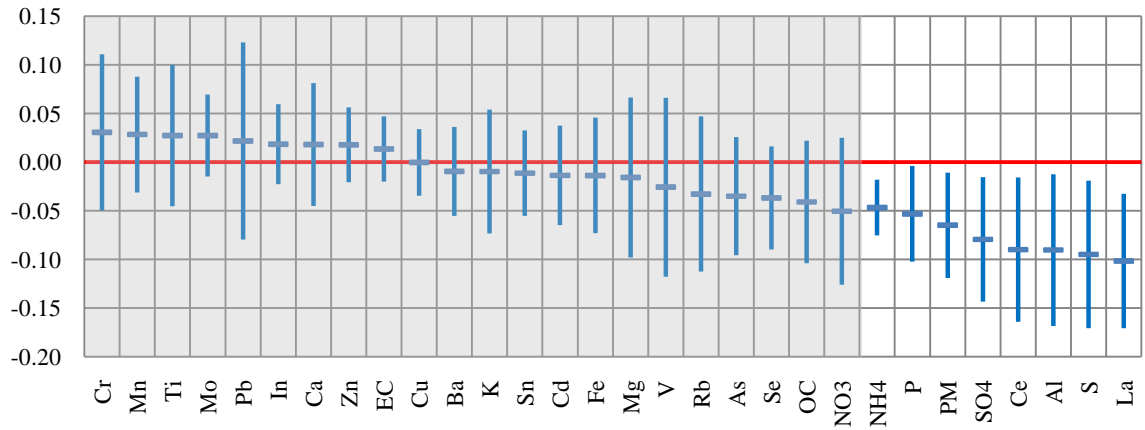


**Figure IV.11 CI Plots for the 8-hour average pollutant concentrations in association with the frequency-domain parameters, (a)  $\ln(\text{HF})$ , (b)  $\ln(\text{LF})$  and (c)  $\text{LF}/\text{HF}$ .**

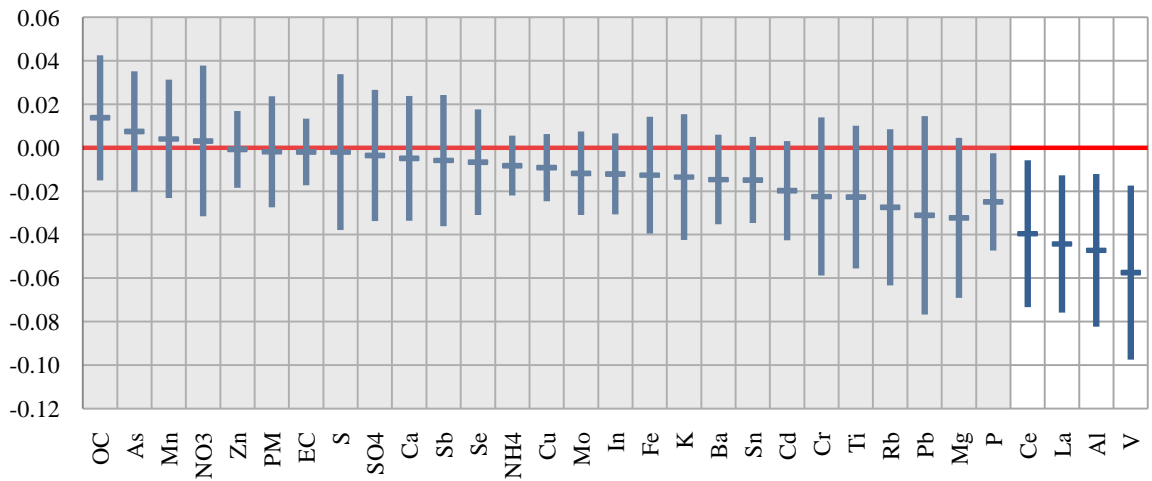
**(a)  $\ln(\text{HF})$**



**(b)  $\ln(\text{LF})$**



**(c)  $\text{LF}/\text{HF}$**



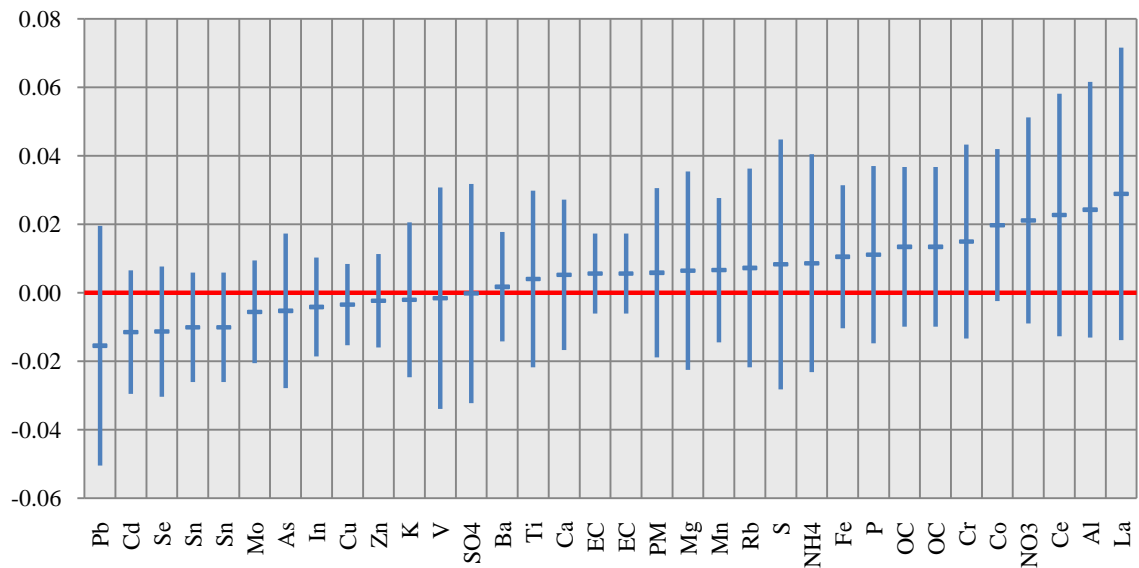
## The Effects Due to Air Pollution on August 2

For ln(SDNN), the increase observed with 8-hour concentrations was unexpected and deserves further analysis. During the Detroit summer intensive, HR increased while both ln(SDNN) and ln(r-MSSD) decreased in conjunction with the associated constituents both in the 8-hour and 30-minute datasets. Looking ahead at the 30-minute CI Plots, ln(SDNN) decreased with constituent concentrations (Figure IV.23). This discrepancy where ln(SDNN) increased along with air pollution concentrations may point to a day when air pollution was high and CAPs Rats saw significantly higher ln(SDNN), thus skewing the associations. Table IV.5 showed that ln(SDNN) on August 2 was significantly higher than all other days and also had the highest PM<sub>2.5</sub> mass. To test the influence of August 2 on the associations with ln(SDNN) and air pollution concentrations, the entire day was removed from the mixed model. New mixed modeling results are shown in Figure IV.6 indicating that no associations with ln(SDNN) remained. Furthermore, significant associations with all the constituents were now lost as indicated in Figure IV.12. Thus, August 2 was responsible for the unusual increase in ln(SDNN). Another test was done to remove data on August 7, the second highest PM<sub>2.5</sub> mass day with similar composition and meteorological conditions (August 2: 951µg/m<sup>3</sup>, August 7: 845µg/m<sup>3</sup>). Removing August 7 did not change the significance between AIR and CAPs Rats, nor did removing August 7 have any effect on the constituents associated with the increase in ln(SDNN).

**Table IV.6 Eight-hour mixed modeling results from the Steubenville summer exposure after removing the first day of exposure (August 2) from the dataset.**

	Mixed Modeling Significance (p<0.05)		
	Group	Date	Group*Date
Heart Rate	0.711	<.0001	0.8098
ln(SDNN)	0.9168	0.0188	0.2861
ln(r-MSSD)	0.6281	0.1237	0.9015
ln(Low Frequency)	0.1386	0.4545	0.2184
ln(High Frequency)	0.5401	0.0047	0.0499
LF/HF Ratio	0.3329	0.0728	0.7149

**Figure IV.12 A CI Plot for ln(SDNN) using 8-hour data from the Steubenville summer intensive but without the first day of exposure.**

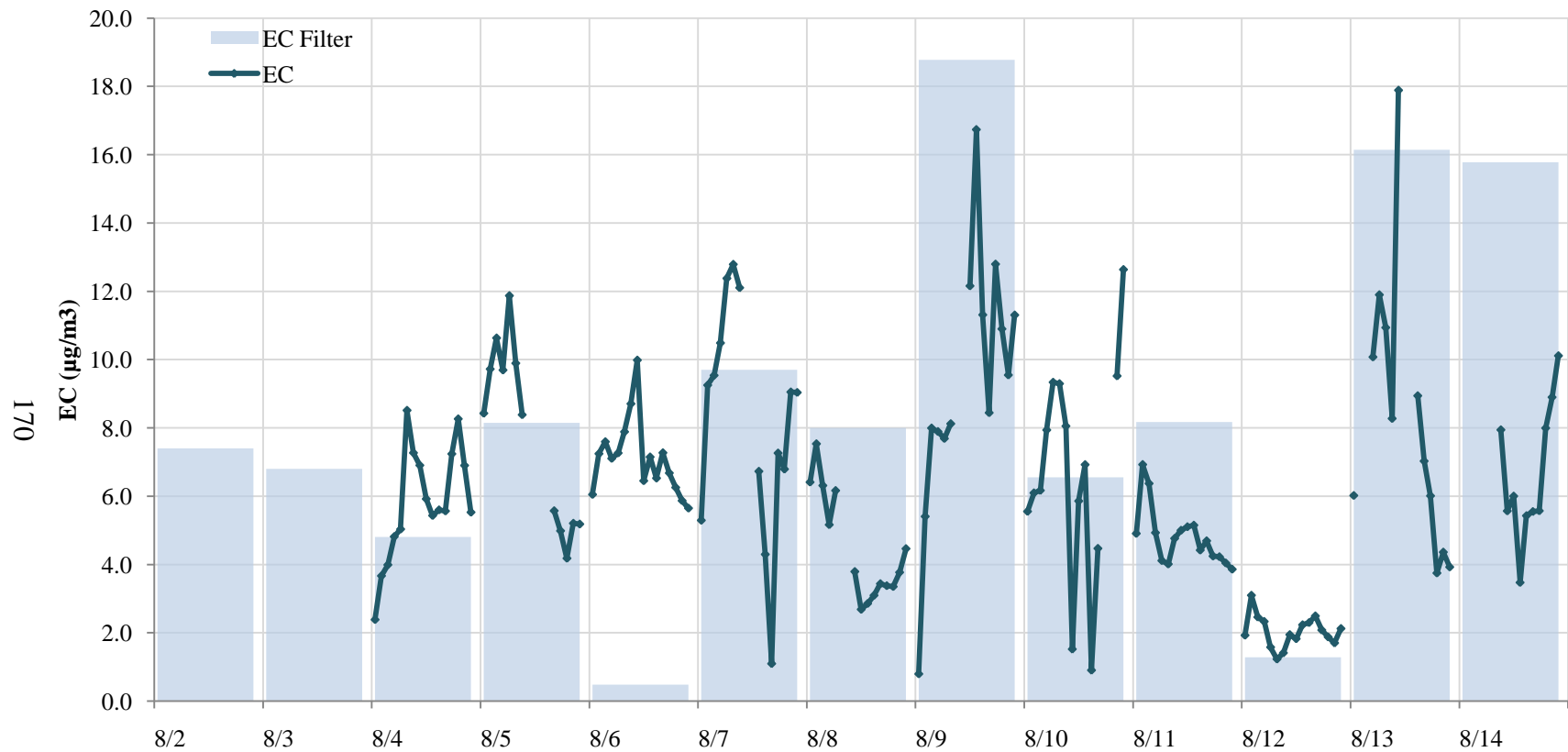


#### IV.1.5 High-Resolution Air Pollution Measurements

In Chapter III thirty-minute resolution data enabled us to detect more significant and minute changes in HRV because (1) the larger dataset providing a larger number of samples, and (2) the ability to detect more subtle differences without drowning out short-term air pollution concentrations within a day. Therefore, 30-minute data from the Steubenville summer study was explored to determine if within-day changes in HRV were detectable and if those changes were associated with continuous air pollution concentrations. In Figure IV.7, continuous CAPs PM<sub>2.5</sub> concentrations varied greatly and those differences could not be captured with one integrated filter sample. Thirty-minute averages for EC were determined and showed variability within a day that was not possible to detect with an integrated sample. However, there are large portions of missing data from the instrument failing to adequately advance the quartz tape the sensor uses to detect the EC concentration. In Figure IV.13, available EC data (74% of the total possible) from August 4 through August 14 were plotted together with PM<sub>2.5</sub> concentrations. Drastic changes in PM<sub>2.5</sub> mass were not always collinear with EC. This occurred most strongly on August 7 and August 14, two days with winds from the SW.

Back trajectories on August 7 suggest that air masses reaching Steubenville had followed the Ohio River Valley. On August 14, the air masses were from the east over Pennsylvania, and remained stationary over the Ohio River south of the sampling site for several hours prior to passing over Steubenville. Both of these days indicate that air pollution was heavily influenced from southwesterly flow that brought a large secondary  $\text{SO}_4^{-2}$  contribution into Steubenville. EC concentrations are significantly higher from the SW than the NE, however, the air pollution on August 7 and 14 does not show that EC mass was affected by the regional inputs to Steubenville, consistent with Detroit findings for EC.

**Figure IV.13 Thirty-minute EC concentrations during each exposure, as well as 8-hour integrated EC concentrations from the Steubenville summer intensive.**



## Trace Element Concentrations

The use of the SEAS in observing the within-day changes in trace metal concentrations was shown in Chapter III as a critical tool in observing changes in pollutants (and source contributions) in association with HR and HRV. Although Steubenville does not experience the wide urban mixture of sources, nor the frequent changes in wind directions throughout the course of the day like Detroit, the 30-minute data will be valuable to observe plumes that may affect the CAPs Rats. In Figure IV.14, S had a significant increase over the course of the day. Moderate winds are from the south-southwest all through the exposure and the concentrations reflect a plume from the Cardinal Power Plant blanketed the river valley. Daily trace element concentrations and averages are summarized in Table IV.7.

**Figure IV.14 Thirty-minute continuous concentrations of S are plotted during the Steubenville summer exposure hours.**

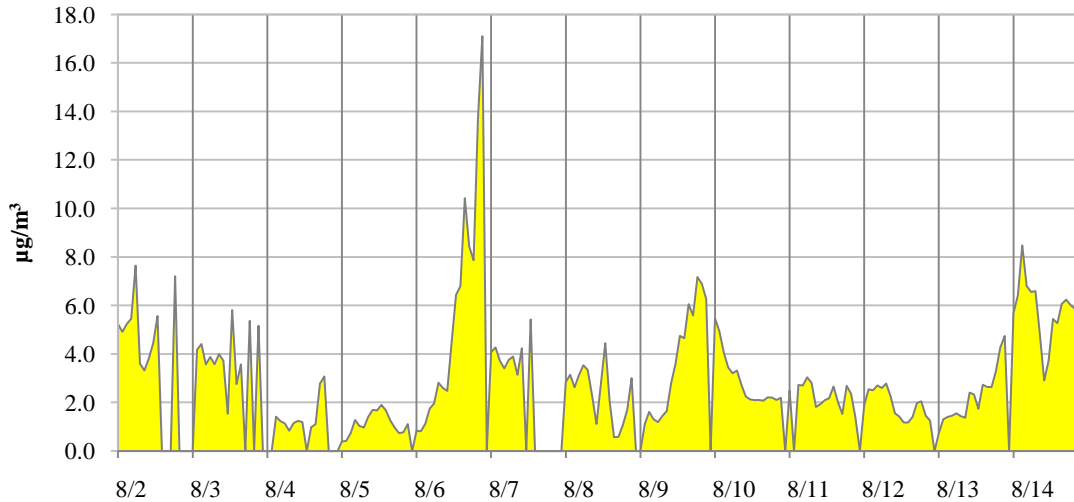


**Table IV.7 Average concentrations of PM<sub>2.5</sub> and components in Steubenville during the summer intensive. Units are in ng/m<sup>3</sup>, \*(Except PM and S in units of µg/m<sup>3</sup>).**

	PM*	EC*	Mg	Al	P	S*	K	Ca	Ti	V	Cr	Mn	Fe	Cu	Zn	As	Se	Rb	Sr	Mo	Cd	Sb	Ba	La	Ce	Sn	Pb
8/2	1375	NA	28.9	31.9	1.5	5.13	40.6	156	0.21	0.71	0.21	3.18	38.4	3.00	16.9	1.03	2.33	0.08	0.64	0.14	0.13	1.78	3.36	0.028	0.051	0.35	5.8
8/3	1252	NA	46.0	35.8	19.1	3.97	47.3	151	0.54	0.90	0.16	2.15	33.5	2.52	9.5	0.62	1.78	0.09	0.76	0.16	0.10	0.64	3.30	0.018	0.032	1.60	3.6
8/4	518	5.81	24.4	23.2	20.5	1.47	32.6	94	0.41	0.31	0.15	1.55	20.5	2.33	9.7	0.39	0.72	0.07	0.37	0.12	0.09	0.51	3.43	0.011	0.020	0.82	1.8
8/5	383	7.81	22.2	20.9	8.0	1.13	43.1	103	0.99	1.88	0.53	2.75	16.0	3.70	39.9	1.00	0.74	0.09	0.35	0.67	1.75	0.74	3.81	0.023	0.032	0.57	3.8
8/6	749	7.10	25.7	37.4	14.7	5.60	57.4	81.0	1.15	2.51	0.44	4.17	81.0	6.64	13.3	1.01	11.0	0.13	0.57	1.19	0.31	0.75	4.23	0.018	0.027	0.33	19.4
8/7	1442	8.29	31.0	24.4	17.6	3.99	41.3	119	0.44	1.01	0.17	9.91	31.8	1.50	9.7	1.14	1.80	0.09	0.61	0.44	0.14	0.79	2.62	0.013	0.024	1.04	1.4
8/8	313	4.46	25.4	32.6	28.1	2.39	27.6	160	1.54	1.41	0.71	4.81	23.3	1.76	16.3	1.04	1.09	0.12	0.59	0.83	0.13	0.65	2.63	0.035	0.045	1.44	2.4
8/9	556	9.36	44.3	39.2	25.2	3.74	74.7	303	2.38	1.37	0.75	7.88	86.6	5.48	81.4	1.02	2.07	0.21	0.80	2.18	1.35	0.99	5.06	0.028	0.047	0.72	13.7
8/10	821	6.73	24.4	18.0	3.9	2.91	23.4	103	0.87	0.51	0.35	2.70	32.7	2.12	13.8	1.31	1.07	0.04	0.39	0.53	0.14	0.89	2.47	0.029	0.039	0.87	2.8
8/11	525	4.80	46.4	29.8	1.9	2.30	25.0	402	2.58	0.99	0.50	7.26	48.1	3.23	19.7	0.72	0.71	0.11	0.91	1.82	0.49	0.89	4.27	0.037	0.062	0.42	5.7
8/12	159	2.04	26.0	27.5	5.4	1.92	35.6	104	0.66	0.26	0.83	2.33	24.0	5.56	7.5	0.62	0.88	0.05	0.32	1.30	0.16	0.65	2.83	0.013	0.019	1.48	8.4
8/13	490	8.26	37.1	30.9	5.3	2.26	91.4	182	1.97	2.79	2.04	3.91	55.5	3.48	115.5	3.40	1.72	0.13	0.80	2.23	3.27	1.19	4.42	0.032	0.050	4.53	32.5
8/14	1319	6.65	66.9	45.3	5.7	5.80	148.1	358	1.62	1.57	0.62	14.3	119.5	3.85	335.0	1.89	4.42	0.39	1.00	0.63	1.25	2.67	5.03	0.030	0.057	0.83	24.9
Mean	737	6.36	34.6	30.7	11.8	3.23	53.9	181	1.25	1.30	0.61	5.09	48.1	3.60	55.9	1.20	2.41	0.13	0.62	1.01	0.78	1.01	3.69	0.025	0.039	1.19	10.3
SD	512	3.14	20.8	25.2	10.5	2.31	53.6	159	1.73	1.50	1.59	5.35	77.4	3.36	151.0	1.11	4.71	0.13	0.41	1.18	1.34	0.96	1.60	0.017	0.025	1.86	15.2
Median	557	6.01	29.5	24.0	7.0	2.69	39.5	124	0.71	0.79	0.34	3.52	30.4	2.77	13.7	0.83	1.17	0.09	0.53	0.58	0.19	0.76	3.24	0.020	0.032	0.47	4.3
5%	138	1.70	16.4	9.5	1.7	0.83	14.7	58.1	0.23	0.25	0.12	1.33	13.2	0.52	4.8	0.26	0.44	0.03	0.23	0.07	0.06	0.35	1.96	0.008	0.014	0.17	0.9
95%	1709	12.10	77.7	68.6	32.5	6.90	122.3	527	4.16	4.40	1.36	13.3	140.7	9.47	171.6	3.79	8.06	0.26	1.35	3.77	3.82	2.50	6.97	0.053	0.077	5.30	37.4



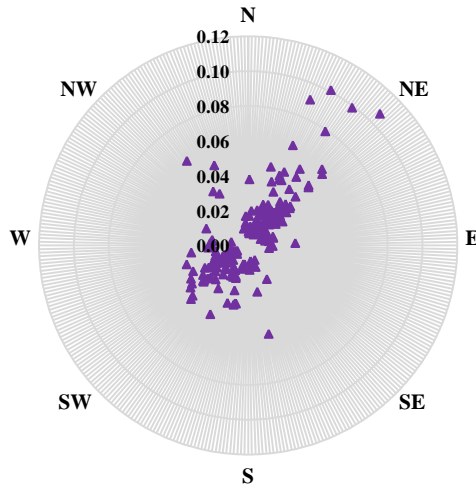
## Trace Element Concentrations and Wind Direction

Thirty-minute constituent concentrations are important because each SEAS sample can be associated with a wind direction, identifying a specific direction with a high contribution of a certain trace element. In Figure IV.15, three pollution roses incorporate the concentrations of S, La and EC, based upon wind direction. These figures show that La concentrations in most directions are moderate ( $<0.04 \text{ ng/m}^3$ ), but when winds are from the NE, a significant increase above background concentrations pointed to a specific source from the NE; this increase in La may be attributable to significant, short-term spikes in concentration. S can also identify short-term peaks in concentrations that would normally be drowned out by an eight-hour integrated sample. Contrary to La and S, EC could not show that one specific direction was stronger than the other. Winds were from the NE or SW, but this pattern was quite similar to the wind rose from Figure IV.2. Thus, EC may be from a more localized source, and less driven by short-term peaks in concentrations or from predominant winds.

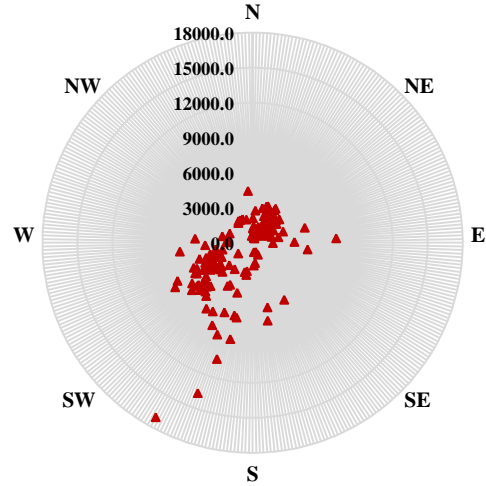
These pollution roses led to the assumption that specific constituents would have higher concentrations in the NE while most others would follow  $\text{PM}_{2.5}$  mass and have higher concentrations from the SW wind direction (Figure IV.5). All the days of this study, with the exception of August 13, had winds that remained unchanged through the eight hours of exposure. Therefore, each day was classified by wind direction, either NE or SW, and August 13 was split, having morning winds from the NE and afternoon winds from the SW. When mean concentrations of all the constituents were plotted, only a handful of constituents appeared to be exclusively from the NE. Mo, Cd, Ba, P, Ti and Ca had notably higher concentrations on exposure day had air flow from the NE than from the SW.

**Figure IV.15 Thirty-minute pollution concentrations of La, S and EC based on wind direction during the Steubenville summer exposure hours.**

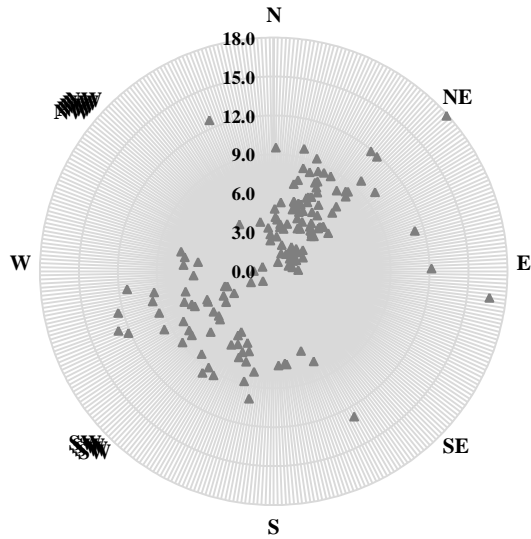
**(a) La**



**(b) S**



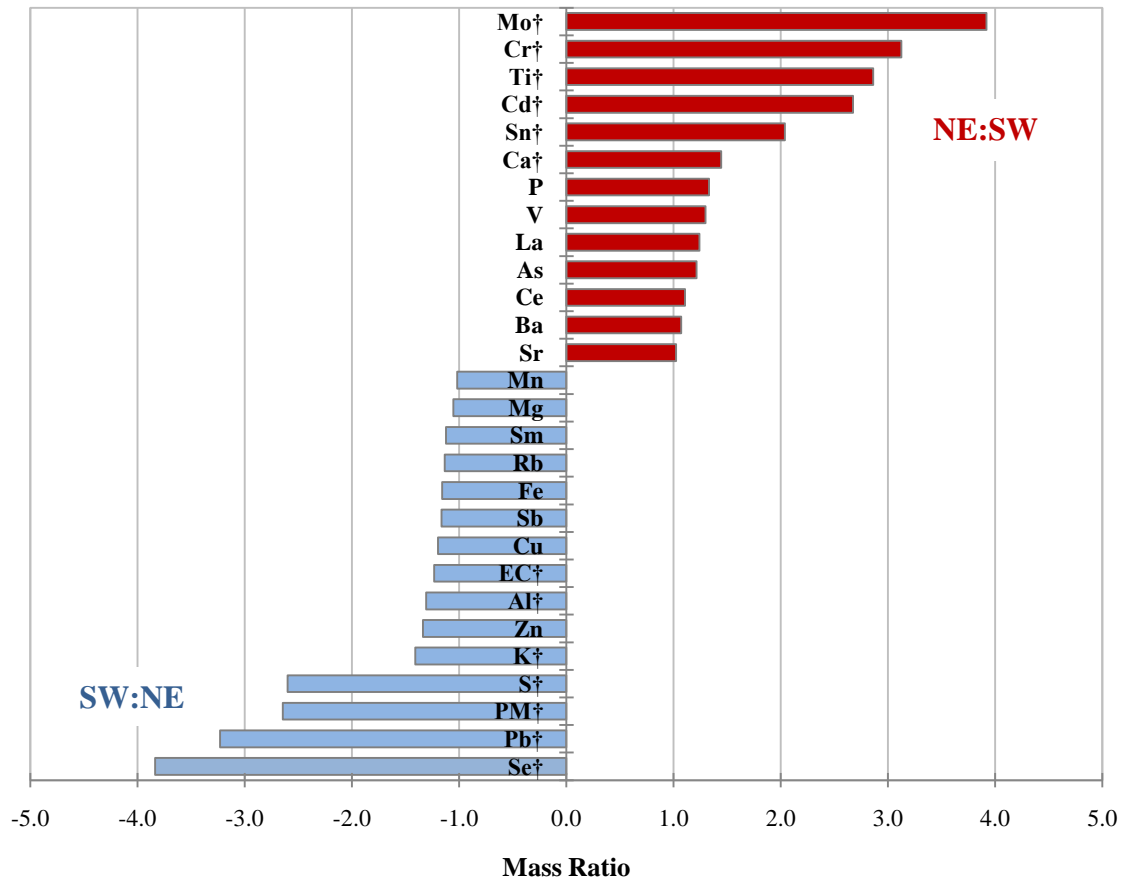
**(c) EC**



### **Mass Ratios by Wind Direction**

Steubenville air flow shows two prominent wind directions: the NE and SW. From the pollution roses, it is apparent that the NE and SW have distinctively different concentrations that influence air pollution concentrations at the sampling site. Although short-term peaks show their prominence (e.g. La from the SW), the mean concentrations from the NE and the SW should be compared. In Figure IV.16, the concentration of each trace element is shown in a ratio, depending on which direction had the larger average mass of the two. The ratio NE:SW (red) and SW:NE (blue) indicates the degree by which mass was higher in one direction than another. Mo, Cr, Ti, Cd and Sn had a mass twice as high from the NE than the SW. Only S, PM, Pb and Se had mass considerably higher from the SW than the NE. These strong directionality differences emphasize how significant predominant winds will influence the contributions of trace elements at the sampling site in Steubenville, and ultimately affect the HRV.

**Figure IV.16 Pollution ratios of air pollutants higher from the NE to SW (red) and ratios higher from the SW to NE (blue).**



Overall, the high-resolution data provide much more insight on which pollutants had an impact on the Steubenville area over the summer exposures in 2006. These data will now be associated with HRV to determine if the patterns found using the 8-hour dataset are also evident using the 30-minute data or if more prominent patterns are now being identified.

#### IV.1.6 High-Resolution HRV Analysis

The 30-minute data identified HR and ln(SDNN) as significantly different between AIR and CAPs Rats. Mixed modeling results are summarized in Table IV.8. Unlike the 8-hour average HR data, the 30-minute time scale determined HR as

significantly different ( $p=0.0018$ ) indicating that changes in HR and more evident on the shorter time scale than averaged over the course of an entire day. For  $\ln(\text{SDNN})$ , differences in the CAPs Rats in relation to the Air Rats were also significant ( $p=0.0031$ ) which is supported by the findings from the 8-hour dataset.

**Table IV.8 Thirty-minute mixed modeling results comparing AIR vs. CAPs Rats for the Steubenville summertime exposure.**

	<b>Mixed Modeling Significance (<math>p&lt;0.05</math>)</b>		
	Group	Date	Group*Date
Heart Rate	0.915	<0.0001	<b>0.0018</b>
$\ln(\text{SDNN})$	0.6574	<.0001	<b>0.0003</b>
$\ln(r\text{-MSSD})$	0.4218	<.0001	0.3162

#### **Associations with Air Pollution and HRV**

The high-resolution HRV data were run in a mixed-model with 30-minute air pollution measurements and presented in CI Plots in Figure IV.17a, 18a and 19a. EC, As, PM, Cd, Fe, V, Sb and Mo are all associated with a significant reduction of  $\ln(\text{SDNN})$ . Some of the trace elements were significantly higher from the NE while others were significantly higher from the SW. It is possible that the effects on HRV were a reflection of the total 13-day exposure; however, it is also possible that SW and NE winds had different impacts upon HRV. Therefore, mixed modeling analysis was run to compare how AIR and CAPs Rats differed when winds came from the NE and from the SW, and these results are summarized in Table IV.9.

**Table IV.9 Mixed modeling analysis broken down by NE and SW winds for the Steubenville summer intensive.**

**North/Northeast**

N=99	Mixed Modeling Significance (p<0.05)		
	Group	Date	Group*Date
Heart Rate	0.7697	<.0001	<b>&lt;.0001</b>
ln(SDNN)	0.914	0.0248	0.3173
ln(r-MSSD)	0.5041	0.0186	0.6007

**West/Southwest**

N=80	Mixed Modeling Significance (p<0.05)		
	Group	Date	Group*Date
Heart Rate	0.7562	<.0001	<b>0.0006</b>
ln(SDNN)	0.4552	<.0001	<b>0.0208</b>
ln(r-MSSD)	0.4843	0.0533	<b>0.0359</b>

Heart rate was significantly different between AIR and CAPs Rats, both from the NE and SW directions; however, ln(SDNN) and ln(r-MSSD) were significantly different only when winds flowed from the SW. These findings indicate that the contributions to PM<sub>2.5</sub> mass to Steubenville from the SW affect HRV whereas winds from the NE do not have any impact on HRV. When run in a mixed model, the larger HR for CAPs Rats from the NE was statistically significant over the HR from the SW. This indicates that the effects on HR from NE and SW were different. The same was not true for HRV; between group differences of ln(SDNN) and ln(r-MSSD) were significant from the SW, but within-group differences of ln(SDNN) and ln(r-MSSD) were not statistically different between the SW and the NE. Therefore, the statistical differences in Table IV.9 may only indicate a trend how the constituents affect HRV, but the impacts were not statistically sound.

The associations of 30-minute trace elements and CAPs Rats HRV were analyzed, including analysis by data from the NE and SW winds. Although HR was the only parameter found statistically different between wind directions, ln(SDNN) and ln(r-

MSSD) will also be investigated to see if a pattern existed across all parameters. Figures IV.17, 18 and 19 present the CI Plots for HR,  $\ln(\text{SDNN})$  and  $\ln(\text{r-MSSD})$ .

Based on mixed modeling analyses of 30-minute air pollution concentrations and cardiac measurements, the only pollutants that associated with HR across both the NE and SW were Mg (associated with a decrease in HR) and La (associated with an increase in HR). From the mass ratios in Figure IV.16, Mg nor La were not significantly higher from a single wind direction. Se, S and Pb associated with HR when winds were from either the NE and from the SW; however, the effects were diametrically opposed. Se, S and Pb significantly associated with a decline in HR when wind came from the NE, but then significantly associated with a rise in HR when winds were from the SW. Se, S and Pb were all significantly higher from the SW than the NE, similar to fine-fraction mass. HR was only associated with  $\text{PM}_{2.5}$  when winds were from the SW. Figure IV.17 shows a clear pattern that, the overall trend of HR was to decrease with higher air pollution concentrations, especially since higher mass for the pollutants (e.g. Se, S and Pb) were higher from the SW than then NE.

The patterns across NE and SW winds for  $\ln(\text{SDNN})$  were not the same as those found for HR. In Figure IV.18, the CI Plots show that As and Sb were associated with a reduction in  $\ln(\text{SDNN})$ , regardless of the wind direction. SW winds only additionally found PM associated with a reduction in  $\ln(\text{SDNN})$ , whereas the NE direction found several, especially Se, Rb and Pb observing the strongest effect estimate in  $\ln(\text{SDNN})$ . The most interesting finding with  $\ln(\text{SDNN})$  was that Fe, EC and Mo all associated when all wind directions were included, but not individually, despite pollution roses for Mo and Fe showing a higher prevalence from the NE. For EC, the mass is evenly distributed and does not appear to have a stronger prominence from one direction or the other.

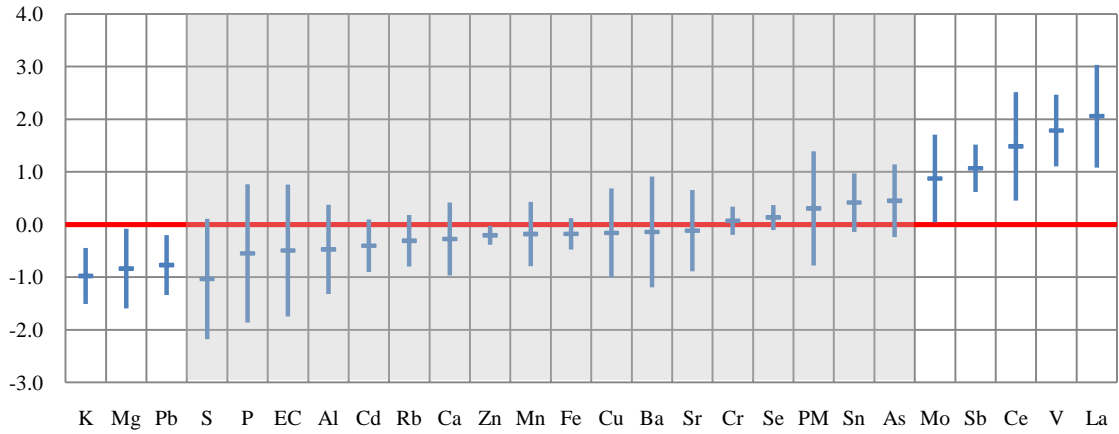
When observing the significant associations with  $\ln(\text{r-MSSD})$ , very few associations were observed in comparison to the large number of constituents associated with HR and  $\ln(\text{SDNN})$ . In Figure IV.19, Mo appears in the CI Plots significantly associated with  $\ln(\text{r-MSSD})$  when winds are from the NE (significant increase) and the SW (significant decline). From the SW, Al is significantly associated with an increase in  $\ln(\text{r-MSSD})$ . Al was the only constituent associated with an increase in  $\ln(\text{SDNN})$ , which also occurred when winds were from the SW direction. Overall, these findings

present strong evidence that wind direction can determine significant differences in the CAPs-exposed rats, and that the effects on HRV are influenced by the pollutants differently, when winds were from the NE or from the SW.

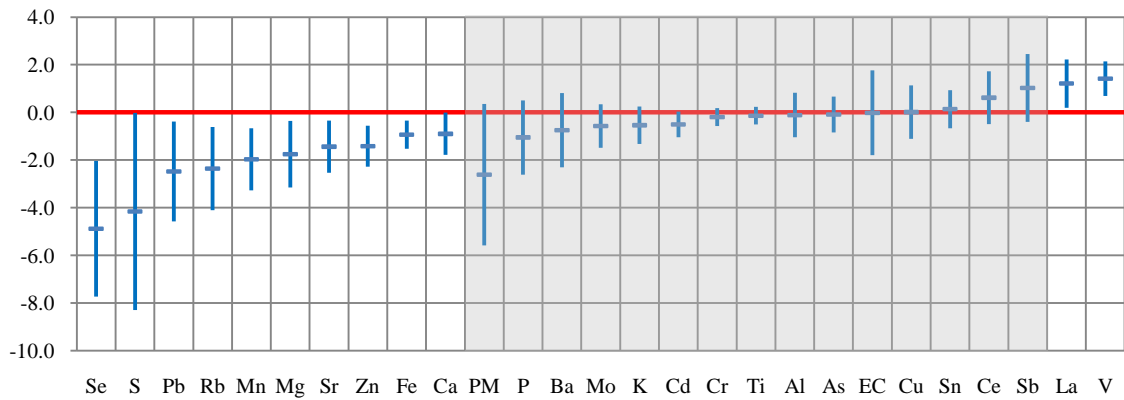


**Figure IV.17 CI Plots for the Steubenville summer 30-minute measurements of HR, and according to NE and SW winds (p<0.05).**

**(a) HR: All Wind Directions (N=1429)**



**(b) HR: Northeast Winds (N=662)**



**(c) HR: Southwest Winds (N=564)**

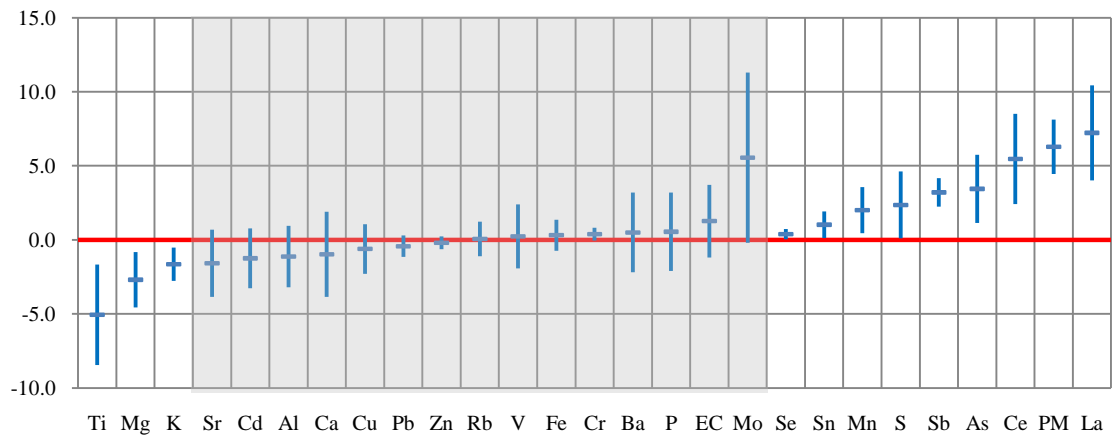
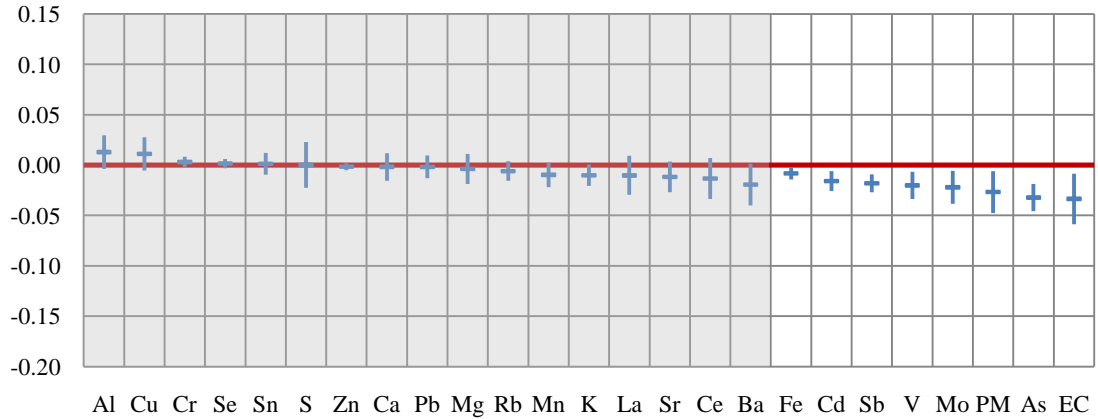
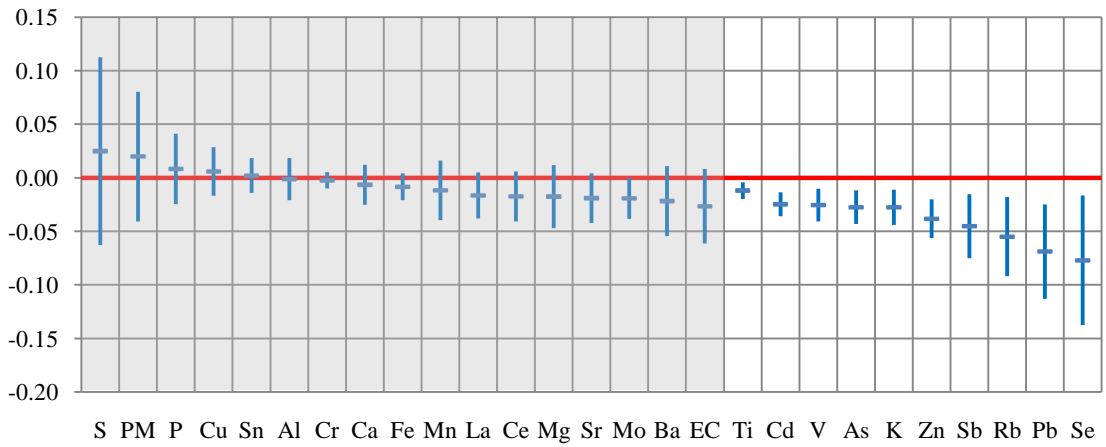


**Figure IV.18 Steubenville summer 30-minute CI Plots for ln(SDNN), and according to wind direction (p<0.05).**

**(a.) ln(SDNN): All Wind Directions (N=1429)**



**(b.) ln(SDNN): Northeast Winds (N=662)**



**(c.) ln(SDNN): Southwest Winds (N=564)**

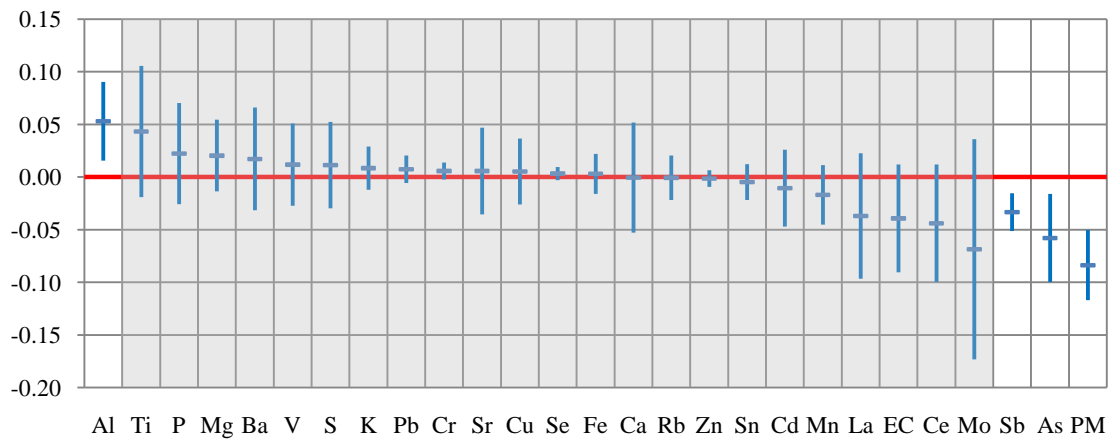
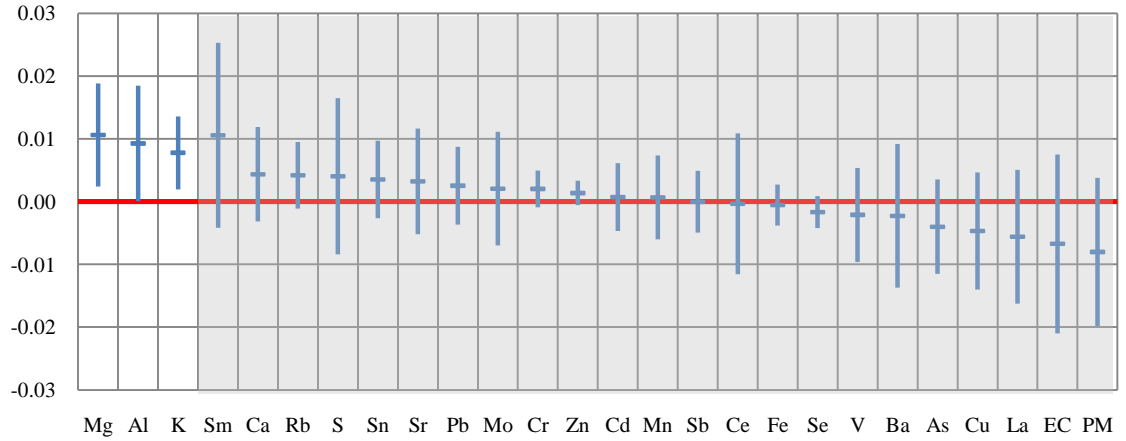
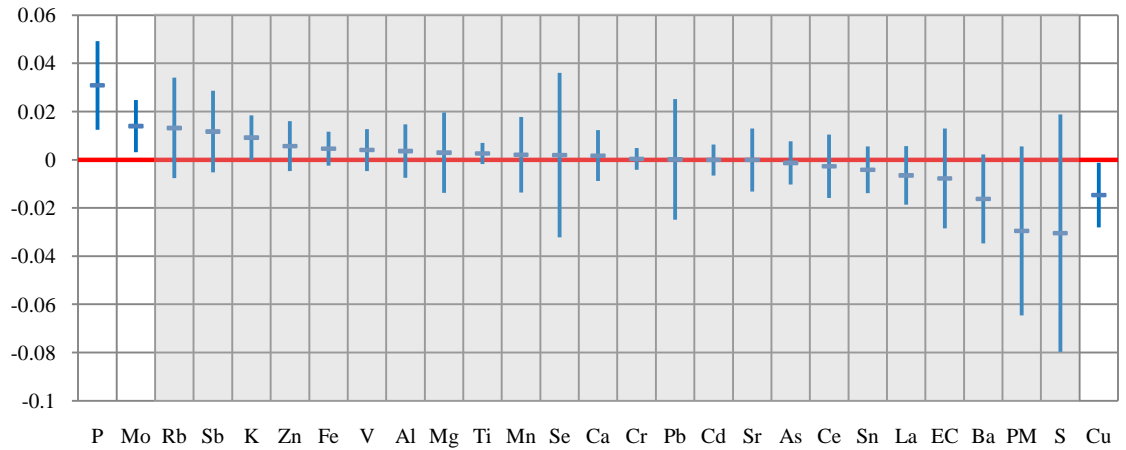


**Figure IV.19 Steubenville summer CI Plots for 30-minute  $\ln(r\text{-MSSD})$  by wind direction ( $p < 0.05$ ).**

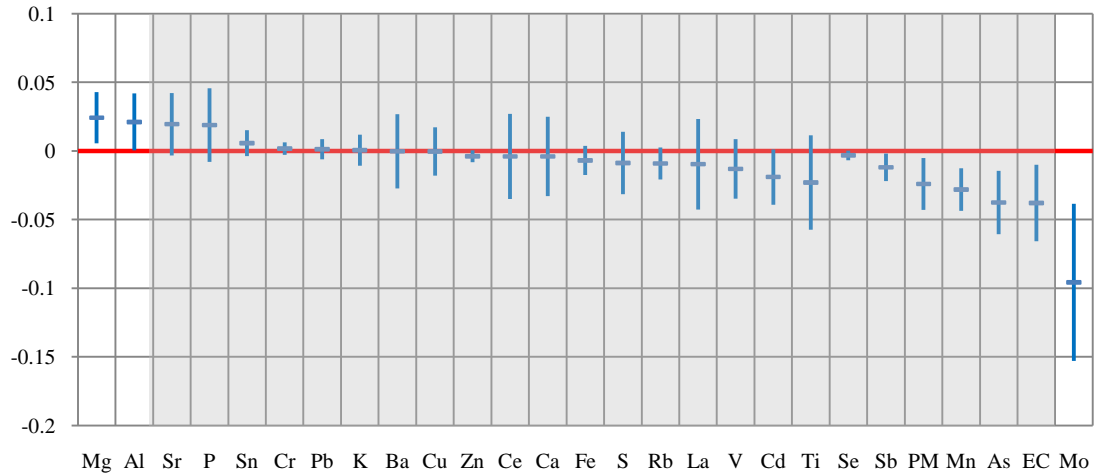
**(a.)  $\ln(r\text{-MSSD})$ : All Wind Directions (N=1429)**



**(b.)  $\ln(r\text{-MSSD})$ : Northeast Winds (N=662)**



**(c.)  $\ln(r\text{-MSSD})$ : Southwest Winds (N=564)**



## IV.6 Steubenville Summer Summary

The findings in the Steubenville summer intensive indicate that varying winds from the NE and SW winds brought significantly different constituent concentrations that may have affected HRV in CAPs-exposed differently. HR was significantly affected by NE and SW winds, whereas AIR and CAPs Rats were significantly different when predominant winds were from the SW. Associations with constituents of PM<sub>2.5</sub> were not consistent, and when CI Plots were broken down by wind direction, differences in the constituents associated from the NE and SW directions were evident. These findings are important in determining that the high-resolution effects of air pollution on HRV can be seen with differences in the wind direction. This can ultimately lead to Chapter V where HRV was associated with source contributions rather than individual constituent concentrations to identify a more strongly associated measure to the changes in autonomic tone.

This analysis could only be conducted using high-resolution 30-minute data, and often the high-resolution findings had surprisingly different associations with HRV than 8-hour integrated data did. This outcome supports the findings from the Detroit summer study that the 30-minute dataset is a more comprehensive measure to be used to analyze the effects in HRV than the 8-hour summaries are. Eight-hour frequency-domain findings did however show that ln(LF) and ln(HF) were significantly different in CAPs Rats than the AIR Rats.

## **IV.2 Steubenville Winter Intensive**

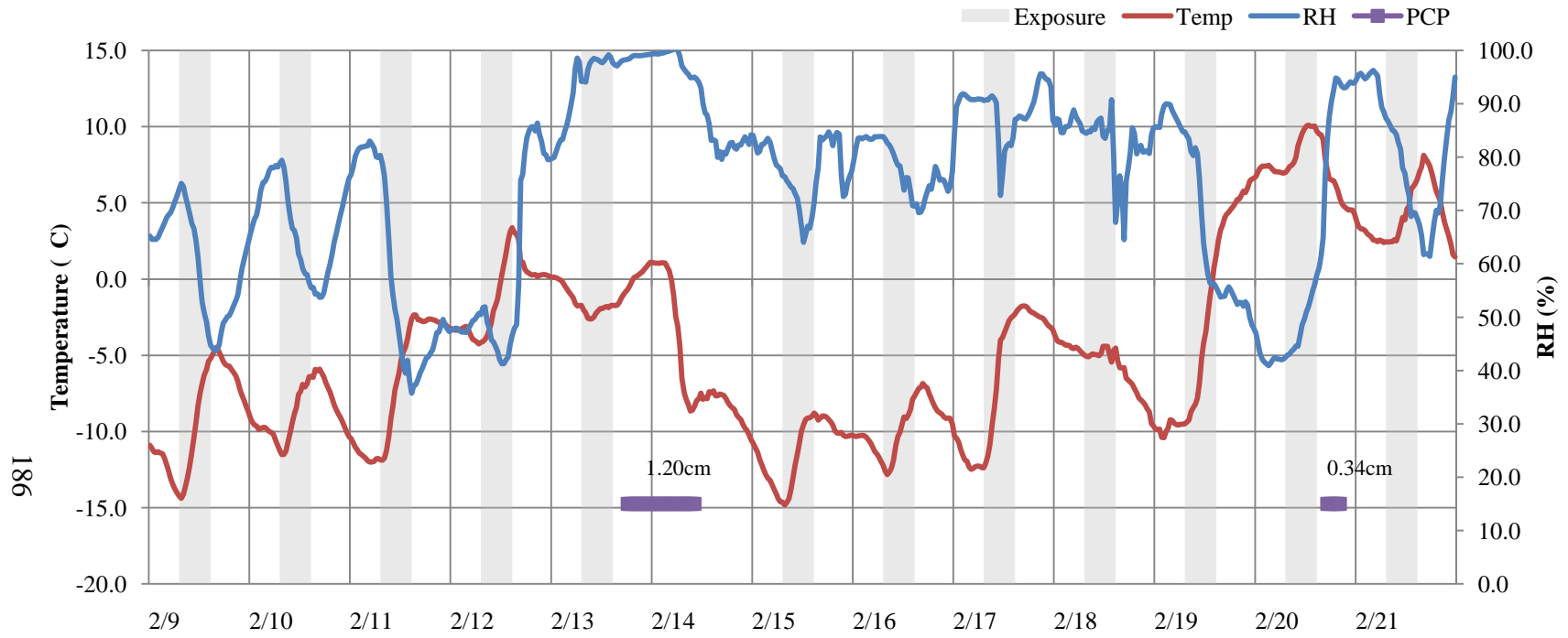
The Steubenville winter study (February 9-20, 2007) had an ambient PM<sub>2.5</sub> average of 13.5µg/m<sup>3</sup>, half of what was found during the summer study. The low PM<sub>2.5</sub> may have been the reason why AIR and CAPs Rats could not be dissociated in any HRV parameter using the 8-hour or the 30-minute dataset. Nevertheless, this intensive provided a unique opportunity to observe the short-term effects of a pollution event that did affect HRV. The first 4 hours on February 17 experienced elevated concentrations of PM<sub>2.5</sub> and many constituents; also a significant drop in ln(SDNN) was observed during the same 4-hour period. An in-depth investigation on this short-term period showed that the 4-hour period had a significant impact on the HRV associations over the entire two-week study. This section will focus on these observations and its implication for future HRV studies.

### **IV.2.1 Meteorological Summary**

#### **Climate**

Steubenville temperatures ranged from -14.8 to 10.1°C during two-week winter exposure. The average temperature was  $-4.4 \pm 6.2^\circ$  (Exposure Hours:  $-4.8 \pm 6.2^\circ$ ) and RH was  $74 \pm 17\%$  (Exposure Hours:  $72 \pm 17\%$ ) showing that the exposure hours did not differ greatly from the 24-hour observations. Despite the similar averages, a consistent trend showed that morning RH was typically higher and dropped over the course of the 8 hours of sampling while temperatures rose (Figure IV.20). Frequent snow flurries were observed to increase the RH; February 13 experienced the highest RH due to the snowfall. February 17 also showed RH at 90% in the morning and rapidly dropped midway through the exposure.

Figure IV.20 Hourly temperature and RH through each day's 8-hour exposure highlighted in grey.



## **Precipitation**

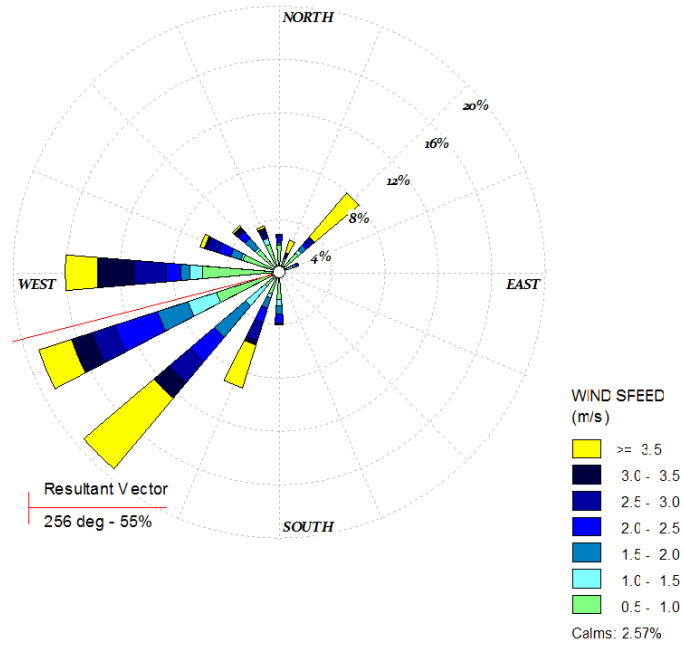
During the two-week winter intensive in Steubenville, two dramatic synoptic events occurred, one being a large stationary front that deposited several centimeters of snowfall on February 13, and the other synoptic event was an extremely large rise in air pollution concentrations on the morning of February 17. Scattered flurries fell throughout the study, but the snowfall from the front on February 13 was the only event that produced measurable accumulation (1.20cm of wet precipitation equivalent). The stationary front remained over Steubenville from the afternoon of February 13 and continued into the night. The front deposited freezing rain, and the storm was so severe that exposures and sampling were suspended on February 14 due to extremely icy conditions. The rise in air pollution concentrations on the morning February 17 may be attributed to a combination of meteorological conditions and a captured pollution event. The impact of this 4-hour period will be analyzed later in this chapter.

## **Wind Patterns**

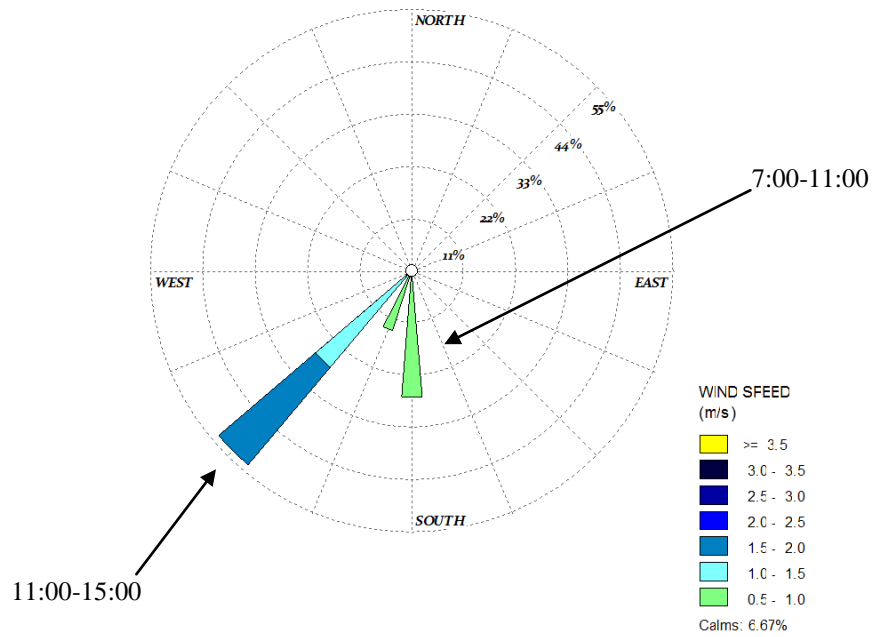
Winds were similar to summer in that flow was primarily from the SW or NE directions. The wind rose for the entire two-week period is presented in Figure IV.21. It can be assumed that air flow will again be a significant factor to Steubenville air pollution as was shown in the summer. One noticeable seasonal difference between the summer and winter winds is that SW winds showed a greater tendency to flow from the west and less from the south during the winter. However, southerly flow was still significant to  $PM_{2.5}$  mass. On the early morning of February 17, when air pollution concentrations were highest, winds were calm ( $<0.5\text{m/s}$ ) and came directly from the south. Later in the day, as pollution concentrations dropped, winds began to pick up and winds flowed from the southwest. Together, the low wind speeds and southerly flow may help explain the elevated concentrations on the morning of February 17.

**Figure IV.21 The wind roses for (a) the entire 2-week period during the Steubenville winter intensive and (b) winds during February 17.**

**(a) Entire 2-Week Period**



**(b) February 17, 2007**





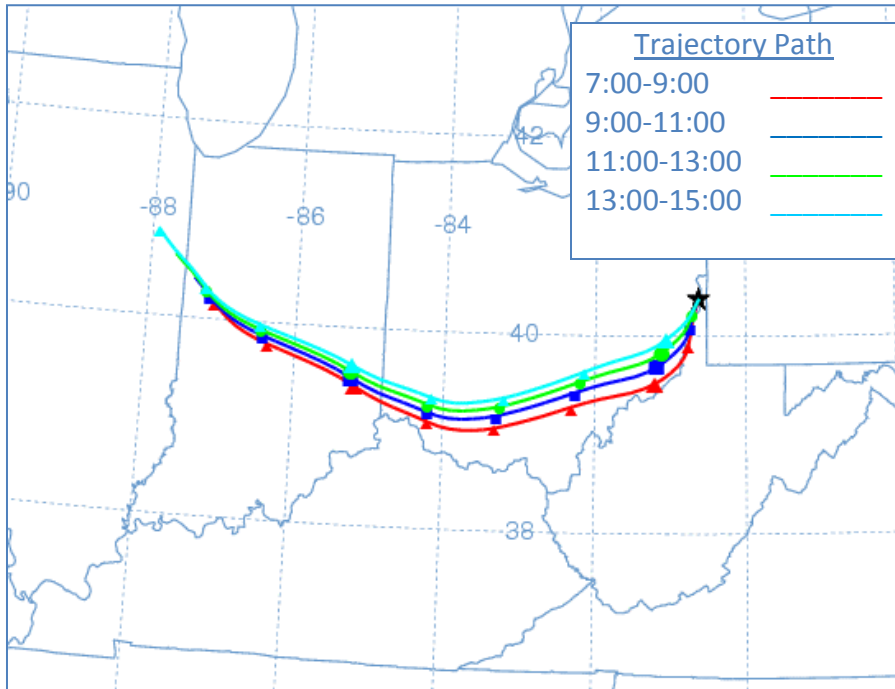
### **Meteorology on the Morning of February 17**

The elevated PM<sub>2.5</sub> concentrations on February 17 were a combination of meteorological conditions with an air mass carrying large source contributions. So far, both high RH and calm winds from the south may have contributed to the large spike in many PM<sub>2.5</sub> constituents. In the absence of a precipitation event, the high RH may be contributing to particle growth and increasing particle formation. The magnitude by which the mass is increased may have also been attributed to a temperature inversion. From daily HYSPLIT models, the mixed layer depth (i.e. mixing height) was calculated on each day. February 17 observed a mixing height of only 29m, in relation to the average mixing height of 206m for the Steubenville winter study. However, a lowered mixed depth was not likely the only driving factor to the elevated PM<sub>2.5</sub> mass. February 19 (Figure IV.22b) also had a low mixed depth of 29m but does not show the same elevated concentrations in mass probably because surface winds were substantially higher, and the back trajectory did not pass over any major industrialized areas. Therefore, several meteorological conditions and source contributions accumulated to observe the peaks in mass concentrations on the morning of February 17.

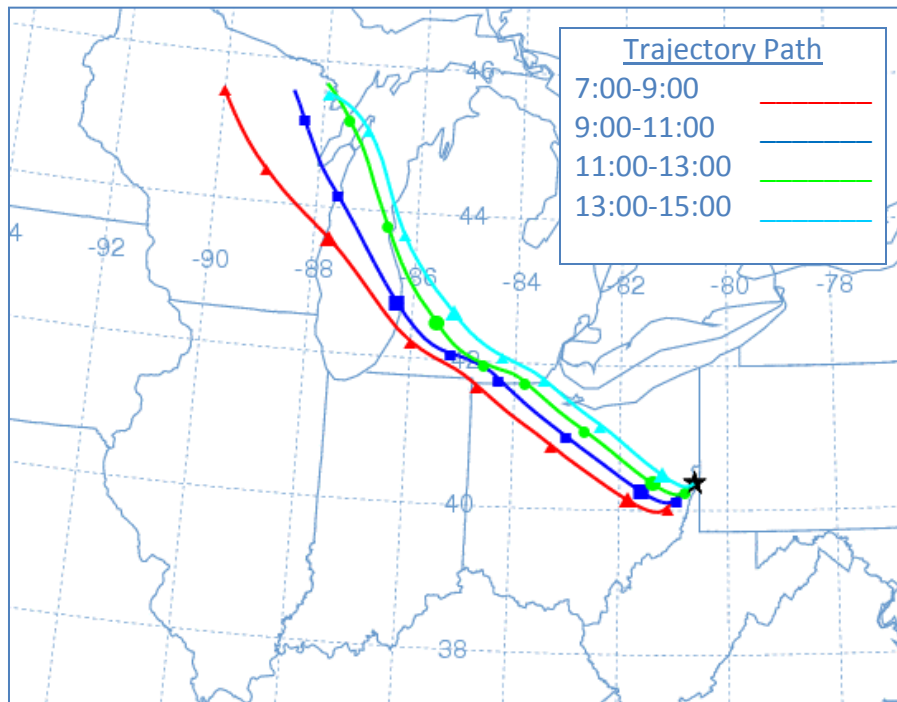
In Figure IV.22a, HYSPLIT showed that back trajectories on the 17 carried an air mass that flowed along the Ohio River Valley south of the site for several hours. This air mass may have captured plumes from steel blast furnaces as well as the Cardinal Power Plant. PM<sub>2.5</sub> mass data showed elevated mass for only the first 4 hours of exposure, but all 4 of the 2-hour trajectories overlapped. Therefore, the reduction in fine mass over the day was not due to a change from the origination of the air mass. Instead, more localized conditions, indicated by RH and a shift in the wind rose, affected the concentrations later that day.

**Figure IV.22 Back trajectories for February 17 and February 19, two exposure days with low mixed depths (29m).**

**(a) February 17:  $27.2\mu\text{g}/\text{m}^3$  (CAPs:  $671.0\mu\text{g}/\text{m}^3$ )**



**(b) February 19:  $12.9\mu\text{g}/\text{m}^3$  (CAPs:  $314.4\mu\text{g}/\text{m}^3$ )**



## IV.2.2 Air Pollution Measurements

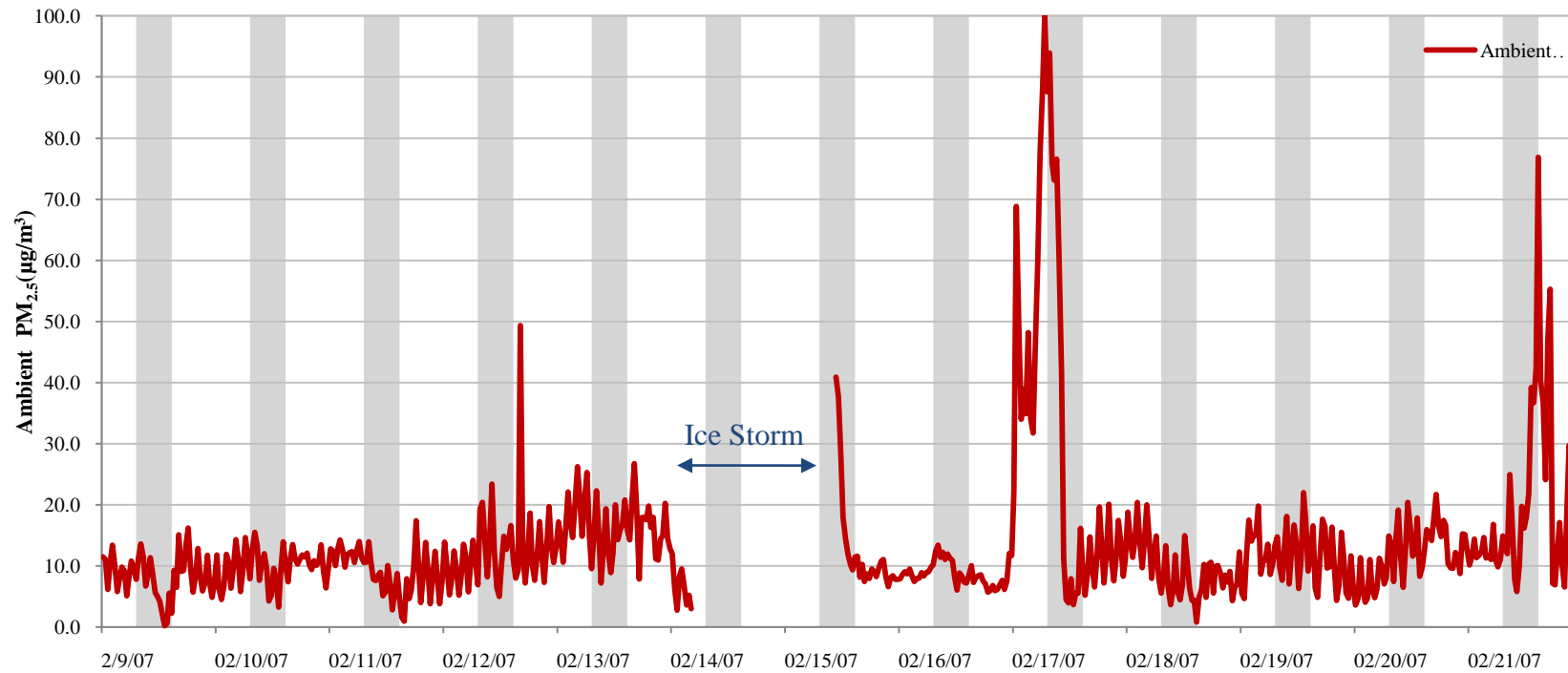
### Ambient Air Pollution

Ambient PM<sub>2.5</sub> mass in Steubenville amounted to  $12.1 \pm 12.3 \mu\text{g}/\text{m}^3$  (Exposure Hours:  $12.6 \pm 14.4 \mu\text{g}/\text{m}^3$ ), which showed that there was strong variability in the mass during the entire two-week study and during exposure hours. PM<sub>2.5</sub> concentrations exceeded  $90 \mu\text{g}/\text{m}^3$  for several hours prior to exposure and during the first 4 hours of the exposure of February 17 (Figure IV.28). The first 4 hours on that morning averaged  $65.0 \pm 27.0 \mu\text{g}/\text{m}^3$ ; in the absence of the 4-hour block of data, the exposure PM<sub>2.5</sub> average and standard deviation dropped to  $11.4 \pm 10.3 \mu\text{g}/\text{m}^3$  thus exemplifying the significant impact of air pollution on that morning had.

For the rest of the study period, there were consistent oscillations in the PM<sub>2.5</sub> mass, but these were on a much higher frequency than the diurnal trends observed in other studies. Both temperature and humidity were significantly different between day and night; however, daytime and nighttime PM<sub>2.5</sub> concentrations ( $12.3$  and  $12.0 \mu\text{g}/\text{m}^3$ , respectively) were not significantly different ( $p=0.44$ ). Furthermore, less evidence suggested that early morning changes in the boundary layer had a substantial impact on the mixed depth without the typical elevated concentrations seen in the other studies. The only exception was the significant rise in mass on the morning of February 17.

**Figure IV.23 Thirty-minute TEOM concentrations of ambient PM<sub>2.5</sub> ambient concentrations ( $\mu\text{g}/\text{m}^3$ ), exposure hours are highlighted by the grey bars.**

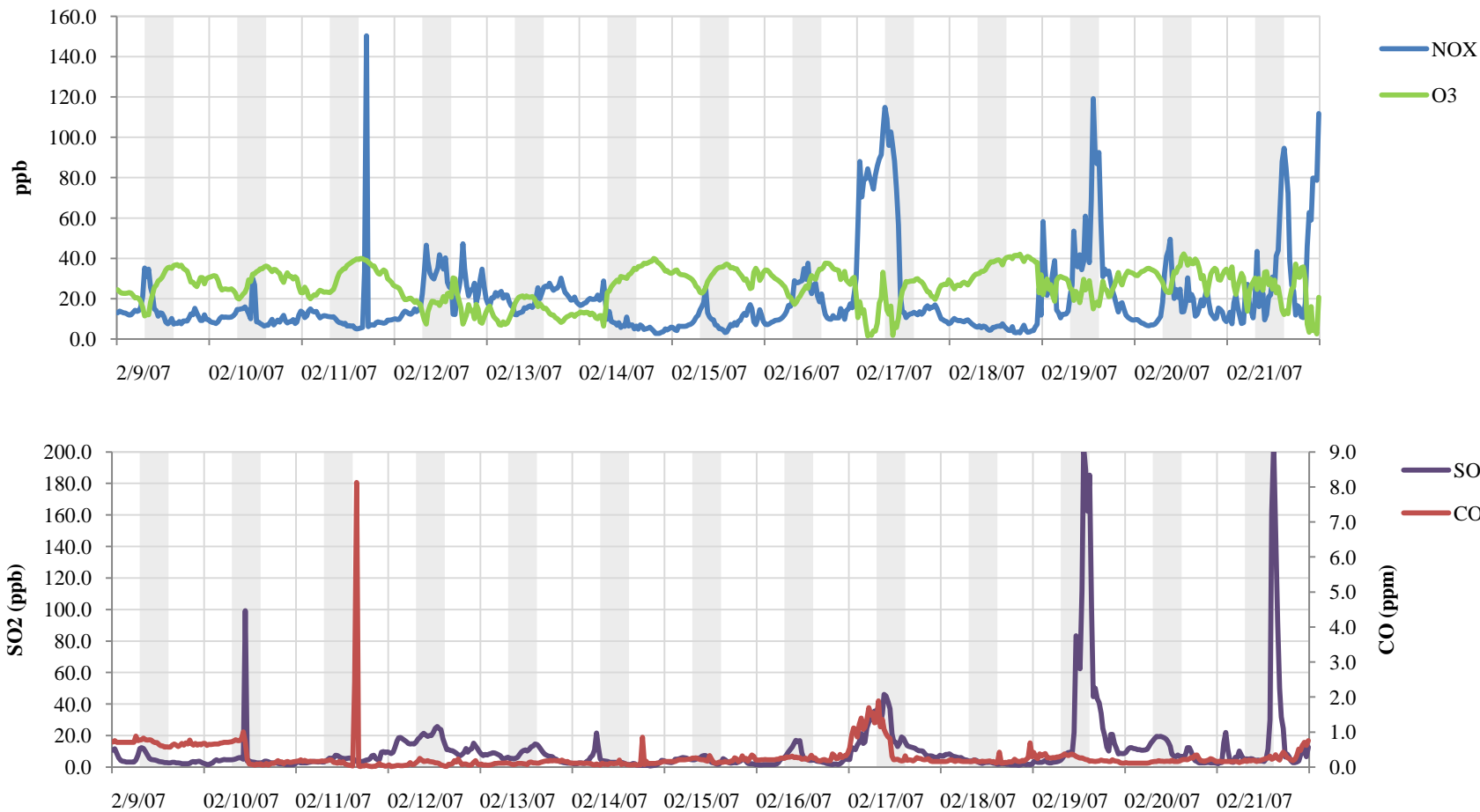
192



## Gas Concentrations

Gaseous pollutant concentrations were monitored during the two-week period and are shown in Figure IV.24. The concentrations of NO<sub>x</sub> and SO<sub>2</sub> were typically near the detection limits of the instruments, except for several peaks in concentrations, such as the inversion observed on February 17; average concentrations for CO, NO<sub>x</sub> and SO<sub>2</sub> were 0.32ppm, 15.8ppb and 6.7ppb, respectively. During the exposure hours, the concentrations were 0.30ppm, 23.8ppb and 4.9ppb. The 4-hour block on the morning of February 17 saw elevated NO<sub>x</sub> and SO<sub>2</sub> concentrations up to 84.3ppb and 1.08ppb, respectively. NO<sub>x</sub> had a secondary peak in concentration on February 19 increasing the daily average of NO<sub>x</sub> to 55.9ppb, which was in fact higher than the daily average on February 17 (52.8ppb). However, the peak on February 19 was not collinear with a peak in PM<sub>2.5</sub> or SO<sub>2</sub>. Back trajectories on both these days illustrated why SO<sub>2</sub> was higher on February 17 than on February 19, despite both days having similar wind patterns. The CO concentration did not peak on either February 17 or with the NO<sub>x</sub> peak on February 19. Instead, CO maintained a steady diurnal pattern throughout the two-week intensive with overnight depressions and gradually increased concentrations throughout the day. For O<sub>3</sub>, the average concentration was 26.3± 9.6ppb (27.0±10.0ppb during exposure hours) and experienced normal diurnal oscillations in concentration, similar to those observed in the summertime exposure. As expected, O<sub>3</sub> concentrations rarely exceeded 40ppb during the winter exposure period whereas summertime O<sub>3</sub> concentrations were often well over 40ppb during the daytime hours.

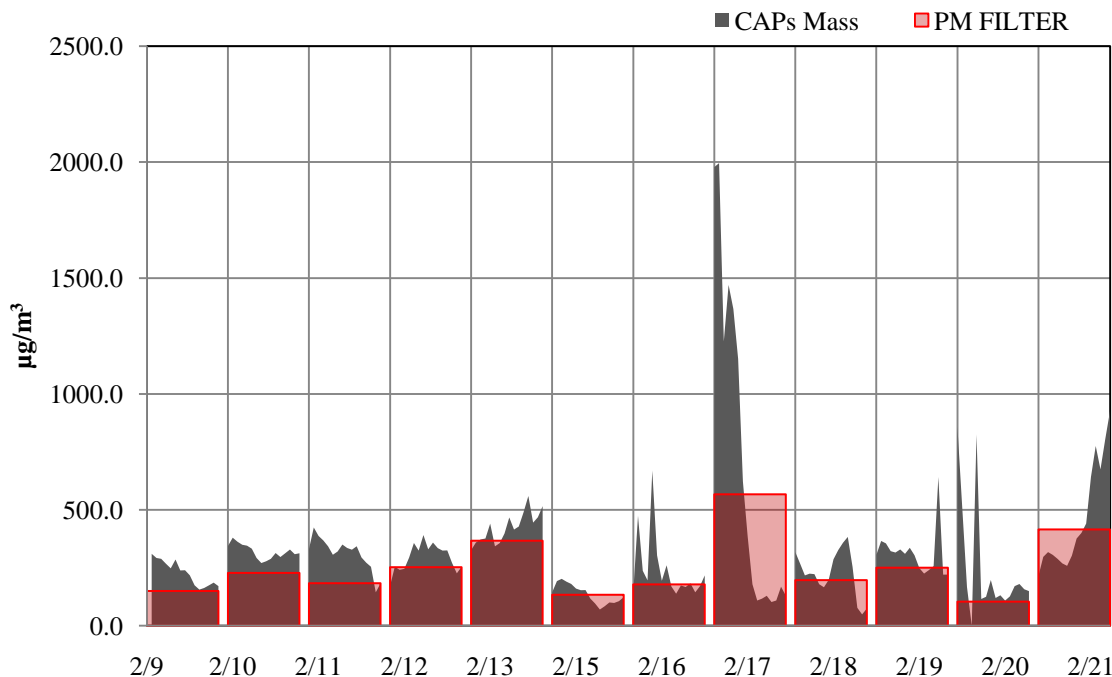
**Figure IV.24 Thirty-minute concentrations of gas measurements during the Steubenville winter study, with exposure hours highlighted by the grey bars.**



### **CAPs Concentrations**

The lowest ambient PM<sub>2.5</sub> concentrations measured at the Steubenville site were during the winter intensive, as was the lowest CAPs mass concentration during the exposures. The fine mass determined from the Teflon filters was  $252.4 \pm 129.2 \mu\text{g}/\text{m}^3$  whereas the TEOM captured higher concentrations and greater variability, which resulted in a mass of  $326.8 \pm 271.0 \mu\text{g}/\text{m}^3$ . Figure IV.25 shows overlays of 30-minute TEOM concentrations over the integrated mass obtained from the filters. Previous studies often observed substantial changes in PM<sub>2.5</sub> mass due to changes in mixing height, temperature gradients and dominant flow that can occur throughout a day. On most days during the Steubenville winter intensive, there is not much a gradient in PM<sub>2.5</sub> mass; therefore there was not a substantial divergence of the TEOM concentrations from the integrated mass concentration. As shown in Figure IV.25, only the February 17 and February 21 experienced within-day variability that may have influenced the higher mean and variability determined by 30-minute PM<sub>2.5</sub> concentrations.

**Figure IV.25 Fine mass concentrations measured in Steubenville during the winter exposure from both the 8-hour exposure filter and the 30-minute TEOM data.**



### PM<sub>2.5</sub> Composition

The composition of PM<sub>2.5</sub> mass in Steubenville in the winter was significantly different than during the summer, similar to the seasonal variability in composition observed in Detroit. Atmospheric formation of secondary SO<sub>4</sub><sup>-2</sup> was limited in the wintertime in these two Midwestern states, and was therefore replaced with NO<sub>3</sub><sup>-</sup> ions binding to NH<sub>4</sub><sup>+</sup> to form particles in the absence of SO<sub>4</sub><sup>-2</sup>.<sup>15</sup> Figure IV.26 shows the contributions of PM<sub>2.5</sub> CAPs mass for each 8-hour exposure. The average composition for SO<sub>4</sub><sup>-2</sup> was 19±13%, and on most days, the range was 10-20%, except on February 17 and February 21 when the composition exceeded 40% of the CAPs mass. These two days of higher mass reflected summertime conditions when SO<sub>4</sub><sup>-2</sup> represented 24±12% of the mass. February 17 surpassed both of these averages by contributing 262.4µg/m<sup>3</sup> of SO<sub>4</sub><sup>-2</sup> to its total mass. In the summer, Steubenville NO<sub>3</sub><sup>-</sup> consisted of <2% of the fine mass whereas winter averaged 16±9% NO<sub>3</sub><sup>-</sup> in the air sample. Table IV.10 provides the daily mass contribution to CAPs mass.



**Figure IV.26 Daily concentrations of the major components of PM<sub>2.5</sub> CAPs collected during the 8-hour Steubenville winter exposures (µg/m<sup>3</sup>).**

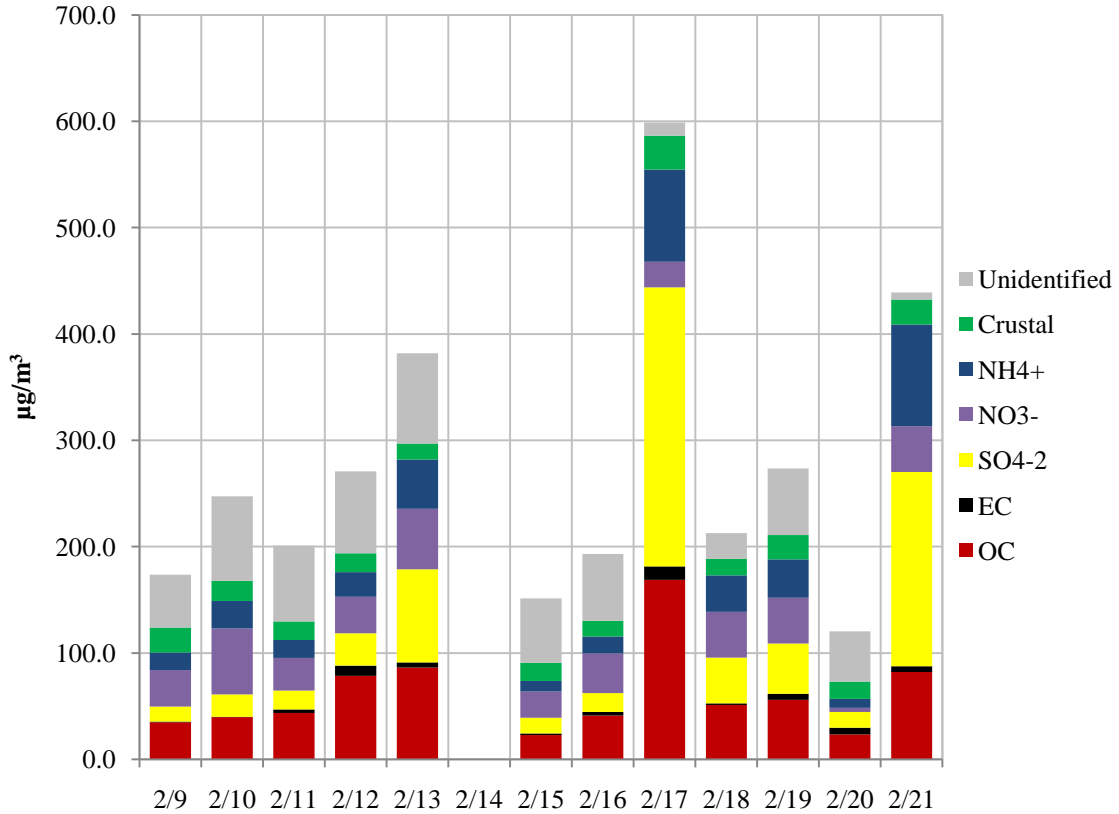


**Table IV.10 Daily concentrations of the major components of PM<sub>2.5</sub> CAPs collected during the 8-hour exposures (µg/m<sup>3</sup>).**

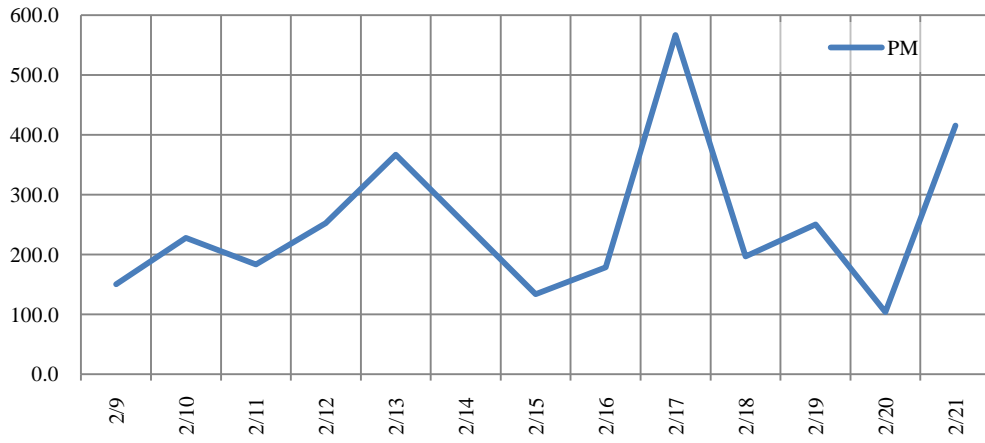
	Mass	OC	EC	SO <sub>4</sub> <sup>-2</sup>	NO <sub>3</sub> <sup>-</sup>	NH <sub>4</sub> <sup>+</sup>	Crustal
2/9	150.2	34.9	0.6	14.1	34.2	16.8	23.4
2/10	228.1	39.6	0.5	20.8	62.2	25.7	19.2
2/11	183.6	43.6	3.3	17.6	30.9	16.6	17.5
2/12	252.8	78.6	9.4	30.4	34.3	23.1	17.9
2/13	367.0	86.4	4.9	87.4	56.9	46.4	15.0
2/15	133.8	22.7	1.7	14.5	24.9	9.8	17.4
2/16	178.6	41.2	3.3	17.8	37.5	15.9	14.6
2/17	567.1	168.8	12.7	262.4	24.1	86.8	31.8
2/18	197.1	51.0	1.5	43.0	43.2	34.4	15.8
2/19	250.6	56.0	5.5	47.3	43.1	36.1	23.0
2/20	104.2	23.5	6.2	14.8	4.0	8.4	16.1
2/21	415.7	82.1	5.3	182.6	43.1	95.9	23.2
Mean	252.4	60.7	4.6	62.7	36.5	34.6	19.6
SD	134.6	40.3	3.7	79.4	15.4	28.8	5.0

## Trace Elements

The trace element concentrations in the wintertime exposure were often highly correlated to the PM<sub>2.5</sub> mass. Most notably, 8-hour concentrations of Fe, Ca, K, Mg, Ti, Mn, Cr and Ba were all significantly correlated with PM<sub>2.5</sub> ( $p < 0.05$ ). Daily concentrations are summarized in Table IV.11. S and Se were not significantly correlated to PM<sub>2.5</sub> mass; instead, S and Se were highly correlated with each other ( $r^2 = 0.8310$ ). Figure IV.27 provides a plot of the PM<sub>2.5</sub> mass and the S concentration of the collected PM. The two days with highest PM<sub>2.5</sub>, February 17 and 21, were two days in which sulfate exceeded 40% of the fine mass. However, when looking at insoluble elemental S, a collinear relationship with either PM or SO<sub>4</sub><sup>-2</sup> did not occur. Thus the majority of the S content in PM<sub>2.5</sub> in Steubenville winter may be in the soluble form. Additionally, the days with highest concentrations of S were relatively low in overall PM<sub>2.5</sub> mass. S had peaks on February 9, 15 and 18, but these days all had CAPs mass at or below 200 µg/m<sup>3</sup>.

**Figure IV.27 Daily CAPs concentrations for (a) PM<sub>2.5</sub> and (b) S during Steubenville winter study.**

**(a) PM (Fe, Ca, K, Mg, Ti, Mn, Cr and Ba)**



**(b) S (Se)**

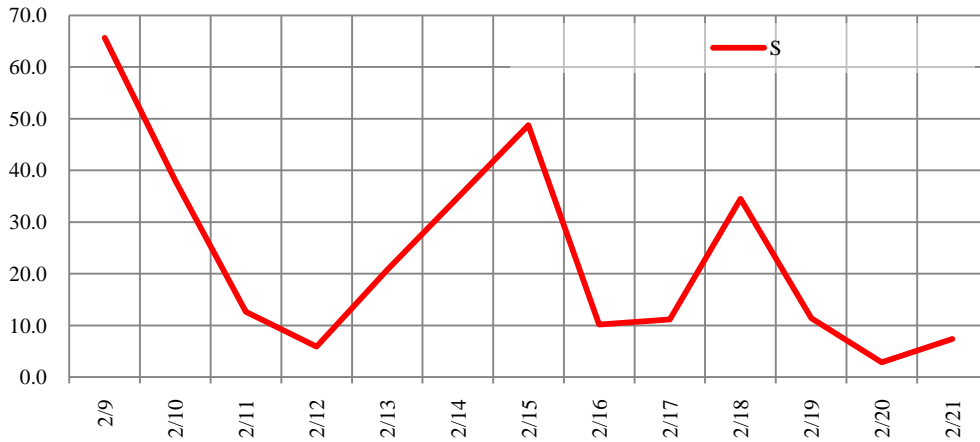


**Table IV.11 Average CAPs mass and trace element concentrations in units of ng/m<sup>3</sup>. \*(PM, Al, Fe and S in units of µg/m<sup>3</sup>).**

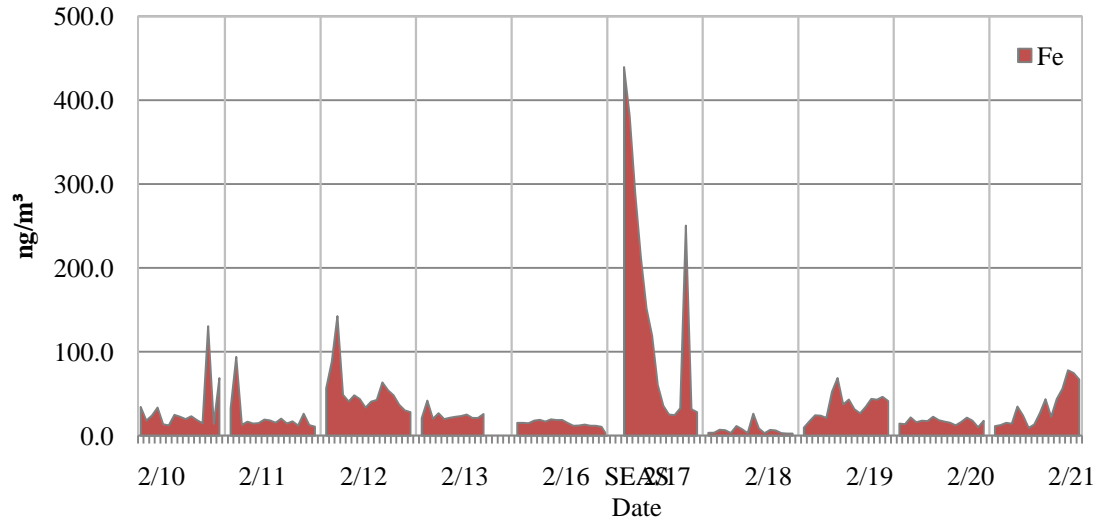
	PM*	Rb	Sr	Mo	Cd	In	Sn	Sb	La	Ce	Pb	Mg	Al*	P	S*	Ti	V	Cr	Mn	Fe*	Co	Ni	Cu	Zn	K	As	Se	Ba	Ca*
2/9	150	3.3	14.8	3.3	24.3	0.25	11.7	12.3	1.95	2.69	147	523	2.02	715	65.7	31.7	18.8	26.9	63.4	2.37	1.1	11.2	40.1	204	882	13.0	63.9	35.9	2.6
2/10	228	2.9	14.1	2.8	13.6	0.23	8.9	5.6	1.16	1.95	98.5	557	1.70	531	38.0	28.2	16.8	25.5	44.0	1.47	1.9	7.9	25.2	121	732	7.9	48.4	29.9	2.4
2/11	184	2.0	9.6	1.8	12.4	0.24	5.7	3.3	0.42	0.93	102	266	1.08	541	12.6	60.2	8.0	15.9	55.9	0.95	0.5	5.1	35.3	128	731	8.8	37.2	29.7	2.6
2/12	253	2.5	9.8	6.2	38.6	0.41	8.0	8.4	0.88	1.24	264	292	1.26	510	5.9	138	23.4	49.0	79.9	1.08	0.7	10.0	67.3	973	782	8.9	12.4	38.5	2.0
2/13	367	2.0	11.6	13.2	13.0	0.25	6.7	7.9	0.55	0.93	124	268	0.92	420	20.8	103.1	24.1	20.1	68.7	0.81	0.8	6.1	30.3	157	692	7.7	147.3	32.5	1.6
2/15	134	2.0	10.6	3.0	11.2	0.22	6.4	6.9	0.52	1.11	94.4	307	1.20	400	48.7	22.1	6.0	25.7	117.5	1.15	0.7	4.4	23.5	82.4	726	11.0	51.2	23.9	2.2
2/16	179	2.2	9.4	7.1	10.4	0.30	4.9	4.4	1.01	1.39	118	325	1.07	468	10.2	85.8	13.2	54.3	144.5	1.40	1.7	45.1	26.6	383	489	7.1	16.0	22.9	2.5
2/17	567	3.1	16.2	34.4	19.8	0.35	8.0	8.4	0.99	1.99	205	719	1.69	565	11.2	234	32.7	64.9	196.0	3.75	1.3	13.8	54.0	1417	1125	9.6	24.6	56.1	5.1
2/18	197	1.9	9.7	5.5	13.5	0.23	5.8	11.6	0.82	1.36	105	282	1.02	439	34.5	20.7	5.2	40.3	58.9	1.22	0.6	4.7	39.1	514	666	12.8	28.4	28.2	1.9
2/19	251	2.4	16.8	9.5	17.8	0.28	6.0	6.9	1.09	2.11	132	700	1.54	462	11.4	80.4	10.6	35.6	148.8	2.34	0.8	8.8	38.7	476	628	7.8	8.7	44.2	5.6
2/20	104	2.0	9.0	11.9	14.6	0.23	3.6	4.3	0.47	0.91	104	368	1.07	556	2.8	20.6	1.6	29.8	46.1	0.86	0.7	6.1	67.0	615	677	2.1	4.4	30.3	2.3
2/21	416	2.4	15.9	36.5	39.3	0.48	18.8	9.4	0.86	1.47	301	523	1.25	469	7.4	138	26.7	46.4	81.4	1.22	1.0	10.8	37.9	1644	993	17.4	14.9	36.6	3.5
Mean	252	2.4	12.3	11.3	19.0	0.29	7.9	7.4	0.89	1.51	150	428	1.32	506	22.4	80.2	15.6	36.2	92.1	1.55	1.0	11.2	40.4	560	760	9.5	38.1	34.1	2.9
SD	135	0.5	3.0	11.9	10.1	0.08	4.0	2.8	0.42	0.56	69.6	169	0.34	85	19.8	65.3	9.7	15.0	48.5	0.86	0.4	11.1	14.9	524	170	3.8	39.1	9.2	1.3

### **Thirty-Minute Trace Element Concentrations**

In the previous three exposure studies, 30-minute and 8-hour findings were discussed separately; but during the winter study in Steubenville, there was only one day with diurnal differences in 30-minute data that diverted from the 8-hour findings: February 17. Table IV.12 summarizes the average SEAS concentrations on each day of exposure. The variability observed throughout each day would bring changing wind patterns and therefore changes in the concentrations of constituents of PM<sub>2.5</sub>. But as was shown in Figure IV.25, only two days displayed somewhat interesting variability over the course of the day. When observing S and Fe, two prominent trace elements in Steubenville, the only substantial within-day change took place on February 17 (Figure IV.28). Therefore, these two trace elements, along with many other constituents of PM<sub>2.5</sub> should not differ greatly from the 8-hour dataset. Neither S nor Fe were significantly correlated with total PM<sub>2.5</sub> mass using 8-hour filter data ( $p=0.2645$  and  $0.0686$ , respectively), but when using 30-minute concentrations for S and Fe with 30-minute mass data, the  $r^2$  improved ( $r^2=.7563$  and  $0.6694$ , respectively), and the correlations were significant ( $p<0.0001$ ). This result should be reflected in similar CI Plots between the two datasets. Later in this chapter, the effect of the pollution episode will be explored to determine if the 4-hour block influenced the changes in HRV and determined the constituents associated with HRV.

**Figure IV.28 Iron (Fe) and Sulfur (S) plots of 30-minute SEAS data during exposure hours.**

**(a) Fe**



**(b) S**

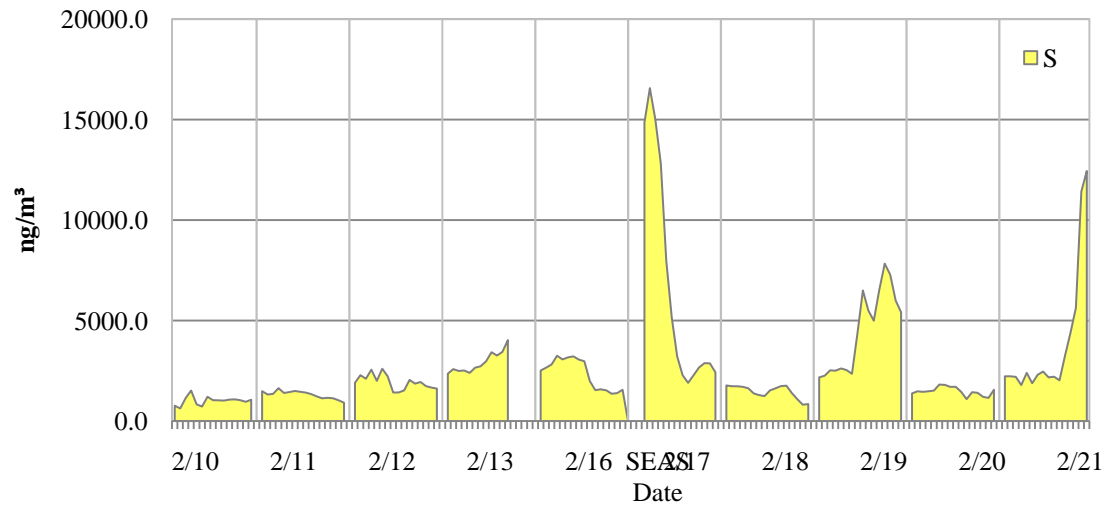


**Table IV.12 Average SEAS fine fraction trace element concentrations in units of ng/m<sup>3</sup> \*( PM, EC, and S in units of µg/m<sup>3</sup>).**

	PM*	EC*	Mg	Al	P	S*	K	Ca	Ti	V	Cr	Mn	Fe	Co	Ni	Cu	Zn	As	Se	Rb	Sr	Mo	Cd	Sn	Sb	Ba	La	Ce	Pb
2/9	235	5.1	NA	NA	NA	NA	NA	NA	NA	NA	NA	NA	NA	NA	NA	NA	NA	NA	NA	NA	NA	NA	NA	NA	NA	NA	NA	NA	NA
2/10	320	5.5	21	20	14	1	48	253	0.2	0.1	1.2	1.7	32	0.1	1.4	7	16	0.2	1.4	0.1	0.6	0.2	0.1	1.3	0.5	3.4	0	0	2
2/11	312	4.4	21	15	4.7	1.3	48	203	0.6	0.2	1.1	1.6	22	0	1.7	4.3	11	0.5	0.8	0	0.5	0.2	0.1	0.2	0.4	5.3	0	0	3.8
2/12	294	9.1	34	36	4.2	1.9	62	140	1.1	0.5	0.3	11	53	0	0.8	3.6	20	1.3	3.9	0.1	1	0.5	0.2	0.3	0.7	1.7	0	0.1	4.4
2/13	424	7.3	118	57	5.5	2.9	76	362	2.9	0.7	1.2	9.6	24	0	1.5	2.8	23	2.2	1.5	0.2	1	0.7	0.5	0.7	0.7	5.9	0.1	0.1	4.4
2/15	136	4.1	72	18	3.1	0.9	32	371	0.5	0.2	0.3	1.9	9	0	1.1	1.7	7.9	0.3	0.3	0.1	0.9	0.3	0.1	0.3	0.1	8.2	0	0	2
2/16	240	5.1	51	31	2.8	2.4	40	405	0.7	0.2	0.4	1.9	15	0	1.1	1.8	17	0.4	1.9	0.1	1.1	0.4	0.1	0.5	0.3	10	0	0.1	4.4
2/17	703	5.4	58	72	7.5	6.6	109	232	1.8	3.5	0.8	11	149	0.1	1.5	3.9	266	3.9	6.2	0.4	1	0.5	0.6	1.6	1.1	2.8	0.1	0.1	28
2/18	225	3.1	20	15	1.2	1.5	38	257	0.3	0.2	0.5	2.1	6.7	0	1.3	1.8	9.6	0.5	0.7	0.1	0.5	0.1	0.1	0.4	0.2	8.3	0	0	1.8
2/19	313	7	31	72	2.7	4.5	50	154	1.1	3	0.4	4	35	0	1.7	3.9	21	1	15	0.1	0.9	0.3	0.1	0.6	0.4	8.4	0.1	0.1	8.6
2/20	263	5.4	34	23	3.1	1.5	70	170	0.7	0.7	0.3	9.9	17	0	1.2	1	14	0.6	1.8	0.2	0.8	0.3	0.2	0.3	0.8	3.9	0	0	2.3
2/21	456	7.8	63	49	5.9	3.8	42	337	1.1	0.4	0.8	5.6	34	0	7.4	3	30	0.7	4.7	0.2	0.9	0.2	0.1	0.4	0.7	6.9	0.1	0.1	6.4
Mean	327	5.7	43	38	5	2.7	57	249	1	0.9	0.7	5.7	38	0	2	3.3	40	1.1	3.8	0.2	0.8	0.3	0.2	0.6	0.6	5.7	0	0.1	6.4
SD	270	2.6	48	36	4.9	2.7	40	191	1.2	1.7	1.4	6.4	59	0	7.5	3	128	1.8	7.4	0.2	0.4	0.2	0.3	0.8	0.5	4.1	0	0.1	10
Median	289	5.2	31	24	3.5	1.8	46	193	0.6	0.3	0.3	2.2	21	0	1.2	2.1	16	0.6	1.5	0.1	0.7	0.3	0.1	0.4	0.5	4.8	0	0	3.7
5%	106	2.8	15	12	1.1	0.9	26	66	0.1	0.1	0.2	1.2	3.6	0	0.6	0.9	8.4	0.2	0.3	0	0.4	0.1	0.1	0.1	0.2	1.5	0	0	1.4
95%	805	11	122	128	16	7.8	98	583	2.9	5.5	1.4	21	131	0.1	2.5	8.7	91	3.1	15	0.4	1.7	0.8	0.6	2	1.8	13	0.1	0.2	22

### IV.2.3 HRV Summary

Mixed Modeling Results comparing the HRV of AIR and CAPs Rats in Steubenville during the winter were not significant for any parameter using either the 8-hour or 30-minute datasets. It appears that daily air pollution concentrations in the winter did not affect the CAPs-exposed rats in a way that would significantly alter their HR or HRV. Tables IV.13 and 14 summarize the mixed modeling findings for the 8-hour and 30-minute datasets. In other studies, the 8-hour integrated averages in air pollution concentrations did not have enough variance to detect day-to-day differences, not to mention a large enough change to detect differences in HRV. But here, using high-resolution data also did not result in any significant differences between AIR and CAPs Rats. As mentioned in the previous section, the 30-minute pollution dataset was closely related to the 8-hour dataset since within-day variations were substantial on only two days (e.g. February 17 and 21). Therefore, a similar result between the two datasets could be expected. For both datasets, ln(SDNN) saw closest to being significantly different between AIR and CAPs Rats ( $p=0.0506$  and  $0.1776$ , respectively). Therefore, this parameter will be used in several examples in this section to illustrate the effects of the pollution episode during the winter study in Steubenville.

**Table IV.13 Steubenville winter daily average statistics for unexposed (AIR) and exposed (CAPs) rats.**

	AIR Rats	CAPs Rats	Mixed Modeling Significance ( $p<0.05$ )		
	N=95	N=84	Group	Date	Group*Date
Heart Rate	307.7	301.8	0.1832	<.0001	0.7354
ln(SDNN)	2.74	2.79	0.2533	<.0001	0.0506
ln(r-MSSD)	1.44	1.47	0.6833	<.0001	0.7443
ln(LF)	-2.87	-2.89	0.7799	0.0036	0.3899
ln(HF)	-2.54	-2.56	0.8662	0.0488	0.3537
LF/HF	0.74	0.77	0.6579	0.0971	0.1128



**Table IV.14 Steubenville winter study mixed modeling results for the 30-minute HRV parameters.**

	Mixed Modeling Significance (p<0.05)		
	Group	Date	Group*Date
Heart Rate	0.1801	<.0001	0.9060
ln(SDNN)	0.2822	<.0001	0.1776
ln(r-MSSD)	0.7075	<.0001	0.9147

**Daily Comparisons of AIR and CAPs Rats**

February 17 was the only day on which average ln(SDNN) for CAPs Rats was lower than AIR Rats throughout the two-week study. Also, AIR and CAPs Rats were different when looking at 30-minute ln(SDNN) data within the 17<sup>th</sup> (p=0.0771). Furthermore, the LS Means test found that the HRV of CAPs HRV was significantly lower on February 17 than on most other days of the exposure. In Table IV.15, the t-values illustrate the directionality of the difference for each day against all others. The results for February 17 were significantly different (in bold) than for every other day, except February 16. Therefore, there is some indication that the substantial peak in air pollutants that morning may have influenced the reduction of ln(SDNN) for the entire day. Only a few short-term, significant reductions in HRV were observed in each exposure study, similar to the findings on February 17. The occurrence of a short-term drop in HRV was not frequent enough to be considered a significant biological effect, and cannot be used in this study to associate a significant drop in HRV with an air pollution episode. However, the 4-hour pollution episode that occurred on February 17 was such a profound effect on both concentrations and HRV that it is possible that future studies can be modified to look at peaks in pollution concentrations and the immediate (or lagged) changes in HRV.

**Figure IV.29 Daily AIR and CAPs Rats averages for ln(SDNN) for the Steubenville winter exposure study.**

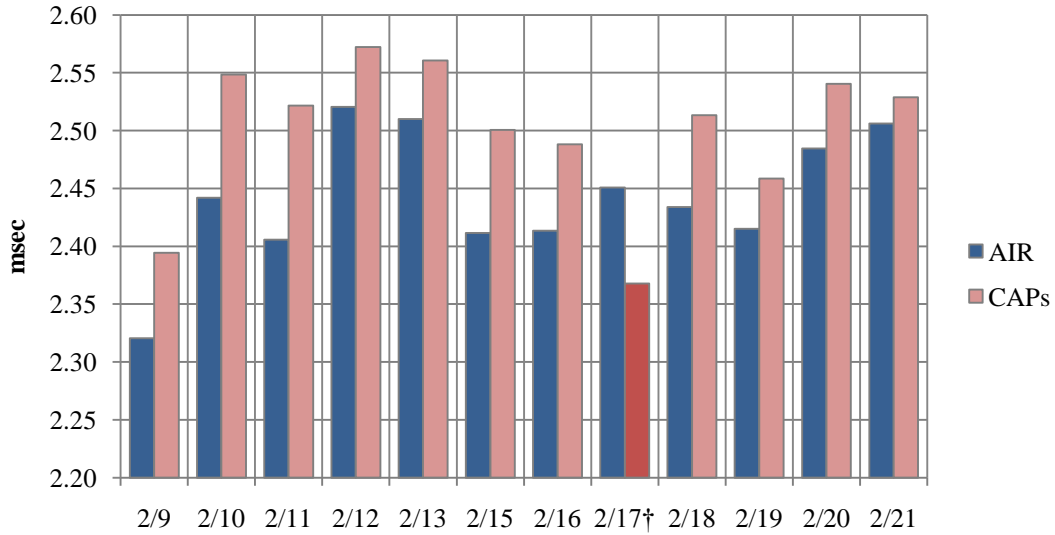


**Table IV.15 Least-squares means analysis showing that ln(SDNN) of CAPs Rats on February 17 was significantly lower than on all other days, except February 16.**

	2/9	2/10	2/11	2/12	2/13	2/15	2/16	2/17	2/18	2/19	2/20
2/10	-0.11										
2/11	-0.7	-0.59									
2/12	<b>-2.83</b>	<b>-2.72</b>	<b>-2.13</b>								
2/13	0.11	0.22	0.81	<b>2.94</b>							
2/15	0.04	0.15	0.74	<b>2.87</b>	-0.07						
2/16	0.8	0.91	1.5	<b>3.63</b>	0.69	0.76					
2/17	<b>2.47</b>	<b>2.58</b>	<b>3.17</b>	<b>5.3</b>	<b>2.36</b>	<b>2.43</b>	1.67				
2/18	0.4	0.5	1.09	<b>3.23</b>	0.29	0.36	-0.4	<b>-2.07</b>			
2/19	0.44	0.54	1.13	<b>3.27</b>	0.33	0.39	-0.37	<b>-2.04</b>	0.04		
2/20	-1.89	-1.78	-1.19	0.94	<b>-2</b>	-1.93	<b>-2.69</b>	<b>-4.36</b>	<b>-2.28</b>	<b>-2.32</b>	
2/21	-0.86	-0.75	-0.16	1.97	-0.97	-0.9	-1.66	<b>-3.33</b>	-1.26	-1.29	1.03

**Eight-Hour Associations between Air Pollution and HRV**

Despite there being no significant differences between AIR and CAPs Rats, the significant change in HRV on February 17 and the peak in fine mass concentrations indicate that air pollution may be affecting cardiovascular function. As with the other studies, Steubenville winter CI Plots were made for both the 8-hour and 30-minute datasets to identify the significance of the effect estimate for each pollutants upon HRV

parameters. For the 8-hour dataset, S, Ce, Al, Rb, Fe, La, Se and  $\text{NO}_3^-$  were significantly associated with an increase in HR. At the same time, Cu, Zn, Cd, Pb, Mo and EC were associated with a decrease in HR. This multi-directionality of HR was similar to that found for HR and HRV during the Steubenville summer intensives.

In the winter, the common pollutants between the HR and HRV were Cu, Cd and EC. Cu and Cd associated with an increase in  $\ln(\text{SDNN})$ , and Cu and EC were associated with an increase in  $\ln(\text{r-MSSD})$ , and all three associated with a reduction in HR. Fe and Ce were both found to be in association with a reduction in  $\ln(\text{SDNN})$  and  $\ln(\text{r-MSSD})$ .  $\text{SO}_4^{-2}$  associated with  $\ln(\text{SDNN})$  while S associated with  $\ln(\text{r-MSSD})$ . It is unclear why the soluble and insoluble forms of S differed so greatly ( $r^2=0.109$ ) and thereby showed different associations between HRV parameters, but the discrepancy indicates that solubility in the Steubenville winter study may have a significant effect on the composition and HRV analysis.

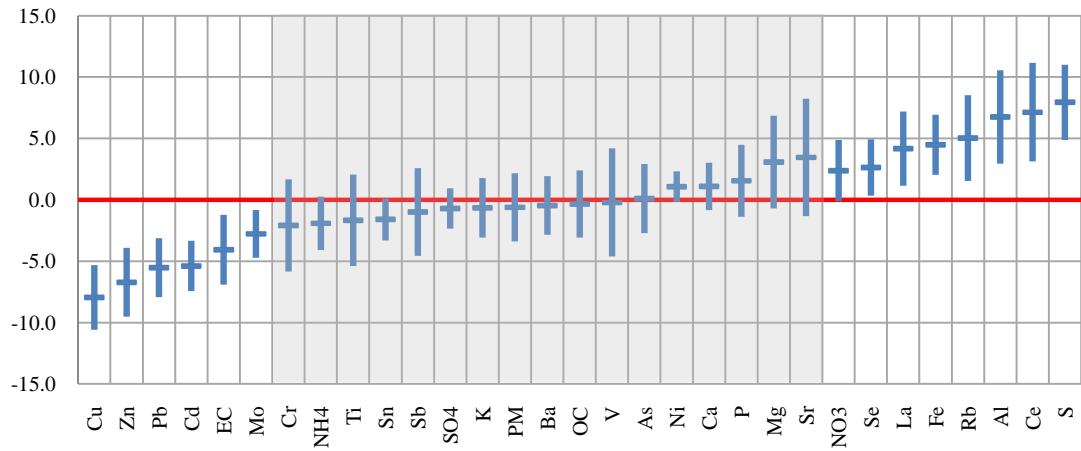
In contrast, S, Fe, Rb, La, Ce and Al were observed to associate with an increase in HR and decrease in one or two HRV parameters. Table IV.16 shows the Pearson's correlations of all the constituents from one group against the other. Cu, Cd, and EC are significantly correlated to each other and most of the other constituents are also significantly related, with exception of Ce. Even though it was found associated with all three HRV parameters, its mass was independent of all other constituents of  $\text{PM}_{2.5}$ . These split findings may relate back to the Steubenville summer study where wind direction was pivotal in determining how specific air pollutants were affecting HRV in CAPs Rats. In the next section, 30-minute concentrations of air pollutants can be linked with wind directions.

**Table IV.16 Pearson's correlation table with two groups of constituents from the 8-hour Steubenville winter intensive that showed opposing effects on HRV.**

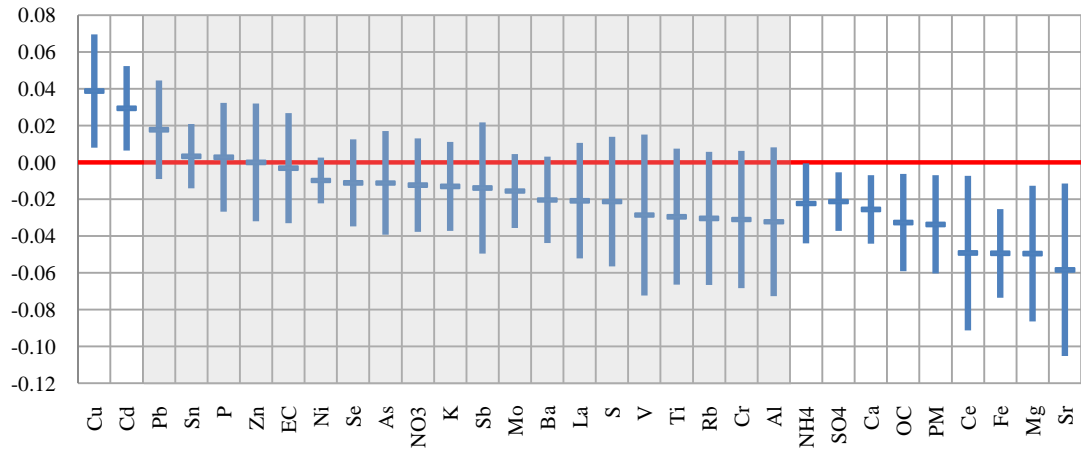
	Cu	Cd	EC	S	Fe	Rb	La	Ce
Cd	0.48541 <.0001	1						
EC	0.69342 <.0001	0.40743 <.0001	1					
S	-0.47076 <.0001	-0.22008 0.0022	-0.68276 <.0001	1				
Fe	0.13529 0.0614	0.07793 0.2826	0.43047 <.0001	0.11555 0.1105	1			
Rb	0.12257 0.0903	0.33186 <.0001	0.18085 0.0121	0.34342 <.0001	0.7543 <.0001	1		
La	-0.06267 0.3878	0.2688 0.0002	-0.20592 0.0042	0.53456 <.0001	0.56189 <.0001	0.80537 <.0001	1	
Ce	-0.07862 0.2784	0.19885 0.0057	-0.08936 0.2177	0.47637 <.0001	0.75589 <.0001	0.85134 <.0001	0.93219 <.0001	1
Al	0.0303 0.6765	0.23558 0.001	-0.00764 0.9162	0.48174 <.0001	0.73931 <.0001	0.93273 <.0001	0.84365 <.0001	0.93388 <.0001

**Figure IV.30 CI Plots for the Steubenville Winter Exposure (8-hour data) ( $p < 0.05$ ).**

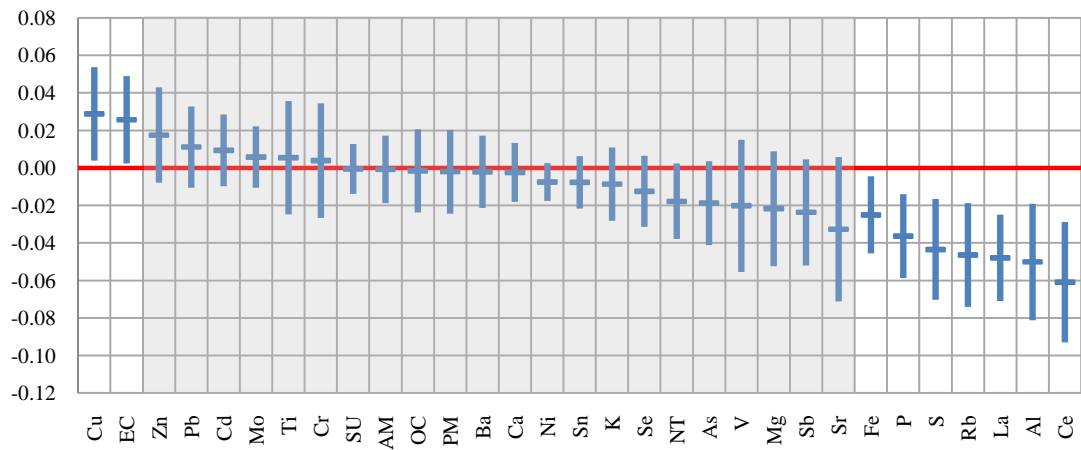
**(a.) Heart Rate**



**(b.) ln(SDNN)**



**(c.) ln(r-MSSD)**

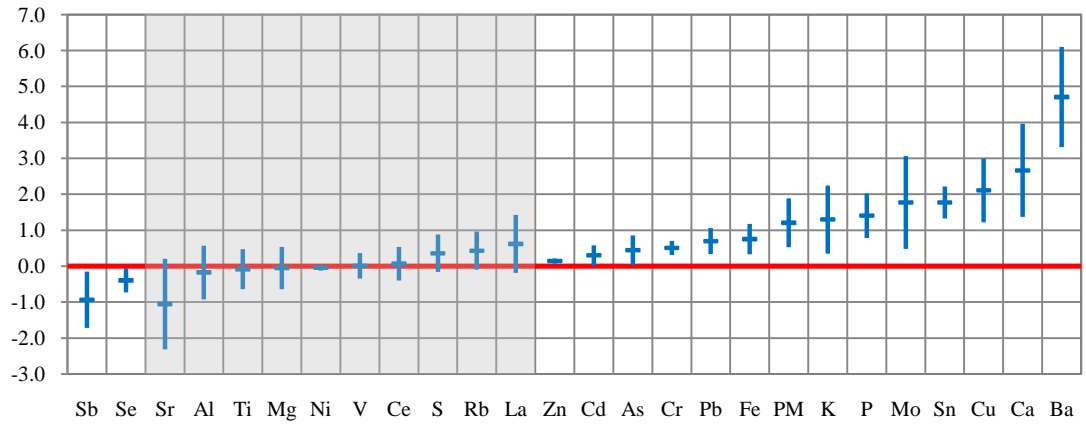


### **Thirty-Minute Associations**

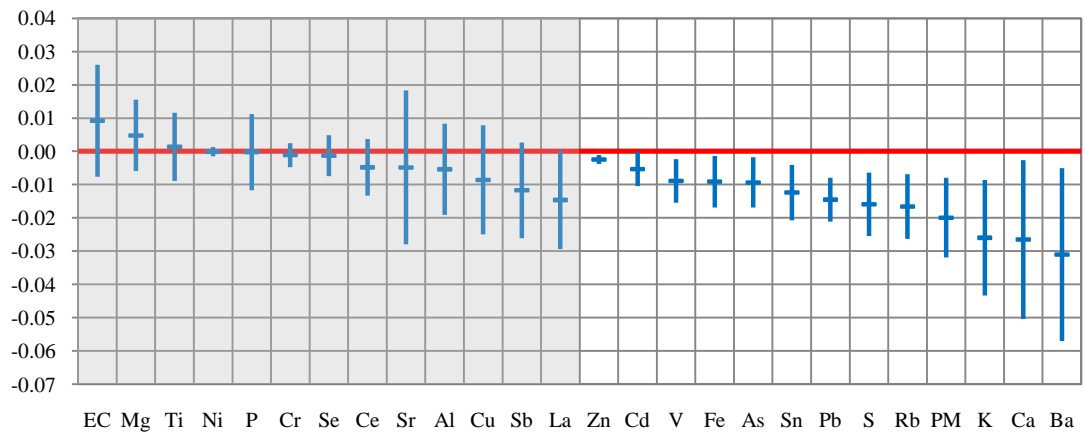
Since within-day variations of most constituents and the  $PM_{2.5}$  mass were not significant, with the exceptions of February 17 and 21, very few differences between the two datasets in terms of the pollutants associated with HRV were expected. In fact, the same general pattern of an increase in HR and a decrease in HRV and with less multi-directionality as was observed in the 8-hour data became evident;  $\ln(\text{SDNN})$  and  $\ln(\text{r-MSSD})$  no longer have constituents associated with an increase in these parameters. The most significant change from the 8-hour dataset is the observation of  $PM_{2.5}$  in each of the parameters. Now, Fe and S were associated with  $\ln(\text{SDNN})$  but not  $\ln(\text{r-MSSD})$ . Both  $\ln(\text{SDNN})$  and  $\ln(\text{r-MSSD})$  are reduced in association with Ca, Ba, Co and Sn and were also associated with an increase in HR. Opposing associations from Cu, Cd and EC were no longer evident. Only Sb and Se associated with a reduction in HR while several other constituents associated with an increase in HR. Overall, both datasets indicate the same general pattern of behavior, but the associated constituents affecting HRV varied greatly using the high-resolution data. Furthermore, the loss of multi-directional effects did not lead to the necessity of investigating the health effects by wind direction.

**Figure IV.31** Thirty-minute CI Plots from the Steubenville Winter exposure ( $p < 0.05$ ).

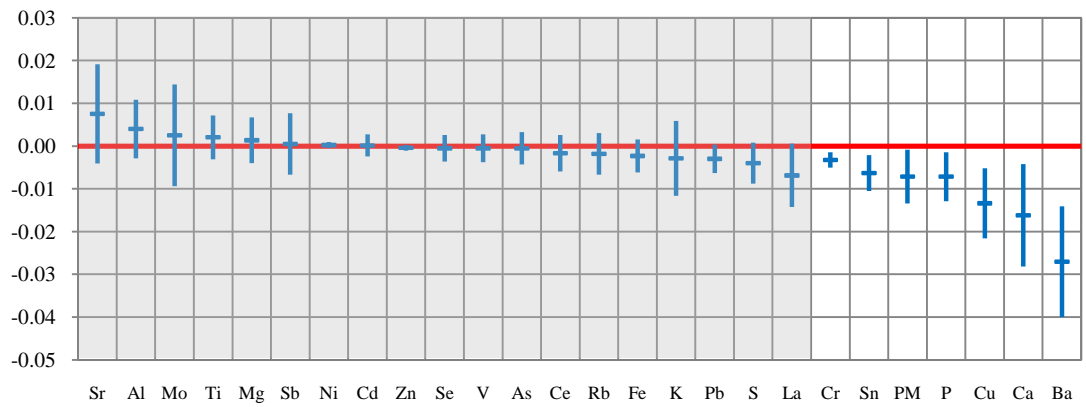
**(a.) Heart Rate**



**(b.) ln(SDNN)**



**(c.) ln(r-MSSD)**



## IV.2.4 Steubenville Winter Discussion

### The Effects on HRV from a Pollution Episode

AIR and CAPs Rats could not be distinguished from each other when looking at HRV within February 17. This outcome may have been due to the significant drop in fine-fraction mass and constituents across the day, therefore, the dataset was broken up into 4-hour blocks to separate the air pollution peak and HRV into AM and PM on each day (Figure IV.32). Even then, mixed modeling results show that when looking at just the 4-hour block of data, AIR and CAPs were still not significantly different from each other. However, the number of constituents associated with HR,  $\ln(\text{SDNN})$  and  $\ln(r\text{-MSSD})$  was greatly affected. The removal of this 4-hour block of data greatly reduced the overall  $\text{PM}_{2.5}$  mass as well as many of the constituents, dropping the already low concentrations during the winter intensive. Table IV.17 shows the concentration of each pollutant during the exposure period in comparison to the concentrations when the 4-hour block is removed. For most constituents, the average mass was substantially higher during the pollution episode than during the rest of the two-week exposure.

**Figure IV.32 Average CAPs mass concentrations according to 4-hour averages during exposure hours.**

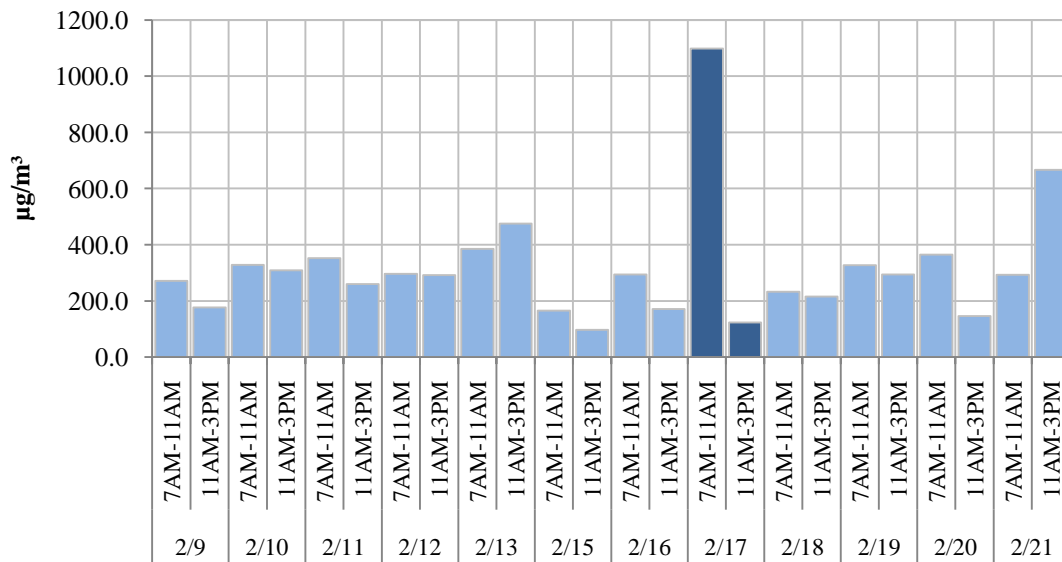




**Table IV.17 The average of each component of PM<sub>2.5</sub> mass during the pollution episode (the first 4 hours of exposure on February 17) was compared to the average during all the other hours of exposure in ng/m<sup>3</sup> (\* μg/m<sup>3</sup>).**

	PM*	EC*	Mg	Al	P	S*	K	Ca	Ti	V	Cr	Mn	Fe	Co	Ni	Cu	Zn	As	Se	Rb	Sr	Mo	Cd	Sn	Sb	Ba	La	Ce	Pb
Episode Average	1153	17	95	112	14	11	183	370	3.1	5.8	1.3	19	236	0.1	2	6	514	6.8	10	0.8	1.5	0.8	1	3.1	1.7	3.1	0.1	0.2	46
All Other Average	286	5.6	41	34	4.6	2.3	51	244	0.9	0.7	0.6	5.1	28	0	2	3.2	18	0.8	3.5	0.1	0.8	0.3	0.2	0.5	0.5	5.9	0	0.1	4.5

### **Air Pollution on the Morning of February 17**

The 4-hour block in the morning part of the exposure on February 17 had considerably higher PM<sub>2.5</sub> mass far beyond all the other AM concentrations, so the influence was not simply due to typical diurnal conditions in Steubenville during the winter. The 8-hour filter data showed that mass on February 17 was higher than on all the other days at 567µg/m<sup>3</sup>, but the magnitude of the early morning peak was lost because the later four hours of exposure on February 17 observed considerably lower PM<sub>2.5</sub> mass (124µg/m<sup>3</sup>).

Along with PM<sub>2.5</sub> mass, several constituents had higher concentrations during the 4-hour block of time that overlapped with the exposures on February 17. PM and S concentrations were both over 4 times greater than during the rest of the study, whereas Rb, Cd and Sn were all 6 times higher. V, Fe and As were 8 times higher, and Pb was over 10 times greater than the average for the rest of the study concentrations. Most of all, Zn was 28 times higher on the early morning of the exposure. The assumption is valid that Zn and all the constituents would be equally increased by the same order of magnitude during an inversion. However, winds directly from the south may be capturing a source contribution for Zn but do not typically explain the exaggerated concentration on that morning.

The pollutants that did not show much difference or even a reduction during the early morning peak were Ni, Ba and Ca. Looking at average concentrations by wind direction, Ni, Ba and Ca all have their highest concentrations from the north and northeast, so it is not surprising that there is a reduction in these concentrations since winds were not coming from these directions. This finding presents an interesting question whether the observed biological effect ln(SDNN) was in response to something unique during the pollution episode or if there was an effect due to winds being predominantly from the south. If the greatest impact on the CI Plots was the 4-hour block of data on February 17, then its removal would produce fewer constituents and even produce similar results found using the 8-hour dataset. This section will test this hypothesis to see if a 4-hour block of high pollution data can affect the resulting constituents associated with changes in HRV.

### **Changes in HRV Associations without the Morning of February 17**

When considering all data, 11 trace elements were associated with an increase in HR: Ba, Ca, Cr, Cu, P, Sn, K, As, Cd, Fe, Pb as well as PM. After removing the 4-hour block, only 6 remained: Ba, Ca, Cr, Cu, P and Sn. Originally, only Sb and Se associated with the decrease in HR, but after the 4-hour block was removed, Al, As, Rb, S, Sr, Ti, V and Zn along with Sb and Se were also associated with a decrease in HR. Additionally, PM was now associated with a decrease in HR and no longer associated with an increase in HR. It appears that removing the pollution episode eliminated the driving influence of PM<sub>2.5</sub> and many of its constituents that drove the increase in HR. Once the pollution episode was removed from the two-week exposure period, a greater influence of constituents to reduce HR became noticeable; but because the pollution episode was so large, many of the reducing constituents were masked by the driving effect of high PM<sub>2.5</sub> mass. When looking at the components that associated with the 4-hour block, K, Rb, S and PM all associated with an increase in HR. The influence of the episode was so large that, Rb, S and PM were associated with a reduction in HR when the 4-hour block was removed. As a result, the 4-hour block from the large pollution episode had a significant effect on the constituents that associated with HR, and the large increase in HR caused by the pollution episode masked the effect of many constituents that would otherwise be associated with a reduction in HR.

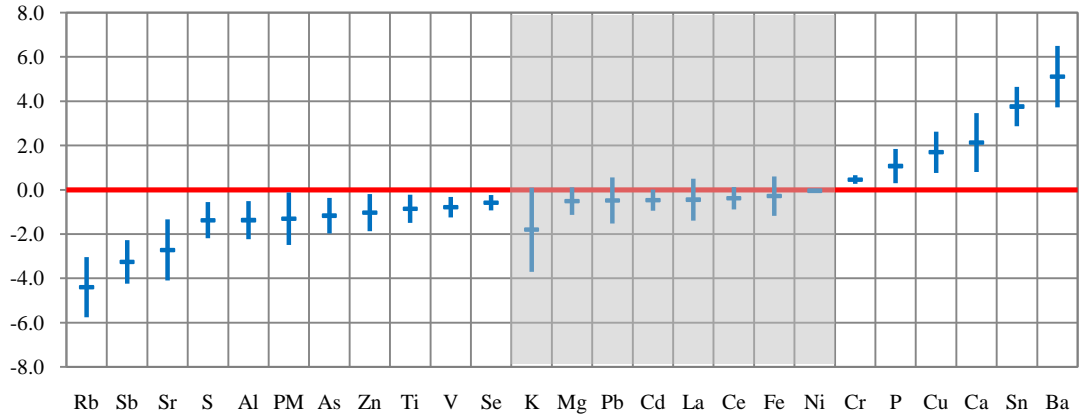
When considering the two HRV parameters,  $\ln(\text{SDNN})$  and  $\ln(\text{r-MSSD})$ , the pollution episode on February 17 drove the  $\ln(\text{SDNN})$  but had very little influence on  $\ln(\text{r-MSSD})$ . When looking at all the data, there were 10 trace elements (As, Ba, Ca, Cd, Fe, K, Pb, Rb, S, Sn, V and Zn) as well as PM<sub>2.5</sub> mass that associated with a decrease in  $\ln(\text{SDNN})$ . Without the pollution episode, only Ba was still associated and none of the other 9 constituents or total mass were significantly associated with a reduction in  $\ln(\text{SDNN})$ . Fe was actually significantly associated with a reduction in  $\ln(\text{SDNN})$  without the pollution episode, again showing how influential that early morning event was on Steubenville air. When looking at components associated with just the 4-hour block, insufficient strength in the dataset prevented identifying any constituent with a change in  $\ln(\text{SDNN})$  or in  $\ln(\text{r-MSSD})$ . However,  $\ln(\text{r-MSSD})$  was not affected by the pollution episode in quite the same way as was HR or  $\ln(\text{SDNN})$ . When considering all

the data, Ba, Ca, Cr, Cu, P, PM and Sn were associated with a reduction in  $\ln(r\text{-MSSD})$ . When removing the 4-hour block from the dataset, the mixed modeling analysis only lost Cr and PM from the associated constituents. Therefore, the pollution episode affected the association with the fine-fraction mass and  $\ln(r\text{-MSSD})$ , but not many of its constituents.

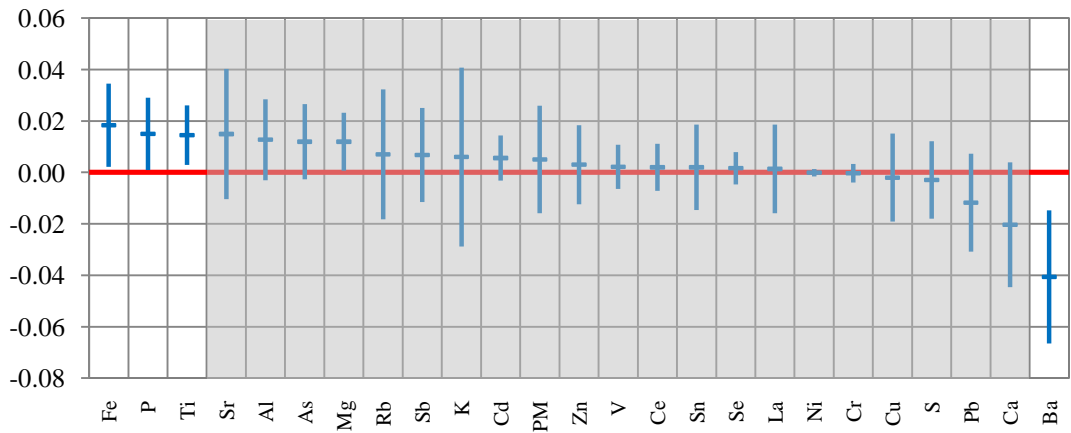
Overall, the influence of a pollution episode, with orders of magnitude different in mass concentrations, can greatly influence the affects of HRV on CAPs-exposed rats within this two-week animal model. The findings from the CI Plots show that without the pollution episode, few constituents are found to be in association with HRV parameters. Furthermore, some constituents appear in the opposite direction. During a temperature inversion, most pollutant concentrations increase, as seen in Table IV.17. This hypothesis could cause a false-positive relationship of constituents, when, in fact, only total mass or a few constituents like Fe or S are driving the health response.

**Figure IV.33 CI Plots for the Steubenville winter intensive in the absence of the 4-hour data block on the morning of February 17.**

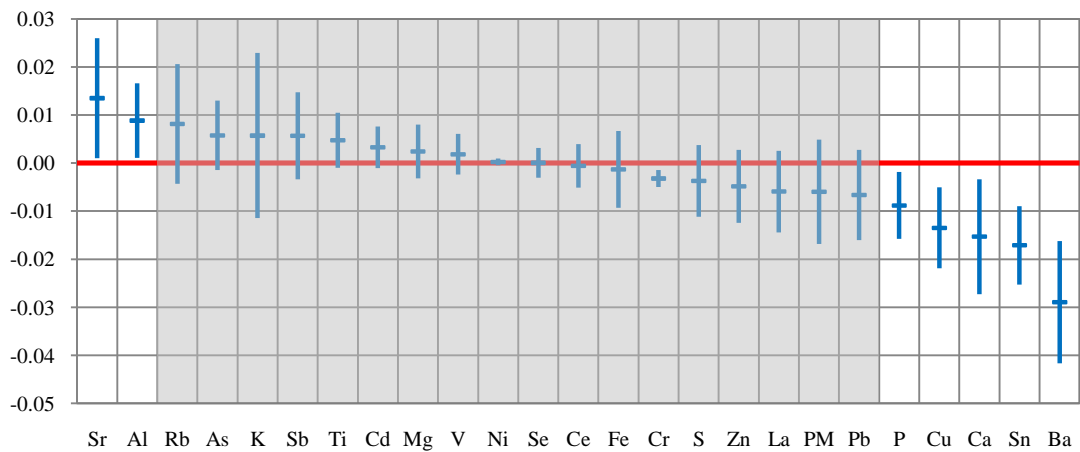
**(a.) Heart Rate**



**(b.) ln(SDNN)**



**(c.) ln(r-MSSD)**



#### IV.2.5 Steubenville Winter Conclusion

Despite the absence of significant differences between AIR and CAPs Rats, the Steubenville winter HRV findings provide an opportunity to investigate the influence of a short-term elevation in pollution concentrations on the associations with HRV, which may prove to be a useful technique in future exposure studies. On February 17, ambient PM<sub>2.5</sub> concentrations began exceeding 100µg/m<sup>3</sup> overnight and carried into the first 4 hours of exposure. On that same day, ln(SDNN) in CAPs Rats was significantly lower than during any other time, although no instantaneous difference between AIR and CAPs Rats was identified. Further investigation found significant associations with several constituents that peaked on that day and HRV. The question arose whether or not the pollution episode drove those associations between constituents of PM<sub>2.5</sub> and HRV. By removing the 4-hour block of data from the model, analysis determined that the pollution episode drove many of the associations observed, and that there was indeed a significant reduction in ln(SDNN) of CAPs Rats that significantly associated with pollution concentrations. Therefore, the Steubenville winter intensive supports the notion that even a short-term increase in air pollution can influence the associations with HRV over the two-week period.

Even with the pollution episode, no significant differences were found between AIR and CAPs Rats with any of the observed HRV parameters. It is possible that there needed to be a total threshold within the exposure chamber that was not reached, except during the pollution episode on February 17. When the 4-hour block of high pollution was removed, many of the associated pollutants with HRV were lost. This loss may indicate that a minimal amount of PM<sub>2.5</sub> CAPs needs to be in the chamber, or else even short-term pollution events can influence the overall findings during a two-week animal model. Furthermore, earlier studies showed that the high-resolution data could identify significant changes in HRV that the 8-hour data could not. During this exposure, SEAS and TEOM data did not observe much within-day gradient in mass concentrations and may have been another reason why high-resolution HRV data could not distinguish between AIR and CAPs Rats. Overall, the Steubenville winter study lacked significant differences between AIR and CAPs Rats, and many of the significant associations with

HRV were related to the 4-hour period of elevated pollution concentrations, not an overall trend in air pollution over the two-week exposure.

### **IV.3 Comparing Summer and Winter HRV Findings in Steubenville**

Steubenville experienced significant differences in the composition of  $PM_{2.5}$  during the summer and winter months typical of a Midwestern area influenced by regional secondary  $SO_4^{-2}$  inputs as well as a large agricultural contribution of  $NH_4^+$ . This result was evident in the major ion compositions for both seasonal intensives summarized by the pie charts shown in Figure IV.34. Winter exposures observed a far greater  $NO_3^-$  concentration in the winter. The  $NO_3^-$  composition increased from <2% in the summer to 16% in the winter, due to  $NO_3^-$  binding to  $NH_4^+$  to form  $NH_4NO_3$  particles. Percentages for  $SO_4^{-2}$  were not as different in each season, likely due to the two large coal-fired power plants within 15km north and south of the site. Nevertheless, the mass contribution in the winter was less than half of that found during the summer. These significant changes in the major ion constituents led to significant reductions in aerosol acidity during the winter and therefore less reactivity of trace elements in the atmosphere. Figure I.7 shows that the Steubenville summer intensive was the only study that had a measurable amount of  $H^+$  ion. Therefore, the aerosol acidity could have also influenced the type of particles in the atmosphere between summer and winter conditions.

Solubility may also affect physiological reactions in the cardiopulmonary system. The higher unidentified portion in the summertime was likely attributed to water content. Water content in the winter was also greatly reduced with less relative humidity as water was captured in snow or it remains as ice in the atmosphere. With less moisture in the air, fewer surfaces exist for trace elements to react and form soluble species. Solubility can be significant in this exposure study because particles can become more reactive with biological tissues in the respiratory system, and ultimately effect the cardiopulmonary system.<sup>55</sup> In addition to wind direction changes from shifts in frontal passages, increased wind speeds in the winter may have also influenced the differences in air pollution in Steubenville. Other factors not measured, like seasonal energy demands and other anthropogenic changes in pollution output (i.e. demand from construction for building materials) could also play a significant role in the differences among pollution

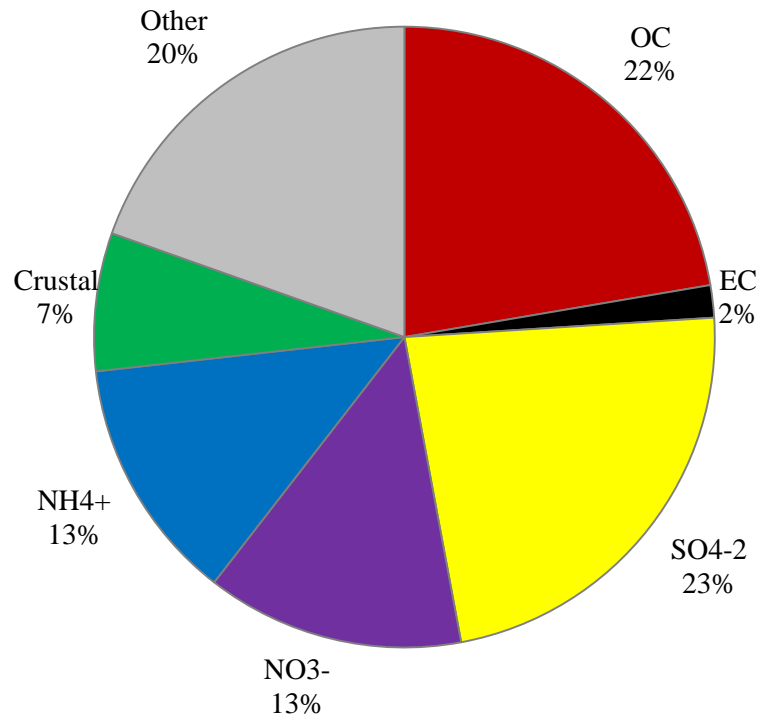
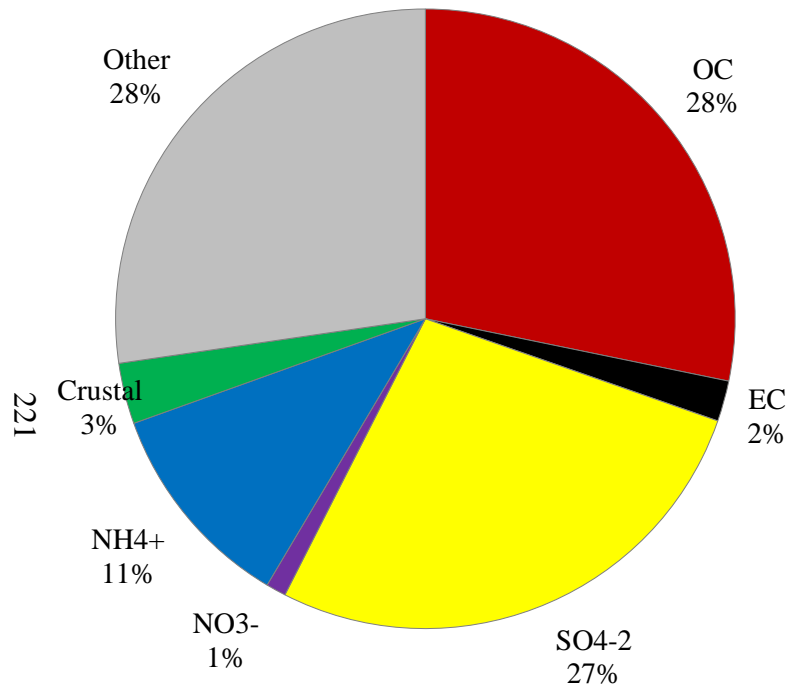
concentrations between summer and winter in Steubenville. Table IV.18 summarizes the 30-minute samples that were observed during each study. Most concentrations are higher in the summer exposure than in the winter.



Figure IV.34 Pie graphs of the PM<sub>2.5</sub> CAPs composition from the Steubenville summer and winter intensives.

(a) Steubenville Summer:  $736.9 \pm 512.1 \mu\text{g}/\text{m}^3$

(b) Steubenville Winter:  $326.1 \pm 271.1 \mu\text{g}/\text{m}^3$



**Table IV.18 Steubenville summer and winter mean concentrations (ng/m<sup>3</sup>) of SEAS trace elements and the total range for each element in each season. (PM<sub>2.5</sub> and EC are in µg/m<sup>3</sup>) The season in bold is to highlight that it has a higher concentration.**

Summer	Mean ± SD	Range	Winter	Mean ± SD	Range
<b>PM</b>	<b>736.9±512.1</b>	<b>(81-2951.0)</b>	PM	326.1±271.1	(49.2-1995.7)
<b>EC</b>	<b>6.36±3.14</b>	<b>(0.79-17.9)</b>	EC	5.69±2.59	(0.043-16.8)
Mg	34.6±37.6	(7.75-144.5)	<b>Mg</b>	<b>43.4±51.1</b>	<b>(9.54-331.3)</b>
Al	30.7±34.4	(6.71-241.8)	<b>Al</b>	<b>37.8±43.5</b>	<b>(9.49-170.7)</b>
<b>P</b>	<b>11.8±13.3</b>	<b>(0.981-47.9)</b>	P	5.04±5.83	(0.971-37.2)
<b>S</b>	<b>3.23±3.56</b>	<b>(0.396-17.1)</b>	S	2.68±3.10	(0.628-16.6)
K	53.9±61.6	(5.48-428.8)	K	56.8±63.1	(22.9-350.2)
Ca	180.8±203.8	(35.9-854.2)	<b>Ca</b>	<b>249.4±279.8</b>	<b>(47.9-1030)</b>
Ti	1.25±1.50	(0.015-17.4)	Ti	0.979±1.16	(0.081-7.38)
<b>V</b>	<b>1.30±1.52</b>	<b>(0.131-10.6)</b>	V	0.930±1.20	(0.093-8.56)
Cr	0.608±0.839	(0.061-21.1)	Cr	0.656±0.881	(0.159-12.75)
Mn	5.09±5.87	(0.763-38.3)	Mn	5.70±6.72	(0.921-30.3)
Fe	48.1±59.4	(8.50-830.7)	Fe	37.6±46.9	(2.61-439.7)
Cu	3.60±4.08	(0.013-32.0)	Cu	3.27±3.75	(0.749-21.2)
Zn	55.9±77.8	(2.16-1407)	Zn	40.4±60.7	(4.07-1176)
As	1.20±1.36	(0.203-6.43)	As	1.05±1.33	(0.114-12.8)
Se	2.41±3.09	(0.302-37.9)	<b>Se</b>	<b>3.78±4.96</b>	<b>(0.229-42.3)</b>
Rb	0.125±0.145	(0.022-0.985)	Rb	0.147±0.176	(0.032-1.25)
Sr	0.624±0.683	(0.112-3.51)	<b>Sr</b>	<b>0.811±0.881</b>	<b>(0.253-2.54)</b>
Mo	1.01±1.18	(0.043-6.26)	<b>Mo</b>	<b>0.324±0.360</b>	<b>(0.053-1.28)</b>
<b>Cd</b>	<b>0.776±0.970</b>	<b>(0.011-7.52)</b>	Cd	0.202±0.249	(0.024-2.27)
<b>Sn</b>	<b>1.19±1.47</b>	<b>(0.104-14.3)</b>	Sn	0.602±0.728	(0.011-5.85)
<b>Sb</b>	<b>1.01±1.15</b>	<b>(0.173-6.89)</b>	Sb	0.562±0.641	(0.086-3.09)
Ba	3.69±3.92	(0.795-10.9)	<b>Ba</b>	<b>5.73±6.39</b>	<b>(0.804-22.9)</b>
La	0.025±0.027	(0.007-0.107)	<b>La</b>	<b>0.046±0.053</b>	<b>(0.005-0.240)</b>
Ce	0.039±0.043	(0.011-0.177)	<b>Ce</b>	<b>0.065±0.077</b>	<b>(0.010-0.816)</b>
<b>Pb</b>	<b>10.4±12.6</b>	<b>(0.513-101.6)</b>	Pb	6.37±8.01	(0.455-72.2)

### Seasonal HRV Comparisons in Steubenville

When observing the percentage changes in ln(SDNN), the most widely accepted time-domain parameter used in HRV analysis, there were several constituents associated with reductions in this HRV parameter in the summer and the winter in Steubenville. In

Figure IV.35, a seasonal comparison of the percent change in HR and HRV are shown. Pollutant concentrations are associated with HR,  $\ln(\text{SDNN})$  and  $\ln(\text{r-MSSD})$  across both studies. HR saw many seasonal differences and multi-directionality with the constituents. In Figure IV.35c, the only trace element found to be significantly associated with HR in the same direction in both seasons was Mo. Summer showed La and Ce (both higher mass in the winter) as well as V and Sb with increased HR. Sb was actually associated with a reduction in HR in the winter and is therefore probably not a driving or influential factor on HR. The same is true for Pb, K and Mg that associated with a reduction in HR in the summer and Mn and Se that also showed a reduction in HR during the winter. Mn and Se were actually higher in concentration in the winter when a reduction was associated with HR.

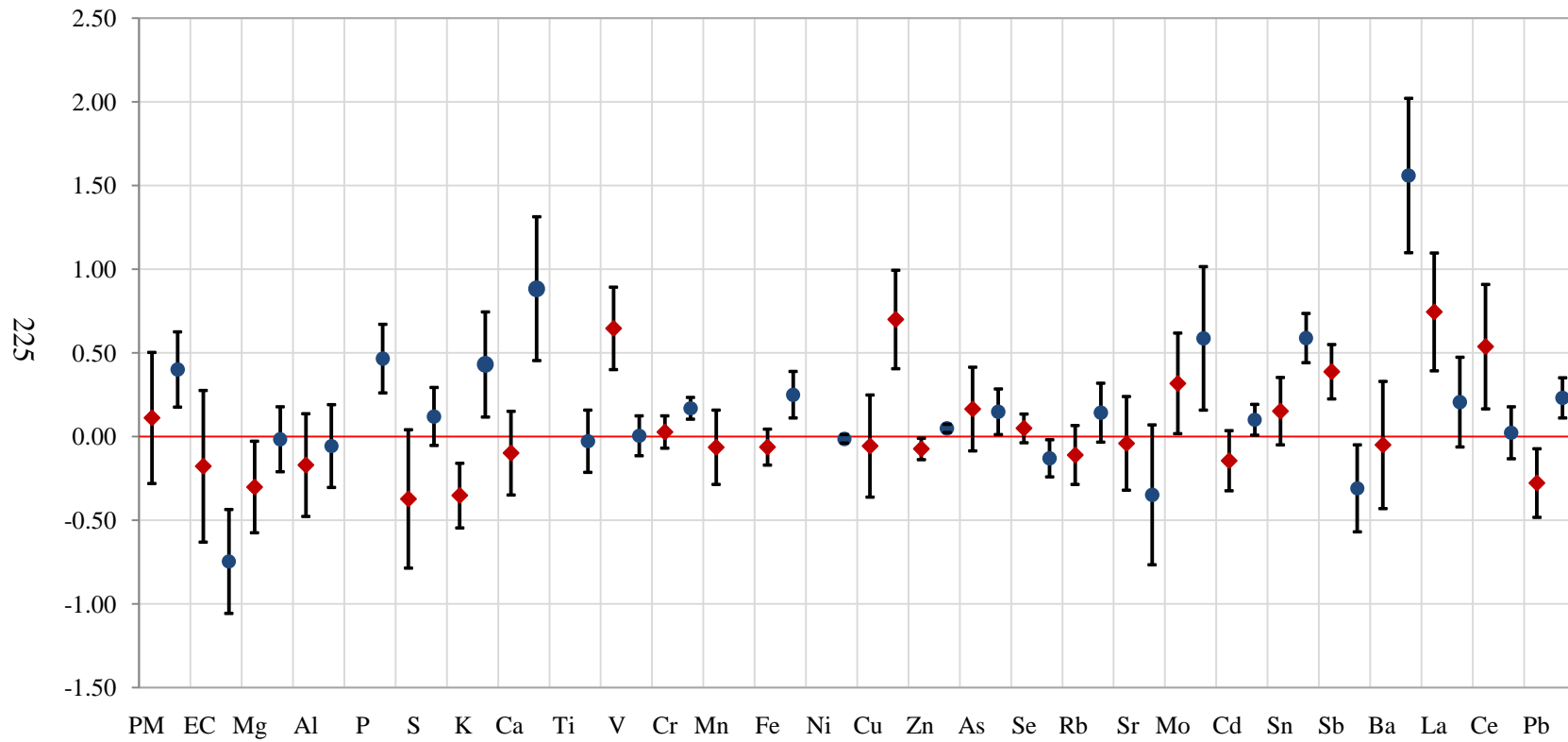
For  $\ln(\text{SDNN})$ , pollutants that were associated with both seasonal intensives were PM, Fe, V, As and Mo. All of these constituents were found to have higher concentrations in the summer than in the winter, which, quite possibly, is the reason that AIR and CAPs Rats are significantly different in the summer but not the winter. Summertime associated air pollutants with  $\ln(\text{SDNN})$  also included Sb and Cd, not found significant during the winter. Both Sb and Cd had higher concentrations in the summer and could also be the reason why summer saw a significant change in HRV and winter did not. Neither seasonal study found any constituents associated with an increase in  $\ln(\text{SDNN})$ .

When comparing the seasonal effect  $\ln(\text{r-MSSD})$  in the summer and winter, there appears to be a significant difference in directionality. In Figure IV35c, it is evident that winter primarily had pollutants associated with a reduction in intensity, (Cr, Sn, PM, P, Cu, Ca and Ba), while summer showed elements associated with an increase in  $\ln(\text{r-MSSD})$ , (Mg, Al, K). Although Mg, Al and K all had significant associations in the summertime, their concentrations were actually higher during the wintertime exposures when they were not associated with a reduction in  $\ln(\text{r-MSSD})$ . Of all the constituents associated with a reduction in  $\ln(\text{r-MSSD})$  in the winter, only Ba, Ca and Cr had higher concentrations in the winter. PM, P, Sn and Cu all had an association, but their concentrations were higher in the summer when no association was identified.

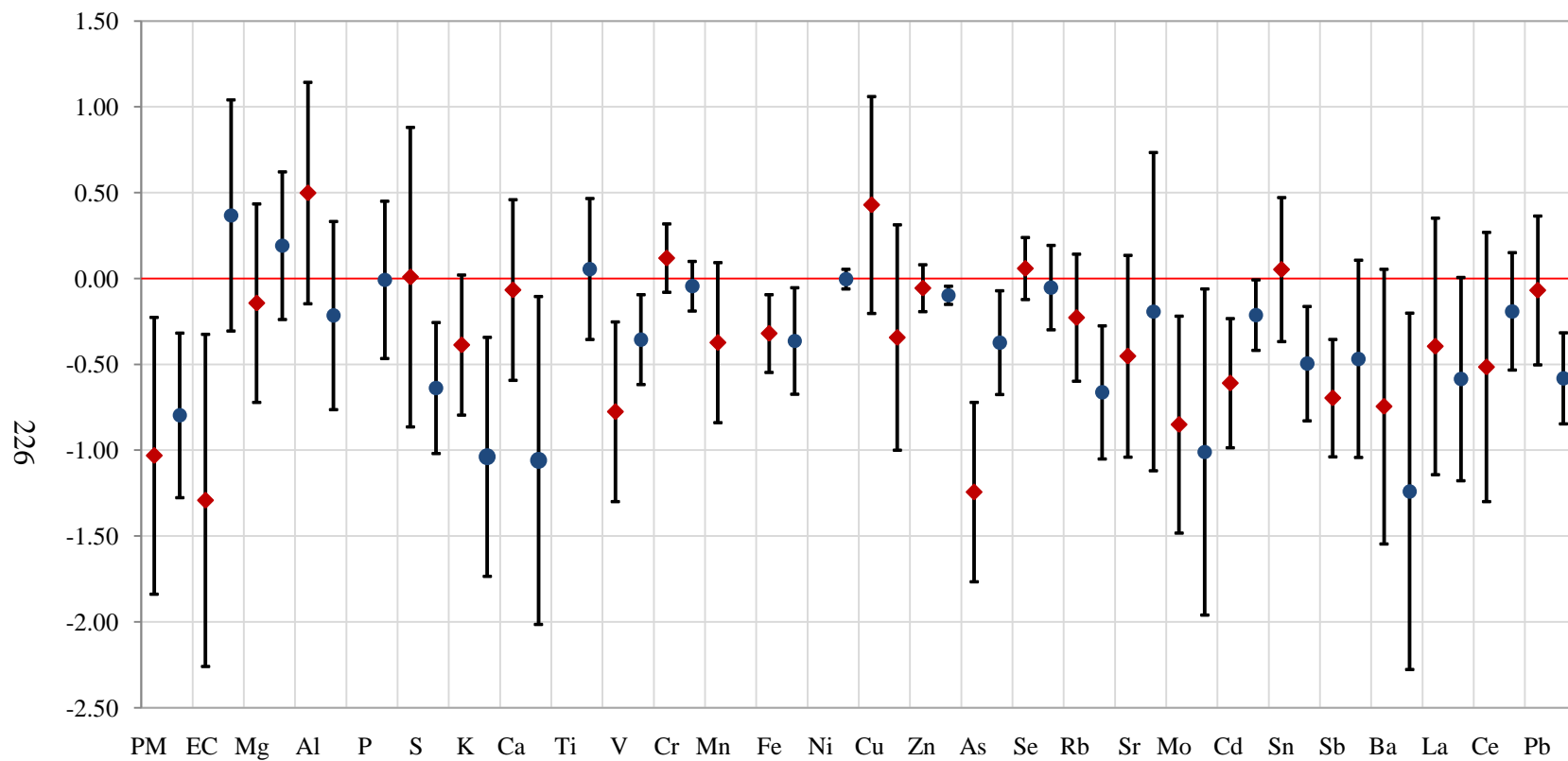
The only interesting note on this observation is that Mn was also found to be associated with an increase in  $\ln(r\text{-MSSD})$  which may mean that Mn is having an opposing effect in relation to the overall general pattern observed in the winter study. The same observation was found in the summer with Mg and K as both were significantly associated with a decrease in HR and an increase in  $\ln(r\text{-MSSD})$ . Although all of these findings are significant associations within a parameter, it is hard to assume that cross-parameter effects were being driven by a sole trace element in opposition to the trend. In fact any sole association would be too loose of an association to make any firm conclusions on the behavior of HRV.

**Figure IV.35 Thirty-minute CI Plots comparing the percent change from the average (a) HR, (b) ln(SDNN) and (c) ln(r-MSSD) for each constituent of PM<sub>2.5</sub> during both Steubenville exposure studies (Summer | Winter).**

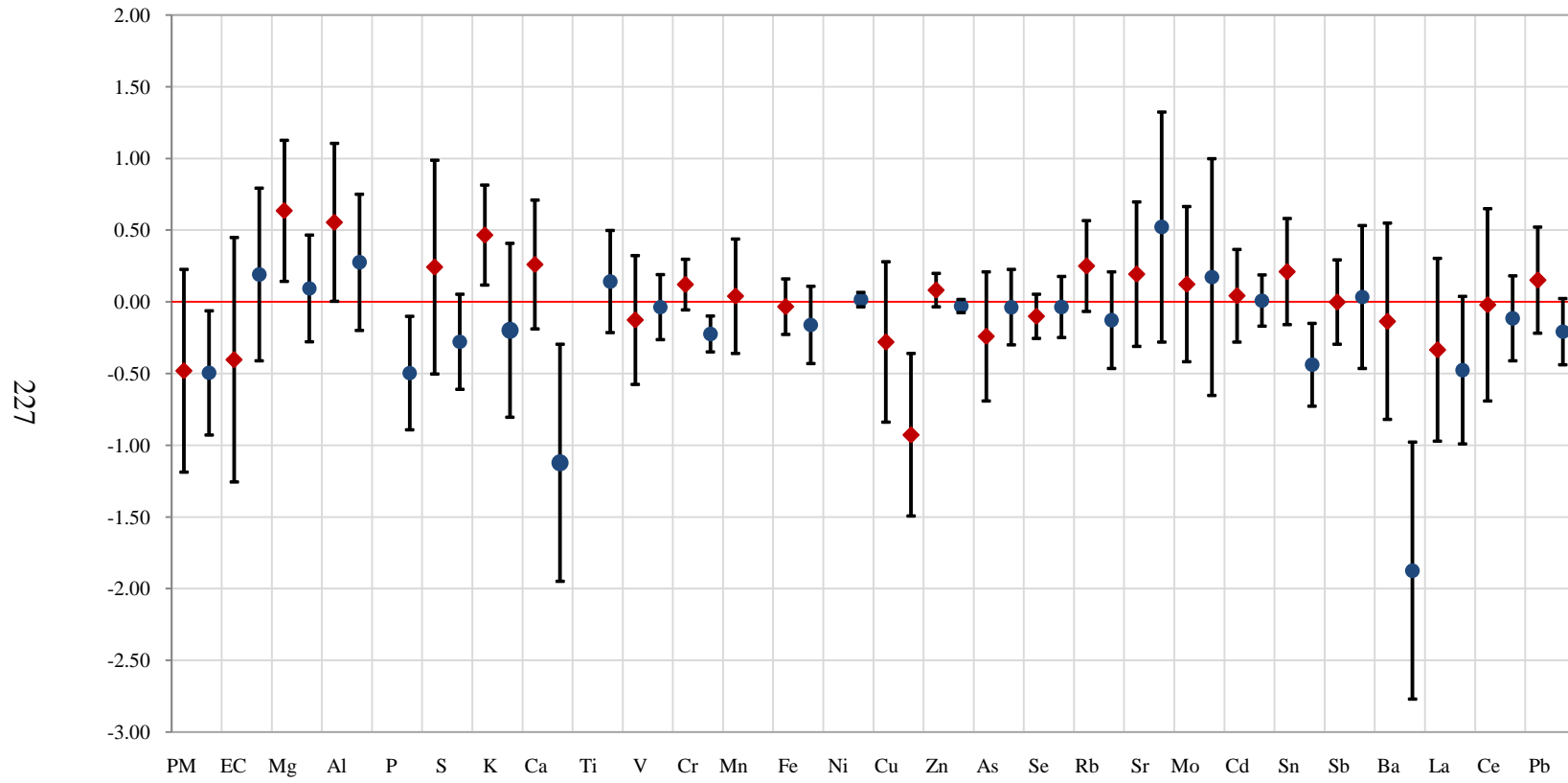
**(a) Steubenville HR**



**(b) Steubenville ln(SDNN)**



(c) Steubenville  $\ln(r\text{-MSSD})$



## **Conclusion**

Thus far, both Detroit and Steubenville have examined individual trace elements and the major constituents of  $PM_{2.5}$  and their association with HRV. It was not always apparent that a higher concentration of a constituent would lead to the associated effect in HRV. In fact, there are several examples that a larger effect estimate or percent reduction in HRV can be attributed to the intensive with a lower average mass concentration. Therefore, the source estimates for the trace elements may provide more specific information that can be related to changes in HRV than when individual constituents were used. An analysis of source contributions may also provide a valuable link to understand site-to-site differences in pollution composition that leads to the variations in the health responses in CAPs-exposed Rats.



## CHAPTER V

### ASSOCIATIONS OF HRV WITH SOURCE CONTRIBUTIONS IN SUMMERTIME EXPOSURES IN DETROIT, MI AND STEUBENVILLE, OH

#### V.1 Introduction

In Chapter III and IV, site and seasonal differences in  $PM_{2.5}$  composition were described, and associations with HRV were determined. For three of the four exposures performed, we found that specific constituents of  $PM_{2.5}$  were more strongly associated to the changes in HRV than  $PM_{2.5}$  mass concentration; the exception was the Detroit summer study where the  $PM_{2.5}$  mass was more strongly related with  $\ln(SDNN)$  in the CAPs Rats. It became apparent from the seasonal results that  $PM_{2.5}$  mass and the mass of constituents did not always determine the strength or the statistical significance of the effect estimate. It appears as though each exposure period presented independently relationships between constituent concentrations and HRV. Findings from Detroit and Steubenville indicate that constituent concentrations were associated with HRV more strongly from one wind direction. Hence, emissions from source contributions may influence the changes in autonomic tone. Receptor-based source apportionment methods, (e.g. PMF), provided an estimate of the mass contributions from specific source factors, in both Detroit and Steubenville, which were then associated with HRV.

#### Constituent Mass and HRV

It was hypothesized that the rats would receive different exposures to  $PM_{2.5}$  in the two sites based upon the differences in source mixtures in these areas. A comparison of the site and seasonal associations for specific constituents with  $\ln(SDNN)$  is given in Table V.1. A Student's t-test was run to determine which season had significantly higher

mass at each site. The table also shows the percent reduction in  $\ln(\text{SDNN})$  during each study. There were three observed outcomes in the data set in terms of how mass of constituents associate with reductions in  $\ln(\text{SDNN})$ : (1) greater seasonal mass led to a greater reduction in  $\ln(\text{SDNN})$ , (2) a significant reductions occurred independent of mass, and (3) a significant reduction in  $\ln(\text{SDNN})$  occurred in the season when lower concentrations were observed. First, it was assumed that higher mass would lead to a greater percent reduction in  $\ln(\text{SDNN})$ . In Detroit,  $\text{PM}_{2.5}$  mass was significantly higher in the summer than in the winter, and  $\ln(\text{SDNN})$  during the summer was significantly associated with PM mass, but not in the winter intensive. In this case, higher  $\text{PM}_{2.5}$  mass did correspond to a significant reduction in  $\ln(\text{SDNN})$ . This was also true for La and Ce. In the Detroit winter study, concentrations of La and Ce were significantly higher than in summer, and both were related to significant reductions in  $\ln(\text{SDNN})$ , larger than those found during the summer. In these three cases, a greater reduction in  $\ln(\text{SDNN})$  was attributed to higher concentrations of PM, La and Ce.

For the second outcome, Sb and As consistently associated with a reduction in HRV across the four seasonal intensives. However, each was significantly associated with a reduction in  $\ln(\text{SDNN})$  in three of the four intensives. The effect estimate for Sb with  $\ln(\text{SDNN})$  was statistically significant during the Detroit summer, Detroit winter, and Steubenville summer exposure studies. The Detroit winter study was the only seasonal intensive in which a significant association with As and  $\ln(\text{SDNN})$  was not observed. Since As concentrations were lowest during the Detroit winter study, a threshold of may have been needed to be achieved for a reduction in  $\ln(\text{SDNN})$  to be significant. However, with only two examples of this outcome, there is insufficient data to suggest that these trace elements will be consistently related to a reduction in  $\ln(\text{SDNN})$ , regardless of the seasonal changes in ambient atmospheric changes or their source.

The most frequent outcome observed in Table V.1 was that higher mass did not correspond with the strength or the significance of the reduction in  $\ln(\text{SDNN})$ . In Detroit, EC was associated with a larger and significant reduction in  $\ln(\text{SDNN})$  in the summer even though EC concentrations were three time greater in the winter than in the summer.

Sr in the winter was significantly higher in Detroit, but the association with  $\ln(\text{SDNN})$  was only significant in the summer. With Ba, neither season in Detroit had a significantly larger mass, but summertime Ba has a 0.77% reduction in  $\ln(\text{SDNN})$  whereas wintertime showed a 0.65 increase in  $\ln(\text{SDNN})$ , although the increase was not statistically significant. Fe in both Detroit and Steubenville was related to a greater, statistically significant reduction in  $\ln(\text{SDNN})$  in the season with the lower concentration of Fe. Multiple examples of this outcome are a strong indication that the effects on HRV are not driven by the concentrations of individual constituents or  $\text{PM}_{2.5}$  mass alone.

From these findings, it is apparent that fine-fraction mass and the concentrations of individual constituents do not completely explain the associations with  $\ln(\text{SDNN})$  across the seasonal intensives. Thus, differences in  $\text{PM}_{2.5}$  composition, atmospheric conditions and chemistry may need to be considered in a real-world model structure to understand the inconsistencies across the seasonal exposure studies. Such a complex model is not within the realm of this thesis; however, using the mass contributions of sources from receptor-based modeling may improve the associations with HRV. Receptor-based modeling would also show that the source of the mass constituents may be more important than the raw mass, potentially explaining the range of findings in Table V.1.

**Table V.1** The average mass and standard deviation for each pollutant during each intensive are shown with the associated percent reduction in ln(SDNN). Season with higher mass are shown in bold, as are significant percent reductions in ln(SDNN). \* indicates concentrations in  $\mu\text{g}/\text{m}^3$ ; all others are in  $\text{ng}/\text{m}^3$ . PM+ indicates that the  $\text{PM}_{2.5}$  mass values presented are from the filter mass.

	DET Summer		DET Winter		STB Summer		STB Winter	
	Mass± Std Dev	% Change	Mass± Std Dev	% Change	Mass± Std Dev	% Change	Mass± Std Dev	% Change
PM+	<b>518±506</b>	<b>-3.04</b>	357±218	-0.04	<b>406±266</b>	<b>-1.03</b>	252±134	<b>-0.80</b>
EC*	1.77±1.19	<b>-2.58</b>	<b>6.20±3.60</b>	-0.48	<b>6.36±3.14</b>	<b>-1.29</b>	5.69±2.59	0.37
Mg	45.1±49.5	<b>-1.74</b>	<b>97.7±110.2</b>	0.51	34.6±37.6	-0.14	<b>43.4±51.1</b>	0.19
Al	16.7±18.6	-0.98	<b>40.9±45.3</b>	0.49	30.7±34.4	0.50	<b>37.8±43.5</b>	-0.22
P	<b>21.2±25.6</b>	-0.27	14.6±17.7	-0.25	<b>11.8±13.3</b>		5.04±5.83	-0.01
S*	<b>1.82±2.11</b>	-0.42	1.27±1.40	-0.43	<b>3.23±3.56</b>	0.01	2.68±3.10	<b>-0.64</b>
K	<b>144.1±234.6</b>	-0.01	67.0±82.9	0.17	53.9±61.6	-0.39	56.8±63.1	<b>-1.04</b>
Ca	240.4±273.3		<b>435.1±505.2</b>	0.50	180.8±203.8	-0.07	<b>249.4±279.8</b>	<b>-1.06</b>
Ti	0.656±0.742	<b>-1.39</b>	<b>1.46±1.69</b>	<b>0.69</b>	1.25±1.50		0.979±1.16	0.05
V	0.525±0.658	-0.01	0.633±0.870	0.07	<b>1.30±1.52</b>	<b>-0.78</b>	0.930±1.20	<b>-0.36</b>
Cr	0.417±0.540	-0.26	0.343±0.394	0.32	0.608±0.839	0.12	0.656±0.881	-0.04
Mn	4.36±4.98	<b>-1.24</b>	<b>6.21±7.22</b>	0.59	5.09±5.87	-0.37		
Fe	44.2±50.3	<b>-2.04</b>	<b>90.9±103.4</b>	0.33	48.1±59.4	<b>-0.32</b>	37.6±46.9	<b>-0.36</b>
Co	<b>0.0705±0.0814</b>	<b>-0.95</b>	0.052±0.061	0.21				
Ni	0.368±0.784	-0.59					1.96±7.47	0.00
Cu	5.07±6.28	-0.23	5.34±7.29	<b>0.22</b>	3.60±4.08	0.43	3.27±3.75	-0.34
Zn	<b>44.9±61.8</b>	<b>-0.24</b>	23.3±25.7	0.28	55.9±77.8	-0.06	40.4±60.7	<b>-0.10</b>
As	<b>0.688±0.802</b>	<b>-1.62</b>	0.361±0.402	-0.16	1.20±1.36	<b>-1.24</b>	1.05±1.33	<b>-0.37</b>
Se	0.708±0.815	<b>-0.86</b>	<b>0.907±1.04</b>	-0.16	2.41±3.09	0.06	<b>3.78±4.96</b>	-0.05
Rb	0.120±0.135	-0.80	<b>0.168±0.194</b>	0.20	0.125±0.145	-0.23	0.147±0.176	<b>-0.66</b>
Sr	1.45±2.11	<b>-1.90</b>	<b>2.31±2.72</b>	0.24	0.624±0.683	-0.45	<b>0.811±0.881</b>	-0.19
Mo	0.545±0.735	0.09	0.659±1.16	0.06	<b>1.01±1.18</b>	<b>-0.85</b>	0.324±0.360	<b>-1.01</b>
Cd	<b>0.222±0.261</b>	-0.47	0.136±0.152	0.25	<b>0.776±0.970</b>	<b>-0.61</b>	0.202±0.249	<b>-0.21</b>
Sn					<b>1.19±1.47</b>	0.05	0.602±0.728	<b>-0.50</b>
Sb	<b>0.922±1.18</b>	<b>-0.58</b>	0.519±0.631	<b>-0.50</b>	<b>1.01±1.15</b>	<b>-0.70</b>	0.562±0.641	-0.47
Ba	5.49±6.27	<b>-0.77</b>	5.82±6.38	0.65	3.69±3.92	-0.75	<b>5.73±6.39</b>	<b>-1.24</b>
La	0.103±0.148	-0.12	<b>0.302±0.393</b>	<b>-0.37</b>	0.025±0.027	-0.40	<b>0.046±0.053</b>	-0.59
Ce	0.0775±0.103	<b>-0.31</b>	<b>0.189±0.237</b>	<b>-0.41</b>	0.039±0.043	-0.52	<b>0.065±0.077</b>	-0.19
Pb	<b>6.22±7.59</b>	<b>-0.56</b>	3.06±3.47	0.30	<b>10.4±12.6</b>	-0.07	6.37±8.01	<b>-0.58</b>

## Source Apportionment Modeling

Thirty-minute trace element data, collected with the SEAS, were used to calculate source factor contributions in Detroit and Steubenville. Positive matrix factorization (PMF) was used to identify trace elements that co-vary, thereby reducing the dimensionality of the dataset from 28 trace elements to six source factors. For example, rather than looking at the concentrations of total Fe on PM<sub>2.5</sub> particles collected in Detroit, PMF determined that more than one source was emitting Fe to the atmosphere; a significant portion of the Fe is from steel production while Fe also was also from motor vehicles. Thus, receptor-modeling results provided a more meaningful dataset for mixed modeling analysis to associate fine mass contributions with HRV.

The following source inter-comparison between Detroit and Steubenville will focus on the summer exposures. PMF model results (Morishita, *et al.*, 2009) determined several “factors” that can then be attributed to a source at each location.<sup>65</sup> These factors were unique to each site based on the chemical mass balance of the constituents.<sup>65</sup> After extensive analysis of the SEAS data in the PMF model, the output was calculated to provide a sum of the fine-fraction mass for each 30-minute sampling period. The PMF model was able to account for 90-95% of the PM<sub>2.5</sub> ambient mass. The normalization of these findings was conducted, as was done for each individual constituent, in order to compare the association with of each factor with HRV.

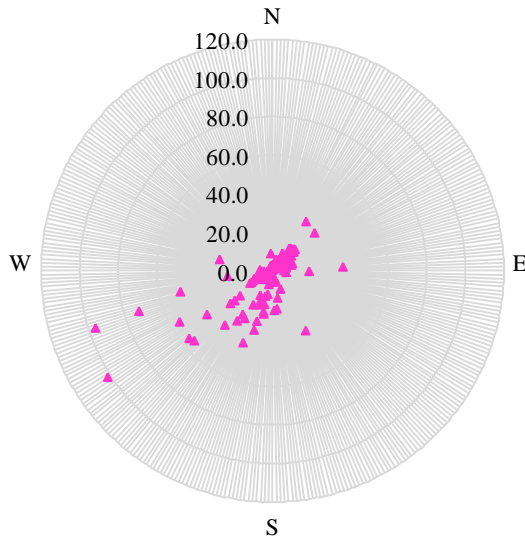
This chapter describes the source influences on HRV by using the same statistical analysis approach discussed in Chapters III and IV. Summertime comparisons between Detroit and Steubenville were made; however, the trace elements that make up a source factor differ from site to site and the sources cannot be assumed to be identical. Therefore, in this study, comparisons can only be used only for descriptive purposes. Also, ambient PM<sub>2.5</sub> mass in Steubenville was larger than that of Detroit (23.1 and 13.9 μg/m<sup>3</sup>, respectively). When looking at the effect estimate plots in Figure IV.5 and IV.6, it is important to note that those values only reflect the mass specifically found during the exposure hours. Further studies would be required to allow for these effect estimates to be absolute (e.g. normalized across studies) to conduct a comprehensive site and seasonal analysis of source contributions.

## V.2 Source Factors in Detroit and Steubenville

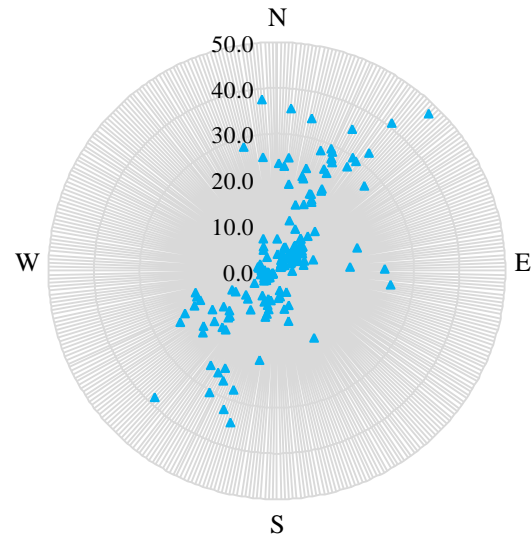
SEAS elemental data from Detroit and Steubenville were analyzed using PMF as described in Morishita *et al.*(2009).<sup>65</sup> In Detroit, PMF results elucidated 6 sources (factors) that contributed to the PM<sub>2.5</sub> mass: (1) Diesel and Motor Vehicle Emissions, (2) Cement Production and Sewage Sludge Incineration, (3) Coal Burning, (4) Metals Processing, (5) Oil Refining and (6) Iron/Steel Production. In Detroit, many of the point sources are in close proximity to each other and thus were in the same upwind direction from the site. PMF could not always differentiate between two sources adjacent to each other such as Cement Production and Sewage Sludge Incinerator. Source factors that were identified by PMF in Steubenville were (1) Coal-Burning, (2) Iron/Steel Production, (3) Metals Processing, (4) Cement Manufacturing, (5) a Lead source, and (6) a Phosphorous source. The Lead and Phosphorus source factors have not yet been assigned to a specific industrial process, but strong candidates is a battery facility known to be SW of the site where we see elevated concentrations of Pb (Figure V.1a). A fertilizer processing facility is known to be NE of the site. When looking at the concentrations of P on a “pollution rose” (Figure V.1b), there are elevated concentrations from the NE direction exceeding 40ng/m<sup>3</sup>, which may be times in which an air shed is carrying P directly from the fertilizer facility.

**Figure V.1 Thirty-minute concentrations of Pb and P in Steubenville by wind direction ( $\text{ng}/\text{m}^3$ ).**

**(a) Elemental Pb**



**(b) Elemental P**



### Site Differences in Source Composition

Three similar source factors were identified in both Detroit and Steubenville: Coal Combustion, Iron/Steel Production and Metals Processing. These factors were identified using specific elemental ratios and source signatures based on previous source apportionment studies. As described earlier, what is referred to as a “Metals Processing” source factor in Detroit was not based on the same trace element ratios that define the “Metals Processing” in Steubenville, due to the fact that different metals are typically being processed in the local smelters. Therefore, this study acknowledges that the two “Metals” are similar, but not identical.

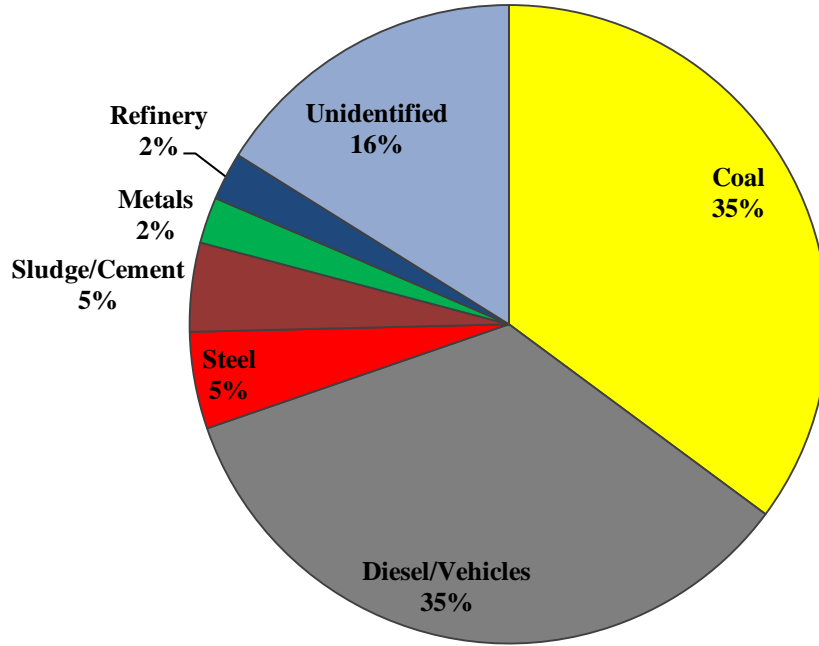
The Regional Coal Combustion factor was estimated to be the largest contributor to the  $\text{PM}_{2.5}$  mass concentrations at both sites, as shown in Figure V.2. Coal combustion accounted for 61% of the fine mass measured during the Steubenville summer intensive ( $14.6 \mu\text{g}/\text{m}^3$ ), whereas Coal Combustion accounted for only 35% ( $4.9 \mu\text{g}/\text{m}^3$ ) of fine mass measured during the Detroit summer study, with Diesel/Motor Vehicle Traffic

contributing 34% of the mass. Iron/Steel Manufacturing in Detroit contributed less than 5% ( $0.68 \mu\text{g}/\text{m}^3$ ); but in Steubenville, this factor was second to Coal Combustion, contributing 17% of the mass ( $3.84 \mu\text{g}/\text{m}^3$ ). The Diesel/Motor Vehicle factor was not identified as a contributor to the fine mass in Steubenville, indicating a distinct contrast in the sources that affected the sites. Metal Processing in Detroit and Steubenville accounted for only 2.3 and 4.4% of the fine mass, respectively. The Detroit analysis also identified Cement/Sewage Sludge Incineration and Oil Refining as two additional factors that influenced the fine-fraction mass during the exposure hours by 4.5 and 2.4%, respectively. The other contributors in Steubenville were the Lead, Phosphorous, and Cement factors contributing to 7.1, 6.3 and 4.5% of the fine mass, respectively.

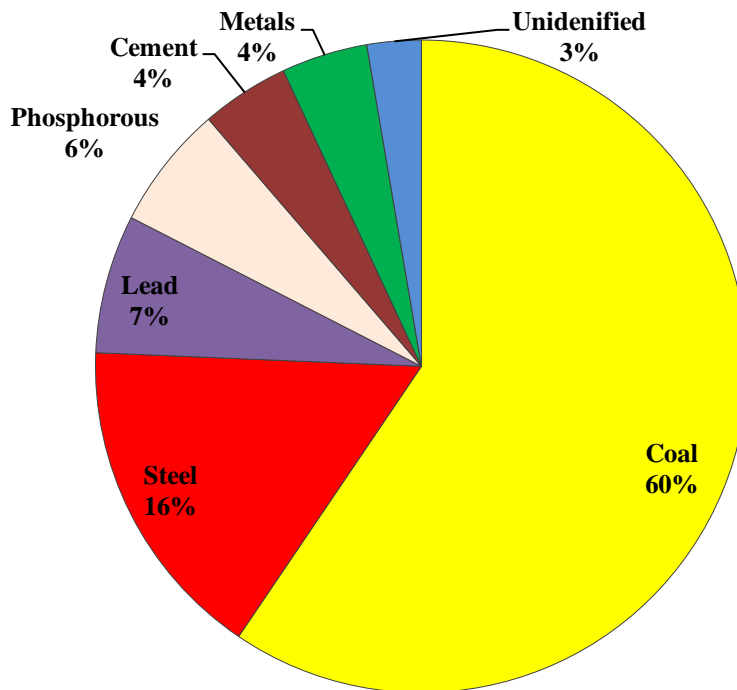


**Figure V.2 Detroit and Steubenville summertime source PM<sub>2.5</sub> mass contributions during exposure hours.**

**(a) Detroit: 13.9±10.9µg/m<sup>3</sup>**



**(b) Steubenville: 23.1±13.7µg/m<sup>3</sup>**



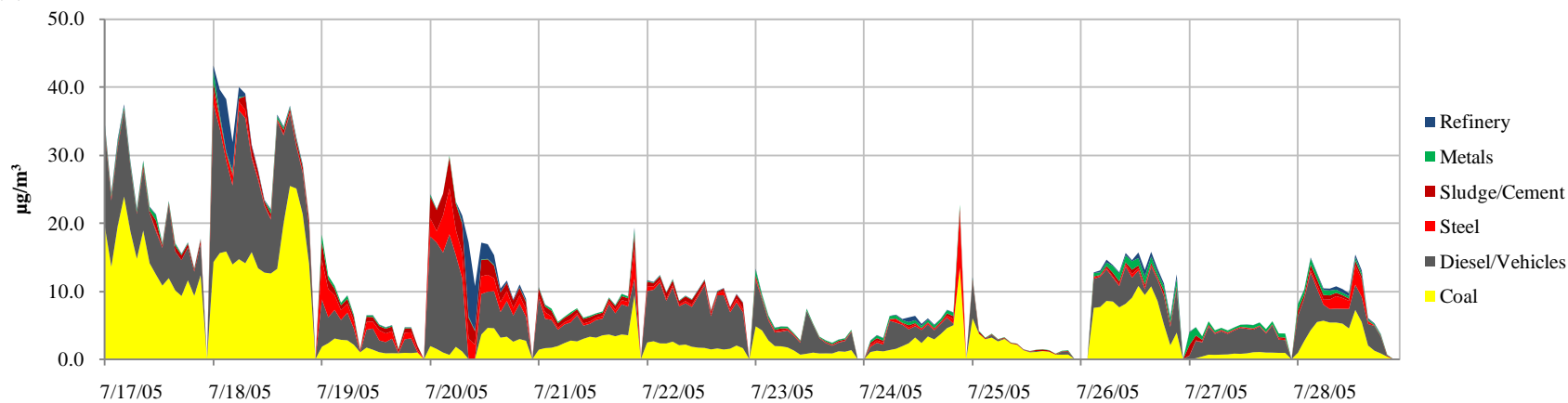
## High-Resolution Observations

One of the advantages of the PMF model was the ability to calculate factor contributions for every sample collected. Figure V.3 shows the source contribution for each 30-minute period during the 13-day exposure. The plot shows how changes in source contributions vary greatly within a daily exposure. In Detroit, results from July 17 provided an example of how the mass of all the contributions co-vary, but on other occasions, as on July 18, the sources that influence the sampling site can change independently and dramatically. While Coal Combustion dominated the mass composition over time, there were intervals where other sources contributed the majority of the PM<sub>2.5</sub>. For example, the Diesel source dominated the fine-fraction mass on the morning of July 20. These findings help support previous conclusions of the importance of high-resolution air pollution data. In Steubenville, Coal contributed even greater than in Detroit and seemed to dominate the PM<sub>2.5</sub> mass composition. Exceptions to this were seen on August 13 when Coal was only a minor contributor and Cement and Metal Processing became dominant sources to the mass.

PMF estimates using the 30-minute trace element data were also used to show how the source contributions change by wind direction. In Figure V.4, the Coal and Iron-Steel contributions in Steubenville are shown as a function of wind direction. The Coal factor was primarily associated with winds from the SW and Iron-Steel Manufacturing is primarily with winds from the NE. Concentrations of S (a tracer for Coal) and Fe (a tracer for Iron/Steel) are also plotted in Figure V.4. Elemental concentrations can often be associated with many wind directions whereas the contribution of Fe, for example, from the iron/steel factor is often related to winds from one or two distinct directions. The analysis suggests that the total amount of Fe, for example, was the sum total of the contributions from several different sources of the element.

**Figure V.3 Thirty-minute PM<sub>2.5</sub> source contributions for exposure hours during the Detroit and Steubenville summer studies.**

**(a) Detroit**



239

**(b) Steubenville**

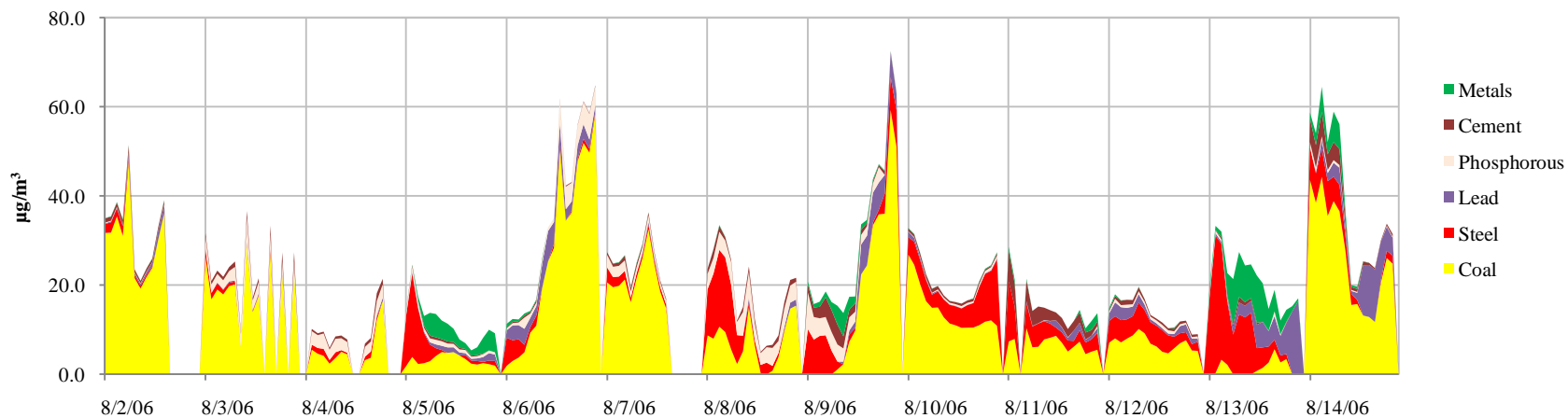
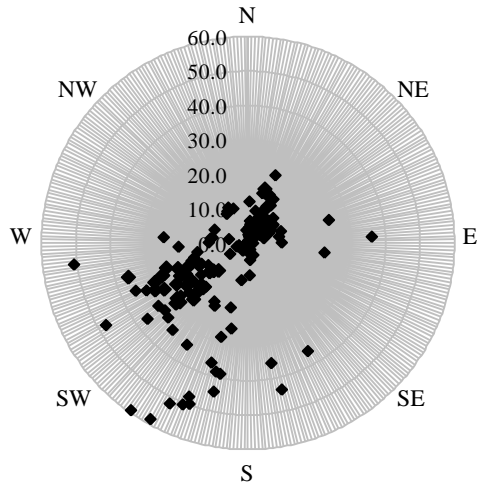
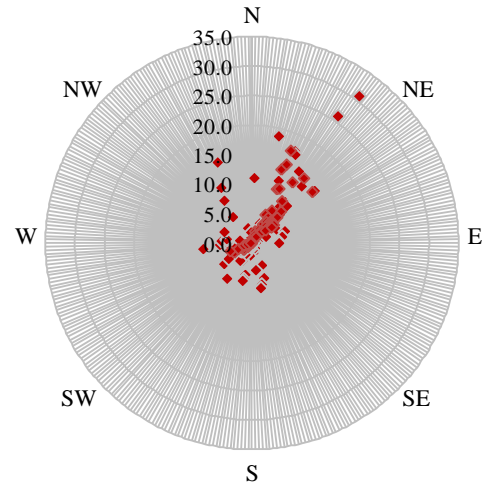


**Figure V.4 Pollution roses for source contributions to Steubenville fine mass using PMF results ( $\mu\text{g}/\text{m}^3$ ) and concentrations of S and Fe ( $\text{ng}/\text{m}^3$ ) from SEAS.**

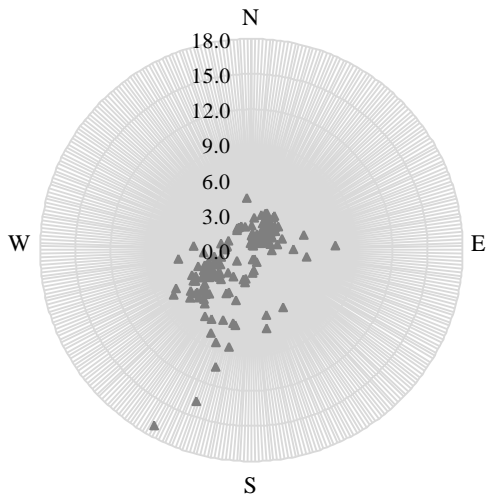
**(a) Coal Factor**



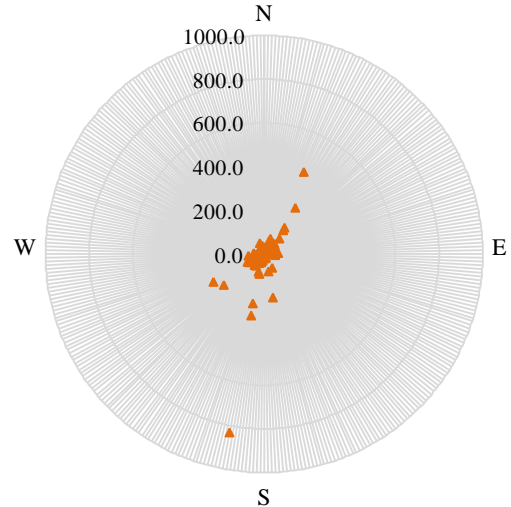
**(b) Iron-Steel Factor**



**(c) Elemental S**



**(d) Elemental Fe**



### **V.3 Source Contributions Associated with HRV**

#### **Detroit**

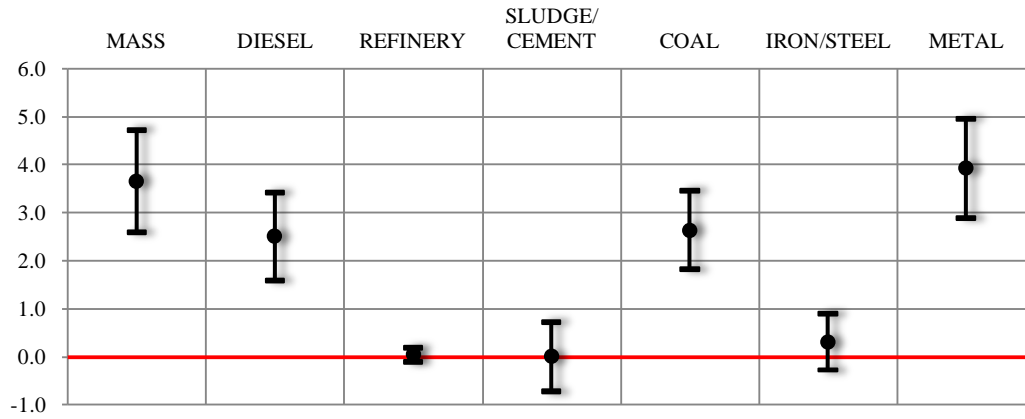
Significant associations between trace elements and HRV during the Detroit summer study provided strong motivation for investigating associations between source contributions and HRV. The normalized source contributions are shown in Figure V.5, displaying the effect estimate each source factor has upon HR and HRV. In Detroit, Metals Processing, Coal Combustion and Diesel/Motor Vehicles all associated with an increase in HR. This was in line with the combined PM<sub>2.5</sub> mass from all the sources (e.g. “Mass”). Metals Processing was more strongly associated to HR than Mass. The associated sources for ln(SDNN) were not consistent with findings for HR. In Figure V.5, it is shown that Diesel/Motor Vehicle, Iron/Steel and Metals Processing were associated with reductions in ln(SDNN), and Diesel was more strongly associated with a reduction in ln(SDNN) than Mass. Furthermore, all the sources, except for the Refinery, were associated with a reduction in ln(r-MSSD). Mass was highly correlated with reduced ln(r-MSSD), however, Metals Processing had a stronger effect estimate than Mass. When considering all the association across HRV parameters, only Diesel and Metals Processing were associated with all three time-domain parameters. Mass was also associated with all the HRV parameters, which is consistent with the findings from Chapter III that mass was more strongly associated to HRV than the constituents. Here again, Mass is highly associated with the indicators of a sympathetic autonomic response.

#### **Steubenville**

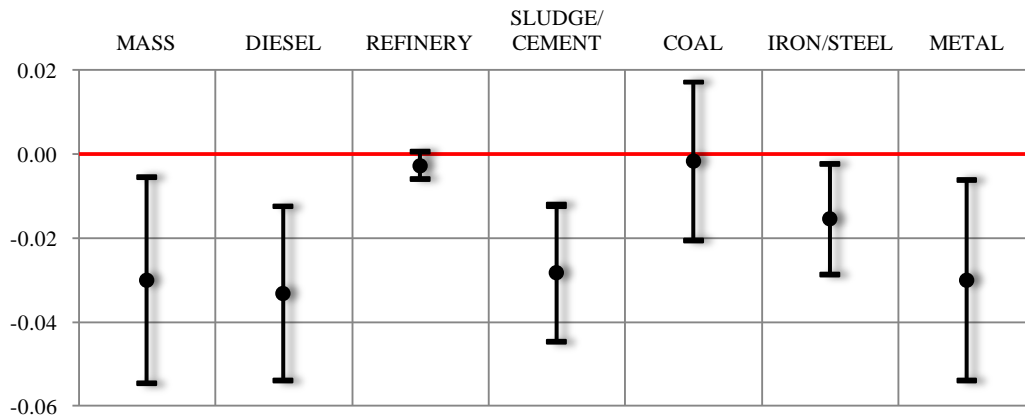
Fewer and weaker significant associations between the HRV parameters and source factors were observed in Steubenville. Mixed modeling results for the source factors in Steubenville were plotted in Figures V.6. Contributions from the Iron/Steel factor were strongly associated with an increase in HR while contributions from Lead were shown to reduce HR. The multi-directional associations with HR and source factors reflect the multi-directionality observed in HR associated with trace elements in Chapter IV. Only Metals Processing was significantly associated with a reduction in ln(SDNN); Phosphorous was significantly associated with an increase in ln(SDNN). Cement and Phosphorous associated with a significant increase in ln(r-MSSD).

**Figure V.5 Detroit confidence intervals of the effect estimate from each identified source for HR and HRV parameters. (msec)**

**(a) HR**



**(b) ln(SDNN)**



**(c) ln(r-MSSD)**

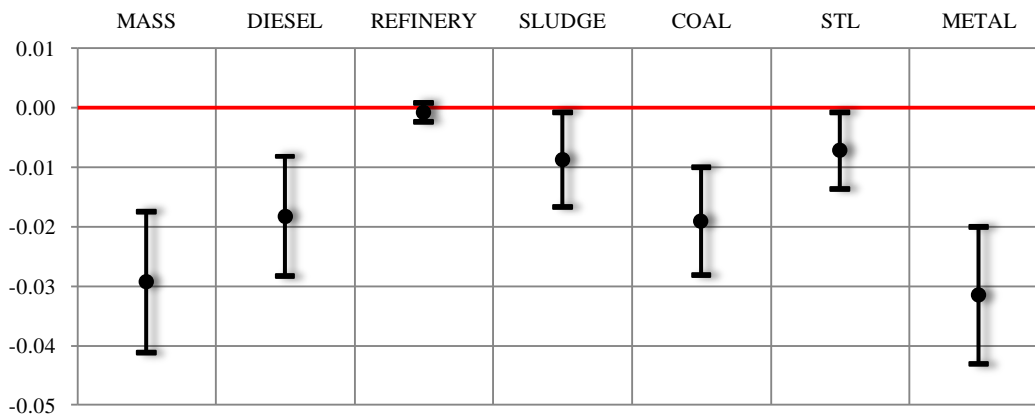
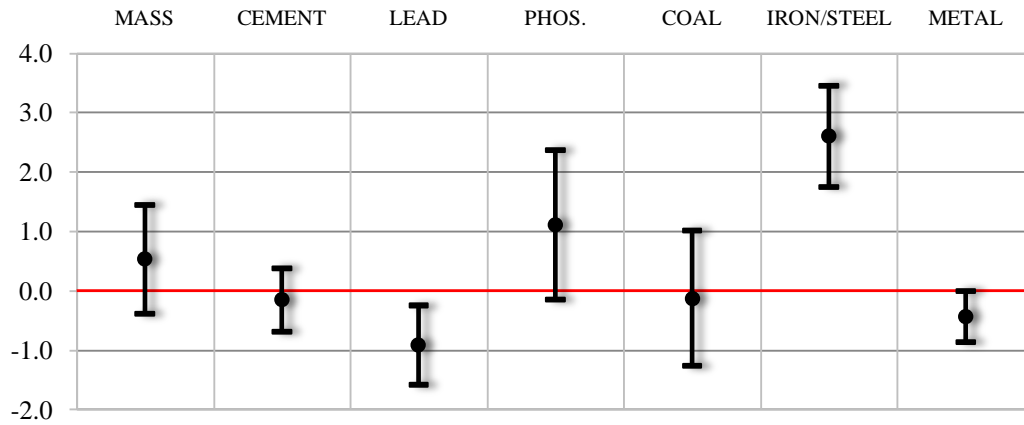
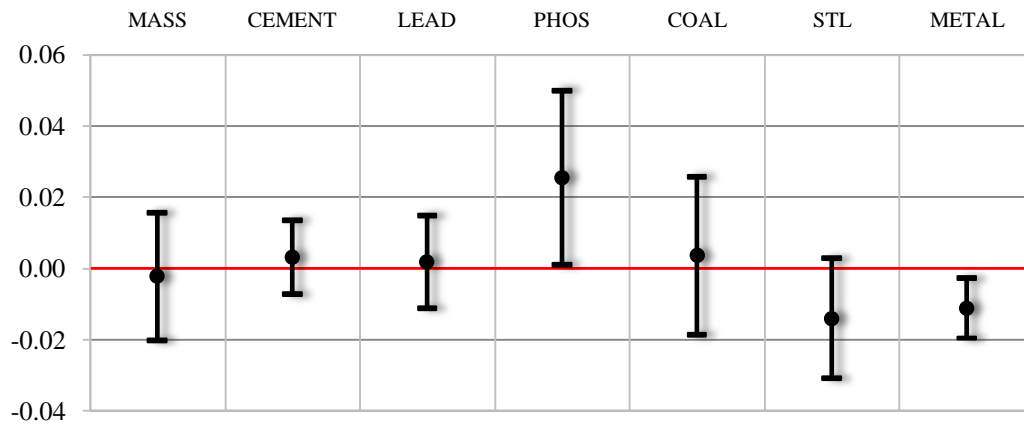


**Figure V.6 Steubenville confidence intervals of the effect estimate from each identified source for HR and HRV parameters. (msec)**

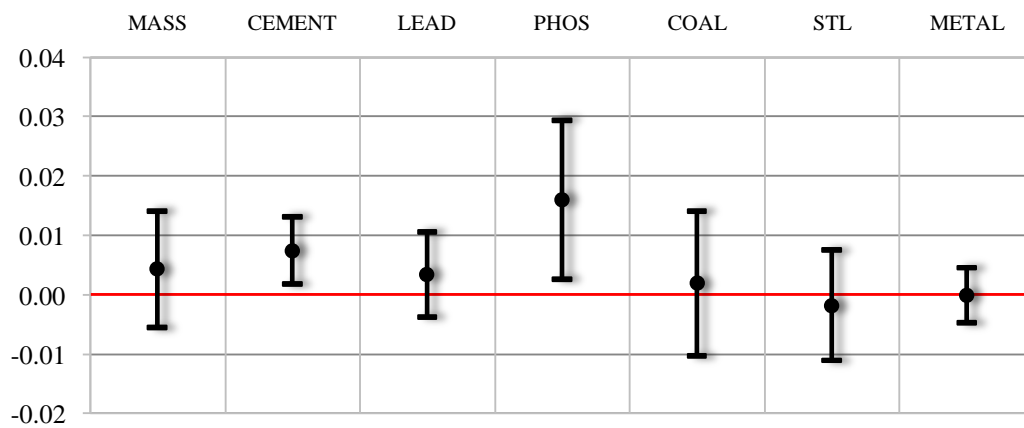
**(a) HR**



**(b) ln(SDNN)**



**(c) ln(r-MSSD)**



#### **V.4 Discussion and Conclusions**

In Detroit, summertime PM<sub>2.5</sub> mass (e.g. “Mass”) was significantly associated with a reduction in ln(SDNN), and may in fact be driving the changes in HRV. Coal Combustion was associated with an increase in HR and a reduction in ln(r-MSSD); there was no association found with ln(SDNN). Rather, Metals Processing and Diesel/Motor Vehicles were associated with a reduction in ln(SDNN) and also had strong association with an increase in HR and a decrease in ln(r-MSSD).

In Steubenville, effects of sources upon HR and HRV were far weaker and fewer than those observed in Detroit. Iron/Steel, attributing to 17% of the mass in Steubenville was the only source that was significantly associated with an increase in HR, but no significant reductions in HRV were found with the estimated contributions from the Iron/Steel source factor. Only the Metals Processing source factor was associated with a reduction in ln(SDNN) but it was not significantly associated with ln(r-MSSD). Cement and Phosphorous source factors were significantly associated with an increase in ln(r-MSSD). Clearly, there was not the same strong percent reduction in HRV in Steubenville as was found with source factors in Detroit. Just as the mass of constituents was not well associated with HRV, so was the mass of source factors in Steubenville.

#### **Site Comparisons**

Cross-study comparisons between Detroit and Steubenville show that the mass from sources that were identified in both locations did not dictate the changes in HRV. For example, Steubenville had four times as much mass from Iron/Steel and three times as much mass from Metals Processing than estimated for Detroit. However, Detroit HRV findings showed stronger percent reductions with these two factors while Steubenville only had negligible associations at best. Diesel in Detroit was also strongly associated with all the HRV parameters. Between Detroit and Steubenville, the percent changes across the HRV parameters appear to be twice as high in Detroit than in Steubenville, even though ambient PM<sub>2.5</sub> mass in Detroit was nearly half of that found in Steubenville during the respective study periods. Not only were the associations stronger in Detroit but there were also far more significant associations with the source factors. Thus the presence of a unique source contribution in Detroit (e.g. Diesel/Motor Vehicles, Sewage



Sludge Incineration) may (1) be most important in influencing the changes in HRV in Detroit, or (2) may cause a synergistic effect with the other sources of PM in Detroit that makes the findings different than those in Steubenville. In future studies, the effects of Diesel/Motor Vehicles and other unique sources could be tested if enough data points can be collected to identify days with high and low Diesel/Motor Vehicle or Sewage Sludge contributions, so that the impact on autonomic tone from each source can be determined.

## CHAPTER VI

### CONCLUSIONS

#### VI.1 Revisiting the Study Objectives

**Objective 1:** Develop a protocol to process and analyze HRV data to determine if and when significant differences in HRV exist between AIR and CAPs-exposed rats.

**Objective 2:** Characterize PM<sub>2.5</sub> constituents between sites and describe seasonal variability within each location based upon atmospheric chemistry and air mass transport.

**Objective 3:** Determine if a relationship exists between HRV in CAPs exposed rats and specific constituents found in concentrated PM<sub>2.5</sub>.

**Objective 4:** Determine if specific PM<sub>2.5</sub> source types are better associated with changes in HRV than PM<sub>2.5</sub> mass alone.

#### **Objective 1 – Comparing AIR and CAPs Rats**

The first objective of this thesis was to develop a protocol to process and analyze HRV data from AIR and CAPs Rats. Extensive analysis was conducted to develop a universal method to statistically eliminate outlying data. These methods are described in Chapter II and can be applied to future studies and subsequent datasets. After raw IBI data was cleaned and processed, then data was available to compare these two groups most appropriately. Although an 8-hour integrated average of rats was used to detect significant changes in HR and HRV parameters, the high-resolution 30-minute dataset allowed for the inclusion of short-term changes in HRV that would otherwise be lost in a single daily average. Therefore, 30-minute HRV data provided a better comparative analysis to determine the statistical differences between AIR and CAPs Rats.

It was determined that ln(SDNN) was significantly different between AIR and CAPs Rats during the Detroit summer study, and HR and ln(r-MSSD) were significantly different between

AIR and CAPs Rats for the Detroit winter study. In Steubenville summer, only HR and  $\ln(\text{SDNN})$  were deemed significantly different between the two groups. No significant differences between AIR and CAPs Rats were identified during the Steubenville winter intensive; however analysis of HRV data did show that there was one morning (February 17) that a short-term, statistically significant reduction in  $\ln(\text{SDNN})$  occurred among the CAPs Rats. This brief but significant reduction in HRV may indicate that in future longitudinal studies, associations can be made with pollution peaks and changes in cardiovascular function.

### **Objective 2 – Characterizing Air Pollution**

The second objective of this study was to characterize and discriminate  $\text{PM}_{2.5}$  composition between two Midwestern sites during two different seasons. Seasonal variability in  $\text{PM}_{2.5}$  mass was evident, with concentrations being higher in the summer at both sites.  $\text{SO}_4^{2-}$  concentrations were greater in the summer with increased photochemistry, whereas  $\text{NO}_3^-$  was higher in the winter, as typically observed in the Midwest. EC concentrations were not significantly different between summer and winter studies at a site, but OC concentrations were significantly higher in the summer at both sites. Higher mass was observed in Steubenville than in Detroit, in both the summer and winter studies.

Detroit and Steubenville were selected for their proximity to major industrial point sources, including coal-fired power plants, metal processing facilities and steel blast furnaces. The Detroit site was impacted by multiple industrial point sources, including waste incineration, sludge incineration and metal processing; however, the strong mobile source contribution was clearly identified by receptor-based modeling as described in Chapter V. Multiple sources were also identified in Steubenville, however, emission contributions were primarily from coal-fired power plants and iron/steel manufacturing. It was shown that Detroit and Steubenville are industrialized areas that share similar seasonal differences in atmospheric chemistry processes, but have different PM composition due to unique source contributions. Consequently, ambient and CAPs analysis of PM composition indicates significant differences between site and between seasons and therefore CAPs Rats were exposed to significantly different  $\text{PM}_{2.5}$  composition during each intensive.

### **Objective 3 – Changes in HRV in Association with Trace Elements**

Chapters III and IV focused on the effects of individual constituents on HRV. Results decidedly showed that 30-minute data was valuable because the high-resolution findings could be

used to identify more subtle changes in HRV that were otherwise masked by averaging HRV over the course of the day. In Detroit, summertime results indicated that 30-minute EC, PM and Fe concentrations were associated with a reduction of  $\ln(\text{SDNN})$ . Winter conditions, with considerably less  $\text{PM}_{2.5}$  mass, showed weak associations with  $\text{PM}_{2.5}$  constituents and HRV. Statistical tests indicated that the associations in the wintertime were not merely the result of lower mass concentrations; but because of seasonal differences in air pollution chemistry.

A few constituents of  $\text{PM}_{2.5}$  in the Steubenville summer study had a stronger association with a reduction in  $\ln(\text{SDNN})$  than  $\text{PM}_{2.5}$  mass; thus, HRV did not appear to be driven by  $\text{PM}_{2.5}$  mass (page 206). Even though Steubenville had higher  $\text{PM}_{2.5}$  mass than found in Detroit, the reduction in  $\ln(\text{SDNN})$  was less than that found in Detroit. This weakened effect was also observed with EC, even though the mean EC concentrations were three times greater in Steubenville than in Detroit. These findings indicate that perhaps  $\text{PM}_{2.5}$  mass and constituent concentrations are not the best determinant for identifying a cardiovascular effect.

#### **Objective 4 – Changes in HRV in Association with Source Contributions**

The final objective was to determine if source contributions more strongly associated with health effects than  $\text{PM}_{2.5}$  mass or the concentration of individual constituents. Mixed modeling results indicated that in both summertime exposure studies, Iron/Steel and Metals Processing were associated with reduced  $\ln(\text{SDNN})$ . Coal was associated with Detroit  $\ln(\text{SDNN})$ , despite the fact that a higher percentage of Coal contributions and a greater amount of mass from Coal was observed in Steubenville. Similarly, the associations with Iron/Steel in Detroit were greater than those observed in Steubenville, even though Steubenville  $\text{PM}_{2.5}$  mass was three times that measured in Detroit. Furthermore, Metals Processing associations were also greater in Detroit. Similar to constituent findings, the mass contributions from source factors cannot be used to estimate the effect upon HRV or determine statistical significance. However, when looking at the differences between the two sites, the Diesel source profile in Detroit stood out as being a large contributor with a strong association with HRV. Therefore, the stronger associations with Iron/Steel and Metals Processing in Detroit could have been caused by a synergistic effect from multiple point sources on HRV. Quite possibly, in the presence of Diesel/Motor Vehicles or Sludge Incineration, a reduction in  $\ln(\text{SDNN})$  an overall greater reduction in  $\ln(\text{SDNN})$  would be observed with Iron-Steel in Detroit than in Steubenville.

This study finds that a difference in source impacts may have varying effects upon HRV, and thus the use of  $\text{PM}_{2.5}$  mass alone may not be the best measure to help reduce the health

impacts upon the cardiovascular system. Findings show that even with greater mass in Steubenville than Detroit, the associated percent reductions were greater in Detroit. Thus, health impacts for each location need to be investigated individually because neither constituents nor sources share the same interactions or percent reductions based on mass alone. The same constituents and sources may not cause the same health effects, as strong contributing factors (e.g. Diesel and Motor Vehicles in Detroit) may greatly influence how other sources interact with HRV.

## **VI.2 Significant Method Developments**

### **HRV Determination**

The initial analysis of HRV required a method development for determination of the appropriate steps necessary to convert raw ECG data into a format that could be used with statistical software. The most challenging component was to determine viable data amongst the large datasets, while also standardizing the techniques such that the same methods could be applied across each data set. In Chapter II, the QA/QC procedure is described in detail, as well as the statistical analysis required to conduct mixed modeling analysis on these data. However, the methods developed in this thesis can be applied in future studies to quickly and reliably determine the acceptable data to include in mixed modeling analysis.

### **Defining a Health Effect**

Another important development through this study was the incorporation of within-group analysis of the CAPs-exposed rats to determine if a significant health effect occurred. In the process of identifying reliable HRV data, it became apparent that the AIR Rats, breathing only to HEPA-filtered air, expressed their own natural fluctuations in HRV. The Least-Squares Means analysis was used to determine if AIR and CAPs Rats were significantly different within each 8-hour (or 30-minute) time period. At times, those differences were determined by a significant change in CAPs Rats; however, the AIR Rats varied in such a way that the more subtle changes in CAPs Rats HRV would not be identified as significantly different. Therefore, statistical tests were conducted on CAPs Rats, independent of the control group. This analysis determined significant changes in HRV do occur within the exposed group. Thus, this study did not rely on AIR versus CAPs Rats alone to state whether a significant health effect occurred. As a result, every HRV parameter was investigated in each season so that trends in the associations with air

pollutants could be explored without the demand of a significant difference from a group of rats that have their own inherent variability.

### **Adopting a Time Scale**

Determining the best dataset to use (8-hour or 30-minute) in these comparative analysis was challenging because the process required an extensive investigation of both HRV data and trace element results. In the end, a consistent pattern was found: 30-minute HRV data revealed intricacies that would otherwise be lost over an 8-hour average. Furthermore, through the introduction of the 30-minute SEAS concentrations of trace elements, this study has gone further than any previous research work on HRV by associating short-term changes in HRV with immediate changes in constituent concentrations. Furthermore, the ability to run PMF on the 30-minute findings and determine the changes in source contributions over the exposure was also ground-breaking in HRV analysis.

### **VI.3 Significant Discoveries**

- (1) Detroit summer findings indicated that  $PM_{2.5}$ , EC and Fe were most strongly associated with a reduction in HRV and an increase in HR, indicating an autonomic response in the cardiovascular system.
- (2) Detroit winter experienced less average mass and health association findings were considerably less profound. However, it was revealed that the differences in atmospheric chemistry are responsible for the seasonal HRV impact differences, not merely reduced mass.
- (3) Significant changes in HRV and significant associations with air pollution varied based upon wind direction during the Steubenville summer study. Statistical analysis revealed that the  $\ln(SDNN)$  from the SW and NE were different, but not statistically significant ( $p=0.0755$ ). Different associations were found with HR,  $\ln(SDNN)$  and  $\ln(r-MSSD)$  depending on wind directions, indicating that different sources impacting a sampling site can affect HR and HRV differently.
- (4) The Steubenville winter study observed the lowest mass concentrations of the four studies, and no significant differences between AIR and CAPs Rats were identified. However, a 4-hour period with elevated concentrations ( $>90\mu\text{g}/\text{m}^3$  of ambient  $PM_{2.5}$  mass), was found to significantly affect HRV and may have been responsible for the significant associations with

constituents. This may be a useful finding when developing future high-resolution HRV studies that capture multiple occurrences of short-term health effects.

- (5) The Iron/Steel Manufacturing and Metals Processing source factors contributed more to PM<sub>2.5</sub> mass in Steubenville than Detroit; however, there were stronger associations of these factors with HRV in Detroit. There may potentially be an additive or synergistic effect of Diesel or other sources in Detroit that enhance the associations with all sources.

#### **VI.4 Comparisons with Other HRV Studies**

In Chapter I, several studies were discussed that monitored a reduction in HRV with ambient air pollution, but very few have characterized the constituents of air pollution to determine which components are most associated with the changes in HRV. These findings will be discussed here in relation to the findings in this study. Murata *et al.* (1991) found that workers had a reduction in HRV in association with Pb, Zn and Cu.<sup>69</sup> Lippmann *et al.* (2006) reported that Ni was associated with changes in HRV in mice, and that Ni and V were both associated with increased risk of mortality in subjects who are part of the National Mortality and Morbidity Air Pollution Study (NMMAPS).<sup>70</sup> Magari *et al.* (2001) determined the opposite response in boilermakers, that in the presence of Ni and V, SDNN was increased without a lag. Thus, there are mixed results, but clear indications that specific trace elements can be associated with HRV.<sup>71</sup>

In the Detroit summer study, Ni was associated with a reduction in ln(r-MSSD) and an increase in HR. Cu was associated with an increase in HR and reduction in ln(r-MSSD). V was also identified in Detroit to increase HR and Mn was associated with a reduction in both ln(SDNN) and ln(r-MSSD). However, it was found in the Detroit study that PM<sub>2.5</sub>, EC and Fe were most associated with HR, ln(SDNN) and ln(r-MSSD). Other constituents that were significantly associated with all three parameters were Sr, Mg, U, As, Ca, Ti, Sm, Co, Se, Ba and Sb. In Steubenville, V was associated with a reduction in ln(SDNN) during both the summer and winter intensives. V also was associated with an increase in HR during the summer. Pb was associated with a decrease in HR in the summer and an increase in HR in the winter. Therefore, these findings show some semblance to the observations found in previous studies, as well as identify several more constituents that are significantly associated with the changes in HRV.

## **VI.5 Study Limitations and Future Advances in HRV Research**

Conducting an exposure study on rats in the field with real-world pollution presented incredible challenges in data collection and processing that, if corrected, could provide a more robust and meaningful dataset. The main challenges with the HRV data were that (1) the AIR Rats had their own natural variability, (2) short intervals did not produce a continuous stream of uninterrupted data, and (3) the two-week study did not capture a large number of air pollution events.

### **AIR Rats**

The most challenging pattern found in this study was that AIR Rats, designated as the controls, had their own natural variability. Therefore, it was difficult to distinguish between the two groups since both exhibited simultaneous changes in HRV. The LS Means approach helped detect changes within the CAPs Rats, independent of the AIR Rats. This way, the possibility of subtle changes in the HRV of CAPs Rats could be identified even if the two groups were not statistically different from each other.

Most health effects studies require a control group . If this study were to be repeated, it would be helpful to use the CAPs Rats as their own control for a period of time to observe a baseline in the day-to-day variability in each CAPs-exposed rat. This would establish that during non-exposure periods, AIR and CAPs Rats are not significantly different, and ensure that the variability from day-to-day in CAPs-exposed rats is not significantly different. Also, to implement a day of non-exposure in the middle of the study to provide another measure of control. For example, CAPs Rats can be placed in the exposure chamber but only breathe HEPA-filtered air rather than ambient air.

### **ECG Sampling Duration**

Continuous IBI data over a short duration of time is critical to determine HRV parameters, especially spectral analysis. For human studies, the sampling interval for HRV is commonly a 5-minute reading every hour. This was translated to rats to be 30 second reading every 5 or 6 minutes. From observations of SH rat ECG data, with preliminary data using 10-second, 30-second and 60-second data, the longer dataset is better for the robustness of the data. Anything shorter cut off possible low-resolution oscillations in the dataset, thus affecting spectral



analysis results. For future studies, a 60-second recording of continuous IBI every 10 minutes is recommended as more comprehensive collection of HRV data. This would be especially advantageous as air pollution data and SEAS samples can be measured over 30-minute intervals. This longer 60 second sampling duration would reduce the amount of compromised data due to lost or broken ECG signals.

### **Sampling Times**

It was determined in this study that the first 60 minutes of sampling greatly affected the HR of AIR and CAPs Rats because of recent handling, and that the rats are still awake when first put in the chambers. The unfortunate part of this finding is that the levels of air pollution in the early morning are often at their highest due to atmospheric processes that occur with the sunrise (i.e. lower boundary layer) producing elevated PM<sub>2.5</sub> concentrations. It is logistically difficult to start running a study 60-90 minutes prior to sunrise, especially in the summertime in the Midwestern states when sunrise is at 6AM EDT. Furthermore, the 7am to 3pm sampling duration captures a working day for most Americans, missing the major traffic contributions that starts prior to 6 in the morning and extends beyond 6 in the evening. What's more, changes in power demand will influence emissions as power plants are affected by load. Another possible effect that may have been missed, based on anecdotal information, are nighttime emissions increases, when plumes are not visible to the population. This was observed first-hand in Steubenville when the odors from the coke ovens, and roller coating were extremely pungent at night and carried on into the morning. This practice would be compounded overnight with a lower boundary layer preventing dispersion into the atmosphere. Therefore, overnight sampling and exposures would help to capture a true exposure of the populations at both locations.

Continuous ambient air monitoring shows significant diurnal and weekly changes in pollution emissions would be lost without a comprehensive air sampling and exposure regimen to produce a true real-world exposure. Nevertheless, there are equipment limitations to running an animal exposure, 24-hours a day. Future advances in concentrator design and operation may allow for the instruments to be unsupervised to capture overnight exposures to CAPs. An unsupervised concentrator would require a programmable sensor feedback that would pause the system if a clog occurred, as identified by a significant change in stage pressure. The concentrator would remain paused until personnel were available for maintenance. If sampling was continuous for 24-hours a day, a 2-3 hour pause in the system over two-week exposures

would not likely disturb the dataset. This would also require a new exposure chamber design that would allow the animals to be exposed continuously by having free access to food and water, and on-call staff available 24-hours a day. Additionally, the facility would need to be located on grounds that were accessible 24-hours a day without also being a public noise nuisance.

### **Study Duration**

These studies lasted nearly two weeks, enough time in Michigan and Ohio to observe some precipitation, considerable changes in temperature from one day to the next, as well as several wind patterns. Yet, when looking at 30-minute data, a peak was rare in a constituent concentration. Without multiple occurrences, the immediate (or lagged) health impacts due to a peak in concentration of a pollutant cannot yet be defined. Future studies that capture multiple peaks may produce a dataset that would provide a valuable type of analysis. Although a variety of meteorological conditions were captured over the two week period, the four seasonal studies were not long enough for peaks from a variety of unique sources to impact the receptor site. Even if the study was drawn out longer, there would be no guarantee that more peaks in concentrations would occur. However, longer study duration would perhaps capture more subtle changes in concentrations of pollutants that could be aligned with HRV to cause the CI Plots to show narrower ranges in the confidence interval for each element, if in fact a true association existed. This would also correct for a change in HRV being falsely attributed to a  $PM_{2.5}$  constituent due to an unusual spike in concentration. Based on the number of peaks that were observed, a four to six week exposure period is suggested.

### **Concluding Remarks**

The findings discussed in this thesis are extensive and profound, and have not yet been published in current scientific literature. The integrated approach of an in-the-field exposure study, alongside state-of-the-art particulate sampling techniques, provided a comprehensive analysis of site and seasonal differences on the source contributions to  $PM_{2.5}$  and how those differences influenced HRV. Ultimately, the goal of any environmental health study is to aid in drafting health standards that can better protect the public. The findings in this thesis will hopefully advance the scientific knowledge required to discover the most adverse pollutants in our atmosphere and help understand the mechanisms by which these pollutants affect human health.

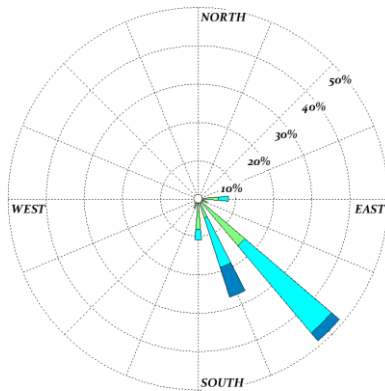
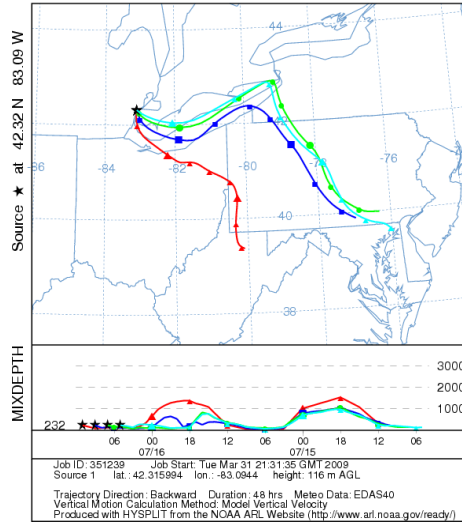
## **APPENDICES**

**APPENDIX A.1**

**BACKWARD WIND TRAJECTORIES (HYPSLIT) AND SURFACE WIND  
ROSES FOR EVERY 8-HOUR EXPOSURE PERIOD IN DETROIT DURING  
THE SUMMER AND WINTER INTENSIVES.**

Detroit: 7/16/05 (Left Rose: 7:00-10:00, Right Rose: 10:00-15:00)

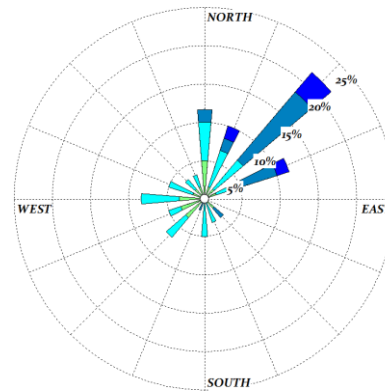
NOAA HYSPLIT MODEL  
 Backward trajectories ending at 1100 UTC 16 Jul 05  
 EDAS Meteorological Data



WIND SPEED  
 (m/s)

- ≥ 3.5
- 3.0 - 3.5
- 2.5 - 3.0
- 2.0 - 2.5
- 1.5 - 2.0
- 1.0 - 1.5
- 0.5 - 1.0

Calms: 0.00%

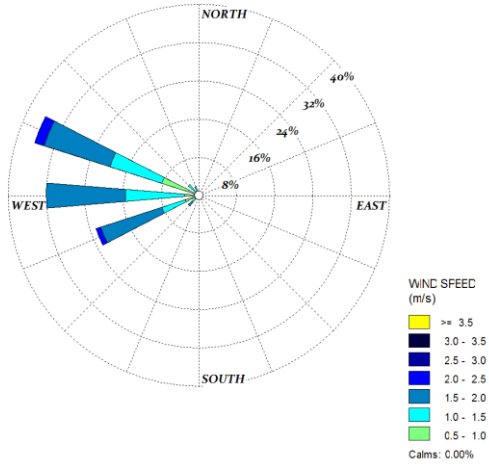
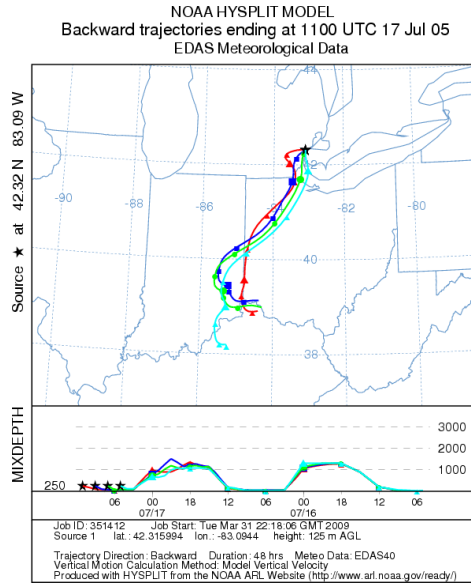


WIND SPEED  
 (m/s)

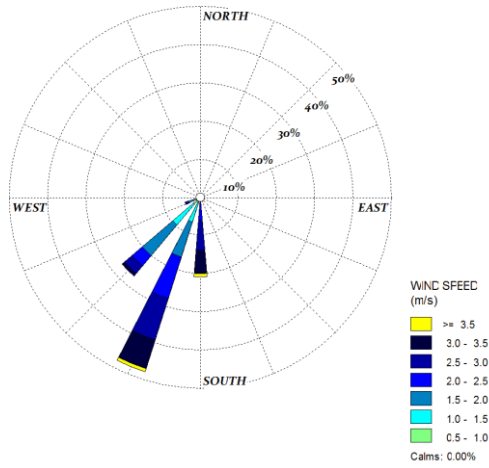
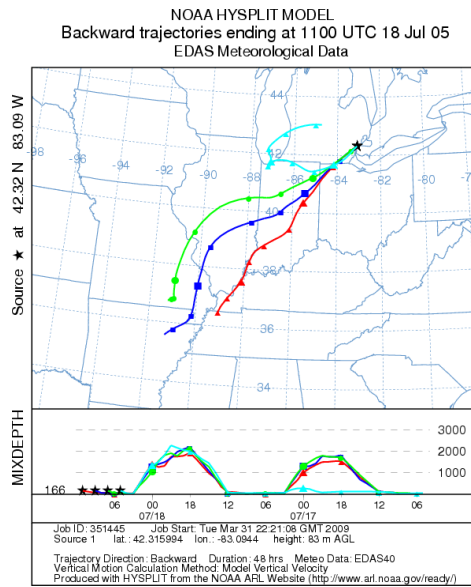
- ≥ 3.5
- 3.0 - 3.5
- 2.5 - 3.0
- 2.0 - 2.5
- 1.5 - 2.0
- 1.0 - 1.5
- 0.5 - 1.0

Calms: 0.00%

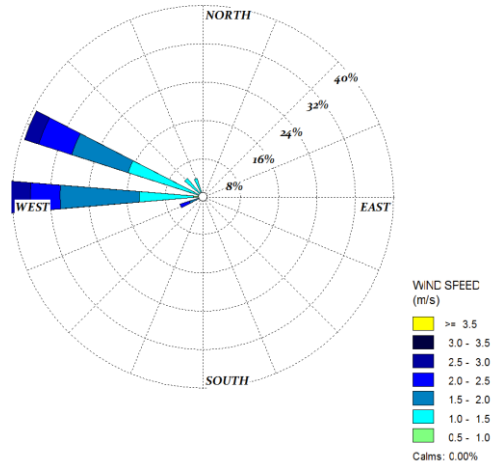
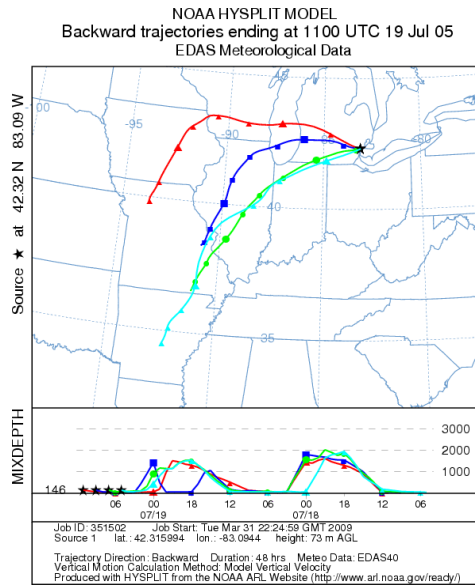
Detroit: 7/17/05



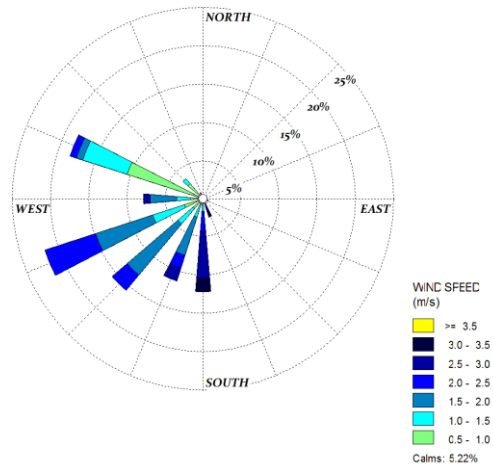
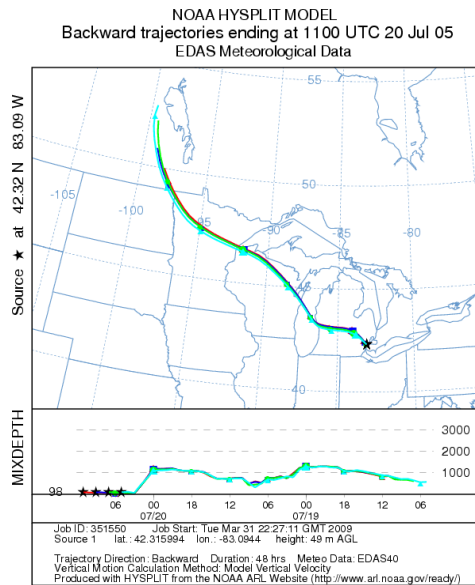
Detroit: 7/18/05



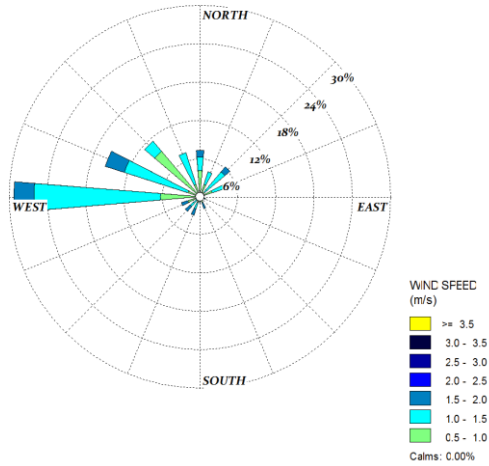
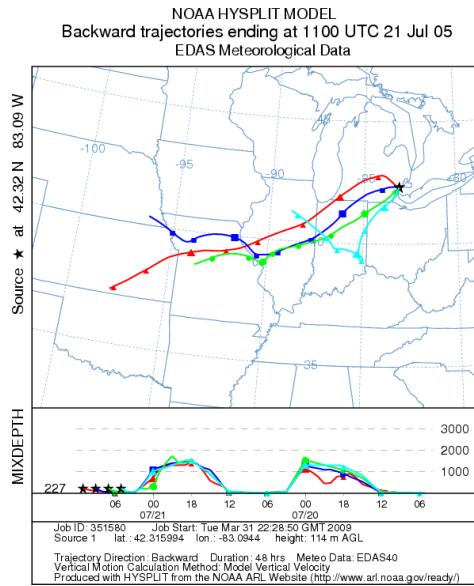
Detroit: 7/19/05



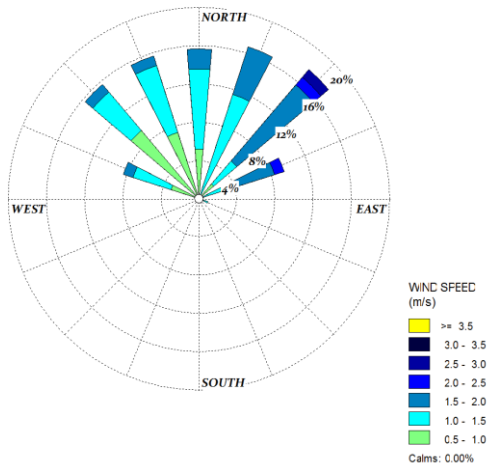
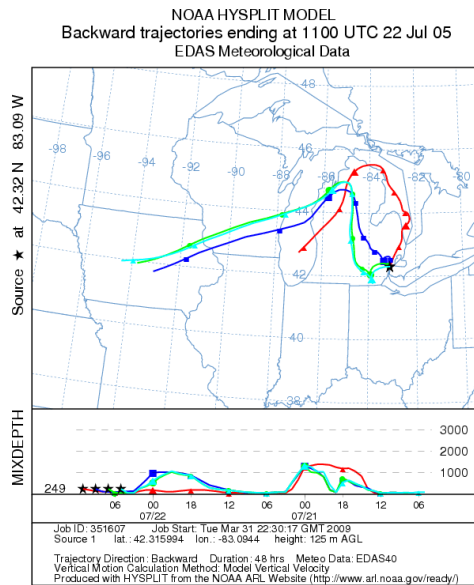
Detroit: 7/20/05



Detroit: 7/21/05

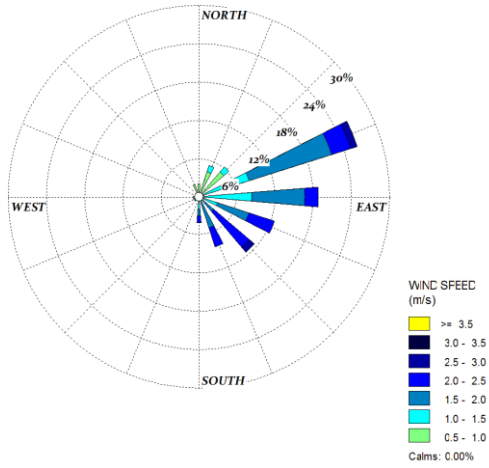
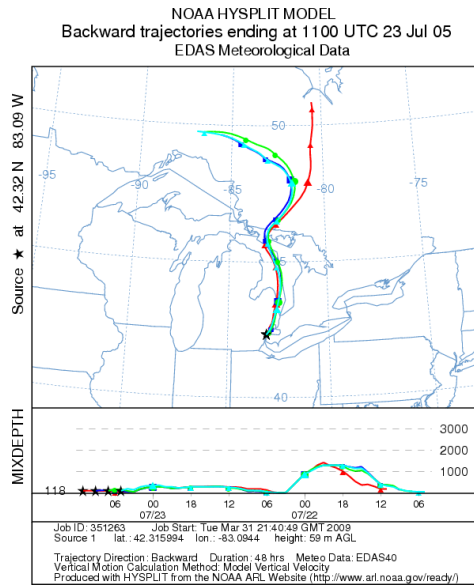


Detroit: 7/22/05

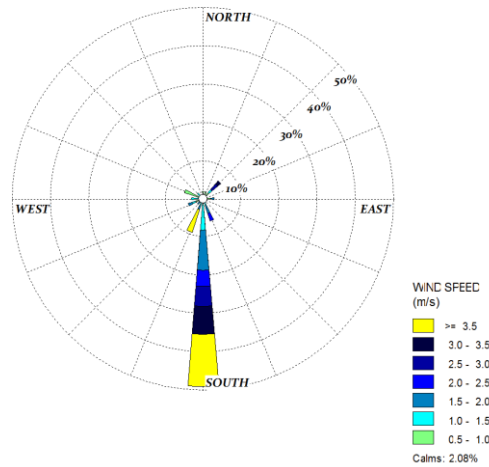
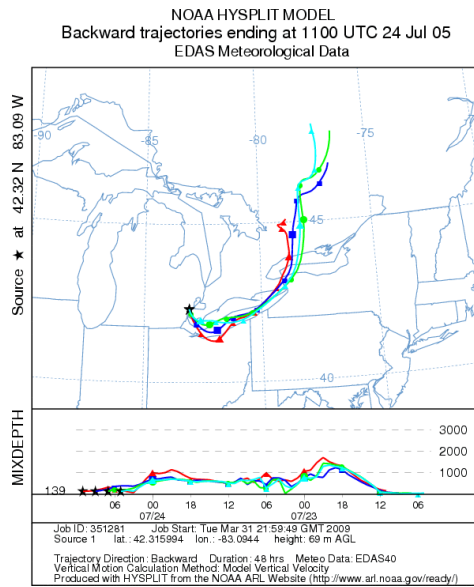




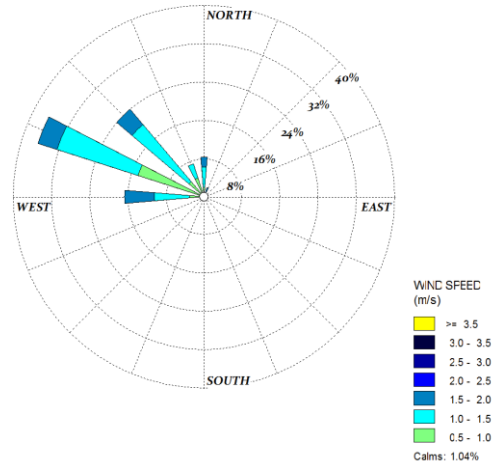
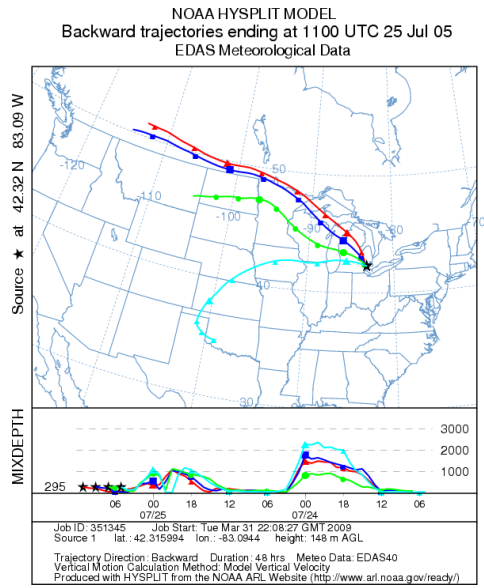
Detroit: 7/23/05



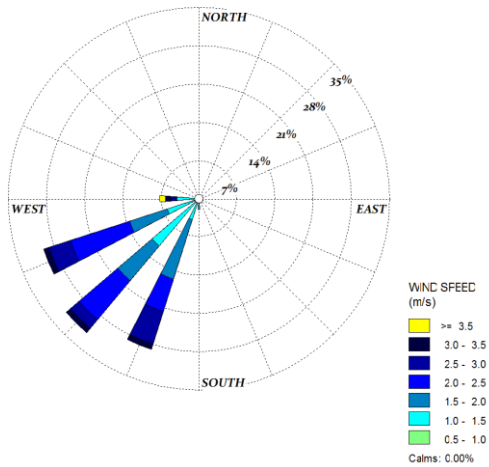
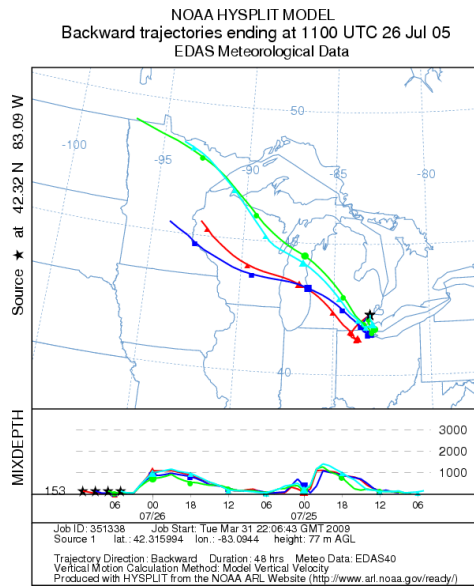
Detroit: 7/24/05



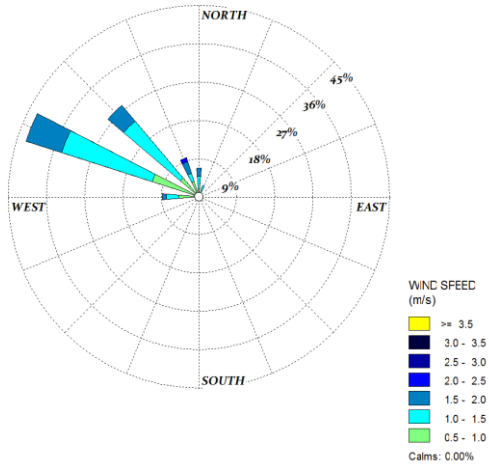
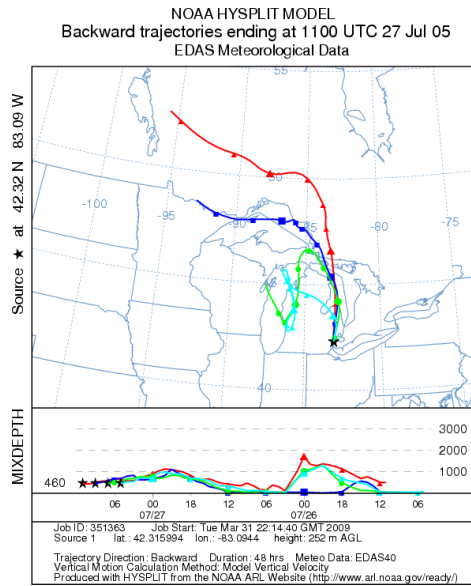
Detroit: 7/25/05



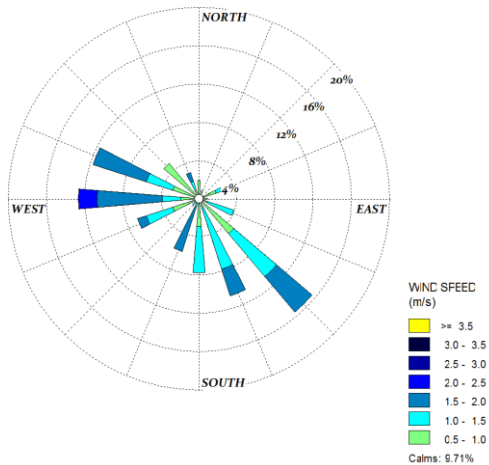
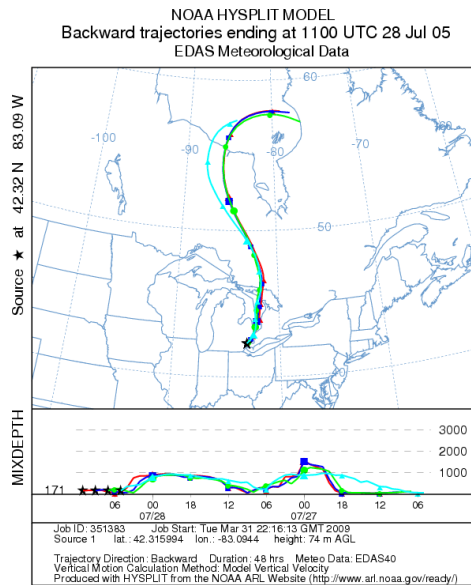
Detroit: 7/26/05



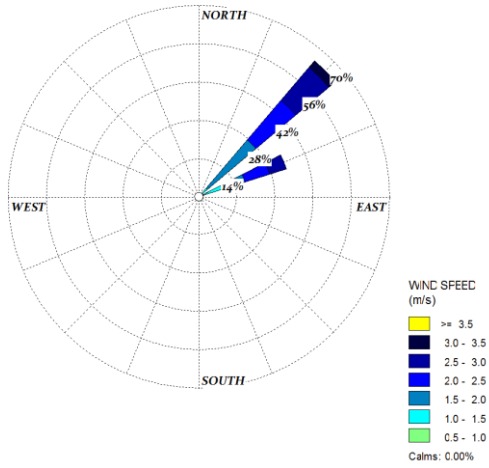
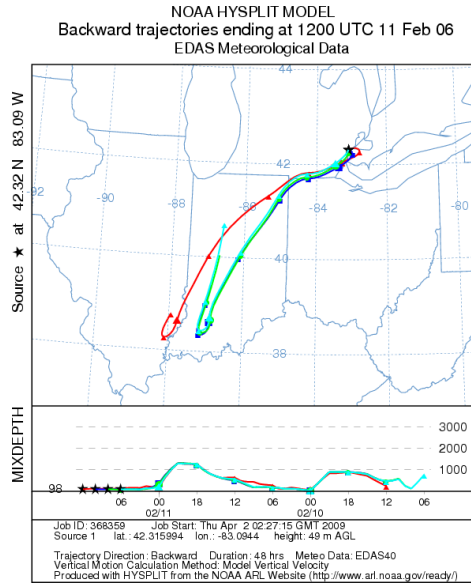
Detroit: 7/27/05



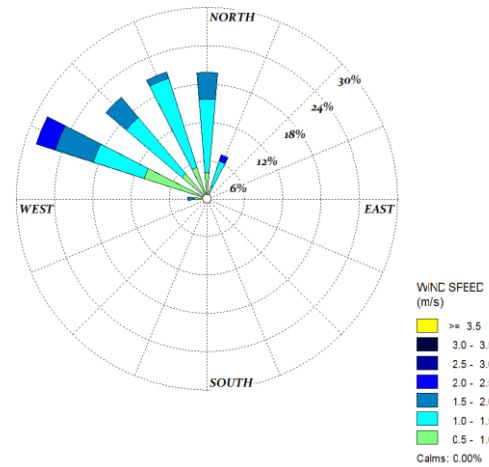
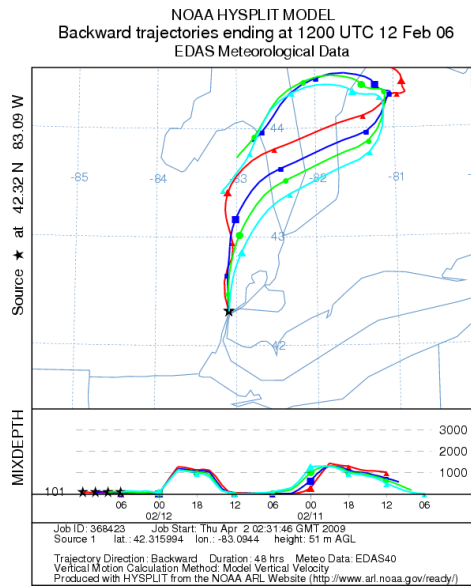
Detroit: 7/28/05



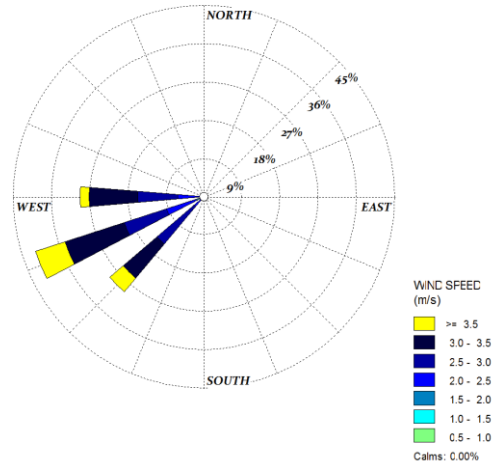
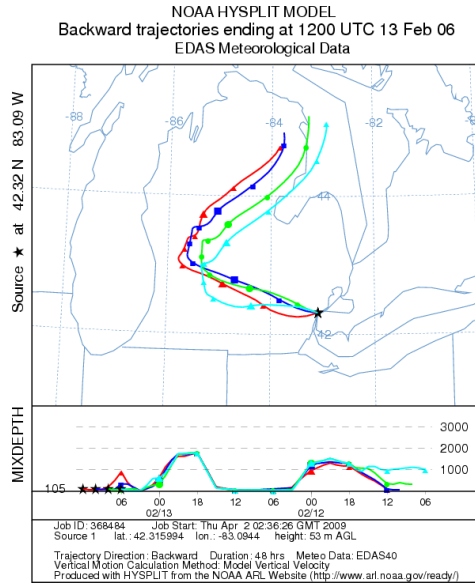
Detroit: 2/11/06



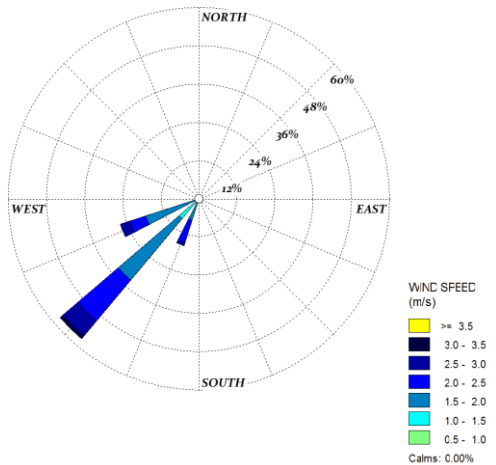
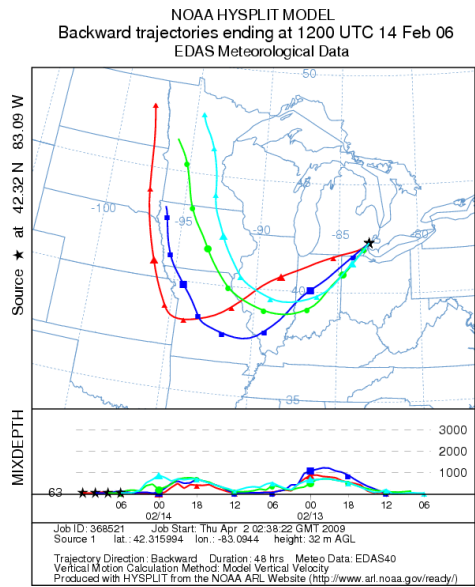
Detroit: 2/12/06



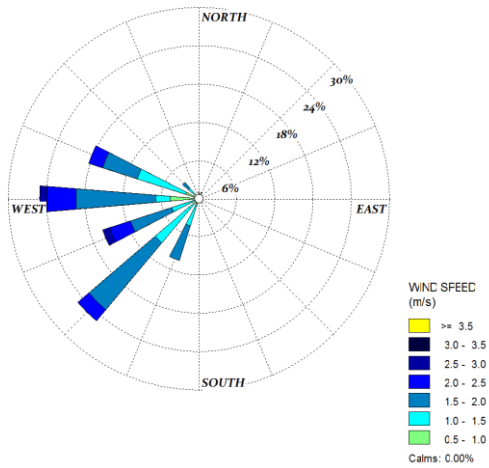
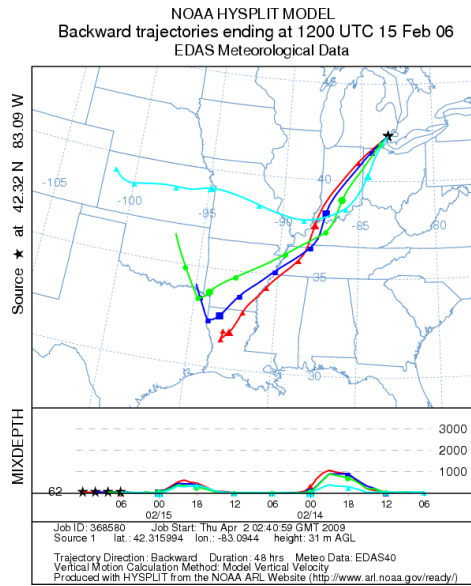
Detroit: 2/13/06



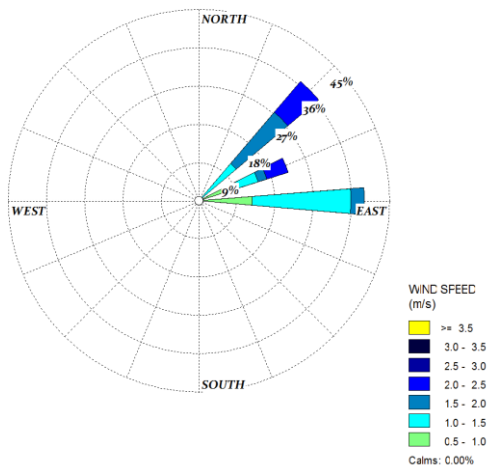
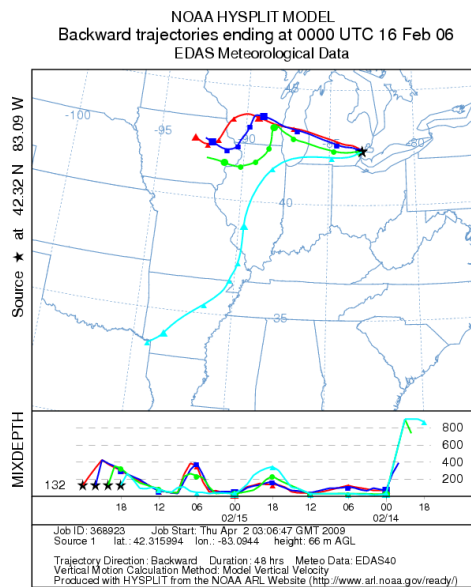
Detroit: 2/14/06



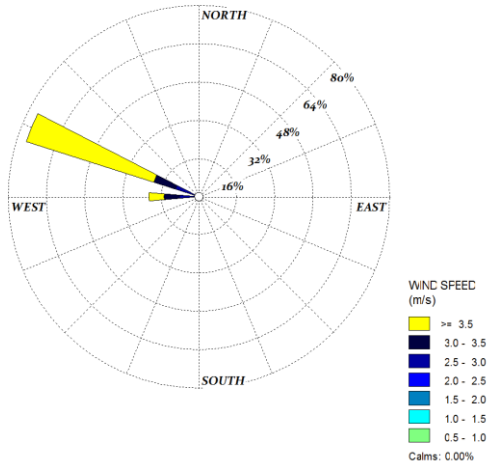
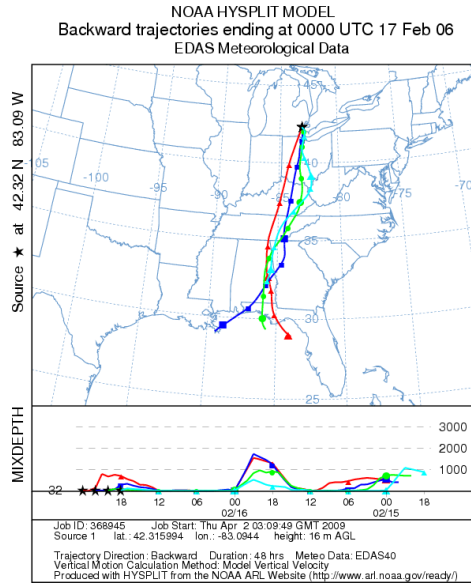
Detroit: 2/15/06



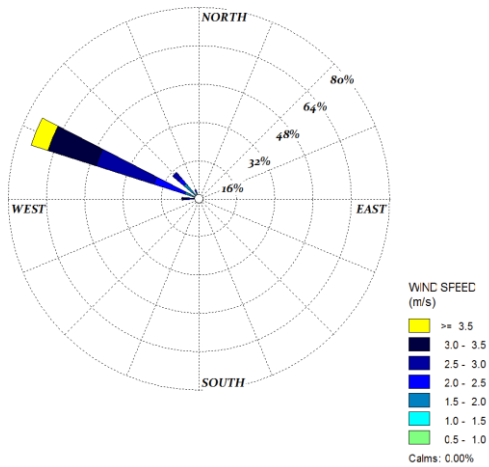
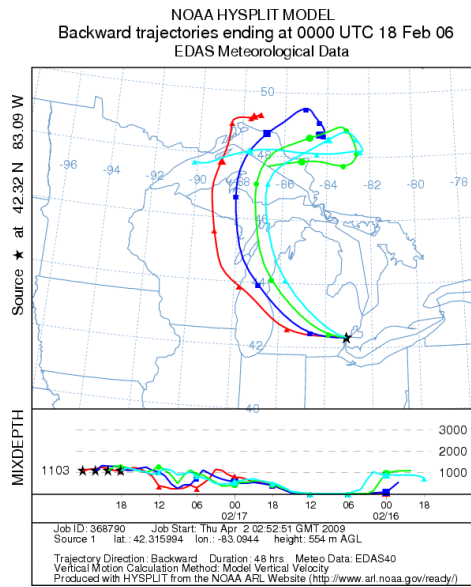
Detroit: 2/16/06



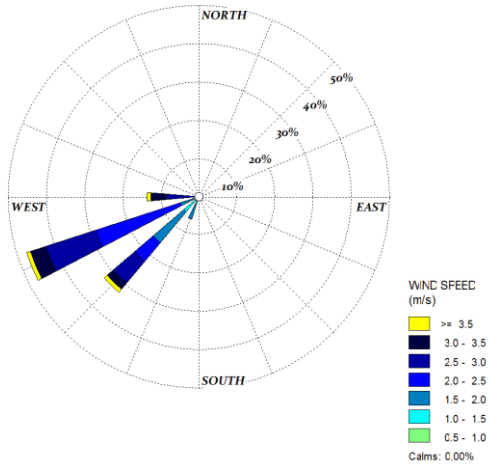
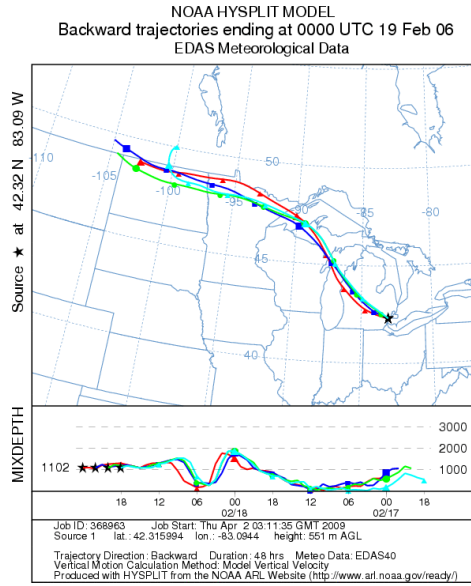
Detroit: 2/17/06



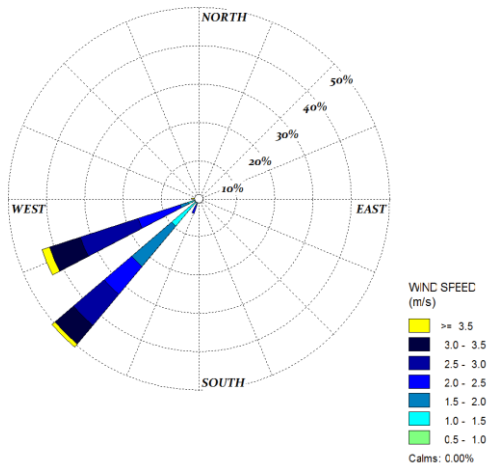
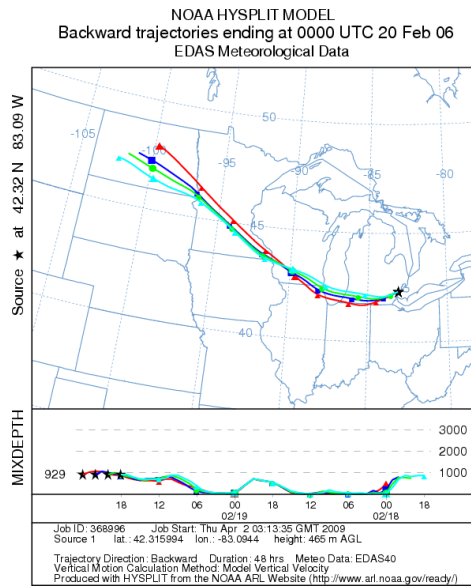
Detroit: 2/18/06



Detroit: 2/19/06

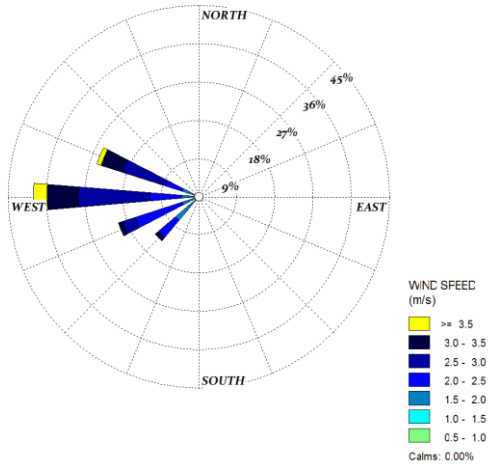
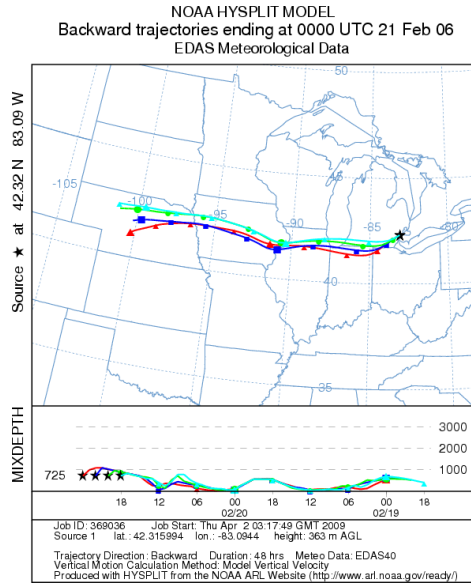


Detroit: 2/20/06

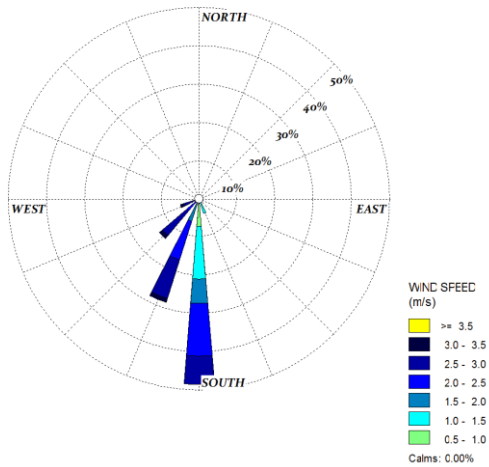
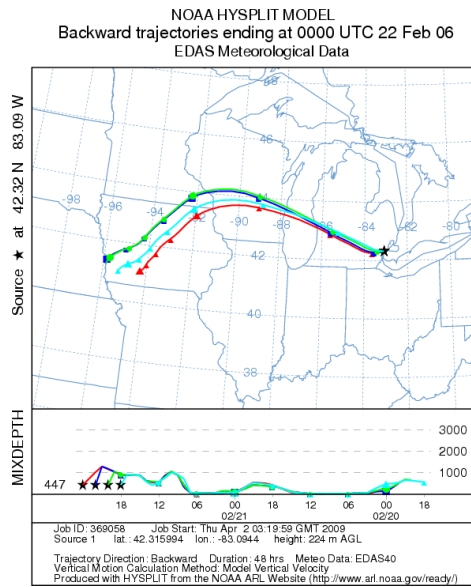




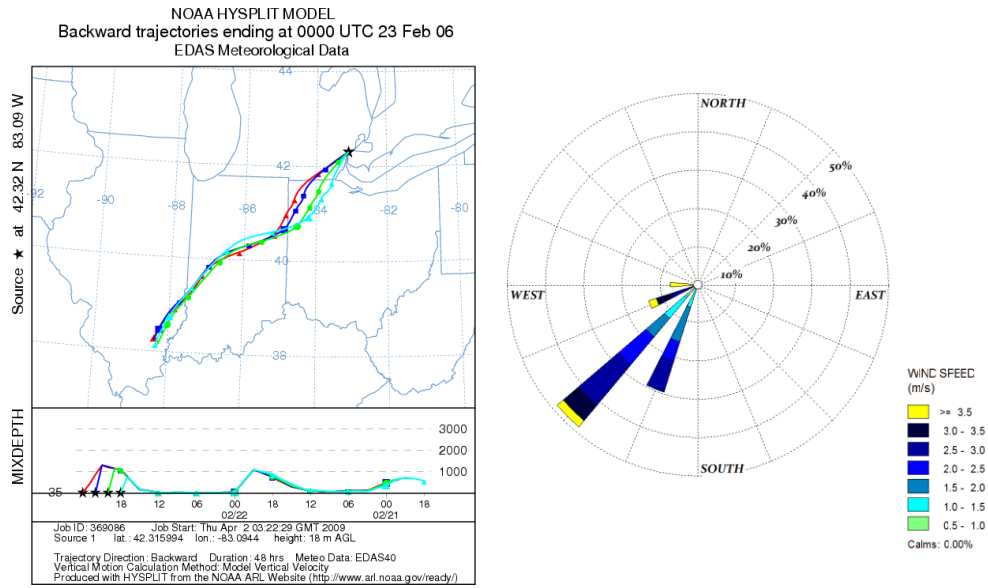
Detroit: 2/21/06



Detroit: 2/22/06



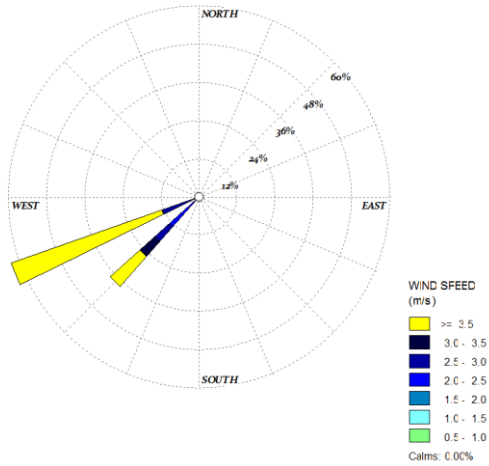
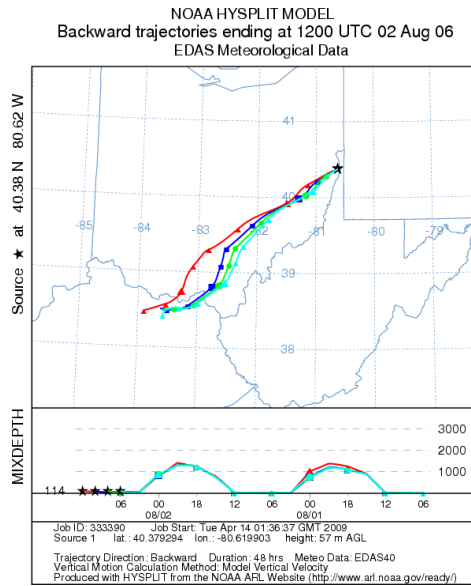
Detroit: 2/23/06



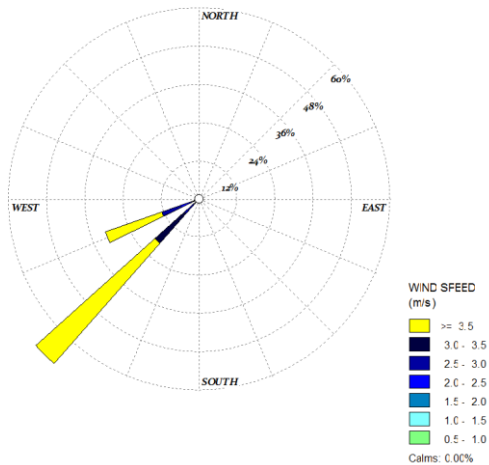
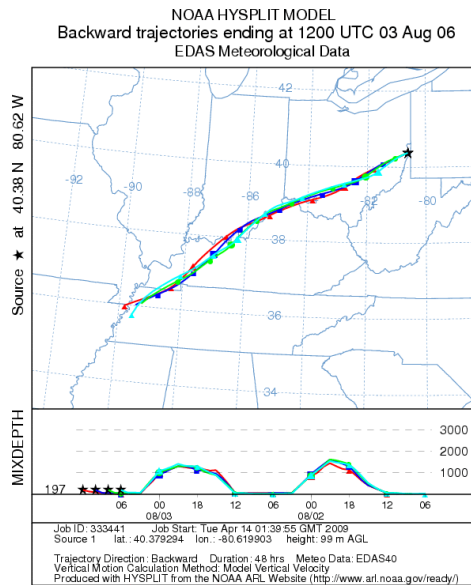
**APPENDIX A.2**

**BACKWARD WIND TRAJECTORIES (HYPSLIT) AND SURFACE WIND  
ROSES FOR EVERY 8-HOUR EXPOSURE PERIOD IN STEUBENVILLE  
DURING THE SUMMER AND WINTER INTENSIVES.**

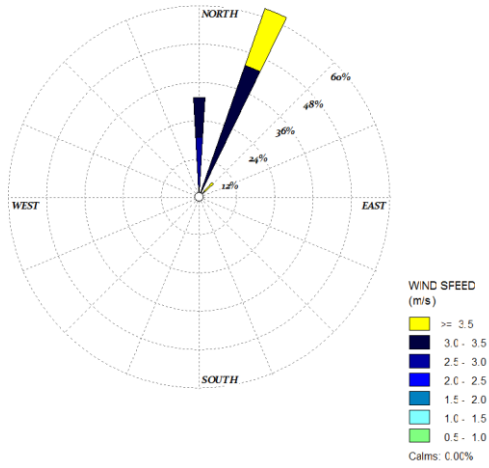
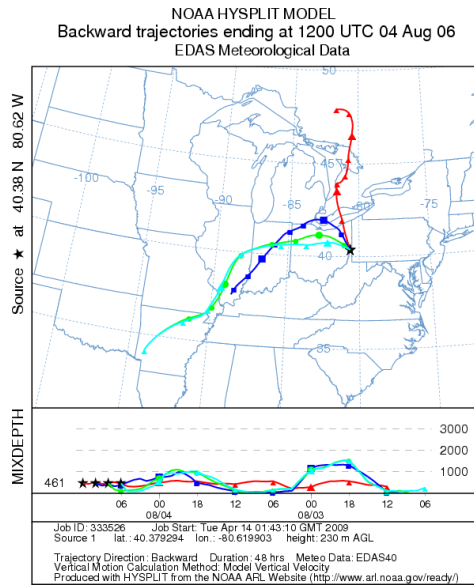
### Steubenville: 8/2/06



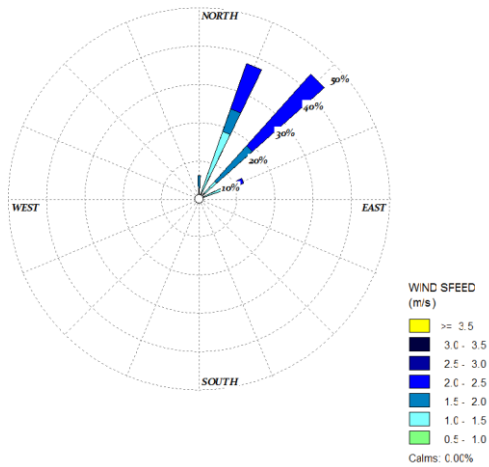
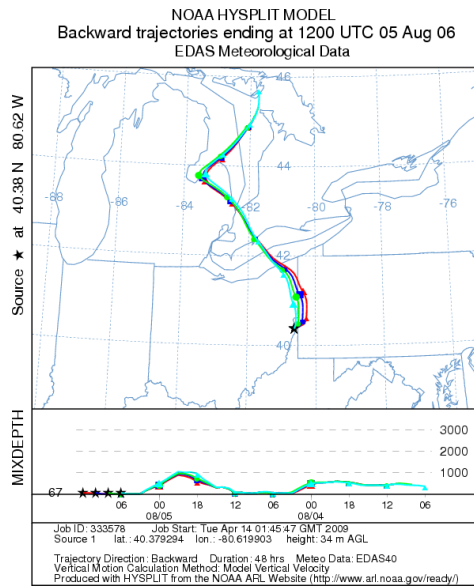
### Steubenville: 8/3/06



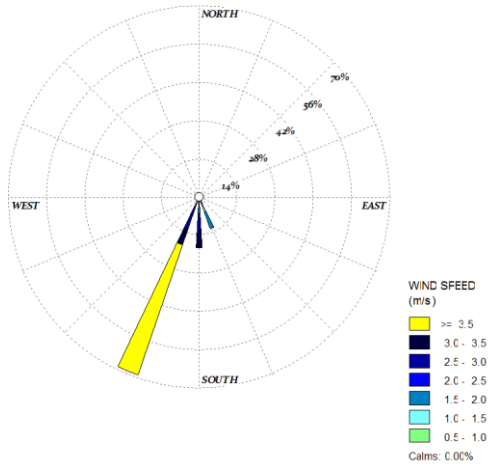
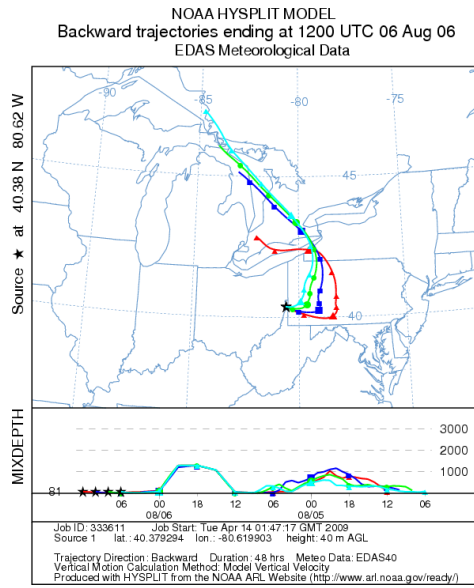
Steubenville: 8/4/06



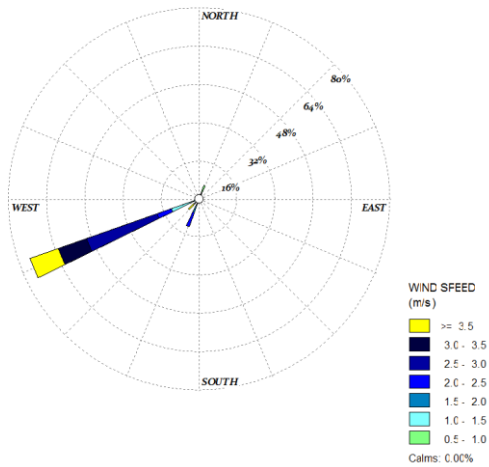
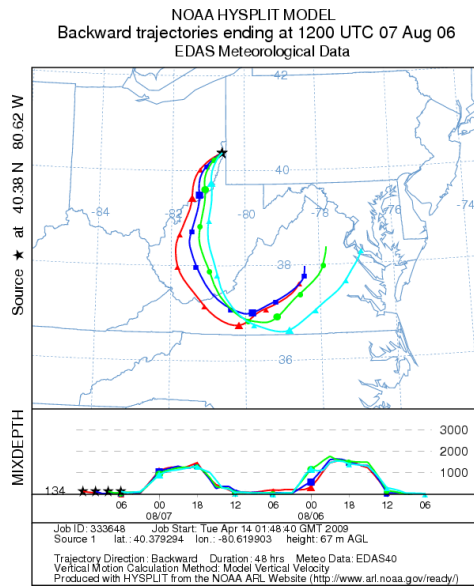
Steubenville: 8/5/06



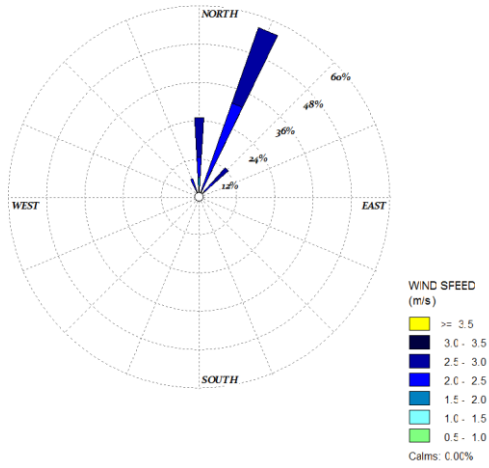
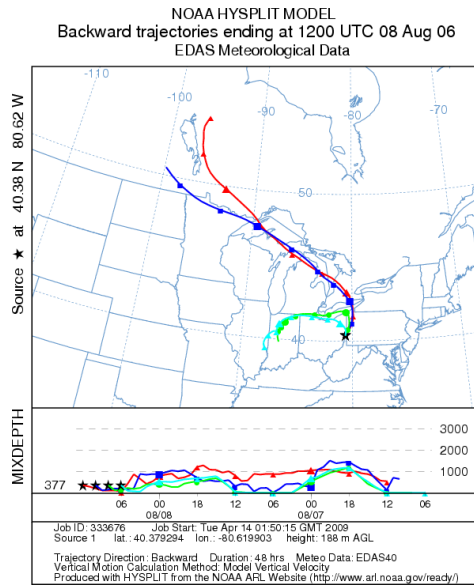
### Steubenville: 8/6/06



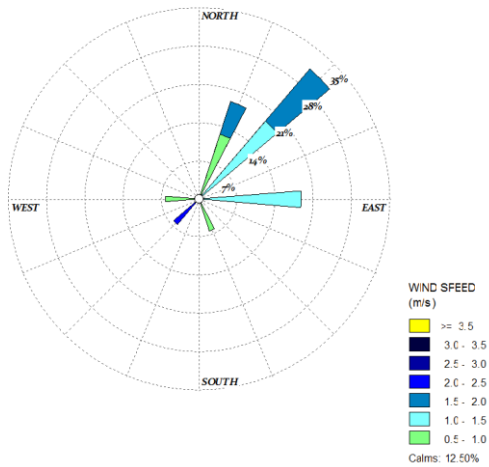
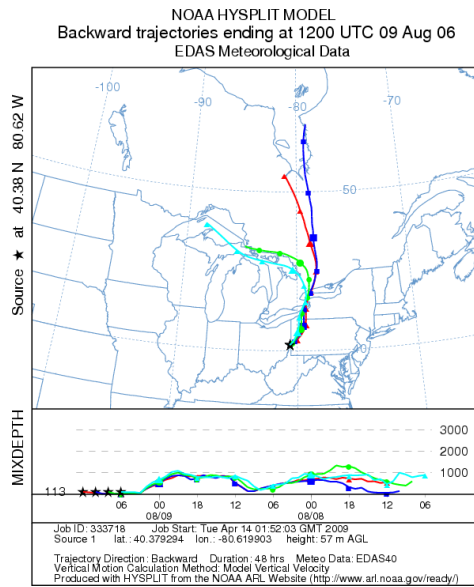
### Steubenville: 8/7/06



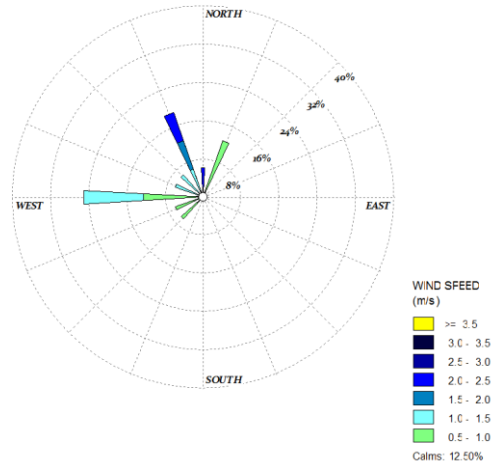
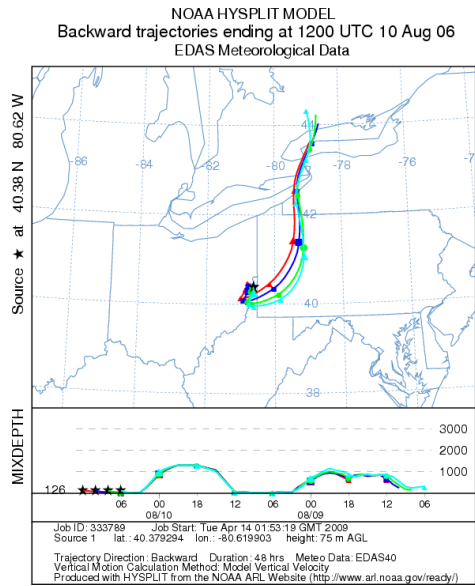
# Steubenville: 8/8/06



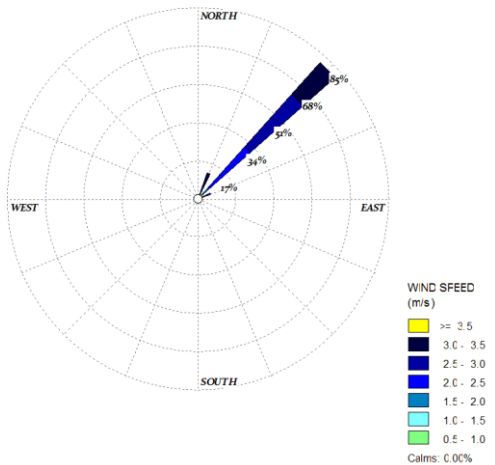
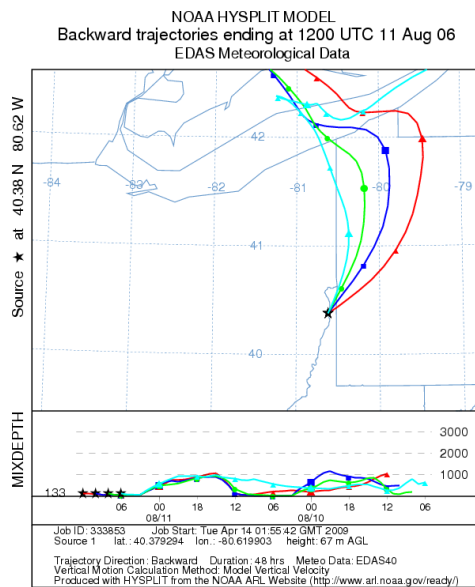
# Steubenville: 8/9/06



# Steubenville: 8/10/06

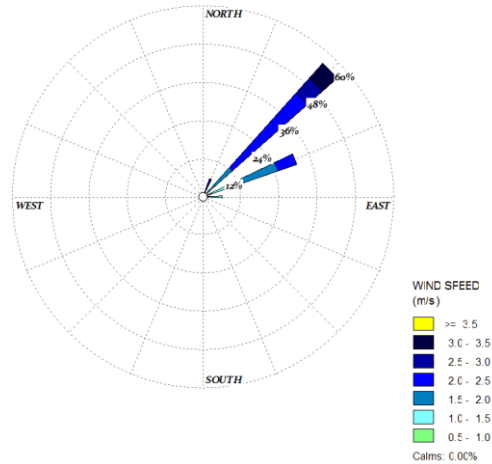
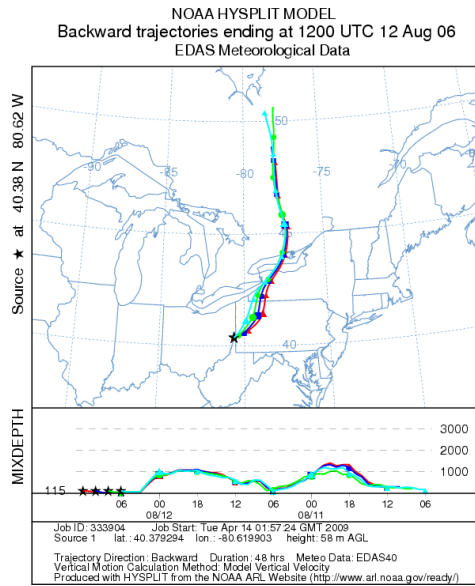


# Steubenville: 8/11/06

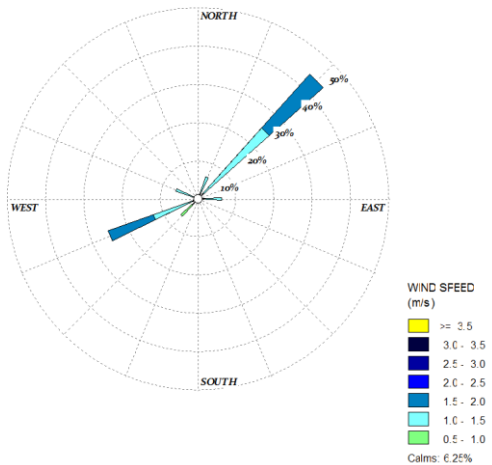
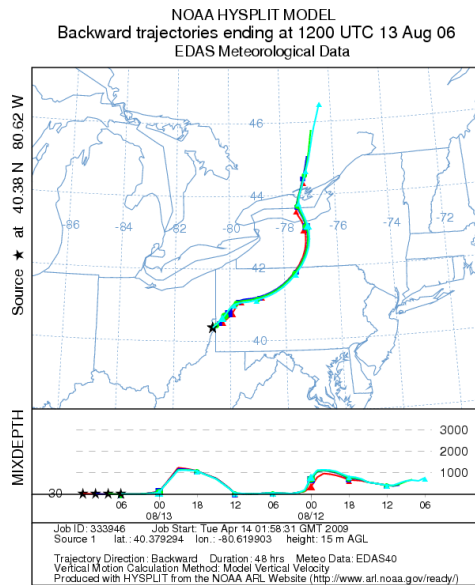




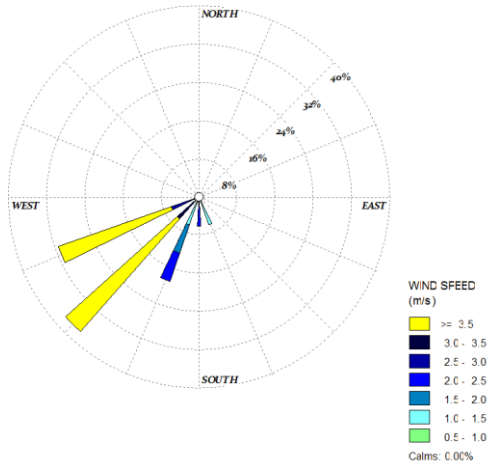
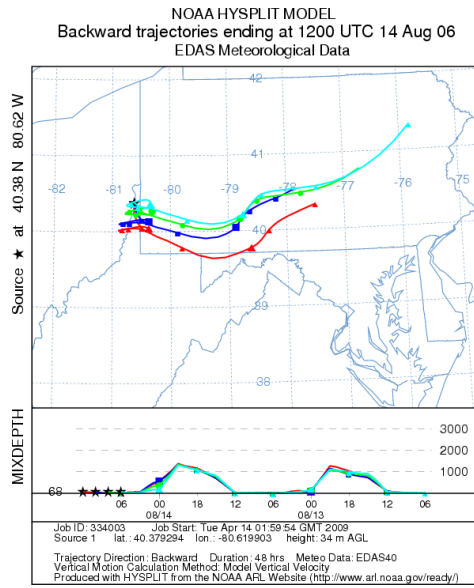
# Steubenville: 8/12/06



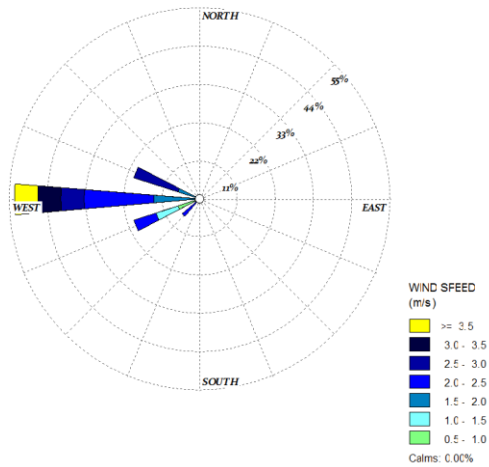
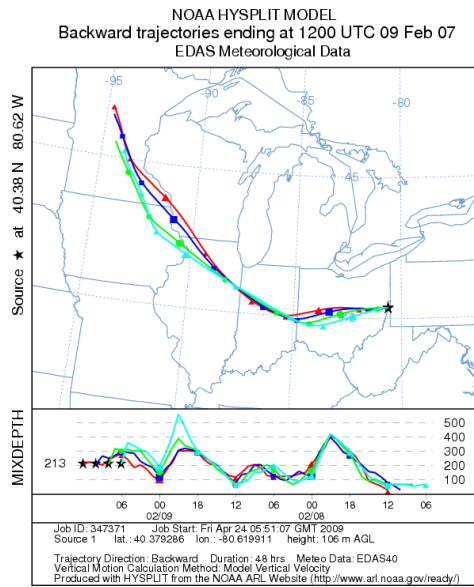
# Steubenville: 8/13/06



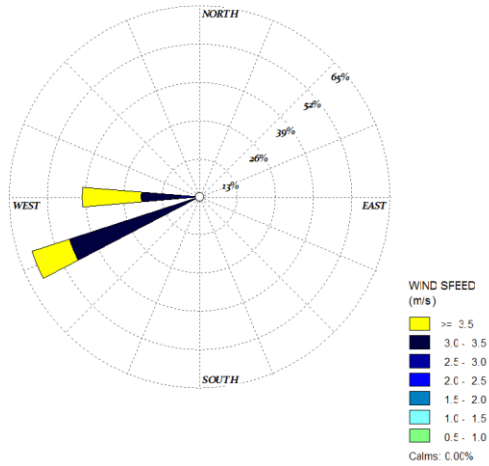
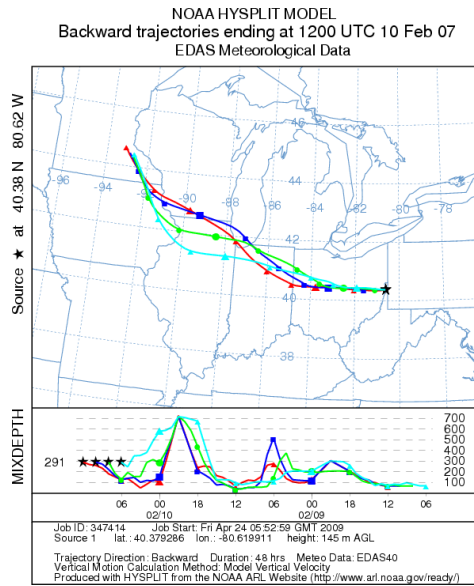
Steubenville: 8/14/06



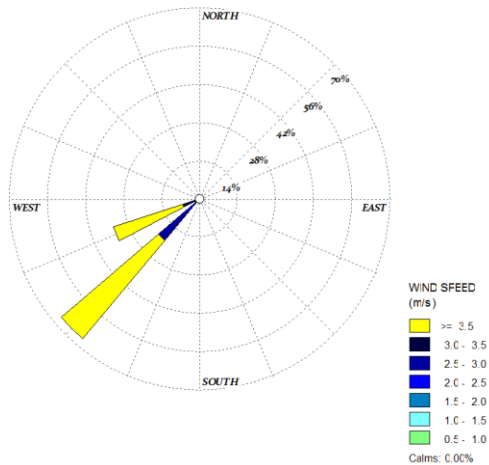
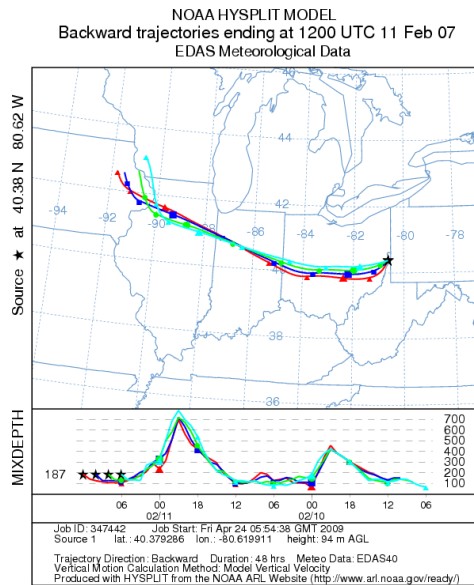
Steubenville: 2/9/07



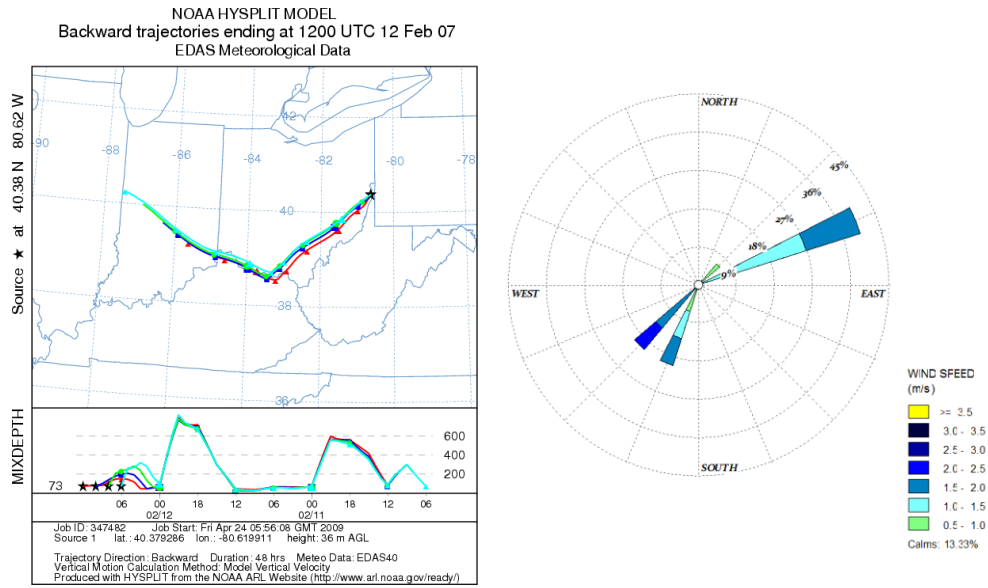
Steubenville: 2/10/07



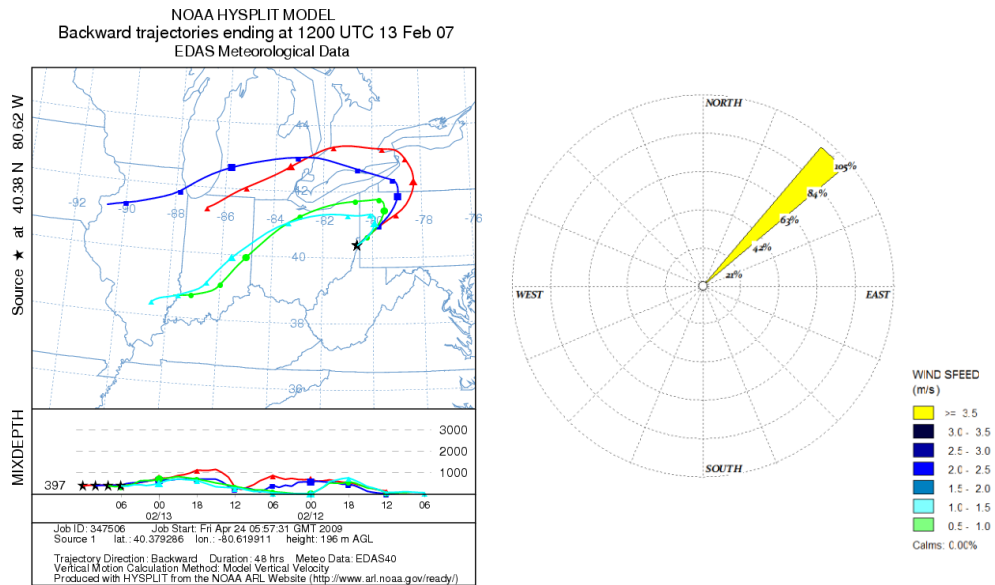
Steubenville: 2/11/07



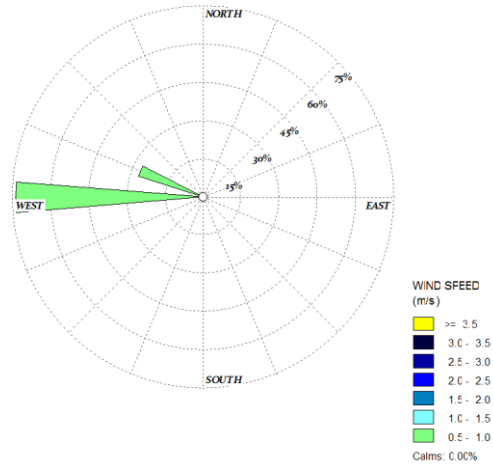
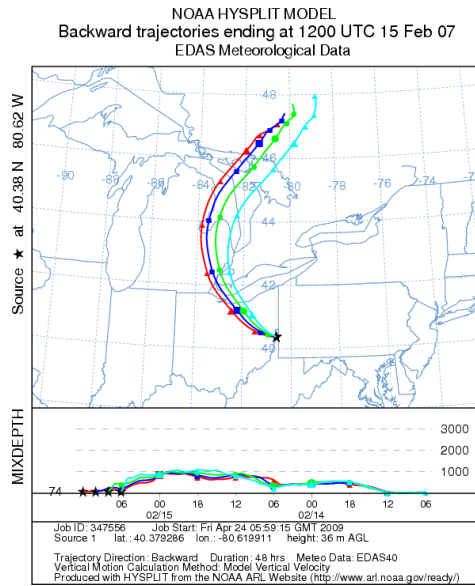
Steubenville: 2/12/07



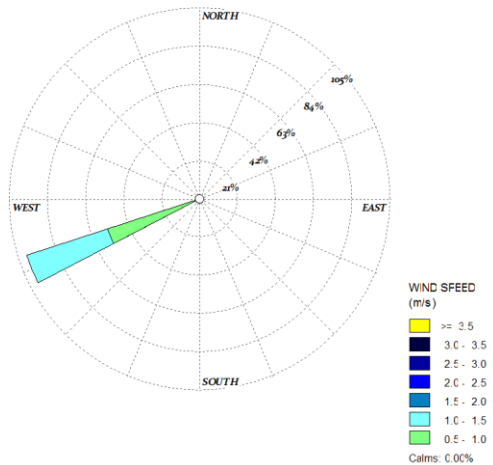
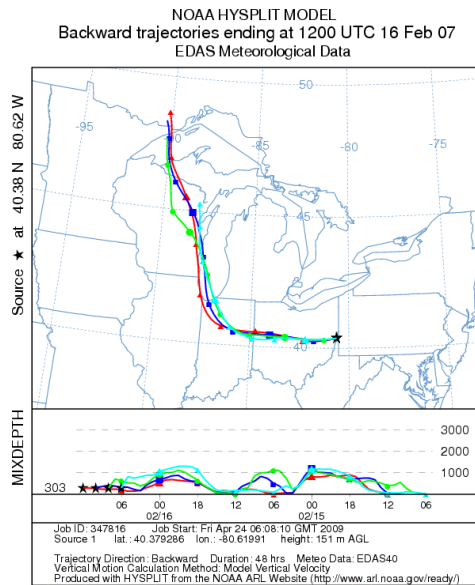
Steubenville: 2/13/07



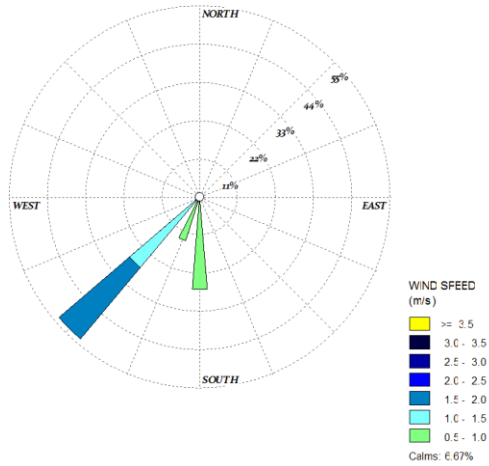
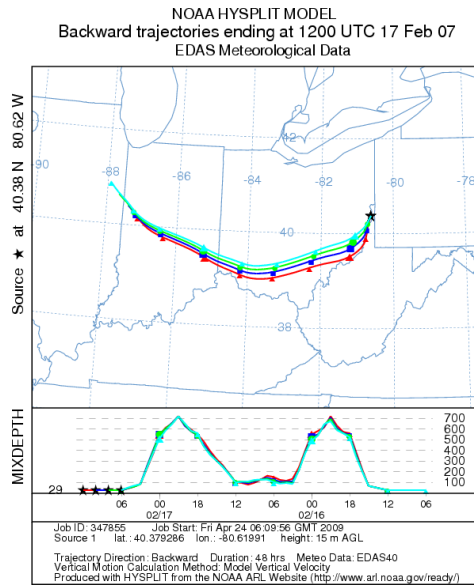
Steubenville: 2/15/07



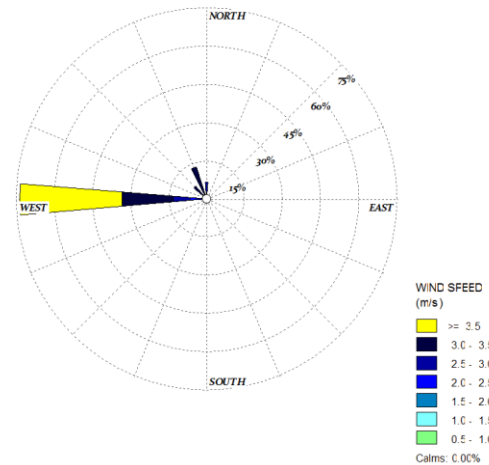
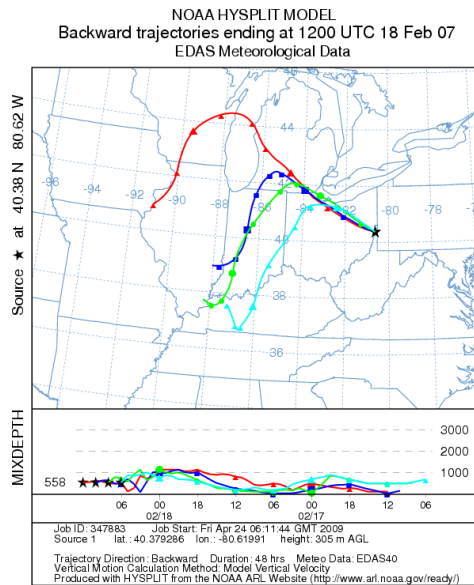
Steubenville: 2/16/07



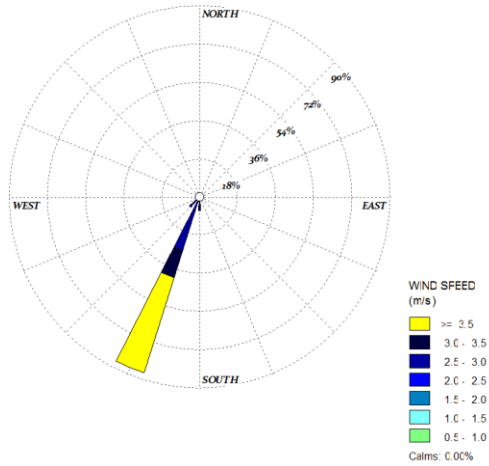
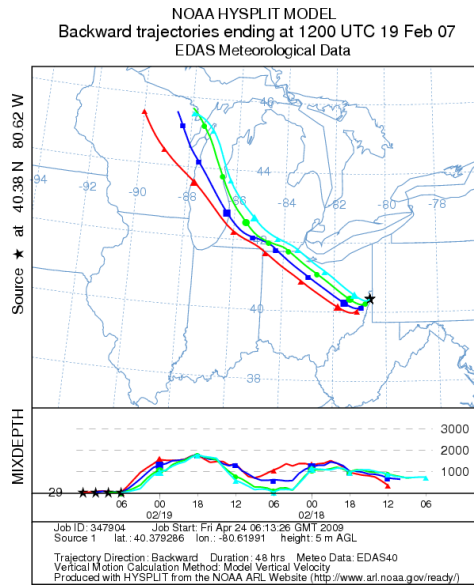
Steubenville: 2/17/07



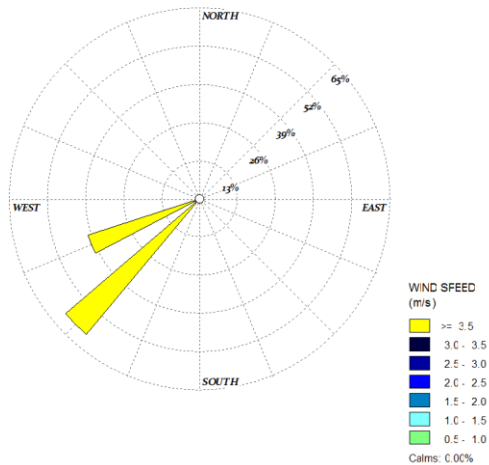
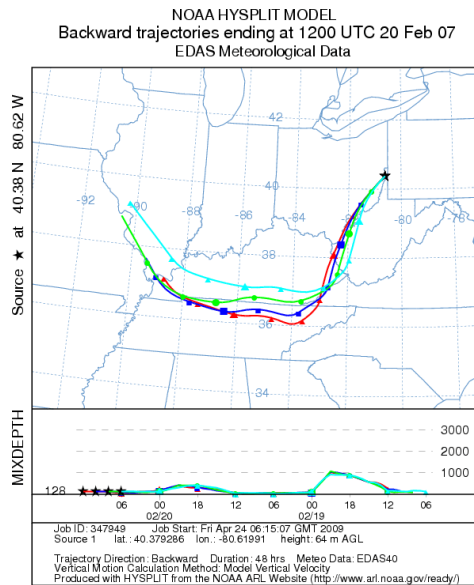
Steubenville: 2/18/07



Steubenville: 2/19/07



Steubenville: 2/20/07



## BIBLIOGRAPHY

1. Samet JM, Dominici F, Curriero FC, et al. (2002) Fine particulate air pollution and mortality in 20 U.S. cities, 1987–1994. *New England Journal of Medicine*. 343:1742–1749.
2. Liao, D, Creason, J, Shy, C, Williams, R, Watts, R, and Zweidinger, R. (1999) Daily variation of particulate air pollution and poor cardiac autonomic control in the elderly. *Environmental Health Perspectives*. 107:521–525.
3. Magari, SR, Schwartz, J, Williams, PL, Hauser, R, Smith, TJ, and Christiani, DC. (2002) The association between personal measurements of environmental exposure to particulates and heart rate variability. *Epidemiology* 13:305–310.
4. Watkinson, WP, Campen, MJ, Costa, DL. (1998) Cardiac arrhythmia induction after exposure to residual oil fly ash particles in a rodent model of pulmonary hypertension. *Toxicological Sciences*. 41(2):209-216.
5. Phalen, RF. The particulate air pollution controversy: a case study and lessons learned. (2002) Kluwer Academic Publishers.
6. Electric Power Research Institute (2006) Tri-City CAPs Project Description. <http://mydocs.epri.com/docs/public/000000000001013705.pdf>
7. Morishita M, Keeler GJ, Wagner JG, Harkema JR. (2006) Source identification of ambient PM<sub>2.5</sub> during summer inhalation exposure studies in Detroit, MI. *Atmospheric Environment*. 40(21):3823–3834.
8. USEPA. (2002) AirData: Access to air pollution data. <http://www.epa.gov/air/data/geosel.html>



9. Grahame, TJ, and Richard B. Schlesinger, RB. (2007) Health effects of airborne particulate matter: Do we know enough to consider regulating specific particle types or sources? *Inhalation Toxicology*. 19(6-7):457-481.
10. USEPA. <http://www.epa.gov/oar/particlepollution/>
11. Berner, EK, Berner, RA. *Global Environment* (1996) Prentice Hall.
12. Keeler GJ, Morishita M, Wagner JG, Harkema JR. (2007) Characterization of urban atmospheres during inhalation exposure studies in Detroit and Grand Rapids, Michigan. *Toxicological Pathology*. 35(1):15-22.
13. Connell DP, Withum JA, Winter SE, Statnick RM, Bilonick RA. (2005) The Steubenville comprehensive air monitoring program (SCAMP) : Overview and statistical considerations. *Journal of the Air & Waste Management Association*. 55(4):467-480.
14. Seinfeld, JH, Pandis, SN (1998). *Atmospheric chemistry and physics*. John Wiley & Sons, Inc.
15. Nemmar, A, Vanbilloen, H, Hoylaerts, MF, Hoet, PHM, Verbruggen, A, and Nemery, B. (2001) Passage of intratracheally instilled ultrafine particles from the lung into the systemic circulation in hamster. *American Journal of Respiratory and Critical Care Medicine*. 164:1665–1668.
16. Whitby, KT, Cantrell, B. (1976) Fine particles, in International conference of environmental sensing and assessment, Las Vegas, NV, Institute of Electrical and Electronic Engineers.
17. Morishita, M. (2003) Doctoral dissertation. An investigation of the source-receptor pathway for anthropogenic fine particulate matter in Detroit, Michigan. The University of Michigan.
18. Lippman, M, Ito, K, Nadas, A, Burnett, RT. (2000) Association of particulate matter components with daily mortality and morbidity in urban populations. *Health Effects Institute*. Number 95.

19. Schlessinger, RB. (1985) Comparative deposition of inhaled aerosols in experimental animals and humans. *Journal of Toxicology and Environmental Health*. 15:197-214.
20. Hopke, PK, Lamb, RE, Natusch, DFS. (1980) Multielemental characterization of urban roadway dust. *Environmental Science and Technology*. 14:164-172.
21. USEPA. Clean Air Status and Trends Network (CASTNET):  
[http://www.epa.gov/castnet/mapconc\\_e.html](http://www.epa.gov/castnet/mapconc_e.html)
22. Kleinman, MT, Phalen, RF, Mautz, WJ, Mannix, RC, McClure, TR, Crocker, TT. (1998) Health effects of acid aerosols formed by atmospheric mixtures. *Environmental Health Perspectives*. 79:137-145.
23. Jacob, DJ, Rokjin JP. (2007) Natural and transboundary influences on particulate matter in the United States: Implications for the EPA regional haze rule. *Powerpoint Presentation (Online)*.
24. Grabroski, MS, McCormick, RL, Yanowitz, J. (1998) HD diesel testing for the Northern Front Range Air Quality Study. *Colorado Institute of Fuels and Engine Research*. Colorado School of Mines.
25. Turpin, BJ, Saxena, P, Andrews, E. (2000) Measuring and simulating particulate organics in the atmosphere: problems and prospects. *Atmospheric Environment*. 34:2983-3013.
26. Schwartz, J, Litonjua, A, Suh, H, Verrier, Gold, DR. (2005) Traffic related pollution and heart rate variability in a panel of elderly subjects. *Thorax*. 60:455-461.
27. Dominici, F, McDermott, A, Zeger, SL, and Samet, JM. (2003) National maps of the effects of particulate matter on mortality: Exploring geographical variation. *Environmental Health Perspectives*. 111:39-43
28. Dockery DW, Pope, CA. (1994) Acute Respiratory Effects of Particulate Air Pollution. *Annual Review of Public Health*. 15:107-132.

29. Loomis D, Castillejos M, Gold DR, McDonnell W, Borja-Aburto VH. (1999) Air pollution and infant mortality in Mexico City. *Epidemiology*. 10(2):118-23.
30. Pope, CA III. (2000) Epidemiology of fine particulate air pollution and human health: biological mechanisms and who's at risk? *Environmental Health Perspectives*. 108(4):713-723.
31. Pope, CA III, Verrier, RL, Lovett, EG, Larson, AC, Raizenne, ME, Kanner, RE, Schwartz, J, Villegas, GM, Gold, DR, Dockery, DW. (1999) Heart rate variability associated with particulate air pollution. *American Heart Journal*. 138:890–899.
32. Godleski, JJ, Verrier, RL, Koutrakis, P, Catalona, P. (2000) Mechanisms of morbidity and mortality from exposure to ambient air particles. *Health Effects Institute*, Number 91.
33. Schwartz, J, Neas, LM. (2000) Fine particles are more strongly associated than coarse particles with acute respiratory health effects in schoolchildren. *Epidemiology*. 11(1):6-10.
34. Dockery, DW, Pope, CA III, Xu, X, Spengler, JD, Ware, JH, Fay, ME, Ferris, BG Jr, Speizer, FE. (1993) An Association between Air Pollution and Mortality in Six U.S. Cities. *New England Journal of Medicine*. 329:1753-1759.
35. Schwartz, J, Morris R. (1995) Air Pollution and Hospital Admissions for Cardiovascular Disease in Detroit, Michigan. *American Journal of Epidemiology*. 142: 23-35.
36. Erin, J, Oberdörster, G. (1990) Increased pulmonary toxicity of ultrafine particles? Particle clearance, translocation, morphology. *Journal of aerosol science*. 21:381-384.
37. Buckeridge D, Glazier R, Harvey B, Escobar M, Amrhein C, Frank J. (2002) Effect of motor vehicle emissions on respiratory health in an urban area. *Environmental Health Perspectives*. 110:293–300.

38. Cascio, WE. (2005) Cardiopulmonary Health Effects of Air Pollution: Is a Mechanism Emerging? *American Journal of Respiratory and Critical Care Medicine*. 172:1482-1484.
39. Gold, DR, Litonjua, A, Schwartz, J, Lovett, E, Larson, A, Nearing, B, Allen, G, Verrier, M, Cherry, R, Verrier, R. (2000) Ambient pollution and heart rate variability. *Circulation* 101:1267–1273.
40. Ulrich, MM, Alink, GM, Kumarathasan, P, Vincent, R, Boere, AJF, and Cassee, FR.(2002) Health effects and time course of particulate matter on the cardiopulmonary system in rats with lung inflammation. *Journal of Toxicology and Environmental Health*. 65:1571–1595.
41. Killingsworth, CR, Alessandrini, F, Murthy, GGK, Catalano, PH, Paulauskis, JD, and Godleski, JJ. (1997) Inflammation, chemokine expression, and death in monocrotaline-treated rats following fuel oil fly ash inhalation. *Inhalation Toxicology*. 9:541–565.
42. Brook, RD, Brook, JR, Urch, B, *et al.* (2002) Inhalation of fine particulate air pollution and ozone causes acute arterial vasoconstriction in healthy adults. *Circulation*. 105:1534-1536.
43. S. D. Adar, SD, Kaufman, JD. (2007) Cardiovascular disease and air pollutants: Evaluating and improving epidemiological data implicating traffic exposure. *Inhalation Toxicology*. 19(s1):135-149.
44. Corey LM, Baker C, Luchtel DL. (2006) Heart-rate variability in the apolipoprotein E knockout transgenic mouse following exposure to Seattle particulate matter. *Journal of Toxicology and Environmental Health*. 69(10):953–965.
45. Malik, M, Camm, AJ. (1995) *Heart Rate Variability*. Futura Publishing Company.
46. The Task Force on Heart Failure at the European Society of Cardiology. (1995) Guidelines for the diagnosis of heart failure. *European Heart Journal*. 16:741–751.

47. Nolan J, Batin PD, Andrews R, Lindsay SJ, Brooksby P, Mullen M, Baig W, Flapan AD, Cowley A, Prescott RJ, Neilson JM & Fox KA (1998) Prospective study of heart rate variability and mortality in chronic heart failure: results of the United Kingdom heart failure evaluation and assessment of risk trial (UK-heart). *Circulation*. 1510–1516.
48. Institute of Heart Math. <http://www.heartmath.org>
49. Watkinson, WP, Campen, MJ, Nolan, JP, and Costa, DL. (2001) Cardiovascular and systemic responses to inhaled pollutants in rodents: Effects of ozone and particulate matter. *Environmental Health Perspectives* 109(s.4):539–546.
50. Corey, LM, Baker ,C, Luchtel, DL. (2006) Heart-rate variability in the apolipoprotein E knockout transgenic mouse following exposure to Seattle particulate matter. *Journal of Toxicology and Environmental Health*. 9(10):953–965.
51. Luttmann-Gibson, H, Suh, HH, Coull, BA, Dockery, DW, Sarnat, SE, Schwartz, J, Stone, PH, Gold, DR. (2006) Short-term effects of air pollution on heart rate variability in senior adults in Steubenville, Ohio. *Journal of Occupational and Environmental Medicine*. 48(8):780-788.
52. Anselme F, Loriot S, Henry JP, *et al.* (2007) Inhalation of diluted diesel engine emission impacts heart rate variability and arrhythmia occurrence in a rat model of chronic ischemic heart failure. *Archives of Toxicology*. 81: 299–307.
53. Campen MJ, McDonald JD, Gigliotti AP, Seilkop SK, Reed MD, Benson JM. (2003) Cardiovascular effects of inhaled diesel exhaust in spontaneously hypertensive rats. *Cardiovascular Toxicology*. 3(4):353–361.
54. Chang CC, Hwang JS, Chan CC, Wang PY, Hu TH, Cheng TJ (2004) Effects of concentrated ambient particles on heart rate, blood pressure, and cardiac contractility in spontaneously hypertensive rats. *Inhalation Toxicology*. 16(6–7):421–429.
55. Peretz, A, Kaufman, JD, Trenga, CA, Allen, J, Carlsten, C, Aulet, MR, Adar, SD, Sullivan JH. (2008) Effects of diesel exhaust inhalation on heart rate variability in human volunteers. *Environmental Research*. 107(2): 178-184.

56. Cavallari, JM, Eisen, EA, Chen, J-C, Fang, SC, Dobson, CB, Schwartz, J, Christiani, DC. (2007) Night Heart Rate Variability and Particulate Exposures among Boilermaker Construction Workers *Environmental Health Perspectives* 115:1046–1051
57. Keenan, DB, Grossman, P. (2006) Adaptive Filtering of Heart Rate Signals for an Improved Measure of Cardiac Autonomic Control. *International Journal of Signal Processing*. 2(1):52-58.
58. Michigan Department of Transportation (2009). Ambassador bridge gateway project brochure.  
[http://michigan.gov/documents/mdot/MDOT\\_Ambassador\\_Gateway\\_brochure\\_219274\\_7.pdf](http://michigan.gov/documents/mdot/MDOT_Ambassador_Gateway_brochure_219274_7.pdf)
59. Environment Canada, National Pollution Release Inventory.  
<http://www.ec.gc.ca/inrp-npri/>
60. Power Plants Around the World. <http://www.industcards.com/ppworld.htm>
61. Sioutas, C, Koutrakis, P, Godleski, JJ, Ferguson, ST, Chong, SK, Burton, RM. (1997) Fine particle concentrators for inhalation exposure-effect on particle size and composition. *Journal of Aerosol Science*. 28:1057-1071.
62. Landis, MS, Keeler, GJ. (1997) Critical evaluation of a modified automatic wet-only precipitation collector for mercury and trace element determinations. *Environmental Science & Technology*. 31:2610-2615.
63. Yoo, SJ. Doctoral Dissertation (2006) Source apportionment of mercury in ambient air and in precipitation at New England region using hybrid receptor model. University of Michigan.
64. Henry, RC. (2002) Multivariate receptor models – current practice and future trends. *Chemometrics and Intelligent Laboratory Systems*, 60:43-48.
65. Morishita, M. *et al.* (2009) Identification of ambient PM<sub>2.5</sub> sources in Detroit, Michigan: Analysis of pollution episodes using semi-continuous measurements. *Manuscript not yet submitted*.

66. Kamal, AS, Keeler, GJ, Mukherjee, B, Morishita, M, Wagner, JG, Harkema, JR. (2009) A Seasonal Comparison of the Impacts of PM<sub>2.5</sub> on Heart Rate Variability in Rats: A Tale of Two Cities. *Manuscript not yet submitted*.
67. Pekkanen J, Peters A, Hoek G, Tiittanen P, Brunekreef B, de Hartog J, *et al.* (2002) Particulate air pollution and risk of ST-segment depression during repeated submaximal exercise tests among subjects with coronary heart disease. The Exposure and Risk Assessment for Fine and Ultrafine Particles in Ambient Air [ULTRA] study. *Circulation*. 106:933–938.
68. Park, SK, O'Neill, MS, Vokonas, PS, Sparrow, D, Schwartz, J. (2005) Effects of Air Pollution on Heart Rate Variability: The VA Normative Aging Study; *Environmental Health Perspectives*. 113:304-309.
69. Murata, K, Araki, S. (1991) Autonomic nervous system dysfunction in workers exposed to lead, zinc and copper in relation to peripheral nerve conduction: a study of R-R interval variability. *American Journal of Industrial Medicine*. 20:663-671.
70. Lippmann, M, Ito, K, Hwang, JS, Maciejczyk, P, Chen, LC. (2006) Cardiovascular effects of nickel in ambient air. *Environmental Health Perspectives*. 114:1662-1669.
71. Magari, SR, Hauser, R, Schwartz, J, Williams, P, Smith, TJ, Christiani, DC. (2001) The association of heart rate variability with occupational and environmental exposure to particulate air pollution. *Circulation*. 104:986-991.